

Functional Expression of Recombinant N-Methyl-D-Aspartate (NMDA) Receptors in Eukaryotic Cell Lines

**Dissertation for the Achievement of the Doctor's Degree of Natural Sciences
Submitted to the Faculty of Biochemistry, Pharmacy and Food Chemistry of the
Johann Wolfgang Goethe-University, Frankfurt am Main**

by

Ralf Dirk Steinmetz

Frankfurt am Main 2000

(DF1)

vom Fachbereich
Chemische und Pharmazeutische Wissenschaften
der Johann Wolfgang Goethe-Universität Frankfurt
als Dissertation angenommen

Dekan: Prof. Dr. Joachim Engels

Gutachter: Prof. Dr. Dieter Steinhilber / Prof. Dr. Theodor Dingermann

Datum der Disputation: 13.12.2000

Ich möchte Herrn Prof. Dr. Dieter Steinhilber dafür danken, dass er mir die Möglichkeit zur Anfertigung der hier vorliegenden Arbeit gegeben hat. Sein stetes Interesse an der Thematik sowie wertvolle Anregungen und Diskussionen haben geholfen, diese Arbeit zum Erfolg zu führen.

Herrn Dr. Johannes Krämer gilt mein Dank für die Ermutigung zur Anfertigung einer Promotionsarbeit sowie für seine jahrelange Freundschaft.

Bei Herrn Dr. Uwe Janßen-Timmen bedanke ich mich für seine wertvollen Ratschläge in vielen technischen Fragen und das freundschaftliche Arbeitsklima.

Herrn Prof. Dr. Pierluigi Nicotera und Eugenio Fava gilt mein Dank für die Unterstützung bei den Untersuchungen zur Charakterisierung des Zelltodes sowie die Gastfreundschaft, die mir bei meinem Aufenthalt in Konstanz zuteil wurde.

Frau Dr. Margret Henseler gilt mein besonderer Dank für ihre Hilfe und das Interesse an meiner Arbeit sowie ihre uneingeschränkte Kollegialität und Freundschaft.

Der grösste Dank gilt meinen Eltern für ihre Unterstützung, Zuversicht und Liebe, die sie mir zuteil werden lassen.

1.	Introduction	7
1.1	Glutamate receptors within the CNS	7
1.2	Structure and function of the NMDA receptor Channel	8
1.2.1	Molecular diversity, nomenclature and primary structure	9
1.2.2	Heteromeric channels	11
1.2.3	Transmembrane topology	12
1.2.4	Channel pore region	14
1.2.5	Ligand binding regions	14
1.2.6	Phosphorylation domain	15
1.2.7	Allosteric modulation regions	16
1.2.7.1	Proton inhibition	16
1.2.7.2	Modulation by polyamines	17
1.2.7.3	Modulation by histamine	18
1.2.7.4	Redox modulation	18
1.2.7.5	Inhibition by zinc	19
1.2.7.6	Effects of magnesium	20
1.3	Distribution within the CNS	20
1.4	Pharmacological diversity of native and recombinant NMDA receptors	22
1.5	Physiological and pathophysiological implications	25
1.5.1	Glutamatergic neurotransmission	25
1.5.2	Long term potentiation	25
1.5.3	Clinical implications	26
1.5.3.1	Epilepsy	26
1.5.3.2	Schizophrenia	27
1.5.3.3	Anxiety	27
1.5.3.4	Acute neurodegenerative diseases	27
1.5.3.5	Chronic neurodegenerative diseases	28
1.5.3.6	Chronic pain	30
1.5.3.7	Drug and ethanol dependence, tolerance and abuse	30
1.5.3.8	Side effects	31
1.6	NMDA receptor agonists and antagonists	33
1.6.1	Agonists and competitive antagonists	33
1.6.2	Glycine site agonists and antagonists	36
1.6.3	Non-competitive antagonists	41
1.6.4	NR2B specific compounds	44
1.6.5	Immunological approach	45
1.7	Apoptosis and necrosis – modes of cell death	46

2.	Aim of the study	48
3.	Results	48
3.1	Transient expression of rat NR1-1a, mouse NR ϵ 1 and mouse NR ϵ 3 in Hek 293 cells	49
3.2	Generation of cell lines stably expressing human NR1-1a / NR2A and NR1-1a / NR2B	52
3.2.1	General considerations	52
3.2.2	Transfection and cell cloning	53
3.2.3	Clone screening	54
3.3	Characterisation of clones L12-G10 and L13-E6	60
3.3.1	RT-PCR analysis	60
3.3.2	Immunoblotting	61
3.3.3	Immunocytochemistry	63
3.3.4	Calcium imaging	65
3.4	Cell death based in vitro assays	68
3.4.1	LDH assay mixture	68
3.4.2	Cell culture models	71
3.4.3	Structure - in vitro activity relationship of a series of thieno[2,3-b]pyridinones	75
3.4.4	Structure - in vitro activity relationship of quinoxaline-2,3-diones	81
3.4.5	Pharmacology of clones	82
3.4.5.1	Cell death caused by NMDA receptors is pH dependent	82
3.4.5.2	Spermine triggers cell death in a subunit specific manner	83
3.4.5.3	Glycine site agonist D-serine enhances L-glutamate induced cell death	85
3.4.5.4	Glutamate and glycine site antagonists inhibit NMDA receptor induced cell death	86
3.4.5.5	Ifenprodil and haloperidol inhibit cell death selectively at NR2B expressing L13-E6 cells in the absence of spermine	87
3.4.5.6	Cell death is not triggered by histamine or activation of PKC	89
3.5	Mechanism of cell death inhibition by cyclosporin A	91
3.6	Characterization of cell death	102
3.6.1	Applied methods for studies on apoptosis and necrosis	102
3.6.2	Results of cell death studies	103
4.	Conclusions	118
5.	Experimental procedures	126
5.1	Transient expression of NMDA receptors in Hek 293 cells	126
5.2	Generation of cell lines stably expressing human NR1-1a / NR2A and NR1-1a / NR2B	126
5.2.1	Transfection	126
5.2.2	Cloning	127

Introduction

5.2.3	Screening	127
5.3	Characterization of clones L12-G10 and L13-E6	128
5.3.1	Reverse-transcription (RT)-PCR analysis	128
5.3.2	Immunoblotting	129
5.3.3	Immunocytochemistry	129
5.3.4	Calcium imaging	130
5.4	Cell death based in vitro assays	131
5.4.1	LDH assay mixture	131
5.4.2	Induction model	132
5.4.3	Differentiation model	133
5.5	Inhibition of cell death by cyclosporin A	134
5.6	Characterization of cell death	136
5.6.1	Plasma membrane damage and morphological characterization	136
5.6.2	Flow cytometry	136
5.6.3	Phosphatidyl serine translocation	137
6.	Materials	138
7.	Zusammenfassung (German summary)	140
8.	References	150
9.	Curriculum Vitae	178

1. Introduction

In the 1970s and 1980s the role of L-glutamate as the major excitatory neurotransmitter in the central nervous system (CNS) was accepted. In fact, it is believed that 70% of the excitatory synapses in the CNS are utilizing L-glutamate as neurotransmitter. The rising interest in excitatory amino acids function has led to the identification and cloning of several subtypes of metabotropic and ionotropic glutamate receptors and glutamate has proved to play a dual role in the brain. Glutamate and its receptors are involved in physiological processes like learning and memory as well as in neurodegenerative diseases. Since the synthesis of N-methyl-D-aspartate by J.C. Watkins in the 1960s, and subsequent pharmacological studies by a number of groups, NMDA receptors have emerged to play a key role in neuronal excitation and toxicity. The present work has focussed on heterologous expression of recombinant NMDA receptors in mammalian cell lines and the development of functional in vitro test systems for compound testing.

1.1 Glutamate receptors within the CNS

Glutamate receptors are found throughout the mammalian brain. The longest known and best-studied glutamate receptors are ligand gated ion channels, also called ionotropic glutamate receptors, which are permeable for cations. They have traditionally been classified into three broad subtypes of receptors based on the discovery of selective agonists: α -amino-3-hydroxy-5-methyl-4-isoxazole propionate (AMPA) receptors, kainate (KA) receptors, and N-methyl-D-aspartate (NMDA) receptors.

AMPA receptors (GluR1–4) are mainly located on the postsynaptic membrane. They form voltage-independent ligand gated channels and are mediating the fast glutamatergic neurotransmission. Under participation of the widely distributed GluR2 subunit, AMPA receptors exhibit a high permeability for sodium and potassium and only a weak calcium permeability. If GluR2 is removed from heteromeric assemblies, the resulting receptors display a substantial calcium permeability. Thus, GluR2 dominantly determines the channel conductance and calcium permeation. GluR2 (as well as KA receptor subunits GluR5 and 6) contains an arginine residue within the channel forming region, whereas the other three subunits carry a glutamine residue in the corresponding position (Q / R site). Site-directed mutagenesis revealed that the distinct channel properties are indeed determined by this arginine or glutamine residue (Burnashev et al., 1992a; Hume et al., 1991). Even more

surprising was the finding that a glutamine codon (CAG) is encoded at the Gln / Arg position in the genomic sequence for all subunits (AMPA and kainate) whereas an Arg codon (CGG) is found in cDNAs of the GluR2 (as well as in GluR5 and 6)(Sommer et al., 1991). This alteration was explained by an RNA editing mechanism, the enzyme-directed, posttranscriptional modification of RNA transcripts.

Native, postsynaptic NMDA receptors form highly regulated channels underlying a variety of modulations, e.g. block by extracellular magnesium at resting potentials, simultaneous stimulation by L-glutamate and glycine, slow depolarisation and modulation by polyamines, histamine, protons and zinc ions. They are supposed to contribute to higher brain functions as synaptic plasticity, learning and memory function. Depending on their subunit composition, the resulting channels are highly permeable for calcium as well as for sodium and potassium. For further details see chapter 1.2.

Only very little is known about KA receptors (GluR5 to 7). Similar to AMPA receptors they show only weak permeability for calcium and seem to play a role in presynaptic regulation. Beside these ionotropic receptors, a group of G-protein coupled receptors has been cloned, also called metabotropic glutamate receptors (mGluR1 to 8). They seem to have modulatory effects upon excitatory neurotransmission. The subtypes of mGluR1 and mGluR5 are coupled to phospholipase C and lead to an intracellular release of calcium from the endoplasmic reticulum via IP₃. In contrast mGluR2–4 and mGluR6–8 are coupled to adenylate cyclase negatively modulating activity of voltage dependent calcium channels. Antagonists at mGluR1 and mGluR5 as well as agonists at mGluR2–4 and mGluR6–8 have been demonstrated to be neuroprotective in ischemic animal models.

The cross-talk of these different receptors in glutamatergic neurotransmission has implications for brain function. Summarizing, the AMPA receptors evoke fast, voltage independent synaptic responses and in turn promote the activation of voltage dependent NMDA receptors. The metabotropic subtypes exert long lasting actions through the activation and inhibition of intracellular signals.

1.2 Structure and function of the NMDA receptor Channel

As this work is focussed on the expression of NMDA receptors, their structure and function is introduced in the following sections.

1.2.1 Molecular diversity, nomenclature and primary structure

The most important result from molecular cloning studies was the elucidation of the diversity of the NMDA receptor channel (Ikeda et al., 1992; Ishii et al., 1993; Kutsuwada et al., 1992; Meguro et al., 1992; Monyer et al., 1992; Moriyoshi et al., 1991; Yamazaki et al., 1992). The identified subunits have distinct distribution throughout the brain, distinct properties and modulation sites. This implies that NMDA receptors are different in their molecular architecture and function, depending on the brain regions and developmental stages (Mishina et al., 1993; Monyer et al., 1992).

Gene	Species	protein Size (aa)	MW (kDa)	References
NR1	rat	920	103	(Moriyoshi et al., 1991)
	mouse (ζ 1)	920		(Yamazaki et al., 1992)
	human	920		(Karp et al., 1993; Le Bourdelles et al., 1994; Planells-Cases et al., 1993)
NR2A	rat	1442	163	(Monyer et al., 1992)
	mouse (ϵ 1)	1442		(Meguro et al., 1992)
	human	1464		(Hess et al., 1996; Le Bourdelles et al., 1994)
NR2B	rat	1456	162	(Monyer et al., 1992)
	mouse (ϵ 2)	1456		(Kutsuwada et al., 1992)
	human	1484		(Adams et al., 1995; Hess et al., 1996)
NR2C	rat	1218	134	(Monyer et al., 1992)
	mouse (ϵ 3)	1220		(Kutsuwada et al., 1992)
	human	1233		(Lin et al., 1996)
NR2D	rat	1329	141	(Ishii et al., 1993)
	mouse (ϵ 4)	1296		(Ikeda et al., 1992)
	human	1336		(Hess et al., 1998)
NR3A (NMDAR-L)	rat	1115		(Sucher et al., 1995b)

Tab. 1 Cloned NMDA receptors

The identified NMDA receptor subunits (see tab.1) share a 22 to 26% homology in amino acid sequence with AMPA or KA receptors and are classified into three subfamilies designated as NR1, NR2 (for mouse receptors GluR ζ and GluR ϵ) and the recently detected NR3. There are four on separate genes encoded members for the NR2 (GluR ϵ) subfamily (NR2A-NR2D / GluR ϵ 1-GluR ϵ 4), whereas only one member is known for NR1 (GluR ζ)

Introduction

except for the seven splice variants. The amino acid sequence identity among the NR1 and NR2 subfamilies is approximately 26%. Within the NR2 subfamily a homology of 42 to 56% is found (Hollmann and Heinemann, 1994). The amino acid sequence identity between human receptors and cDNAs from mouse and rat is 95 to 100%.

For NR1 subunits eight splice forms from NR1-1a to NR1-4b have been described. The alternative splice variants differ by the presence or absence of three nucleotide cassettes into the NR1 sequence (see tab. 2). The first N-terminal cassette inserts 21 predominant basic amino acids after residue 190. This cassette is present in splice forms NR1b / 2b / 3b / 4b. Its absence in NR1-1a / 2a / 3a / 4a is one requirement for polyamine modulation of receptors. Deletion of C-terminal cassette 2 removes 37 amino acids after residue 863. Deletion of cassette 3 removes 38 amino acids and the stop codon, resulting in a new 22 amino acid carboxy terminal end. The most common transcripts in brain contain cassette 2 and / or 3, but not cassette 1 (NR1-1a to NR4a).

Tab. 2 **Presence and absence of N-terminale and C-terminale cassettes in the different splice variants of the NR1 subunit and related nomenclature after Nakanishi (Nakanishi et al., 1992) and Zukin & Bennett (Durand et al., 1993).**

<i>Nakanishi</i>	<i>Zukin & Bennett</i>	cassette 1 (N-term.)	cassette 2 (C-term.)	cassette 3 (C-term)
NR1-1a	NR1 ₀₁₁	-	+	+
NR1-2a	NR1 ₀₀₁	-	-	+
NR1-3a	NR1 ₀₁₀	-	+	-
NR1-4a	NR1 ₀₀₀	-	-	-
NR1-1b	NR1 ₁₁₁	+	+	+
NR1-2b	NR1 ₁₀₁	+	-	+
NR1-3b	NR1 ₁₁₀	+	+	-
NR1-4b	NR1 ₁₀₀	+	-	-

The recently discovered subunit NR3A (formerly termed NMDAR-L or chi-1) is expressed primarily during brain development. NR3A seems to be a regulatory NMDA receptor subunit during brain development since genetic knockout of NR3A in mice results in enhanced NMDA responses and increased dendritic spines in early postnatal cerebrocortical neurons

(Das et al., 1998). Under co-expression with NR1 / NR2 subunits in *Xenopus Oocytes*, NR3A attenuates NMDA receptor currents but has no effect when tested with non-NMDA receptors or expressed alone (Sucker et al., 1995a).

1.2.2 Heteromeric channels

Native NMDA receptors are thought to consist of an association between multiple distinct subunits. Many differences in the functional properties of NMDA receptors are observed in electrophysiological and pharmacological studies with recombinant receptors depending on the used subunits to generate the glutamate gated ion channels. Although it was found that in *Xenopus laevis* oocytes expression of only one single splice variant of the NR1 subunit generates a functional ion channel regulated by glutamate and glycine (Durand et al., 1992; Moriyoshi et al., 1991) and expression of single NR2 subunits will not, in mammalian cell lines functional channels are not detected upon single NR1 expression (McIlhinney et al., 1996). For mammalian cell lines functional recombinant receptors most similar to native NMDA receptors are obtained by co-expression of both NR1 and NR2 subunits. This observation leads to the conclusion that native NMDA receptors are heterooligomeric proteins assembled using NR1 and NR2 subunits in currently unknown ratios and stoichiometries (although there seems to be some evidence for a tetrameric structure (Laube et al., 1998)). This is supported by the reported localization models of the distinct glutamate and glycine binding sites on NR2 and NR1, respectively. The major determinants for glutamate binding are localized in the N-terminal extracellular domain and the M3-M4 loop region of the NR2 subunit (Laube et al., 1997). Similar features were found for the glycine binding site localized on the NR1 subunit (Hirai et al., 1996b; Kuryatov et al., 1994; Laube et al., 1997; Wood et al., 1997).

All these results were obtained from recombinant receptor expression systems. Using immunoprecipitation and quantitative immunoblot analysis of subunits NR1 / NR2A / NR2B, it was found that the majority of NMDA receptor complexes in the adult rat cerebral cortex contains at least three different subunits (Luo et al., 1997). A smaller fraction was composed of only two subunits, NR1 / NR2B or NR1 / NR2A and no complexes were found that contained NR2A / NR2B and do not contain NR1. As well, fractions of unassembled NR2A and NR2B were detected.

1.2.3 Transmembrane topology

Alternative models of the transmembrane topology of ionotropic glutamate receptors have been proposed for NR1 (Moriyoshi et al., 1991) and AMPA / KA receptors (Hollmann et al., 1994) (Bennett and Dingledine, 1995). The currently accepted consensus model for ionotropic glutamate receptor subunits (Hirai et al., 1996b) is shown in fig. 1. It consists of a three transmembrane structure (M1 / M3 / M4) with an extracellular located N-terminal region and an intracellular C-term. The M2 domain forms an intramembrane reentry loop which contributes to the channel pore region. The M3–M4 loop has an extracellular location. For NMDA receptors, a contribution of the M3–M4 loop to the glycine binding site at NR1 and the glutamate binding site at NR2 has been reported (Laube et al., 1997).

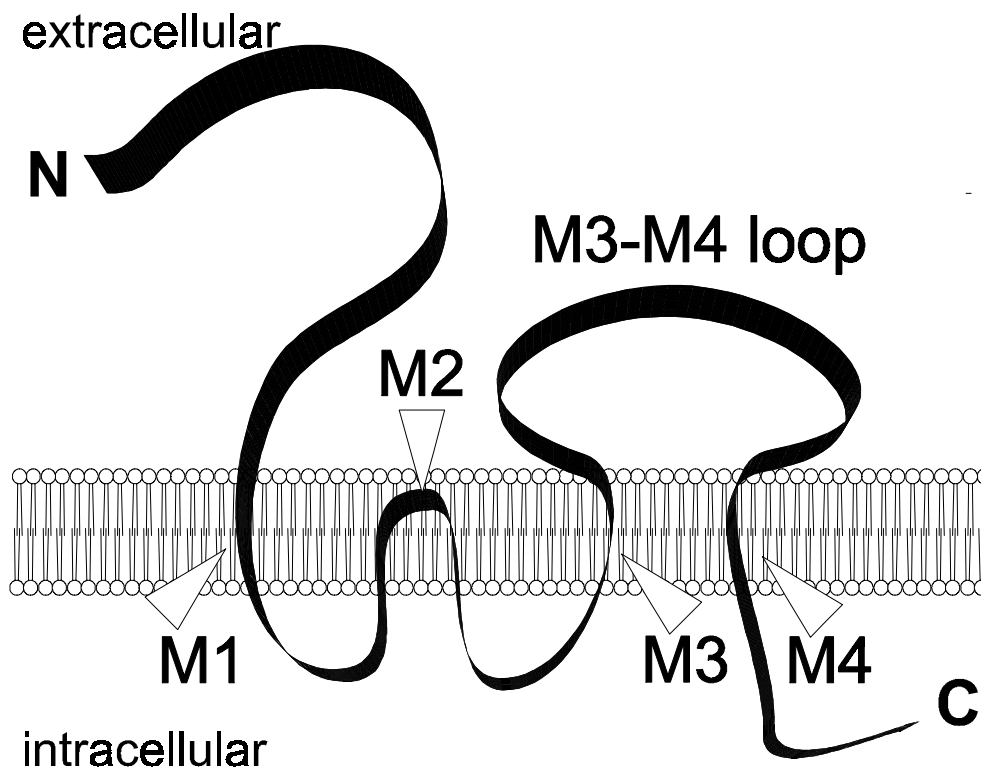


Fig. 1 Transmembrane topology of ionotropic glutamate receptors

NMDA receptors recognition sites are displayed in fig. 2. The co-agonists L-glutamate and glycine (or D-serine) bind to recognition sites on distinct subunits. The binding site for L-glutamate or the specific agonist N-methyl-D-aspartate is located on subunit NR2 whereas the binding domain of glycine or D-serine has a distinct location on subunit NR1. Under resting membrane potentials the channel is blocked by extracellular magnesium. Polyamines such as spermine or spermidine are positive modulators if the contributing NR1 splice variant

is lacking the N-terminale cassette. At higher concentration levels polyamines can either block the receptor channel. Open channels mediate influx of sodium and calcium ions as well as efflux of potassium. Synthetic compounds such as MK801, ketamine, dextromethorphan, phencyclidine and memantine block the open channel in a non-competitive manner. Channel opening is either blocked by competitive antagonists like 2-amino-5-phosphono-pentanoic acid (AP5), 4-(3-phosphonopropyl)piperazine-2-carboxylic acid (CPP) for the glutamate recognition site or by glycine site antagonists such as 5,7-dichloro-kynurenic acid (DCKA) or L-701,324. Splice variants of NR1 provide phosphorylation domains for protein kinase C (PKC). Phosphorylation on serine residues decreases receptors inhibition by calmodulin. Zn^{2+} negatively modulates receptor activity in a voltage-dependent and independent manner. In addition, receptors are influenced by redox agents and protons. More details concerning the mentioned recognition sites are given in the following sections.

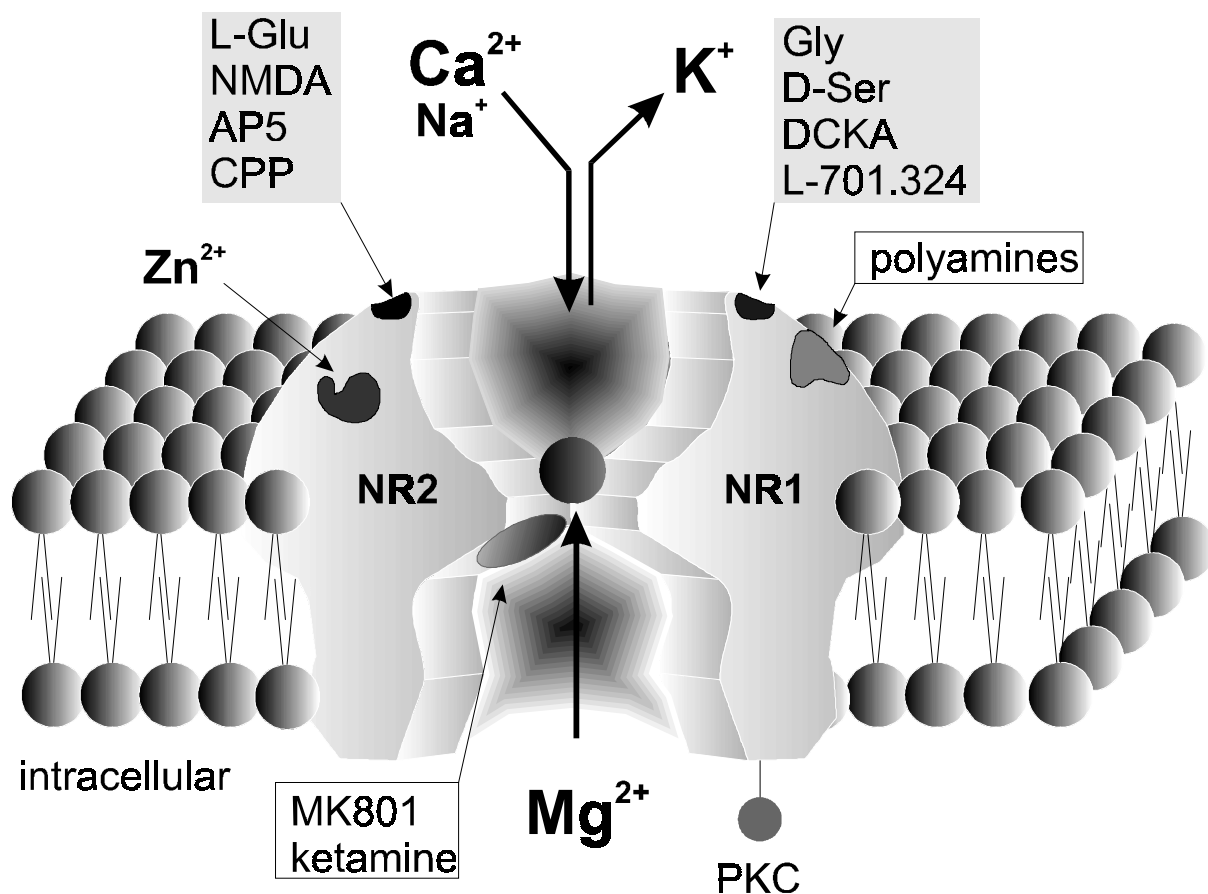


Fig. 2 Recognition sites of the NMDA receptor

1.2.4 Channel pore region

The putative channel forming region consists of the membrane domain M2 (see fig. 1). High permeability for calcium ions and sensitivity to channel block by extracellular Mg^{2+} are mediated by an asparagine residue within the M2 domain of NR1 and NR2 (Burnashev et al., 1992b). This asparagine is in a position homologous to the so called Q / R site of the AMPA / KA receptors (see section 1.1), that is occupied by either glutamine or arginine and that controls divalent cation permeability of the AMPA / KA receptors. Replacement of either glutamine or arginine with asparagine led to altered AMPA channels with a high permeability for calcium compared to magnesium (Burnashev et al., 1992a). Replacement of the respective asparagine in NR1 (N598Q) reduced calcium permeability in NR1 (N598Q) / NR2A assemblies. Substitution of the homologous asparagine in NR2A (N595Q) led to reduced magnesium block in NR1 / NR2A (N595Q) assemblies (Mori et al., 1992) (Sakurada et al., 1993). This suggests that the asparagines of both subunits form the selectivity filter of the NMDA receptor for both magnesium and calcium ions. These findings are of a special relevance since the high calcium permeability and the voltage dependent block by extracellular magnesium are thought to be important for the function of NMDA receptors in mediating long term changes in synaptic plasticity. In addition, it was found that substitution of asparagine 598 in NR1 strongly reduced the sensitivity to blockade by ketamine and phencyclidine (Yamakura et al., 1993a) whereas the sensitivity to MK801 was only slightly affected. For MK801 resistance asparagine mutations in both subunits were required. Hence, these results suggest a common recognition site for open channel blockers and magnesium within the channel forming region M2.

1.2.5 Ligand binding regions

Besides saturating concentrations of L-glutamate, maximum activation of NMDA receptor channels requires co-agonism of glycine. This effect of glycine was first observed in mouse brain neurons (Johnson and Ascher, 1987). D-alanine and especially D-serine were found to mimic the effects of glycine (Kleckner and Dingledine, 1988). Site-directed mutagenesis of the NR1 subunit revealed that aromatic residues at positions 390, 392, and 466 localized in a domain preceding the M1 membrane segment are crucial determinants of glycine binding. Glutamate efficacy was little affected by mutations at these positions (Kuryatov et al., 1994). Mutations to aspartate 481 and lysine 483 produced receptors with up to 160-fold lower affinities for glycine, as well as other agonists and partial agonists, without affecting

maximum current size or the degree of agonist efficacy (Wafford et al., 1995). Contribution of the M3–M4 loop to the glycine recognition site was shown by substitution of the phenylalanine residues at positions 735 and 736. Mutation of both residues caused a >100-fold decrease in glycine affinity (Hirai et al., 1996a). Interestingly the mutated residues in both domains (M1 preceding domain and M3–M4 loop) correspond to positions forming the binding site of homologous bacterial amino acid-binding proteins, in particular the glutamine-binding protein from *E. coli* and LAOBP (leucine alanine ornithine binding protein). These findings have suggested a phylogenetically conserved amino acid-binding fold.

It should be noted that NR2 subunits contribute to the affinity of glycine. Homomeric NR1 receptors exhibit K_i values for glycine from 1 to 5 μ M whereas heteromeric receptors display K_i values in the nanomolar range (Grimwood et al., 1995).

The location of the glutamate binding site on the NR2B subunit has recently been demonstrated (Laube et al., 1997). The glutamate site is located in homologous regions compared to the glycine site on NR1. Mutation of residues within the N-terminal domain and the loop region between membrane segments M3 and M4 significantly reduced the efficacy of glutamate in channel gating.

Homology-based molecular modelling of the glutamate and glycine binding domains are indicating that the NR2B and NR1 subunits use similar residues to ligate the agonist's α -aminocarboxylic acid groups, whereas differences in side chain interactions and size of aromatic residues determine ligand selectivity. In the model of the NR1 subunit ligated to glycine, the carboxyl group of glycine interacts with arginine 505 and threonine 500, whereas the amino group is hydrogen bonded to glutamine 387 and the backbone carbonyl group of proline 498. These binding residues are very similar to those of L-glutamate in NR2B, where the α -carboxyl group interacts with arginine 493 and threonine 488 and the amino group of L-glutamate is hydrogen bonded to glutamate 387 and the backbone carbonyl group of serine 486. The γ -carboxyl group of L-glutamate forms a salt bridge with arginine 493 and can interact with lysine 463 and arginine 667.

1.2.6 Phosphorylation domain

In neurons and transfected Hek 293 cells, phosphorylation domains have been detected on the C-terminal domain of NR1 (Tingley et al., 1993). PKC phosphorylation occurred on several distinct sites on the NR1 subunit. Splice variants differed in the extent to which they could be potentiated by activators of protein kinase C (PKC) from 3- to 20-fold. Presence of the N-terminal insert and absence of the C-terminal sequences increased potentiation by PKC

(Durand et al., 1993). These results demonstrate that alternative splicing of the NR1 messenger RNA regulates its phosphorylation by PKC, and that mRNA splicing is a mechanism for regulating the sensitivity of glutamate receptors to protein phosphorylation. Using the yeast two-hybrid system, it was found that calmodulin interacts with the C-terminus of the NR1 subunit and inactivates the channels in a calcium-dependent manner. Protein kinase C (PKC)-mediated phosphorylation on serine residues of NR1 decreases its affinity for calmodulin (Hisatsune et al., 1997). This suggests that PKC-mediated phosphorylation of NR1 prevents calmodulin from binding to the NR1 subunit and thereby inhibits the inactivation of NMDA receptors by calmodulin.

However, it has been reported that the NR1 subunit is not responsible for the potentiation by PKC activator 12-O-tetradecanoylphorbol 13-acetate (TPA) treatment in *Xenopus* oocytes (Yamakura et al., 1993b). Treatment with TPA potentiated the response to GluR ζ 1 / GluR ϵ 1 and GluR ζ 1 / GluR ϵ 2, but not in GluR ζ 1 / GluR ϵ 3 and GluR ζ 1 / GluR ϵ 4 assemblies (Kutsuwada et al., 1992; Mori et al., 1993). Functional analysis of chimeric receptors demonstrated that the C-terminal region of GluR ϵ 2 is responsible for the potentiation of GluR ζ 1 / GluR ϵ 2 receptors by treatment with TPA.

Additionally, protein-tyrosine kinases (PTKs) and protein-tyrosine phosphatases (PTPs) are highly expressed in the central nervous system. They represent key enzymes in signal-transduction. They are involved in the regulation of neurotransmitter receptors. Some evidence was found that in the CNS tyrosine phosphorylation regulates the function of NMDA receptors (Wang and Salter, 1994).

1.2.7 Allosteric modulation regions

NMDA receptor channel activity is influenced by various allosteric modulators. Modulating effects of protons, polyamines, histamine, redox agents, Zn²⁺ and Mg²⁺ ions are described in the next sections.

1.2.7.1 Proton inhibition

Sensitivity of NMDA receptors in cerebellar neurons to protons has been described (Traynelis and Cull-Candy, 1990). NMDA receptor responses was selectively inhibited by protons, with a 50% inhibitory concentration of pH 7.3 that was close to physiological pH 7.4, implying that NMDA receptors are not fully active under normal conditions. (S)-AMPA and kainate responses remained unchanged at similar pH levels. Proton inhibition was voltage-insensitive and did not result either from fast channel block, a change in channel conductance, or an increase in the 50% excitatory concentration (EC₅₀) of aspartate/NMDA or glycine. Instead,

protons seemed to decrease markedly the opening frequency of NMDA channels. Studies with recombinant receptors revealed that the proton sensitivity of NMDA receptors depends on the contributing splice variants of NR1 (Traynelis et al., 1995). Splice variants lacking the N-terminal cassette (exon 5) such as NR1-1a are much more sensitive to proton inhibition (IC_{50} pH 7.3) compared to those containing exon 5 (IC_{50} pH 6.8).

1.2.7.2 Modulation by polyamines

Polyamines such as spermine, spermidine and putrescine are endogenous compounds in the CNS, although their function in the brain is largely unknown. These compounds modulate NMDA receptor activity by at least three distinct mechanisms, maybe occurring at distinct recognition sites. (i) Under subsaturating concentrations of glycine, polyamines are increasing receptor's affinity for the co-agonist (glycine-dependent stimulation). (ii) Under saturating glycine concentrations they potentiate receptor's response (glycine-independent stimulation). In *Xenopus oocytes* glycine-independent stimulation is seen at homomeric receptors with NR1 splice variants lacking the exon 5, such as NR1-1a and at heteromeric receptors containing NR1-1a and NR2B but not at NR2A, NR2C and NR2D (Williams et al., 1994). Because the potentiation occurs at homomeric NR1-1a receptors as well as in heteromeric NR1-1a / NR2B receptors the polyamine binding site for this kind of modulation may be located at NR1 subunit. Using amino acid sequence identity analysis, the NR1 subunit was compared to known sequences of bacterial polyamine binding proteins (PotD and ESAT) (Kashiwagi et al., 1996b). Aspartate residue 669 located in the extracellular M3-M4 loop of NR1-1a was found to control sensitivity to spermine and to protons. In the N-terminal region, residues glutamate 342 and 339 of NR1-1a have been implicated in the control of polyamine stimulation (Williams et al., 1995). Glutamate 201, located in the N-terminal region of NR2B, was found to contribute to the glycine-independent stimulation (Gallagher et al., 1997). Meanwhile, it was suggested that the glycine-independent stimulation by polyamines at heteromeric NR1-1a / NR2B receptors is caused by the relief of proton inhibition through shielding receptor's proton sensor (Traynelis et al., 1995). (iii) At higher concentrations (200-300 μ M) polyamines block NMDA receptors in a voltage dependent manner and reduce the receptor affinity for L-glutamate (Rock and MacDonald, 1992; Williams et al., 1995). These different effects of polyamines may involve at least three distinct polyamine recognition sites at the receptor.

1.2.7.3 Modulation by histamine

Histamine is a neuromodulator in the brain, and the hippocampus is one of the brain regions that is innervated by histaminergic neurons. It has been reported that glutamate enhances histamine release through NMDA receptors located at histaminergic nerve terminals (Okakura et al., 1992). When applied to cultured hippocampal neurons, histamine selectively increased the amplitude of the component of synaptic transmission that was mediated by NMDA receptors (Bekkers, 1993). In a subpopulation of rat cortical neurones, histamine potentiated NMDA-induced ion currents by slowing the kinetics of onset of desensitization (Zwart et al., 1996). These results suggest that histamine may modulate processes involving NMDA receptors, such as the induction of long-term potentiation. In voltage-clamp records of recombinant NMDA receptors expressed in *Xenopus Oocytes*, histamine potentiated responses to NMDA ($EC_{50} = 10 \mu\text{M}$) at heteromeric NR1 / NR2 receptors containing splice variants of the NR1 subunit that lack the amino-terminal insert (exon 5), together with the NR2B subunit but not the NR2A or NR2C subunit. This effect of histamine was not blocked by classical histamine receptor antagonists (Williams, 1994b).

1.2.7.4 Redox modulation

Disulfide-reducing agents such as dithiothreitol (DTT) or endogenous glutathion (GSH) potentiate NMDA receptor evoked currents in cultured neurons (Aizenmann et al., 1989). In contrast thiol oxidizing agents such as 5,5'-dithiobis-2-nitrobenzoic acid (DNTB) inhibit NMDA-evoked currents, but not completely. Interestingly, potentiation of NMDA-mediated currents is not modified by N-ethyl-maleimide (NEM) which irreversibly alkylates cysteine residues (Tang and Aizenman, 1993). Studies with recombinant receptors expressed in *Xenopus oocytes* showed that homomeric assemblies consisting of subunit NR1 are not significantly redox modulated (Omerovic et al., 1995). In contrast, heteromeric receptors are modulated by sulfhydryl redox agents (Sullivan et al., 1994). Unexpectedly, two cysteines (cysteine 744 and 798) in the NR1 subunit were identified to be required for redox modulation of NMDA induced currents in oocytes expressing NR1 / NR2B, NR1 / NR2C or NR1 / NR2D receptors. Mutation of these two cysteines also eliminated potentiation by spermine and shifted the IC_{50} for proton inhibition and the EC_{50} for NMDA.

Redox modulation of heteromeric NR1 / NR2A receptors appeared to be different from that of the other heteromeric receptors. NR1 / NR2A channels exhibit a reversible component of potentiation in addition to the persistent one found with all other heteromeric assemblies (Kohr et al., 1994). In heteromeric expressed NR1 / NR2A channels in *Hek 293* cells DTT rapidly potentiated L-glutamate-activated whole-cell currents. A part of the current

potentiation disappeared upon washout (reversible component). The remaining potentiation (persistent component) was abolished by an oxidizing agent (DNTB). In cells expressing the NR1 / NR2B, NR2C, or NR2D channels DTT elicited only a slowly developing, persistent potentiation and increased the deactivation time course. In these, but not in NR1 / NR2A, the DTT effect was rendered insensitive to reoxidation by alkylation. Reduced glutathione mimicked the DTT effects only in the NR1 / NR2A receptor. Hence, distinct NMDA receptor assemblies differ profoundly in their responses to sulfhydryl redox agents. As the reversible component of redox potentiation only occurs at NR1 / NR2A receptors and the used reducing agents have also chelating abilities, the relief of tonic zinc inhibition of NR1 / NR2A was proposed as mechanism for this reversible kind of potentiation by reducing agents.

1.2.7.5 Inhibition by zinc

Zinc has been shown to be present in synaptic vesicles in a number of glutamatergic vesicles and is co-released with L-glutamate during presynaptic neurotransmitter release (Xie and Smart, 1991). In addition, zinc ions have been proposed to allosterically modulate native NMDA receptors. Zinc inhibits NMDA receptors at two independent sites (Christine and Choi, 1990; Legendre and Westbrook, 1990). A low affinity zinc site is located inside the channel pore and binding of zinc to this site causes a voltage-dependent open channel block, similar to the one exerted by magnesium. A high-affinity site is located outside the channel on extracellular domains and causes voltage-independent inhibition of NMDA receptors. These two effects were initially described for zinc concentrations in the micromolar range and this fits well to the estimated zinc concentrations in the synaptic cleft following glutamate release. Using recombinant receptors expressed in *Xenopus oocytes* and *Hek 293* cells, the subunit specificity of these two effects was examined (Paoletti et al., 1997). The comparison of NR1-1a / NR2A and NR1-1a / NR2B receptors shows that the voltage-dependent inhibition is similar in both types of receptors but that the voltage-independent inhibition occurs at much lower zinc concentrations in NR1-1a / NR2A receptors (IC_{50} in the nanomolar range) than in NR1-1a / NR2B receptors (IC_{50} in the micromolar range). The high affinity of the effect observed with NR1-1a / NR2A receptors was attributed mostly to the slow dissociation of zinc from its binding site. By analyzing the effects of zinc on varied combinations of NR1 (NR1-1a or NR1b) and NR2 (NR2A, NR2B) it was shown that both subunit families contribute to the voltage-independent zinc inhibition (NR1-1a>NR1-1b and NR2A>NR2B). Further it was observed that the addition of low concentrations of heavy metal chelators (EDTA or tricine) markedly potentiates the responses of NR1-1a / NR2A receptors, but not of

NR1-1a / NR2B receptors. This result suggests that traces of a heavy metal (probably zinc) contaminate standard solutions and tonically inhibit NR1-1a / NR2A receptors. Chelation of zinc even could account for the reversible component of redox potentiation produced by reducing compounds like DTT or glutathione (Paoletti et al., 1997).

Recently, it has been reported that tyrosine kinase Src potentiates NMDA receptor currents by reducing the tonic zinc inhibition (Zheng et al., 1998). Src only acted on receptors assembled from NR2A subunits and a restricted group of NR1 splice variants (Kohr and Seeburg, 1996). In addition, zinc is known to be cytotoxic due to entry into the cell. Cell death in neurons induced by exposure to zinc is increased by glutamate and can be reduced by NMDA receptor antagonists (Koh and Choi, 1994). This suggests that zinc entries into neurons via NMDA receptors, which appear to be both blocked by and permeable to zinc.

1.2.7.6 Effects of magnesium

Extracellular Mg^{2+} , which blocks NMDA channels in a voltage-dependent manner and increases the receptors affinity for glycine, has been shown to potentiate NMDA responses at saturating glycine concentrations. This potentiation, induced by millimolar concentrations ($EC_{50} = 3mM$) of Mg^{2+} , is not mimicked by Ca^{2+} and Ba^{2+} and is voltage independent. The potentiation is variable in native receptors of cultured mouse central neurons; in recombinant receptors, this potentiation is only seen in receptors containing the NR2B subunit and prevented by NR1 splice variants containing the N-terminal insert. Mg^{2+} also induces a shift of the pH sensitivity of NMDA receptors. These effects of Mg^{2+} are quite similar to those of spermine and suggest that Mg^{2+} may be the physiological agonist acting at the subunit-specific spermine site (Paoletti et al., 1995).

1.3 Distribution within the CNS

Distribution of the NMDA receptor channel subunit mRNAs in the adult rodent brain was examined by in situ hybridisation analysis (Akazawa et al., 1994; Ishii et al., 1993; Kutsuwada et al., 1992; Monyer et al., 1992; Moriyoshi et al., 1991; Watanabe et al., 1992; Watanabe et al., 1993; Watanabe et al., 1994a; Watanabe et al., 1994b; Watanabe et al., 1994c; Watanabe et al., 1994d; Watanabe et al., 1994e). In adult rodents NR1 subunit mRNA is distributed throughout the brain (fig. 3A) consistent with its role as the key-subunit of NMDA receptors. NR1 subunits containing cassette 1 (exon 5) are found in most brain regions with higher levels in the thalamus, midbrain, cortex, CA3 hippocampus and cerebellum. Although, it should be mentioned that the most common NR1 transcripts have a deletion of cassette 1. Cassette 2 shows high expression levels in the striatum, septum,

cerebral cortex, hippocampus and cerebellar granule cells. The expression of NR1 transcripts containing cassette 3 is very similar to the cassette 2 distribution with high concentrations found throughout the cerebral cortex, hippocampus, cerebellum, striatum and septum.

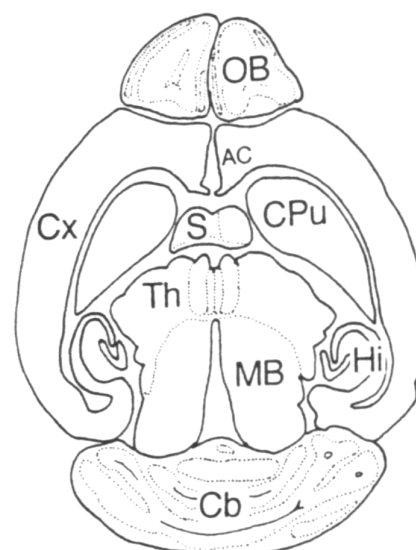
The NR2A ($\epsilon 1$) subunit is distributed widely in the brain (fig. 3B) with higher expression levels in the cerebral cortex, the hippocampus region and cerebellum, especially in cerebellar granula cells. In contrast, the NR2B ($\epsilon 2$) subunit is only expressed in the forebrain with higher expression levels in the cerebral cortex, hippocampus region, the septum, caudate–putamen, the olfactory bulb and the thalamus (fig. 3C). The NR2C ($\epsilon 3$) subunit mRNA is found predominantly in the cerebellum (fig. 3D). Higher levels of NR2D ($\epsilon 4$) expression are appearing in early developmental, peri– and neonatal stages. In the adult brain lower levels of mRNA are found in the thalamus, brainstem and the olfactory bulb (fig. 3E).



Fig. 3 Horizontal sections of the adult mouse brain with distinct NMDA receptor subunit expressing regions (for details see text above).

(A) oligonucleotide probes, that recognizes all NR1 splice variants. (B)–(E) oligonucleotide probing specific for NR2A (B), NR2B (C), NR2C (D) and NR2D (E).

Abbreviations: AC, anterior cingulate cortex; Cb, cerebellum; CPu, caudate–putamen; Cx, cortex; Hi, hippocampus; MB, midbrain; OB, olfactory bulb; S, septum; Th, thalamus (taken from Watanabe et al., 1993).



It should be added, that expression of NMDA receptors is not absolutely restricted to the brain. NMDA receptor subtypes NR1 and NR2D were briefly detected in rat and human osteoblasts and osteoclasts, suggesting that glutamate is also involved in the signalling pathway between bone cells and may be an important local regulator of bone cell functions.

(Patton et al., 1998) (Chenu et al., 1998). NMDA (and non-NMDA) receptors have been identified in pancreatic islets (Inagaki et al., 1995) modulating insulin secretion and in unmyelinated axons in the skin (Carlton et al., 1995) suggesting that peripheral glutamate receptors are involved in the mediation of pain.

1.4 Pharmacological diversity of native and recombinant NMDA receptors

The NR1 and NR2 subunits represent the molecular basis for the pharmacological heterogeneity of native NMDA receptors. It is thus significant that some of the pharmacological properties (provided by radioligand binding studies), that distinguish subtypes of native receptors, correlate to the presence of identified NMDA receptor subunits. It seems, that the presence of NR2C subunits contributes to the distinct pharmacological properties of cerebellar NMDA receptor subtypes. For example, NMDA receptor agonists quinolinate and homoquinolinate as well as competitive antagonists bind with a lower affinity in the cerebellum than in the forebrain (Beaton et al., 1992; Yoneda and Ogita, 1991). It was found that, relative to NR1 / NR2A and NR1 / NR2B receptors, oocyte-expressed NR1 / NR2C receptors had a lower affinity for both D-CPP-ene (D-3-(2-carboxypiperazin-4-yl)-1-propenyl-1-phosphonic acid) and homoquinolinate (Buller et al., 1994). Allosteric modulation sites of NMDA receptors in the cerebellum differ also from those in the forebrain region. The binding of [³H]-MK801 to NMDA receptors in the cerebellum appears to be less sensitive to polyamine modulation (Reynolds and Palmer, 1991). This finding is consistent with a higher amount of NR1 splice variants containing the 5'-insert expressed in the cerebellum.

Forebrain NMDA receptors can be subdivided in quantitative autoradiographic studies by their relative affinity for agonists and antagonists. In the lateral thalamus, NMDA receptors exhibit a higher affinity for antagonists than do NMDA receptors in the medial striatum with unchanged rank order. Vice versa, receptors in the medial striatum have higher affinities for agonists than do receptors from the lateral thalamus. Therefore, these populations have been described as “antagonist“- and “agonist“-preferring receptor populations. The distribution of NR2A mRNA is very similar to that of antagonist preferring receptors determined by [³H]-CPP autoradiographic studies (Buller et al., 1994), whereas NR2 subunit mRNA expressed in the medial striatum is predominantly NR2B. Again studies of NMDA receptor subunits expressed in *Xenopus oocytes* revealed the higher affinity of NR1 / NR2B assemblies for

agonists compared to antagonist preferring NR1 / NR2A receptor channels (Kutsuwada et al., 1992). The reported EC_{50} values of the different NMDA receptor channels are given tab. 3:

Tab. 3 **Reported diversity of agonists efficacy at distinct NMDA receptor channels**
EC₅₀ values are effector concentrations for half-maximum response in electrophysiological records at transfected Xenopus Oocytes (taken from Kutsuwada et al., 1992).

heteromeric channels	Affinity for agonists EC_{50} [μ M]	
	L-glutamate	glycine
NR1- ζ 1 / NR2A- ϵ 1	1.7	2.1
NR1- ζ 1 / NR2B- ϵ 2	0.8	0.3
NR1- ζ 1 / NR2C- ϵ 3	0.7	0.2
NR1- ζ 1 / NR2D- ϵ 4	0.4	0.1

It should be emphasized, that beside these distinct native receptor populations, the majority of NMDA receptors e.g. in the cortex consist of three different subunits (NR1, NR2A, NR2B) (Luo et al., 1997) exhibiting pharmacological properties that are between those of NR1 / NR2A and NR1 / NR2B assemblies.

Regarding recombinant receptors other pharmacological diversities are apparent. Some functional diversities between recombinant NMDA receptor channels have already been discussed in other sections, such as glycine-independent potentiation by polyamines of NR1-1a / NR2B receptors (see 1.2.7.2), reversible component of redox modulation of NR1 / NR2A channels (see 1.2.7.4) and high affinity voltage-independent zinc inhibition of NR1 / NR2A receptors (see 1.2.7.5). Concerning the voltage-dependent block by magnesium, NR1 / NR2A and 2B channels are more sensitive compared to NR1 / NR2C and 2D receptors. Open channel blocker MK801 has even a higher affinity to NR1 / NR2A and 2B, whereas ketamine and phenylcyclidine exhibit only slight variations in receptor affinity. Expression of heteromeric NR1 / NR2 receptors in *Hek 293* cells led to cell death depending on the subunit composition (Chazot et al., 1994). Co-expression of NR1-1a / NR2A resulted in 100 % cell death of transfected cells whereas transfection of NR1-1a / NR2C subunits apparently did not result in significant cell death. In contrast co-transfection of all three subunits again resulted in cell death. The rate of dying cells depended on the transfected ratio of subunits. Increasing the proportion of NR2C to NR2A cDNA led to decreasing cell death rates.

Introduction

These results may be explained by the decreased calcium permeability of NR1 / NR2C channels. However it has been reported that these two receptors have similar calcium permeability (Monyer et al., 1994), but higher conductance states of NR1 / NR2A (and 2B) receptors (Stern et al., 1992) may account for the higher cell death rate.

As mentioned in section 1.2.6, treatment with the PKC activator TPA potentiated the response of NR1 / 2A and 2B receptors expressed in *Xenopus oocytes* but did not alter response of NR1 / NR2C and 2D channels (Kutsuwada et al., 1992; Mori et al., 1993).

Compounds such as ifenprodil and haloperidol were identified to selectively inhibit NMDA receptors containing the NR2B subunit (Chenard and Menniti, 1999). These compounds exhibit a selectivity by inhibition of NMDA receptor responses in forebrain neurons compared to neurons from cerebellum. More recent compounds such as CP-101,606 or Ro 25,6981 have similar abilities. Some findings, e.g. the displacement of high affinity [³H]-ifenprodil binding by spermine and spermidine (Carter et al., 1989; Carter et al., 1990), indicate an interaction with the binding site involved in glycine-independent polyamine stimulation.

Recently, glycine site antagonist CGP 61594 was shown to have some selectivity for the NR2B subtype (Honer et al., 1998).

1.5 Physiological and pathophysiological implications

1.5.1 Glutamatergic neurotransmission

In brain, L-glutamate is synthesized in the nerve terminals from two sources: from glucose via the Krebs cycle and transamination of α -ketoglutarate and from glutamine that is synthesized in glial cells, transported into nerve terminals and locally converted by glutaminase into L-glutamate. In the glutamate containing nerve terminals, glutamate is stored in synaptic vesicles. Upon depolarization of the nerve terminal, it is released by a calcium-dependent exocytotic process. At the post synaptic membrane, L-glutamate interacts with its distinct receptors. Activation of fast depolarizing AMPA receptors causes the loss of the voltage-dependent magnesium block within the NMDA receptor channel pore and together with its co-agonist glycine (or D-serine), L-glutamate evokes strong calcium and sodium inward currents. Besides the binding to ionotropic receptors, L-glutamate can activate metabotropic glutamate receptors coupled either to PLC or to adenylate cyclase. The action of synaptic glutamate is terminated by a high affinity uptake process via plasma membrane glutamate transporters on presynaptic nerve terminals or on glial cells. The glutamate, taken up into glial cells, is then converted by glutaminase into L-glutamine and transported into the neighboring nerve terminals, where it serves as precursor for L-glutamate. In astrocytes, glutamine can also be oxidized into α -ketoglutarate which is in turn actively transported into the neuron to replace the α -ketoglutarate lost during the synthesis of neuronal L-glutamate.

1.5.2 Long term potentiation

The term “long-term potentiation“ (LTP) refers to a long lasting enhancement of synaptic transmission (10 minutes to days depending on testing conditions) after a high-frequency, high-intensity period of afferent pathway activation. The effect is measured as increased amplitudes of excitatory postsynaptic potentials (EPPs). The transductive mechanism of electrophysiological changes at the synaptic level has become a candidate to link learning and cellular changes in vivo. This special form of enhanced synaptic transmission is exerted by glutamatergic pathways and takes place in the hippocampal formation known to be involved in functions like memory and learning. The possible involvement of NMDA receptors into learning process raised following the finding of Collingridge et al., that NMDA receptor activation is a critical step in the induction of hippocampal LTP (Collingridge et al., 1983). It was assumed, that synaptic alterations mediated by NMDA receptors are underlying memory.

Competitive antagonists like AP5 or open channel blocker MK801 offer now the pharmacological tools to block this kind of synaptic plasticity and investigate effects upon learning and memory. Besides this, there are possible interactions or synergisms between NMDA receptors and mGluRs in the induction of LTP. Calcium influx via NMDA receptors causes activation of kinases and facilitates the activation of mGluRs. Stimulation of PLC coupled mGluRs results in the generation of diacylglycerol and inositol-1,4,5-triphosphate (IP₃) which in turn is involved in the activation of kinases and the release of calcium from intracellular stores (endoplasmic reticulum). Additionally, activation of mGluRs facilitates the activation of the NMDA receptor system.

1.5.3 Clinical implications

Several therapeutic applications have been proposed for drugs modulating excitatory amino acid systems. In the next sections the most important proposed targets will be described.

1.5.3.1 Epilepsy

A very early observation related to the application of excitatory amino acids to the brain was their ability to evoke convulsions and epileptic seizures (Hayashi, 1954). Therefore, some forms of clinical epilepsy may be related to an excessive sensitivity of NMDA receptor mediated responses.

NMDA receptor antagonists show anticonvulsive activity in a number of seizure models. In kindled rats, representing a model for complex partial seizures, non-competitive and competitive NMDA receptor antagonists have only a weak efficacy at doses producing significant motor side effects (Löscher, 1993). This was later confirmed in clinical trials with the competitive L-glutamate antagonist D-CPP-ene (SDZ EAA-494) being poor anticonvulsant in epileptic patients with complex seizures in doses causing side effects like impaired concentration, sedation, depression, ataxia and amnesia (Sveinbjornsdottir et al., 1993). These results suggest that these compounds will not be clinically useful antiepileptics against partial and secondarily generalized seizures.

In contrast, systemically active glycine site antagonists like L-701,324 have been reported to prevent audiogenic seizure in DBA/2 mice (Carling et al., 1997; Kulagowski et al., 1994). A series of tricyclic pyrido-phtalazine-diones inhibited pentylenetetrazol-, NMDA- and maximum electroshock-induced convulsions in mice (Parsons et al., 1997a). Besides their higher efficacy, glycine site antagonists seem to provide a more acceptable side effect profile since they induce less behavioural effects like motor incoordination and ataxia and failed to

induce psychotomimetic and neuropathological changes like PCP or MK801 (Leeson and Iversen, 1994).

1.5.3.2 Schizophrenia

Compounds such as phenylcyclidine, ketamine and MK801 as well as competitive antagonists evoke psychotomimetic activity in patients. Hence, a glutamatergic hypothesis of schizophrenia has been developed, suggesting hypofunction of some glutamatergic systems in certain brain regions which may be responsible for the expression of symptoms (Javitt and Zukin, 1991). This hypothesis is supported by the finding that the glutamate release from synaptosomes of schizophrenia patients is decreased (Sherman et al., 1991). Application of NMDA receptors glycine site partial agonists like D-cycloserine improved some of the schizophrenic symptoms in animals and patients (Toth and Lajtha, 1986; Waziri, 1988). Additionally, it has been demonstrated that glycine site antagonists block the activation of the mesolimbic dopamine systems induced following amphetamine administration in the rat (Bristow et al., 1995).

1.5.3.3 Anxiety

Results from anxiety animal models indicate that competitive NMDA receptor antagonists show anxiolytic response, but are different in many respects from benzodiazepines (Liebmann and Bennett, 1988). Additionally, antagonists acting as non competitive open channel blocker or glycine site antagonists exhibit potential anxiolytic activity (Kehne et al., 1995; Kehne et al., 1991). For glycine site antagonists inconsistent results have been reported. Although anxiolytic activity has been demonstrated for compounds like DCKA (Kehne et al., 1991), D-cycloserine or (R)-HA-966 (Anthony and Nevins, 1993) other high affinity glycine site antagonists like L-701,324 and MRZ 2/576 failed to be effective (Karcz-Kubicha et al., 1997). Since observed the anxiolytic efficacy of glycine antagonists was far weaker than that of benzodiazepines, it seems that glycine antagonists currently are not considered to be new powerful tools in anxiolytic therapy.

1.5.3.4 Acute neurodegenerative diseases

Ischemic damage to the central nervous system by **stroke** or **trauma** is a very prominent target in excitatory amino acid research. Glutamate or similar agonists induce neuronal cell death by excessive activation of NMDA receptors. This term called **excitotoxicity** is involved in many types of acute neurodegenerative disorders (for chronic neurodegenerative diseases see 1.5.3.5). Brain microdialysis studies indicate that the concentrations of extracellular L-glutamate rises rapidly upon the induction of ischemic situations or traumatic brain injuries

(Andine et al., 1991; Lees, 1993; Meldrum and Garthwaite, 1990). The concentration of co-agonist glycine is also increased (Globus et al., 1988). Energy deficits seem to be involved in excitotoxic effects of glutamate as they cause high intracellular sodium concentrations leading to a reversal of sodium dependent glutamate uptake and in consequence to a presynaptic non-vesicular release of glutamate (see fig. 4).

Depolarisation of the postsynaptic membrane (e.g. via fast depolarizing AMPA receptors) and subsequent massive calcium influx via NMDA receptors results in the activation of different calcium dependent enzymes such as NO-synthase, phospholipase A₂, protein kinase C, ornithine-decarboxylase, proteases and endonucleases. Some resulting metabolites such as polyamines or arachidonic acid may in turn trigger the activation of NMDA receptors. Damage of calcium buffering mitochondria causes the release of apoptosis inducing factors like AIF or cytochrome C activating the apoptotic cascade or radicals from the respiratory chain leading to plasma membrane damage and necrosis.

Numerous preclinical studies indicate the efficacy of glutamate antagonists in various animal models of acute ischemic damage (Bordi et al., 1997; Bullock et al., 1990; Warner et al., 1995).

1.5.3.5 Chronic neurodegenerative diseases

Excitotoxicity mediated by L-glutamate may even be involved in chronic neurodegenerative disorders. It has been proposed that the neurodegeneration of the substantia nigra dopaminergic pathways in **Parkinson's disease** depend to some extent to glutamate evoked excitotoxicity. NMDA receptor antagonists prevent substantia nigra neurons from undergoing cell death due to application of MPP⁺ (Camins et al., 1997; Turski et al., 1991), a dopaminergic neurotoxin (inhibitor of complex I of the respiratory chain) used in animal models to induce Parkinson's disease. In fact, the NMDA channel blockers amantadine and memantine have been used for the symptomatological treatment of Parkinson's disease.

Related to Parkinson's disease are disorders like **amyotrophic lateral sclerosis (ALS)** and **Alzheimer type dementia** with respect to loss of neurons in discrete brain areas such as neurones in cortex and motoneurons in the spinal cord or cholinergic neurons of the basal forebrain, respectively. Some evidence for an involvement of the glutamatergic pathway in Alzheimer's disease was given by the loss of NMDA binding sites in the cortex and hippocampus of post mortem brains (Greenamyre, 1986). The treatment of the resulting cognitive deficits with glycine site agonists like D-cycloserine was proposed. But this is probably not a valid approach since the positive effects of D-cycloserine disappeared after repetitive administration (Randolph et al., 1994). Recently, it was found that a β -amyloid

fragment (25-35) inhibited [³H]-glycine binding and stimulated [³H]-MK801 binding but only when glycine concentrations were low (Cowburn et al., 1997). This suggests an enhancement of NMDA receptor function mediated by glycine recognition site agonism. Therefore, a neuroprotective potential of glycine antagonists is likely.

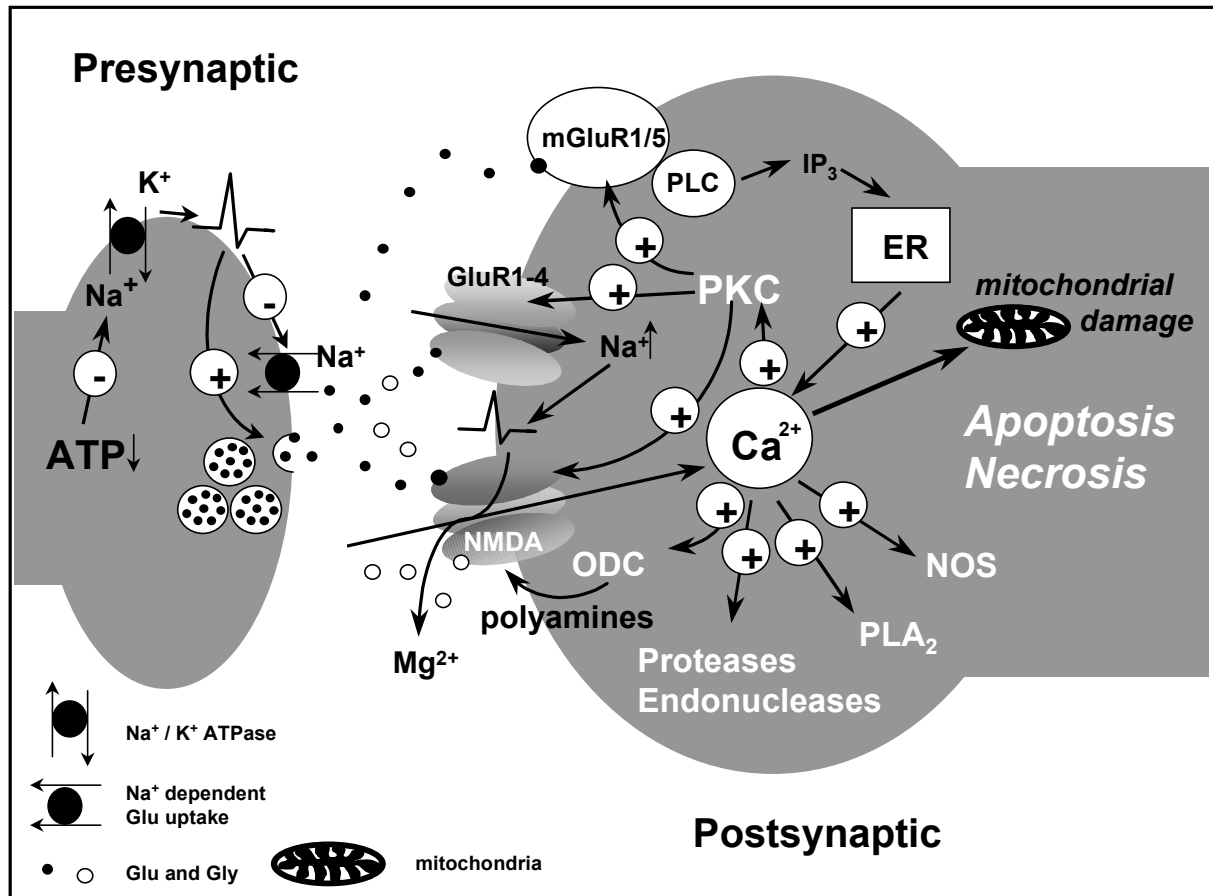


Fig. 4 Simplified scheme of processes involved in glutamate mediated excitotoxicity

There is also an excitotoxic hypothesis for the pathogenesis of ALS. It was first proposed on the basis of data that showed changes in glutamate levels in plasma, cerebrospinal fluid and post mortem brain tissue (Allaoua et al., 1992). Further more, an impaired glutamate uptake in vesicular preparations from post mortem spinal cord and motor cortex of ALS patients was shown (Rothstein et al., 1992). Additionally, the vesicular transmitter release inhibiting compound riluzole (sodium channel blocker) has been shown to be neuroprotective and to slightly extent survival in ALS.

The acquired immunodeficiency syndrome is often accompanied by neurological symptoms including dementia (**AIDS dementia**). It was suggested that the gp 120 coat protein of HIV-1 might indirectly stimulate NMDA receptors causing L-glutamate induced cell death (Toggas

et al., 1996; Wu et al., 1996). These findings suggest that clinically tolerated NMDA receptor antagonists may be useful in the prevention of neuronal damage in HIV-1-infected patients. **Huntington's disease** is a dominantly inherited, progressive neurodegenerative disorder caused by selective neuronal death in the basal ganglia. The pathophysiology is as yet unknown, but evidence suggests that the neurotoxicity may result from endogenous substances acting at excitatory amino acid receptors (DiFiglia, 1990).

The low non-competitive NMDA receptor antagonist remacemide and its metabolite remacemide des-glycine (FPL 12495) block also voltage dependent calcium channels (VSCCs). Remacemide has been used in clinical trials to improve Huntington's disease (Kieburtz et al., 1996). As glycine levels in Huntington's disease patients have been reported to be increased (Reilmann et al., 1997), glycine site antagonists may have some therapeutical benefit.

1.5.3.6 Chronic pain

The involvement of glutamatergic pathways and NMDA receptors in the development of chronic pain is now well established. Besides the increased sensitivity of primary afferent nociceptors, hyperalgesia depends on NMDA receptor mediated central changes in synaptic excitability. Ketamine, which is a widely used dissociative anaesthetic, offers good analgesic properties (Klepstad et al., 1990). Since there is evidence for the presence of NMDA (and non-NMDA) receptors in small, unmyelinated sensory nerve terminals in the skin (Carlton et al., 1995), peripheral NMDA receptors may also contribute to the development of chronic pain (Warncke et al., 1997; Zhou et al., 1996). Other NMDA receptor antagonists such as MK801, ACEA 1011 (Vaccharino et al., 1993) L-701,324 (Laird et al., 1996), memantine (Carlton and Hargett, 1995), amantadine (Pud et al., 1998) or CPP (Kristensen et al., 1994), were shown to exert analgesic effects, too. All these preclinical data suggest that NMDA receptor antagonists will find clinical use in the treatment of chronic pain.

1.5.3.7 Drug and ethanol dependence, tolerance and abuse

One major obstacle with the use of opioids, especially morphine, is the development of tolerance with respect to the antinociceptive effects. Unfortunately, tolerance does not refer to the side effects like the development of respiratory depression and reduction of intestinal motility. Beside the development of tolerance, drug abuse is another important therapeutic challenge associated to the chronic use of these compounds. In various studies, NMDA receptor antagonists and partial antagonists block the development of tolerance to opiates and inhibited withdrawal signs and motivational aspects of drug abuse (Popik and Skolnick, 1996;

Tiseo and Inturrisi, 1993; Trujillo, 1995; Trujillo and Akil, 1991). Ethanol inhibits NMDA receptors with affinity in the low-millimolar range by decreasing the affinity of glycine. After prolonged abuse, this inhibition seems to cause an upregulation of NMDA receptors (Hu et al., 1996) (Chandler et al., 1999), whose activity is responsible for the occurrence of ethanol withdrawal seizures (Hoffman et al., 1995). Hence, NMDA receptor antagonists have been shown to normalize withdrawal syndromes in ethanol dependence, too (Danysz et al., 1992).

1.5.3.8 Side effects

There are some typical side effects of excitatory amino acid modulating drugs like neuronal vacuolization, psychotomimetic effects and amnesia which are discussed in this section.

Neuronal vacuolization and damage was first observed after postischemic treatment of rats with high affinity non-competitive NMDA receptor antagonists like MK801 (Olney et al., 1989). Only specific brain areas are affected and under low doses vacuolization is temporary. High doses may cause necrosis. As reason for this vacuolization, the activation of metabolic activity and the lysosomal proteolytic system of neurons has been proposed (Hetman et al., 1997). These changes have been suggested to be a class specific effect but also competitive antagonists have been shown to induce some vacuolization (Hargreaves et al., 1993) whereas the effect seems to be absent with glycine site antagonists (Hawkinson et al., 1997).

This side effect has been studied in rat and mice and there is some evidence for species differences in susceptibility to and location of vacuolization induced by NMDA receptor antagonists (Auer, 1994; Raboisson et al., 1997). Therefore, the importance of this side effect is certainly unknown.

As mentioned above (1.5.3.2) PCP exhibit **psychotomimetic effects**. It has been mainly used in psychiatric research and in drug abuse (“angel dust“). Psychotomimetic effects have also been seen with other NMDA receptor antagonists such as ketamine, MK801 and competitive antagonists (Krystal et al., 1994; Loscher and Honack, 1991; Willetts et al., 1990). Glycine site antagonists seem to exert minor psychotomimetic effects (Kretschmer et al., 1997). If these effects should be caused in general by blockade of the NMDA receptor channel, then their use is restricted to acute indications.

Systemical application of competitive and non competitive NMDA receptor antagonists at anti-epileptic and neuroprotective doses typically results in some **impairment in motor behaviour, ataxia and hyperactivity** (Loscher and Honack, 1991; Murata and Kawasaki, 1993). For systemic administration of full glycine site antagonists ataxia / myorelaxation seem to be the major side effect (Baron et al., 1997; Parsons et al., 1997b).

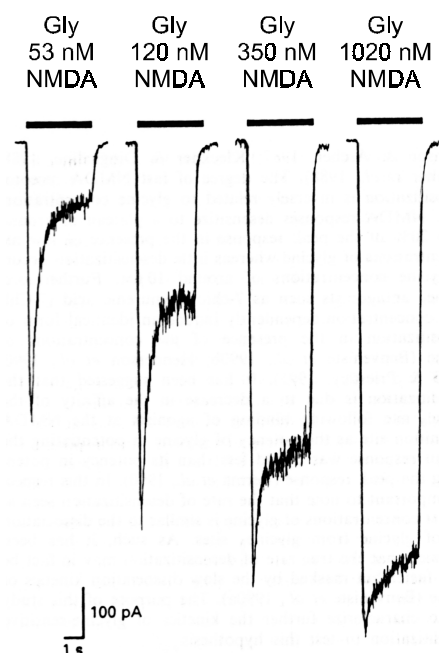
Since the activation of NMDA receptors seems to play an important role in the induction of

LTP (see 1.5.2) neuroprotective agents completely blocking NMDA receptor channels also induce **amnesic effects**. However, impairment of memory may depend on compounds blocking mechanism. The low affinity, voltage-dependent open channel blocker memantine, which has been used in Germany since the early 1980s as both an anti-parkinson agent and an antispastic agent in a variety of chronic neurological diseases including multiple sclerosis, has been shown to act neuroprotective (Kornhuber et al., 1994) in an use-dependent manner. Pathological activity is blocked while physiological activity is unchanged. This is achieved with a high voltage-dependency and a fast channel blocking kinetic (Parsons et al., 1993a). In contrast MK801, which offers only weak voltage-dependency compared with slow kinetics blocks both forms of NMDA receptor activation.

Maintenance of normal synaptic transmission under pathophysiological conditions may also be achieved using glycine-site antagonists. As shown in fig. 5 the co-agonist glycine is potentiating both, peak response to NMDA application (representing physiological response) and the desensitisation plateau (representing the pathophysiological phase). However, the effect of glycine in potentiating peak response is five fold lower than that for plateau responses (Parsons et al., 1993b). Hence, rising concentrations of glycine during ischemic periods predominantly inhibit the physiological receptor desensitization and induce long-term neurotoxic NMDA receptor activation. Abolishment of the desensitization inhibition by glycine antagonists may therefore prevent pathophysiological activation under preservation of physiological peak response and hence, leading to drugs with improved side effect profiles.

Fig. 5 *Desensitization of neurons response to NMDA depends on glycine concentration.*

NMDA (200 μ M) response of a single cell in the presence of rising glycine (53nM, 120nM, 350nM, 1020nM) concentrations. (taken from Parsons et al., 1993b).



It should be added that glycine full antagonists vary in their ability to induce glycine – sensitive desensitization. The quinolone derivate L-701,324 reveal only little desensitization whereas compounds such as 7-chloro–kynurenic acid or DCKA showed 10 fold higher potencies against plateau responses (Karcz-Kubicha et al., 1997; Molnar and Erdo, 1996).

1.6 NMDA receptor agonists and antagonists

1.6.1 Agonists and competitive antagonists

A major feature of NMDA receptor agonists (and antagonists) is the necessity of three ionizable groups. Compounds lacking the amino group or one or both acidic groups failed to show any activity. The α -carboxyl residue seems to be of certain importance since the α -phosphonyl analogue of L-glutamate has low receptor affinity. In addition, an optimal separation of the two acidic groups of either two (aspartate length) or three (glutamate length) carbons is needed for high affinity agonists.

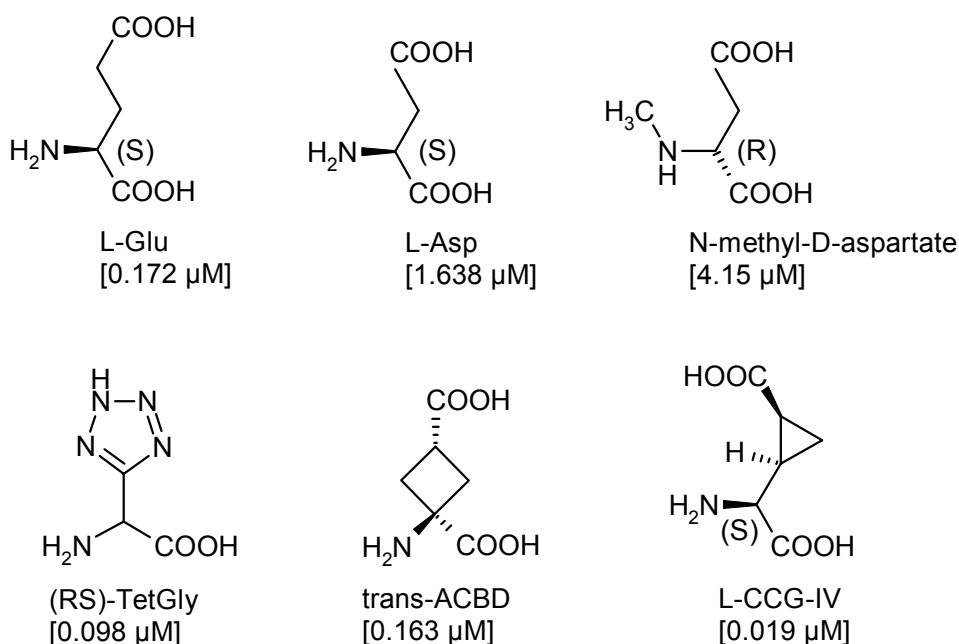


Fig. 6 Structures of NMDA receptor agonists.

K_i values (determined for displacement of [3 H]-CGS 19755) for (S)-Glu, (S)-Asp, NMDA, (R/S)-TetGly and trans-ACBD are taken from Lunn et al., 1992. K_i value of L-CCG IV was determined by displacement of [3 H]-CPP (Kawai et al., 1992) (K_i for reference compounds: NMDA = 15.0 μ M; (S)-Glu = 0.327 μ M).

Among the open chain agonists, the (S)-enantiomer of glutamate (L-glutamate) has the highest affinity and (R)- and (S)-glutamate show the widest enantiomeric difference. (S) isomers of agonists of glutamate chain length are more active than the corresponding analogues of aspartate chain length.

Alkylation of the α -amino group is usually detrimental to the activity of the compounds except the N-methylation of (R)-aspartate (NMDA). NMDA has the same affinity as the parent compound. Many potent and selective NMDA receptor agonists represent cyclic structures. The (R/S)-TetGly has twice the affinity of (S)-glutamate (92 nM vs. 172 nM) and is a potent neurotoxic and convulsant compound. In this structure, the tetrazole group acts as an isosteric replacement for $\text{CH}_2\text{-COOH}$. Higher homologues such as ω -tetrazole substituted aspartate or glutamate have lower affinity. Other highly active and specific compounds incorporate a tri- or tetracyclic ring in the interacidic carbon chain. In these series glutamate analogues which mimic a folded rather than an extended conformation of (S)-glutamate such as trans-ACBD and L-CCG-IV showed enhanced activity. The (2S, 3R, 4S)-CCG is one of the highest affinity NMDA receptor agonists with a 10 fold increased affinity compared to (S)-glutamate (Kawai et al 1992). The same phenomenon is seen with the corresponding cyclobutane analogue ACBD where the trans isomer has substantially higher affinity than the cis isomer (cis-trans ratio of K_i values = 80).

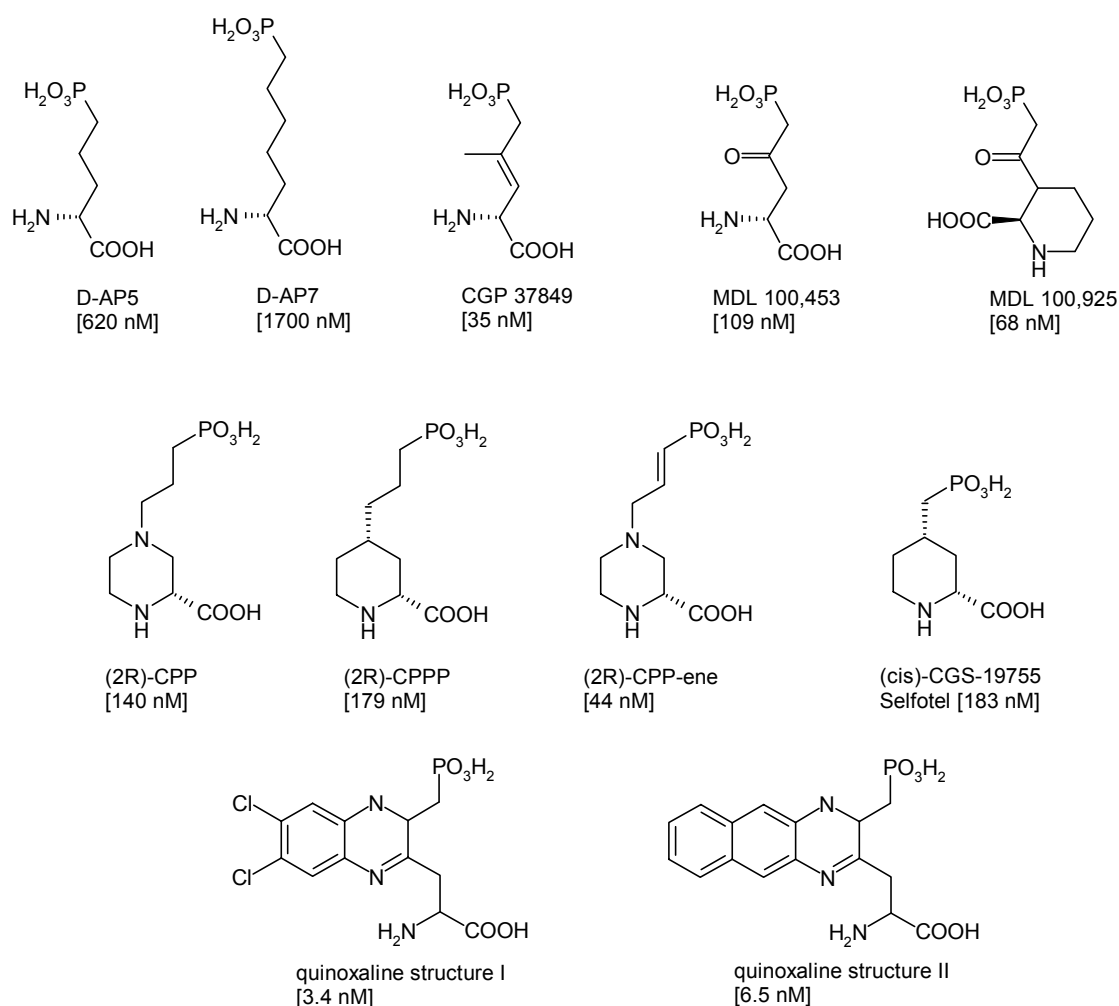
Competitive NMDA receptor antagonists are typically higher homologues of glutamate / aspartate where the number of atoms in the chain separating the α -carbon and the ω -acidic group is either three (AP5-length) or five (AP7-length). In most compounds the enantiomer with the (R) configuration at the α -terminus has the highest affinity, the R/S potency ratio being usually 10–50. Compounds include AP5, AP7, CPP, CPPP, CPP-ene, CGS 19755, CGP 37849, MDL 100,453, MDL 100,925 and quinoxaline (structure I and II) derivatives. Concerning the ω -acidic terminus, the rank order of potency for NMDA antagonism is $\text{PO}_3\text{H}_2 > \text{tetrazole} > \text{COOH} > \text{SO}_3\text{H}$.

AP5 and AP7 can be regarded as lead compounds for the development of competitive glutamate antagonists, since almost all following structures derived from these two open chain antagonists. Other compounds have been synthesized that have substituents incorporated in the interacidic group chain. Besides the (cyclic) piperazines with AP7-length, compounds with a C-4 keto group like MDL 100,453 or MDL 100,925 or the methyl substituted CGP 37849 showed an increased affinity. The latter compounds can be regarded as substituted AP5.

Introduction

Chronologically, CPP and then CGS 19755 were the first compounds reported to have higher affinity than AP5 and AP7 as competitive NMDA antagonists. These piperazine and piperidine compounds can be regarded as cyclic AP7 and AP5 analogues, respectively. In the piperidine group the AP5-length compound CGS 19755 and AP7-length compound CPPP have near equal affinity but CGS 19755 shows higher in vivo potency. In the 4-substituted piperazines, however, peak activity is seen in the AP7-length compounds CPP and CPP-ene. In a reported quinoxaline series of NMDA-receptor antagonists the AP6-length analogues with a 6,7-dichloro substitution (structure I) (Baudy et al., 1993) or 6,7 annealed phenyl moiety (structure II) showed highest affinity. These compounds represent two of the most potent competitive NMDA-receptor antagonists with K_i values of 3.4 and 6.5 nM, respectively.

Fig. 7 Structures of competitive antagonists at the glutamate binding site of the NMDA receptor (Collingridge and Watkins, 1994)



The strong increase in affinity of these bulky compounds may be caused by the use of a large hydrophobic pocket within the binding site. In addition to its high affinity, the 6,7-dichloro compound is of particular interest, since an IC_{50} value of $0.6\mu M$ has been reported for the displacement of [3H]-glycine binding. This presumably results from its close structural similarity to the quinoxalinediones and 6,7-dichlorokynureate.

1.6.2 Glycine site agonists and antagonists

The action of glycine on NMDA receptors is mimicked by other small neutral amino acids, notably by (R)-serine (D-serine) and (R)-alanine. These (R)- α -amino acids act as enantioselective agonists with submicromolar affinities (McBain et al., 1989). Glycine and (R)-serine are present in the CNS at micromolar levels (Matsui et al., 1995) and uptake mechanisms have been described for both. For glycine, cloning studies revealed the existence of GLYT1, a Na^+ and Cl^- dependent uptake transporter specific for glycine (Smith et al., 1992), expressed in glia cells and colocalized with NMDA receptors (Fedele et al., 1993). Glycine uptake via GLYT1 was demonstrated to efficiently regulate local glycine levels (Supplisson and Bergman, 1997). Intracerebroventricularly (i.c.v.) injected (R)-serine accumulates in glial cells (Wako et al., 1995), suggesting the existence of a (R)-serine uptake mechanism in astrocytes (Schell et al., 1995). There are indications that the reversal of the described uptake mechanisms play a major role in increasing the concentration of these amino acids near the synaptic cleft. Since both amino acids, (R)-serine and glycine exhibit heterogeneous and partially complementary distribution within in the CNS (Schell et al., 1997) it remains elusive whether glycine and / or (R)-serine represent the native co-agonist(s) of NMDA receptors.

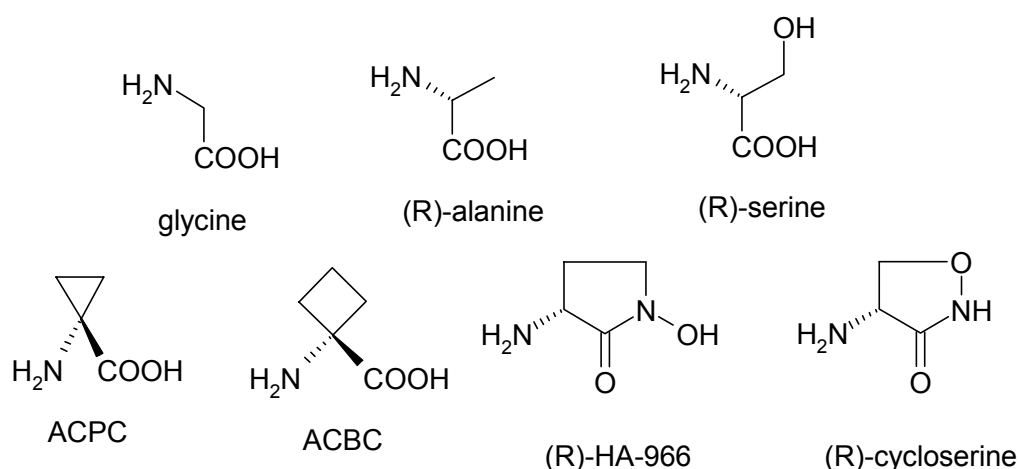


Fig. 8 Structure of compounds acting as agonists and partial agonists at the glycine recognition site of the NMDA receptor

Exogenous full and partial agonists derived from α -amino acid structures. Cyclic amino acids ACPC and ACBC contain cyclopropane and cyclobutane residues, respectively. In vitro, ACPC represents a partial agonist (Watson and Lanthorn, 1990) with an intrinsic activity of approximately 90%. However, in vivo ACPC showed antidepressive, anxiolytic and neuroprotective effects with good penetration to the CNS. ACBC, with its bigger ring and much lower affinity and intrinsic activity, has not been studied extensively. (R)-HA-966 has been recognised as a partial agonist (Foster and Kemp, 1989) with a very low efficacy (<10% of glycine) and anticonvulsant action in vivo, whereas the (S)-enantiomer does not bind to the glycine recognition site of the NMDA receptor. The structurally related aminohydroxamate (R)-cycloserine, which has been formerly used as an antibiotic for the treatment of tuberculosis, is a systemically active partial agonist with high affinity for NR1 / NR2C and NR2D assemblies and higher efficacy than HA-966.

Kynurenic acid was the first glycine site antagonist after the discovery of glycine as a co-agonist of the NMDA receptor (Birch et al., 1988). Optimization strategies led to a 7-chloro substitution, which enhances the affinity for the glycine site by 70-fold (Kemp et al., 1988). This substitution is usually found in all subsequently developed high affinity compounds. Further improvement of affinity led to the 5,7-dichloro derivate known as DCKA (Baron et al., 1990). The development of dihydrokynurenate series led to the highly potent phenylurea derivate L-689,560 (Foster et al., 1992). Further reported kynurenic acid derived compounds were a cyclic hydrazide (M 241,247) and the recently reported pyrido-phthalazine-dione MRZ 2/576 (Parsons et al., 1997b). These two latter tricyclic compounds are glycine site antagonists with only moderate potency, but provide a relative good penetration into the CNS. This is in contrast to the other kynurenic acid derived high affinity antagonists which are inactive in vivo due to poor brain penetration and bioavailability in the CNS, although they provide optimized affinities in the nanomolar level.

The essential features of the kynurenic acid pharmacophore are also present in the indole-2-carboxylic acids. The potency of the propanoic acid derivate MDL 29,951 (Salituro et al., 1992) is comparable to the corresponding DCKA. Unfortunately, like kynurenic acids, most of these compounds show poor bioavailability and are active after i.c.v. administration only (Baron et al., 1992). MDL 105,519 which has an IC_{50} for the displacement of [3H]-glycine binding of 10nM, is widely used as tritiated radioligand of the glycine recognition site (Baron et al., 1996). GV 150526A (Gavestinel) belongs to a series of 2-carboxyindole derivatives in which chain substitutions at position 3 increased affinity to the low nanomolar range. However, Gavestinel is active against convulsions in mice after i.v. and peroral administration

(Di Fabio et al., 1997) and is currently under development by Glaxo Wellcome for the treatment of stroke.

Quinoxaline derivatives derived from the finding, that CNQX and DNQX, which were the first antagonists at AMPA non-NMDA receptors, had also substantial affinity for the glycine recognition site of the NMDA receptor (Randle et al., 1992). ACEA 1021 has been reported to have improved affinity and selectivity (Woodward et al., 1995) and was active in various models of glutamate induced pathogenesis (Lutfy and Weber, 1996; Takaoka et al., 1997; Warner et al., 1995). The tricyclic quinoxalinedione compound 20-g (Nagata et al., 1994) incorporates structural features from the bulky 4-position of the tetrahydroquinoline L-689,560 leading to comparable affinities. The in vivo data of this compound are in common with those of kynurenate and indole classes. Based on the structural features of the kynurenic acids and the quinoxalinediones, a putative model of the binding pocket was developed (Leeson and Iversen, 1994), which is given in fig. 9.

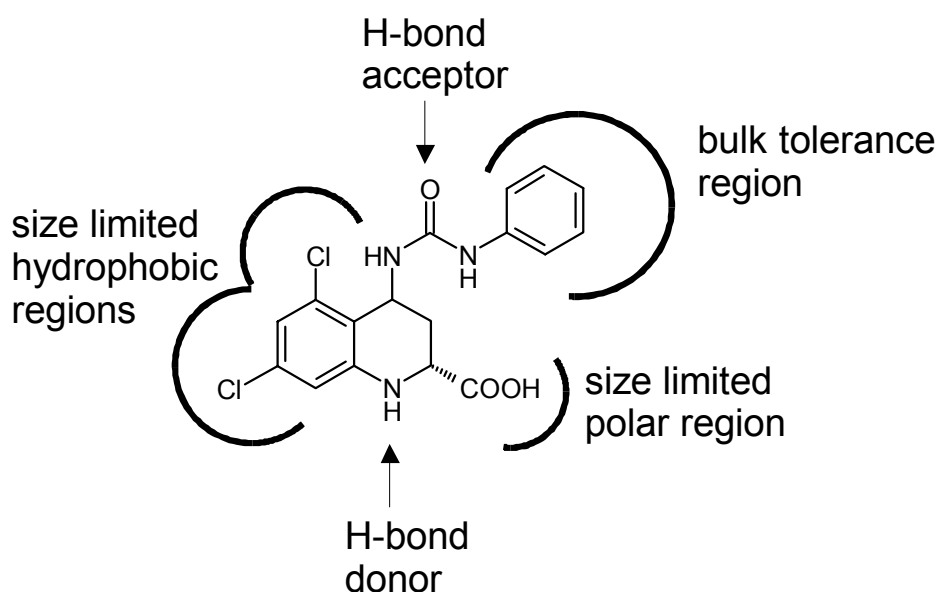


Fig. 9 Pharmacophore for glycine site antagonists after Leeson and Iversen, 1994

The pharmacophore contains a H-bond donor and acceptor moiety, a size limited hydrophobic region, and on the opposite site of the pharmacophore a bulk tolerance and a size limited acidic region. Based on this pharmacophore 2-quinolone derivatives have been synthesized. The 2-quinolones lack the carboxylic group ($pK_a \sim 4$) present in indole-2-carboxylic acids and kynurenic acid derived compounds, whose dissociation was thought to be detrimental to brain penetration. Instead, the compounds hold the acidic function within the fused heterocyclic ring, delocalized to the 2-carbonyl and leading to an increased pK_a value of ~ 5 .

Introduction

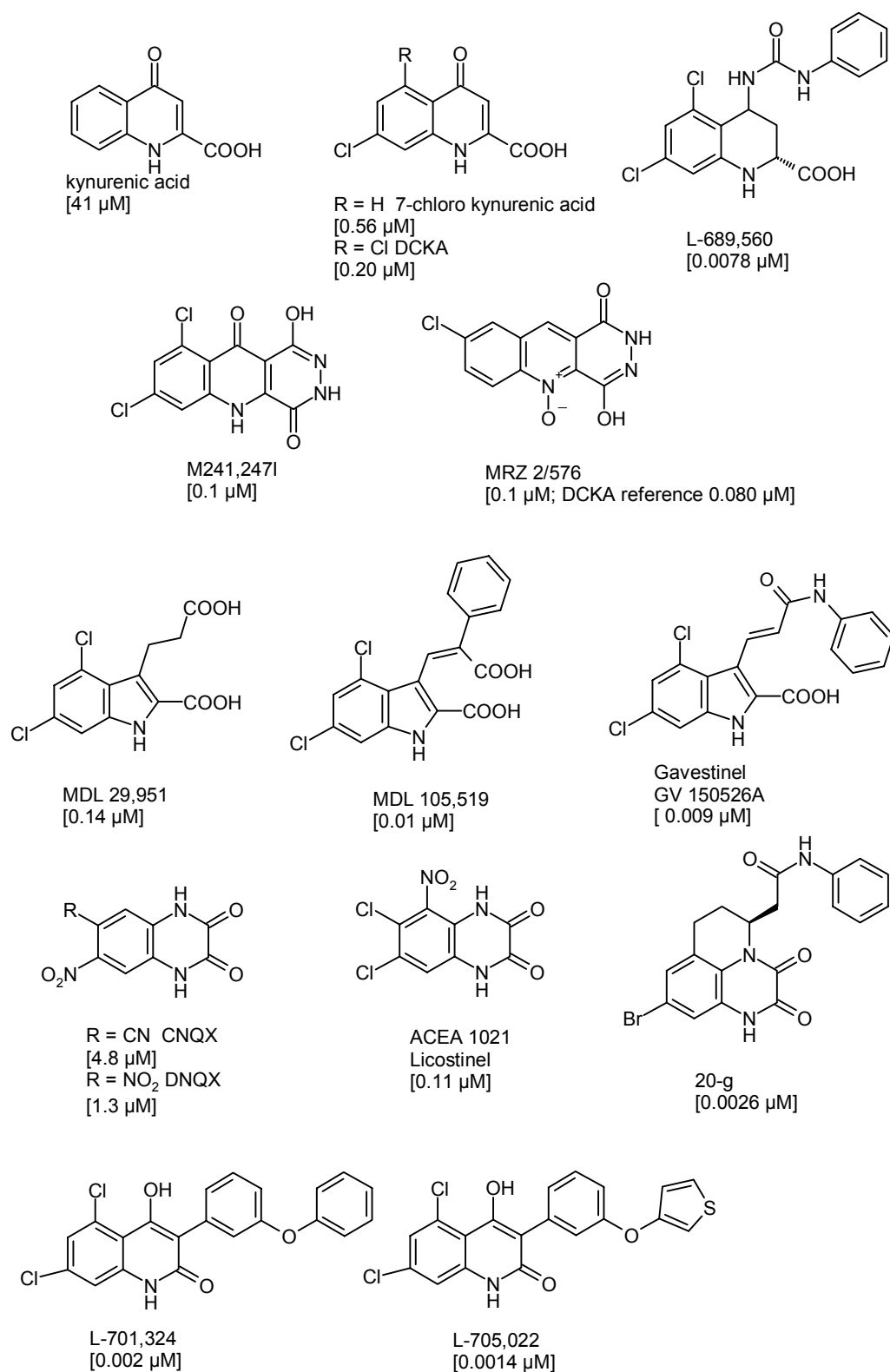


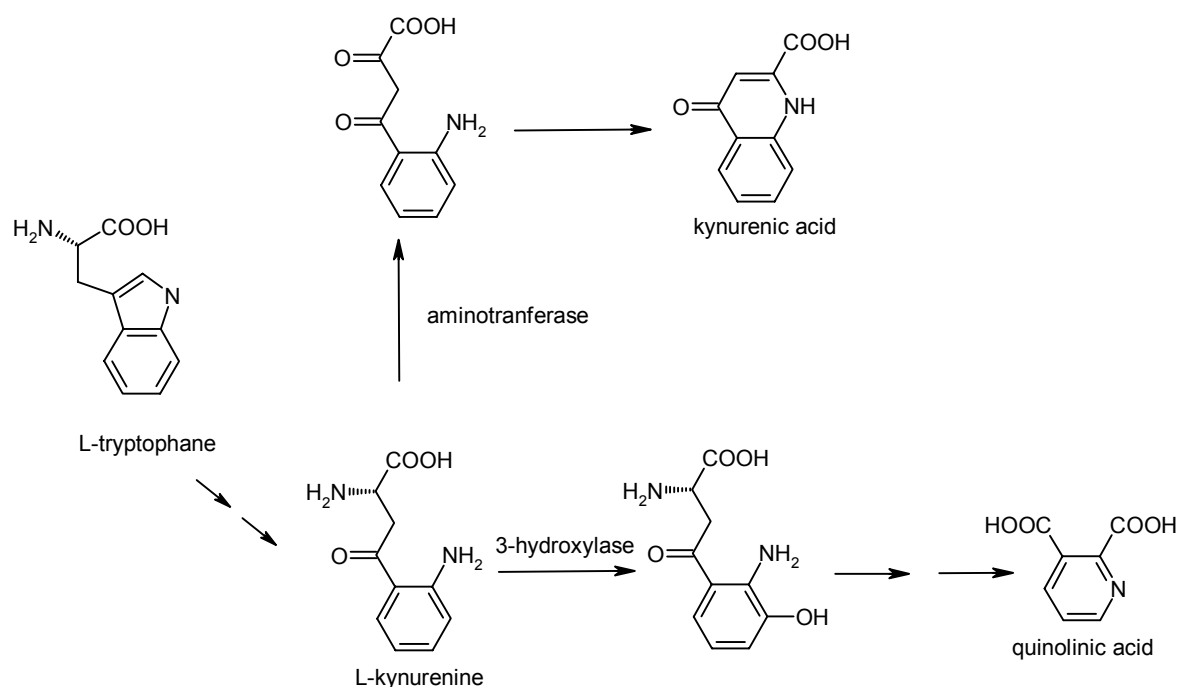
Fig. 10 Structures of glycine site antagonists

Affinities are expressed as IC_{50} values from displacement of [³H]-glycine (taken from Leeson and Iversen, 1994 and Danysz and Parsons, 1998). IC_{50} of MRZ 2/576 was determined by displacement of [³H]-MDL 105,519 (Parsons et al., 1997b).

A series of 4-hydroxy-2-quinolone represents a class of glycine antagonists with consistent bioavailability and in vivo activity. The potency of this series of compounds depends on the nature of the 3-substituent. A breakthrough in systemic activity was found in the 3'-aryloxy-3-phenyl derivatives. Compounds L-701,324 and L-705,022 (Kulagowski et al., 1994) are two of the most potent glycine antagonists with high in vitro and in vivo potency, yet described.

Bioavailability problems of most glycine site antagonists arise from poor penetration into the brain due to ionization of acidic groups or a rapid transport out of the brain mediated by the organic acid transporter in the choroid plexus. However, the bioavailability in the CNS was found to be improved by co-application of probenecid which seems to inhibit drugs outflux via the mentioned organic acid transporter (Moroni et al., 1988; Parsons et al., 1997a; Santamaria et al., 1996). Another bioavailability problem rises from the binding to plasma proteins (Rowley et al., 1997b). It was proposed that on one hand, the affinity at the glycine site increases with lipophilicity. But on the other hand, increased lipophilicity also leads to an enhanced binding to plasma proteins (e.g. albumin) limiting the amount of free compound to diffuse across the blood-brain barrier. This hypothesis was supported by the finding that warfarin increased in vivo potency of some high affinity compounds in vivo (Rowley et al., 1997a).

Another approach to influence the activity of NMDA receptors via the glycine binding site is the use of the L-kynurenine pathway of L-tryptophane in a prodrug concept (Moroni et al., 1988; Russi et al., 1992; Schwarcz, 1993; Stone, 1993). Via this pathway, L-kynurenine is transformed into the antagonistic kynurenic acid and the agonistic quinolinic acid. Central injection of 4-chloro-L-kynurenine led to the in vivo formation of its metabolite 7-chloro kynurenic acid in neuroprotective quantities (Wu et al., 1997). As advantage of this prodrug system, the facilitated penetration of substituted kynurenines via large amino acid transport systems is proposed. Another approach is the inhibition of the kynurenine-3-hydroxylase, a key enzyme in the formation of the agonistic quinolinic acid. Blockade of kynurenine-3-hydroxylase should lead to decreased quinolinic acid levels whereas the endogenous kynurenic acid levels should be increased by facilitating metabolism. An applied compound in this approach is FCE 28833A [(R/S)-3,4-dichlorobenzoylalanine] (Speciale et al., 1996). But unfortunately, since kynurenic acid represents a glycine antagonist with only weak affinity, the estimated antagonist levels after high dose treatment were more than 1000 fold lower than the respective K_i value of kynurenic acid (15 μ M) (Kessler et al., 1989).

Fig. 11 Kynurenine pathway of L-tryptophane

1.6.3 Non-competitive antagonists

Non-competitive antagonists include the dissociative anaesthetics phencyclidine and ketamine (Ketanest[®]), the morphinan dextromethorphan (NeoTussan[®]), the adamantanes memantine (Akatinol-Memantine[®]) and amantadine (PK-Merz[®]), the dibenzocycloalkenimine MK801 and the substituted guanidine CNS 1102, which has been reported to be neuroprotective in vitro and in vivo. PCP was developed in the 1950s as an anaesthetic agent and has been used in psychiatric research as a model of schizophrenia. It is also encountered as a drug of abuse (“angel dust”). Ketamine is an analogue of PCP with lower affinity for the NMDA receptor ion channel. It is a racemic compound widely used for anaesthesia. Like PCP it induces catalepsy and psychotomimetic effects. Dizocilpine (MK801) is the agent with the highest affinity for the NMDA receptor ion channel. It was the first drug consistently shown to be neuroprotective (Park et al., 1988). Unfortunately, induced hallucinations and histological changes in brain of rats (Horvath et al., 1997) led to safety concerns. Aptiganel (CNS 1102 / Cerestat) is a diarylguanidine with high affinity for the NMDA receptor ion channel (Reddy et al., 1994).

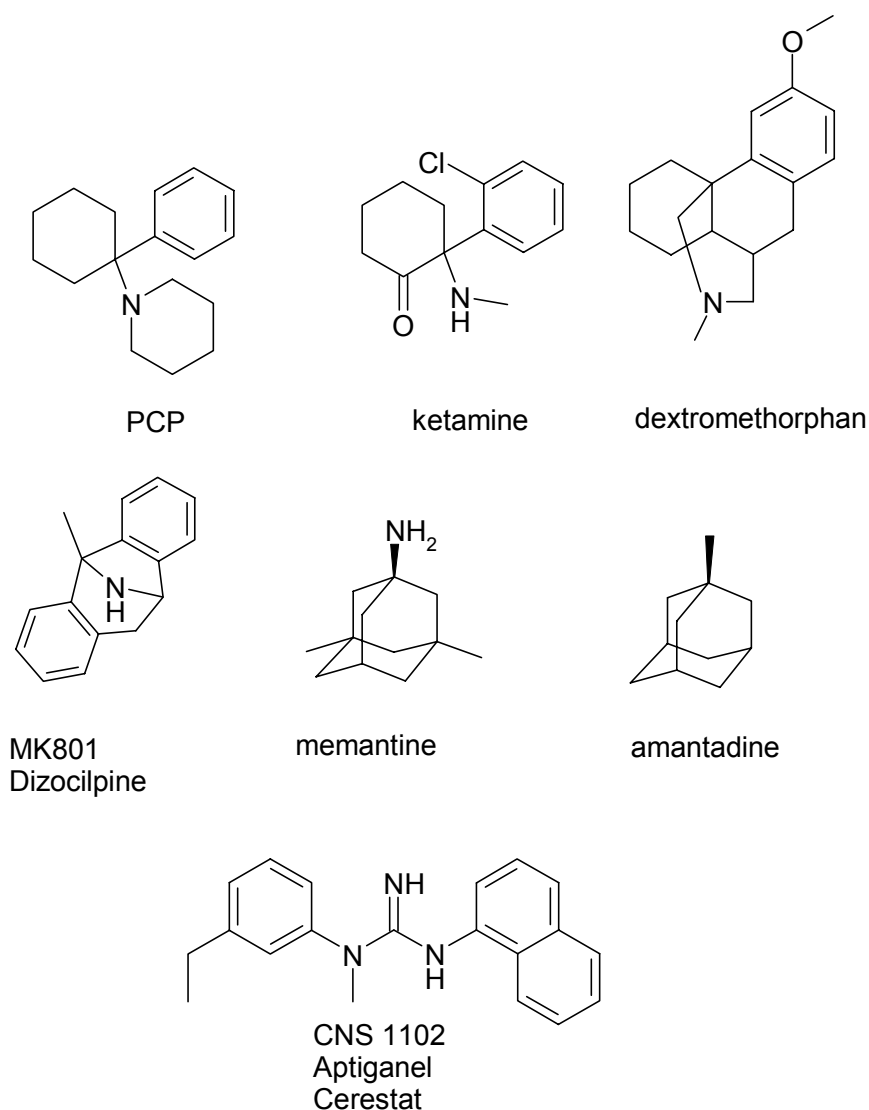


Fig. 12 Structures of non-competitive NMDA receptor antagonists

Clinical trials with this compound in phase I reported symptoms of sedation and central nervous excitation (Muir et al., 1994; Muir et al., 1997). Even in phase III studies with aptiganel, increased systolic blood pressure and an excess of CNS effects were both observed (Dyker et al., 1999). Dextromethorphan has been used as an antitussive for many years before its recognition as a low-affinity open channel blocker of NMDA receptors. A Clinical trial (phase II) in amyotrophic lateral sclerosis did not result in an improvement in 12-month survival (Gredal et al., 1997). The low-affinity non-competitive NMDA antagonists memantine and amantadine have been used as antiparkinson, antimentia and antispastic agents since the early 1980s. They were recognised as NMDA ion channel blockers well after their introduction to clinical practice.

Introduction

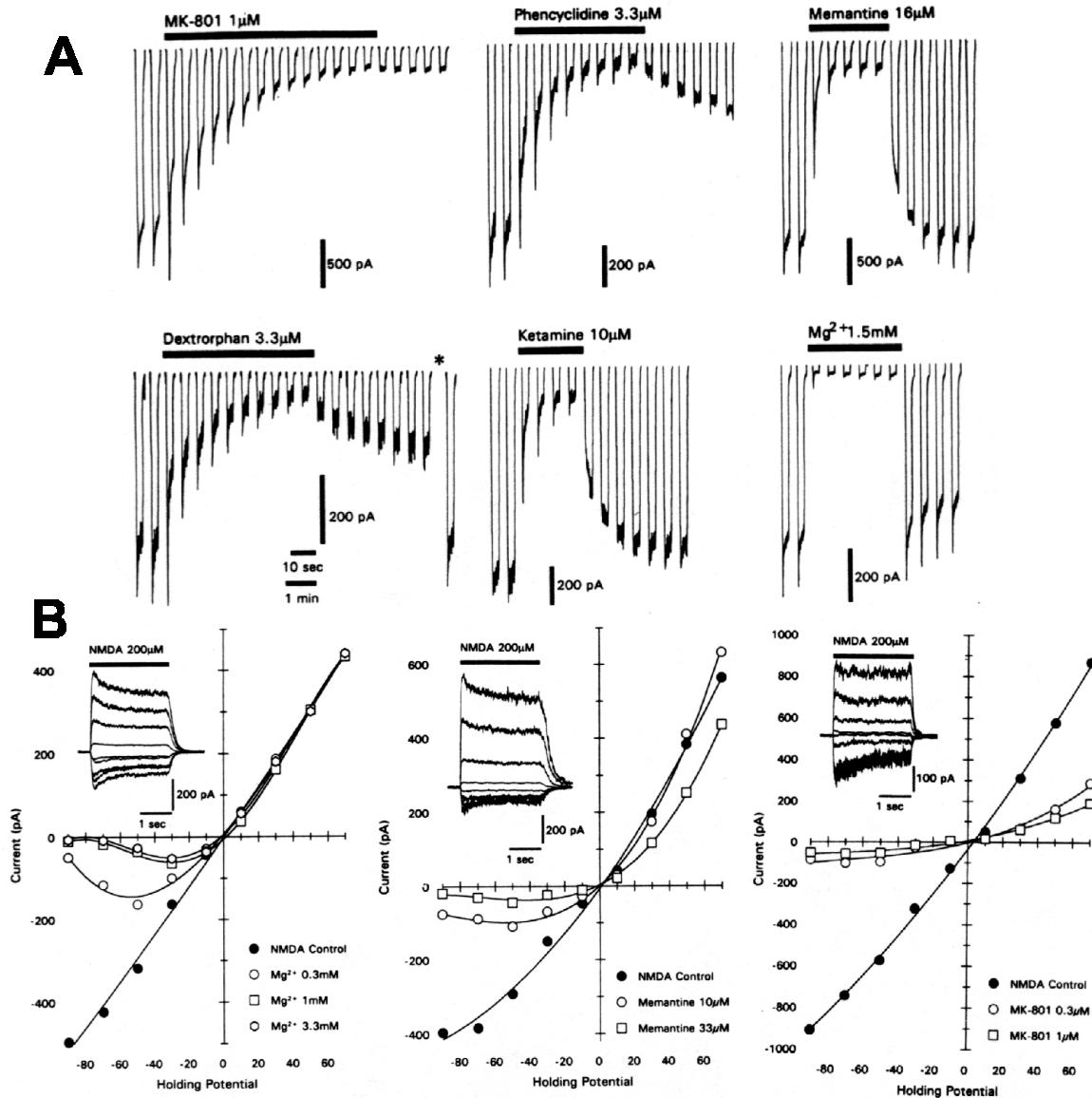


Fig. 13 Use- and voltage-dependency of non-competitive NMDA receptor antagonists Patch clamp studies at hippocampal neurons (taken from Parsons et al., 1993a).

The described compounds differ in their kinetics for NMDA receptor binding. The low-affinity compounds memantine and ketamine bind to NMDA receptors strongly use-dependent similar to magnesium. In contrast, MK801 and PCP showed much slower kinetics (see fig. 13-A). (Parsons et al., 1993a). Even the voltage-dependence of memantine resembles that of magnesium, whereas the blockade by PCP and MK801 is weak (see fig. 13-B).

1.6.4 NR2B specific compounds

This class of compounds is selective for the subtypes of NMDA receptors containing the subunit NR2B. CGP 61594 is a competitive glycine antagonist, which was shown to have some selectivity for the NR2B subtype (Honer et al., 1998). Ifenprodil is the prototype of NR2B selective NMDA receptor antagonists (Williams, 1993b) but exhibits also affinity to α 1 adrenergic, serotonin and sigma receptors (Chenard et al., 1991). High potency and selectivity for the NR2B subtype was found in single enantiomers from erythro and threo ifenprodil (Avenet et al., 1996). Eliprodil was the first ifenprodil analogue to be described with NMDA antagonist properties. This compound is equipotent at α 1 adrenergic receptors and showed some calcium channel blocking activity (Biton et al., 1994). Nevertheless, clinical trials with this compound as a neuroprotectant for stroke and traumatic brain injury were performed. Haloperidol is an antipsychotic drug with affinity for dopamine and sigma receptors. Electrophysiological studies concluded that haloperidol specifically inhibits NR2B containing NMDA receptors (Coughenour and Cordon, 1997).

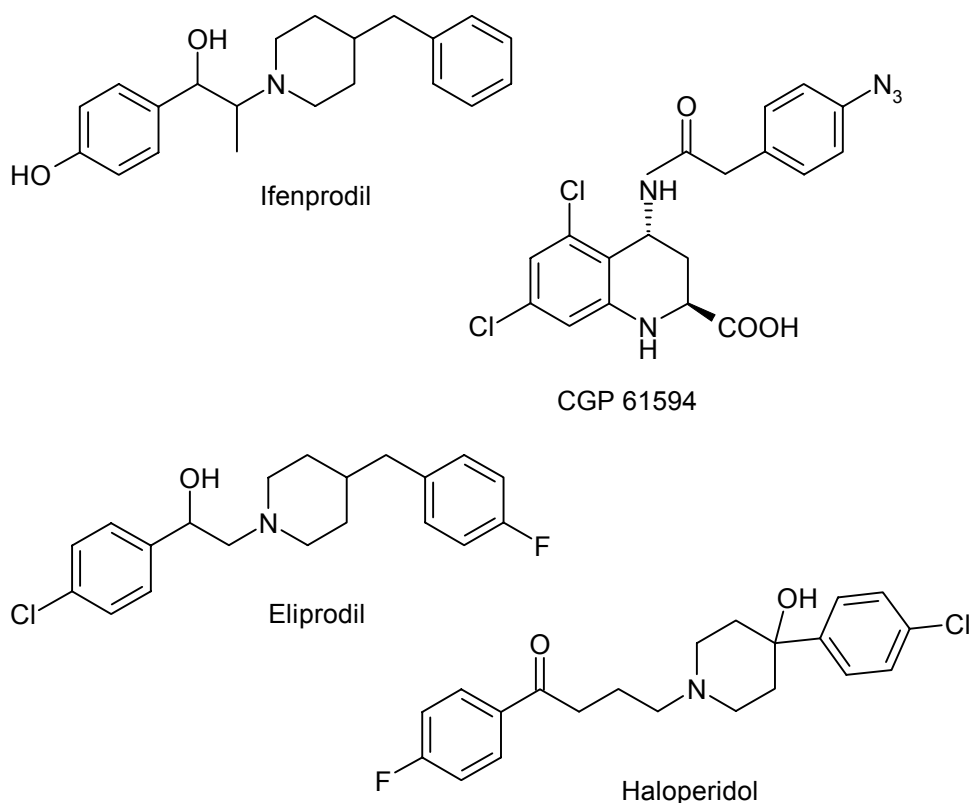


Fig. 14 Structures of NR2B selective NMDA receptor antagonists

1.6.5 Immunological approach

Recently, it has been reported, that a humoral autoimmune response targeting the NR1 subunit of the NMDA receptor has antiepileptic and neuroprotective effects (During et al., 2000). Oral genetransfer of mouse NR1 to intestinal, antigen presenting lamina propria cells was performed using an adeno-associated virus (AAV) vaccine and induced the generation of antibodies against a range of NR1 epitopes. Serum from AAVNMDAR1-immunized rat showed specific binding to peptides that correspond to functional domains within the extracellular NH₂-terminal side of M1 and the M3-M4 loop containing critical residues for glycine binding. In a model of kainate induced epilepsy one month following vaccination the status epilepticus frequency was significantly reduced by ~ 68% and prevented even seizure induced neurotoxicity. In an endothelin-1 model of experimental stroke the total infarct volume of AAVNMDAR1-immunized rats was reduced by ~ 70%. In contrast to administration of NMDA receptor antagonists, vaccination did not result in an impairment of motor behaviour. Besides the lack of this typical side-effect, the most promising feature of this approach seem to be an “on demand delivery“ of neuroprotective agent. Under physiological conditions, vaccinated animals showed low levels of NMDAR1 antibodies in the cerebrospinal fluid (CSF). After kainate treatment, a tenfold increase in CSF levels of NMDAR1 autoantibodies was observed. Since glutamate itself has been reported to alter the blood-brain-barrier (BBB) permeability (Mayhan and Didion, 1996), the authors conclude, that increased glutamate levels after an cerebral insult may lead to a local increase of BBB permeability, resulting in an facilitated passage of antagonistic autoantibodies from the periphery into the CNS. The observed neuroprotection by autoantibodies against NR1 is consistent with the results of a human study in Russia, which showed the presence of NMDA receptor autoantibodies in the serum of patients after stroke (Gusev et al., 1996). A neurological recovery occurred only in individuals with significant antibody titers whereas a poor prognosis or death was correlated to the absence of NMDA receptor autoantibodies. The described approach suggests the possibility of prophylactic vaccination for patients with a high risk of stroke or other cerebral insults and difficult forms of epilepsy as well as a direct treatment of stroke patients with NMDA receptor antibodies.

1.7 Apoptosis and necrosis – modes of cell death

Cell death can occur by either of two distinct mechanisms, apoptosis or necrosis. The term apoptosis or programmed cell death characterizes a structurally distinctive mode of cell death, responsible for the loss of cells within living tissues (Kerr et al., 1972). In contrast, necrosis occurs when cells are exposed to extreme variance from physiological conditions, e. g. hypothermia or hypoxia.

Necrotic cell injury is initiated by the damage of the plasma membrane. The leakage of the plasma membrane causes an impairment of the cell's ability to maintain homeostasis, leading to an influx of water and extracellular ions. Intracellular organelles, most notably the mitochondria, and the entire cell swell and rupture (cell lysis). Due to the ultimate breakdown of the plasma membrane, the cytosolic contents including lysosomal enzymes are released into the extracellular fluid. Therefore, in vivo, necrotic cell death is often associated with extensive tissue damage and an intense inflammatory response.

The main morphological features of apoptosis are cell shrinkage, accompanied by blebbing from the surface, and culminating in separation of the cell into a cluster of membrane-bound vesicles (apoptotic bodies). Besides a usually intact organellar structure, the nucleus undergoes a characteristic chromatin condensation resulting in densely heterochromatic regions. Changes in surface molecules ensure that in vivo apoptotic cells are immediately recognised and phagocytosed by macrophages, microglia or other phagocytes. Due to this removal, no inflammatory response is elicited. In vitro, the apoptotic bodies as well as the remaining cell fragments ultimately swell and finally lyse. This terminal in vitro phase has been termed "secondary necrosis".

"Physiological" apoptosis is responsible for cell death in development, normal tissue turn over, negative selection in the immune system, the mediation of cell killing by TNF and the prevention of tumours and carcinogenesis. Furthermore it accounts for many cell deaths following exposure to cytotoxic compounds, viral infections, hypoxia / stroke and in chronic neurodegenerative processes including Alzheimer's or Parkinson's disease.

Several key elements of the apoptotic pathway have been described: **(i)** Death receptors, like the CD-95 (Fas / APO-1) and the TNFR1 receptor ligand systems. After binding of the respective ligand (FasL / TNF α) and a subsequent trimerization of the receptors, an intracellular recruitment of "death domain" containing factors (FADD or TRADD/FADD) is described, leading to the activation of caspase 8 (Nagata, 1997). **(ii)** Protease cascades have been characterized, in which caspases (**cysteiny-** **aspartate-specific proteases**) play a pivotal

role in the initiation (caspase 9 and 8) and execution of apoptosis (caspase 3) by the cleavage of target proteins such as poly(ADP-ribose)polymerase (PARP) (Nicholson et al., 1995) or ICAD / DFF45 (inhibitor / chaperone of caspase-3 activated DNase CAD (Enari et al., 1998). Caspase-3 activation seems to be required for nuclear apoptosis and DNA fragmentation (Janicke et al., 1998). **(iii)** During apoptosis mitochondrial permeability is altered. Caspase activator cytochrome C is released from mitochondria (Andreyev et al., 1998; Yang and Cortopassi, 1998). Together with dATP, cytochrome C (Apaf-2) promotes the caspase activation in the cytosol by binding to Apaf-1 (Zou et al., 1997) (mammalian homologue of CED 4 in *C. elegans*) and therefore activating Apaf-3 (caspase 9)(Li et al., 1997). Another pathway is the release of proapoptotic AIF (apoptosis inducing factor) (Susin et al., 1996). AIF is a caspase-1-like protease (inhibited by z-VAD.fmk) capable of activating a caspase-3-like protease to induce nuclear apoptosis. The release is mediated by mitochondria undergoing permeability transition. Permeability transition is a phenomenon characterized by the opening of pores in the inner membrane of mitochondria (Bernardi et al., 1998). These pores are induced by the disruption of the inner membrane potential ($\Delta\Psi_m$) e.g. by elevated intracellular calcium or protonophores (FCCP).

Although apoptosis and necrosis are considered as distinct forms of cell death, there is increasing evidence that classical apoptosis and necrosis represent only the extreme ends of a continuum of possible types of cell death. In some cases, both forms share common steps since the execution of apoptosis in neurons and lymphoid cells depends on intracellular ATP levels and can be switched to necrosis by depletion of ATP (Ankarcrona et al., 1995; Leist and Nicotera, 1997; Leist et al., 1999; Nicotera et al., 1998). This suggests, while initial events may be common to both types of cell death (e.g. overstimulation of NMDA receptors in neurons), certain metabolic conditions (maintenance of mitochondrial function and ATP levels) would be required to activate downstream switches which direct cells to the execution of apoptosis. Since glutamate induced neuronal cell death requires mitochondrial calcium uptake (Stout et al., 1998a) and the resulting mitochondrial dysfunction is a primary event in glutamate induced neurotoxicity (Schinder et al., 1996), mitochondrial function and intracellular ATP-levels seem to be critical factors that determine the mode of neuronal death in excitotoxicity. Correspondingly, it is not surprising that both modes of cell death can be found in experimental stroke models (Charriaut-Marlangue et al., 1996). In the ischemic core, necrosis is the predominant form of cell death whereas in the less severely compromised penumbra or border regions a delayed apoptotic cell death occurs.

2. Aim of the study

After the cloning of the rodent NMDA receptor subunits (Ikeda et al., 1992; Ishii et al., 1993; Kutsuwada et al., 1992; Monyer et al., 1992; Moriyoshi et al., 1991) these cDNAs have been used in heterologous transient expression systems like *Xenopus* oocytes for electrophysiological studies (Le Bourdelles et al., 1994; Monyer et al., 1992; Wafford et al., 1993) or mammalian cells for radioligand binding studies (Cik et al., 1993; Grimwood et al., 1995; Laurie and Seeburg, 1994; Lynch et al., 1994). Cloning of human cDNA clones (Karp et al., 1993; Le Bourdelles et al., 1994; Planells-Cases et al., 1993) (Grimwood et al., 1996b; Hess et al., 1996; Hess et al., 1998; Lin et al., 1996) now allows studies at recombinant human NMDA receptors. Since it has been reported that expression of NMDA receptors in the nonneuronal cell line *Hek 293* leads to cell death (Anegawa et al., 1995) the establishment of a cell death based in vitro test system was intended. As expression system we favoured nonneuronal cell lines, stably transformed with recombinant NMDA receptors, since comparable cell lines have proved to be robust and reliable expression systems (Grimwood et al., 1996b; Uchino et al., 1997; Varney et al., 1996).

3. Results

3.1 Transient expression of rat NR1-1a, mouse NRε1 and mouse NRε3 in Hek 293 cells

Human embryonal kidney cells (*Hek 293*) have widely been used for the heterologous, transient expression of recombinant NMDA receptors in mammalian cells. These cells were immortalized by exposure to shared fragments of adenovirus type 5 DNA (Graham et al., 1977). A portion of the adenovirus genome is expressed in these cells including the adenovirus E1a and E1b proteins. E1a proteins have been shown to inhibit the immediate early region (IE) of the SV40 promoter through a mechanism of enhancer repression but do not inhibit the IE region of the human cytomegalovirus (HCMV) promoter (Gorman et al., 1989). In contrast E1b proteins transactivate the IE region of HCMV. Hence, the HCMV promoter is superactivated in *HEK 293* cells. The expression of the rat NR1-1a, mouse NRε1 and mouse NRε3 containing pCIS constructs is therefore under the control of the constitutively active HCMV promoter.

As already mentioned, cell death after heterologous expression of recombinant NMDA receptors has been reported (Anegawa et al., 1995). To examine the effects of rat NR1-1a co-transfected with mouse NRε1 or NRε3 on cell viability, 3×10^6 cells were plated in 10 cm cell culture dishes. After 48 hours, transfection was performed using the calcium phosphate precipitation method (Chen and Okayama, 1987) with 10µg total DNA. Cells were transfected with pCIS (control) and with either pCIS NR1-1a / pCIS NR2A-ε1 (1:3 ratio) or pCIS NR1-1a / pCIS NR2C-ε3 (1:3 ratio). Transfections were carried out in triplicates. 24 hours after transfection, cells were removed from the plates with a cell culture rubber, centrifuged and cell death was determined by trypan blue exclusion. Transfection of NR1-1a / NRε1 led to a 4-fold increase in cell death (28.2 ± 3.7 %) compared to pCIS transfected population (7.3 ± 2.5 %). In contrast, subunits NR1-1a / NRε3 did not affect the cell death rate significantly (8.7 ± 2.1 %). To confirm that the observed cell death resulted from the expression of functional NMDA receptors and not from unspecific toxic effects of different transfected constructs, the ability of the competitive antagonist (R/S)-AP5 (150µM) to prevent cell death was tested. 150µM APV reduced cell death to 16.5 ± 1.5 % representing a

Results – transient expression

reduction of approximately 50% compared to positive control. These results are in good agreement with former studies (Anegawa et al., 1995; Cik et al., 1993). Cik et al. reported a cell mortality rate of $21.7 \pm 3\%$ for the co-transfection of rat NR1-1a and NR ϵ 1 (ratio 1:3) 20 hours post-transfection. The presence of AP5 (200 μ M) reduced cell death rate to $8.3 \pm 2.6\%$. Anegawa et al. reported a 48 hour cell death rate of approximately $57.9 \pm 5.2\%$ for rat NR1-1a / NR 2A expression and an unchanged cell death rate for rat NR1-1a / NR2C. The observed cell death under transient co-expression of NR1-1a and NR2A subunits might be caused by the activation of functional NMDA receptors and subsequent influx of calcium ions. Transfection was carried out in DMEM medium which contains 4 mM glutamine known to produce high glutamate levels within the cell culture medium. Additionally, supplemented fetal calf serum (10%) may contribute to higher concentrations of L-glutamate and glycine.

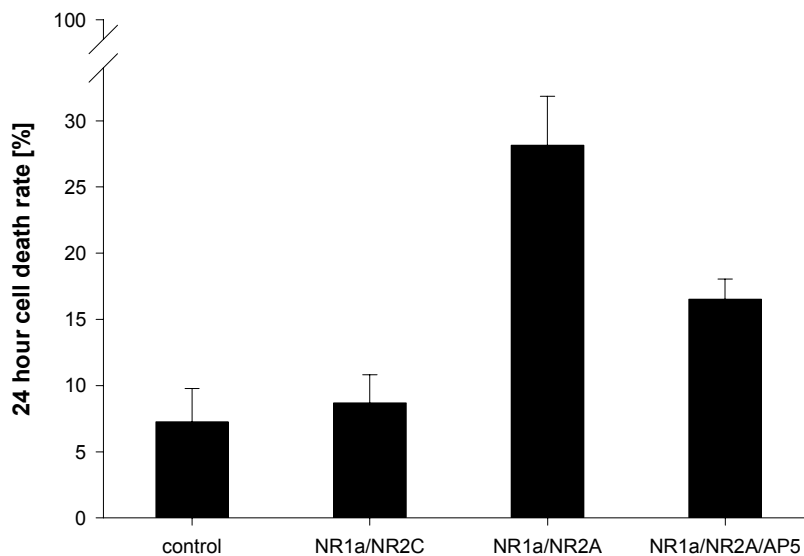


Fig. 15 *Transient expression of NMDA receptor subunits in Hek 293 cells leads to cell death dependent on subunit composition.* Expression of NMDA receptor subunits NR1-1a and NR2A (NR ϵ 1) led to an increased cell death 24 hours post transfection which could be partially reduced with the competitive antagonist (R/S)-AP5 at a concentration of 150 μ M. Increased cell death was not observed after transfection of subunits NR1-1a / NR2C (NR ϵ 3) compared to pCIS control vector transformed populations.

Due to the use of calcium phosphate precipitation method the concentration of free calcium in the cell culture medium is increased. Block of opened channels by magnesium, present in DMEM medium in active concentrations (0.7mM), might be reduced as the resting membrane potential of *Hek 293* is in the range of -15 to -50 mV (Cik et al., 1993). Therefore, activation of functional NMDA receptors is likely to occur. Elevated intracellular calcium levels may

Results – transient expression

then damage calcium buffering mitochondria resulting in increased cell death rates.

The absence of increased mortality under co-transfection of NR1-1a / NR2C agrees with findings from other groups (Anegawa et al., 1995; Chazot et al., 1994). This may be explained by a decreased calcium permeability of this expressed NMDA receptor subtype. In fact, higher NMDA-induced currents in *Xenopus* oocytes expressing NR1 / NR2A compared to NR1 / NR2C have been reported (Monyer et al., 1992).

3.2 Generation of cell lines stably expressing human NR1-1a / NR2A and NR1-1a / NR2B

3.2.1 General considerations

Compared to transient expression systems, cell lines stably expressing human recombinant NMDA receptors have been proved to represent a more reliable, convenient and robust heterologous expression system (Grimwood et al., 1996a; Uchino et al., 1997; Varney et al., 1996). They offer some advantages, since the expression level does not depend upon transfection efficiency limiting parameters such as purity and batch homogeneity of used DNA and other critical transfection conditions, e.g. pH of transfection buffer and medium, cell cycle and growth state of cultures (Graham and Van der Eb, 1973). Furthermore, these stable cell lines offer the possibility of a high throughput screening of compound libraries to discover compounds selectively acting on specific NMDA receptor subtypes. For these reasons, the generation of cell lines stably expressing different recombinant NMDA receptor subtypes was intended.

Since expression of recombinant NMDA receptors in non neuronal cell lines is known to induce cell death, an inducible expression system should be preferred. The mammalian expression vectors pMSGNR1-1a, pMSGNR2A and pMSGNR2B (see fig. 16) represent suitable expression systems, since the expression of the NMDA receptor subtypes is under the control of the mouse mammary tumor virus (MMTV) promotor. The transcription of cloned genes is stimulated by the addition of glucocorticoid hormones, such as dexamethasone, to the cell culture medium. The hormonal stimulation of the MMTV promotor activity is mediated by intracellular glucocorticoid receptors (Lee et al., 1981). These receptors are involved in the regulation of gene transcription by the nuclear translocation of the steroid–receptor complex and the subsequent association with the DNA which favours the binding of RNA polymerase II and the transcription of the encoded gene. Hence, the cell lines intended to be transfected with these constructs should possess glucocorticoid receptors. Therefore we chose the mouse *L(tk-)* fibroblasts as host cells (American Type Culture Collection CCL1.3)

Two transfection strategies were followed to obtain *L(tk-)* fibroblasts expressing functional NMDA receptors. As mentioned before, functional recombinant NMDA receptors consist of the assembly of NR1 and NR2 subunits. Hence, one transformation strategy was the co–transfection of either pMSGNR1-1a / pMSGNR2A or pMSGNR1-1a / pMSGNR2B. The

second strategy intended the co-transfection of pCISNR1-1a, containing the NR1-1a subunit of the rat constitutively expressed by human CMV promotor, and inducible pMSGNR2A or pMSGNR2B. It has been reported that the cell surface expression of the human NMDA receptor subunit NR1-1a requires the co-expression of the NR2 subunit (McIlhinney et al., 1996). Hence, the combination of these constructs should also lead to stable cell lines expressing functional NMDA receptors upon dexamethasone addition.

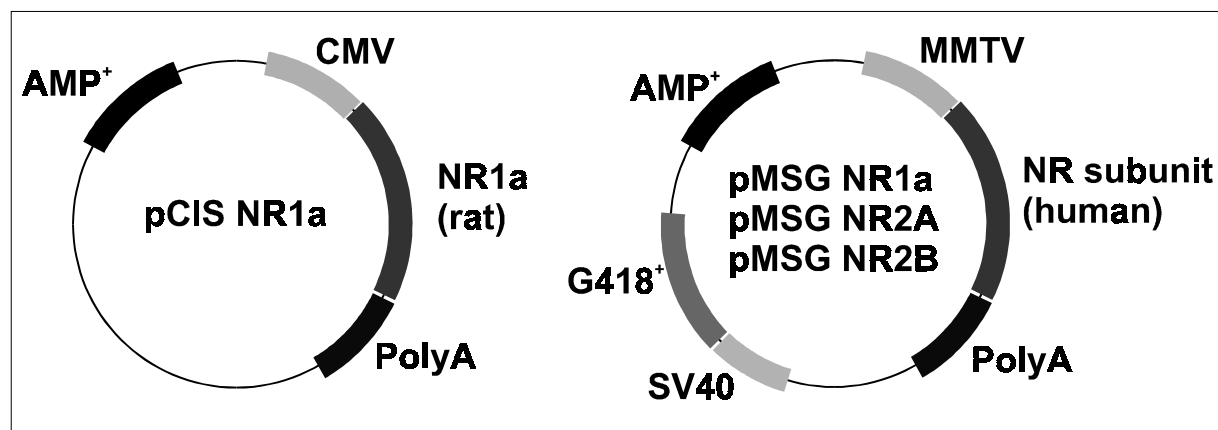


Fig. 16 *Constructs used for stable transfection of L(tk-) cells. In pMSG vectors the expression of cDNAs encoding the human NMDA receptor subunits NR1-1a, NR2A and NR2B is under the control of the dexamethasone inducible MMTV promotor. The SV40 splicing and polyadenylation sites provide RNA processing in mammalian cells whereas the E. coli neomycine resistance gene driven by the SV40 early promotor allows selection of transformants growing in media containing G418 antibiotics. Ampicillin resistance gene allows selection in E. coli strain (DH5 α). The pCIS vector contains the cDNA encoding the rat NR1-1a subunit whose expression is driven by the constitutive expressing enhancer–promotor sequence of the immediate early gene of the human cytomegalovirus (CMV). The vector also contains Poly A site and ampicillin resistance gene for prokaryotic selection. For eukaryotic selection the G418⁺ resistance of the cotransfected pMSGNR2A or 2B vectors was used.*

3.2.2 Transfection and cell cloning

To avoid increasing concentrations of L–glutamate within the cell culture medium due to hydrolysis of L–glutamine, L(tk-) cells were grown in MEM medium (lacking L–glutamine) supplemented with 2 mM alanylglutamine (Glutamax I[®] by Gibco), known to have a higher stability in the cell culture medium. MEM medium was further supplemented with 10% heat inactivated fetal calf serum (FCS), 0.5 mM sodium pyruvate, 100 U/ml penicillin and 100 μ g/ml streptomycin. In the following, this medium is designated as growth medium. Transfections were performed using the calcium phosphate precipitation method (for details

Results – generation of cell lines

see experimental procedures 5.1). In brief, 20 μ g of total DNA were used for the transfection of 5×10^5 cells. Co-transfection of NR1 and NR2 constructs was performed in an 1:5 ratio. 48 hours after transfection cells were exposed to increasing concentrations of geneticine (final 2mg/ml). To avoid selection due to NMDA receptor background expression, 100 μ M ketamine were included. After 4 weeks of selection, pool cultures were cloned using limiting dilution in 96 well plates (0.3 cells per well). After 10 to 14 days, various numbers of clones were obtained (see tab. 4).

Tab. 4 Number and code of clones obtained from limiting dilution

co-transfected vectors	Code	Number of clones
pMSGNR1-1a & pMSGNR2A	L12	62
pMSGNR1-1a & pMSGNR2B	L13	16
pCISNR1-1a & pMSGNR2A	L42	48
pCISNR1-1a & pMSGNR2B	L43	45

3.2.3 Clone screening

The obtained clones were monitored for NMDA receptor activity by detection of cell death 24 hours after induction of NMDA receptor expression. Cell toxicity assays were carried out in growth medium containing 5% FCS and 1 μ M dexamethasone using the CytoTox 96[®] cytotoxicity assay. This assay is based on the determination of lactate dehydrogenase (LDH) activity from cell culture supernatants. LDH represents a stable cytosolic enzyme, that is released into the cell culture medium upon cell lysis. To control response to NMDA receptor antagonists, the open channel blocker ketamine was included into clone screening at a final concentration of 500 μ M. To examine, whether mortality of clones could be triggered under increased agonist concentrations effects of 100 μ M L-glutamate and glycine were also tested. In brief, clones from 96 well plates were subdivided into 4 wells. Three wells were treated with either growth medium containing 5% FCS and 1 μ M dexamethasone or additionally 500 μ M ketamine or 100 μ M L-glutamate and glycine for 24 hours. The fourth well was maintained for further cultivation. Celltoxicity was determined after 24 hours. Clones showing highest cell death rates and response to ketamine inhibition were preselected. Results of preselected clones are given in table 5.

Results – generation of cell lines

Tab. 5 Results of preselected clones from cytotoxicity clone screening

clone	growth medium	Cytotoxicity [%]	
		500µM ketamine	100µM L-glu / gly
L12-B6	32.7	18.4	47.8
L12-B10	20.0	8.5	27.3
L12-D3	28.4	15.5	40.8
L12-D8	27.5	14.4	37.7
L12-D9	20.9	9.8	27.9
L12-E3	44.0	26.6	60.7
L12-E6	24.6	13.7	35.3
L12-E10	26.3	15.0	32.3
L12-F8	27.4	15.0	27.7
L12-G5	65.2	7.7	81.4
L12-G10	75.6	5.3	82.9
L13-C1	19.5	8.5	20.1
L13-C5	41.1	39.9	64.0
L13-E5	26.6	14.3	33.7
L13-E6	45.3	27.3	58.7
L13-F6	17.0	7.2	17.3
L42-C6	33.4	25.8	67.2
L42-D9	19.2	13.2	69.3
L42-E1	94.7	n.d.	95.5
L42-F5	62.1	42.7	72.4
L42-G6	52.9	21.9	47.8
L42-G8	23.3	6.0	20.3
L43-B9	23.6	9.8	24.6
L43-C4	28.7	23.8	38.2
L43-C10	22.0	20.10	25.4
L43-C11	31.6	12.3	26.1
L43-E8	26.1	10.2	33.4
L43-F8	15.6	10.0	20.9
L43-G4	18.3	11.2	18.7

Results – generation of cell lines

All preselected clones were frozen. Clones marked in tab. 5 were chosen for further pharmacological monitoring. Reproducibility of screening results and responsiveness of clones to various competitive and non-competitive antagonists were examined. The results of this second clone screening are given in fig. 17.

Four of twelve clones were dropped, since they showed neither upregulation of cell death upon exposure to dexamethasone (L13–E5, L42–D9, L43–B9) nor accurate response to the distinct antagonists or high unspecific cell death (L12–G5).

Clones L12–B6, L12–E3 and L12–G10 displayed an upregulation of cell death after treatment with 1 μ M dexamethasone in a range of approximately 35 to 55%. In contrast, cell mortality without dexamethasone was not increased (<10%), although 100 μ M L-glutamate and glycine were present. This indicates a lack of functional NMDA receptors in the absence of dexamethasone. The open channel blocker ketamine (100 μ M) and MK801 (100 μ M) as well as the competitive antagonist (R/S)–AP5 (100 μ M) and glycine site antagonist DCKA (100 μ M) reduced cell death to control levels. Response to antagonists acting at distinct recognition sites of the NMDA receptor channel complex demonstrated the functionality of expressed NMDA receptors in these three cell lines. It also shows, that cell death occurring after heterologous expression of NMDA receptors in non-neuronal cell lines is caused by their functional assembly within the plasma membrane, since the cell penetration of the hydrophilic compound (R/S)–AP5 is unlikely and its recognition site has been determined to be extracellularly located (Laube et al., 1997). Addition of 100 μ M L-glutamate and glycine to dexamethasone failed to significantly increase the cell mortality. This could be explained by saturated concentrations of agonists within the incubation medium (MEM cont. 10% FCS).

Anegawa et al. (1995) reported L–glutamate levels of ~180 μ M determined in MEM (10% serum) from cell cultures 24 hours post transfection. Although this medium contained L–glutamine it is likely that supplemented serum already provides high concentrations of L–glutamate and glycine. This hypothesis is confirmed later on, as it was shown that cell death is strictly dose dependent on L–glutamate in the absence of serum. Even the second transfection strategy combining constitutively expressing pCISNR1-1a construct and dexamethasone inducible pMSGNR2A vector led to clones (L42–C6, L42–E1, L42–F5) which showed an increased cell mortality upon exposure to dexamethasone compared to control.

Results – generation of cell lines

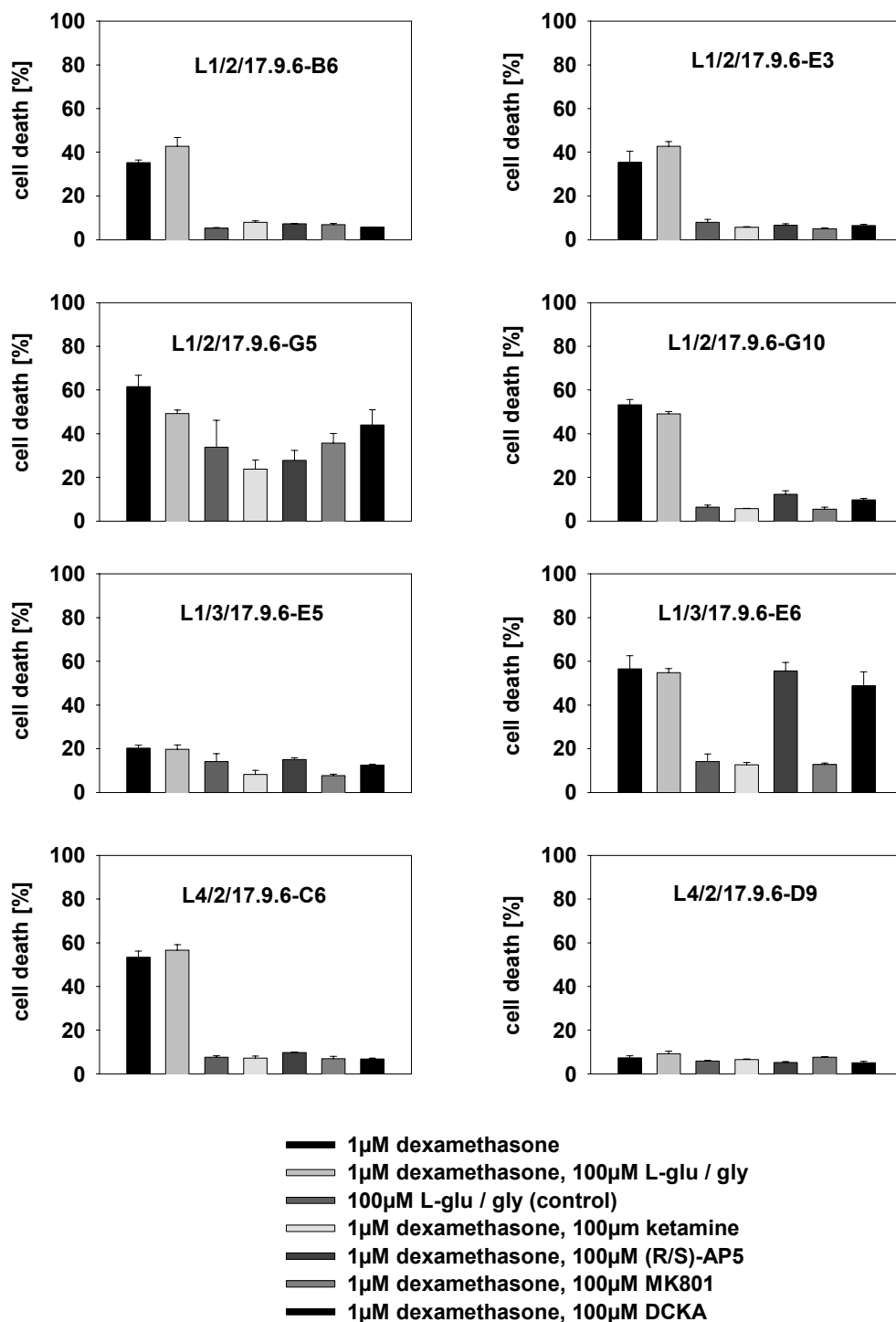


Fig. 17 Screening of selected clones

Clones, cultured in growth medium containing 5% FCS, were exposed to (a) 1µM dexamethasone, (b) 1µM dexamethasone and 100µM L–glutamate / glycine, (c) 100µM L–glutamate / glycine w/o dexamethasone (control), (d) 1µM dexamethasone and 100µM ketamine, (e) 1µM dexamethasone and 100µM (R/S)-AP5, (f) 1µM dexamethasone and 100µM MK801, (g) 1µM dexamethasone and 100µM DCKA. Cell death was measured after 24 hours.

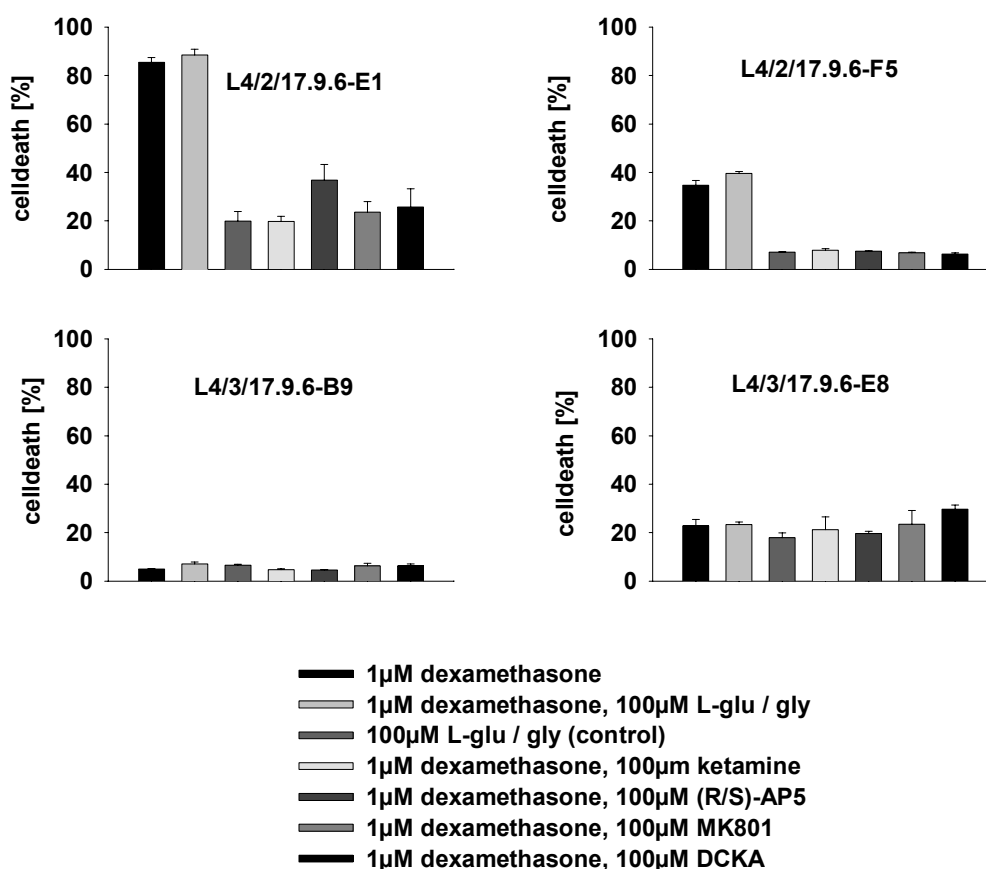


Fig. 17 Screening of selected clones (continued)

Clones, cultured in growth medium containing 5% FCS, were exposed to (a) 1µM dexamethasone, (b) 1µM dexamethasone and 100µM L–glutamate / glycine, (c) 100µM L–glutamate / glycine w/o dexamethasone (control), (d) 1µM dexamethasone and 100µM ketamine, (e) 1µM dexamethasone and 100µM (R/S)–AP5, (f) 1µM dexamethasone and 100µM MK801, (g) 1µM dexamethasone and 100µM DCKA. Cell death was measured after 24 hours.

The observed NMDA receptor mediated cell death was in the range of 35 to 85%. Control levels of L42–C6 and L42–F5 were comparable to those of L12–clones (<10%), whereas L42–E1 displayed a higher rate of unspecific cell death (20%). Similar to L12–clones, L42–cells, exposed to selective NMDA receptor antagonists, displayed a viability comparable to control cells (except the treatment of L42–E1 with 100µM (R/S)–AP5 which was slightly increased to control). The similarity between the pharmacological profiles of L12– and L42–clones demonstrates the possibility of functional assemblies between subunits cloned from rat and human. This is predicted by the great amino acid sequence identity between rat and human NR1 subunits (95 to 100%).

Results – generation of cell lines

L42-clones showed no increased mortality while stimulated in growth medium lacking dexamethasone. This is quite remarkable, since the rat NR1-1a subunit is under the control of the constitutive expressing human CMV promotor and should be expressed even in dexamethasone free medium. Cell death in L42-cells only occurred after exposure to dexamethasone and subsequent induction of subunit NR2A expression. This fact supports the finding of McIlhinney et al., who reported that successful surface expression of recombinant NMDA receptors in heterologous cell systems depends on the co-expression of both NR1 and NR2 subunits. Single NR1 expression does not yield to functional receptors (McIlhinney et al., 1996).

Unfortunately, the rat NR1-1a / human NR2B expressing clone L43-E8 showed only unspecific increase in cell death upon exposure to dexamethasone since cell death was not significantly decreased by NMDA receptor antagonists. Since even control levels were increased, this clone was dropped. In contrast, clone L13-E6 expressing subunits hNR1-1a and hNR2B, both under the control of the MMTV promotor, displayed an increase in cell mortality after induction of receptor expression with dexamethasone which was blocked by application of open channel blockers ketamine and MK801. No or only slight response was observed to 100 μ M (R/S)AP5 and DCKA. Since heterologous NMDA receptors consisting of subunits NR1-1a and NR2B are supposed to exhibit an agonist preferring status, the lacking response to competitive antagonists is caused by a reduced affinity of these compounds. As shown later, we demonstrate that a competitive antagonism at the glutamate and glycine recognition sites takes place under defined agonist concentrations.

From these results it can be summarised, that the co-transfection of inducible vectors pMSGNR1-1a and pMSGNR2A or pMSGNR2B as well as the co-transfection of constitutive expressing pCISNR1-1a (rat) and inducible pMSGNR2A led to cell lines stably expressing functional recombinant NMDA receptors. These cell lines provide a functional in vitro test system for competitive antagonists and channel modulating compounds based on the prevention of cell death mediated by heterologous NMDA receptor expression. For further characterization by RT-PCR analysis, immunoblotting, immunocytochemistry and calcium imaging, clones L12-G10 and L13-E6 were chosen.

3.3 Characterisation of clones L12-G10 and L13-E6

For further characterization of selected clones L12-G10 and L13-E6 RT-analysis, immunoblotting and immunocytochemistry of subunit NR1-1a and calcium imaging were performed. The results of these experiments are given in the next four sections.

It should be added, that the immunological characterization was restricted to NR1 subunits since it has been suggested that heterologously expressed NMDA receptor subunits are assembled in the endoplasmatic reticulum and that co-synthesis of the subunits is necessary for their successful cell surface targeting and functionality (McIlhinney et al., 1998). In addition a C-terminal truncation of NR2 subunits was reported which complicates the immunological detection of NR2 subunits; so far all commercially available antibodies were directed against a C-terminal polypeptide region.

3.3.1 RT-PCR analysis

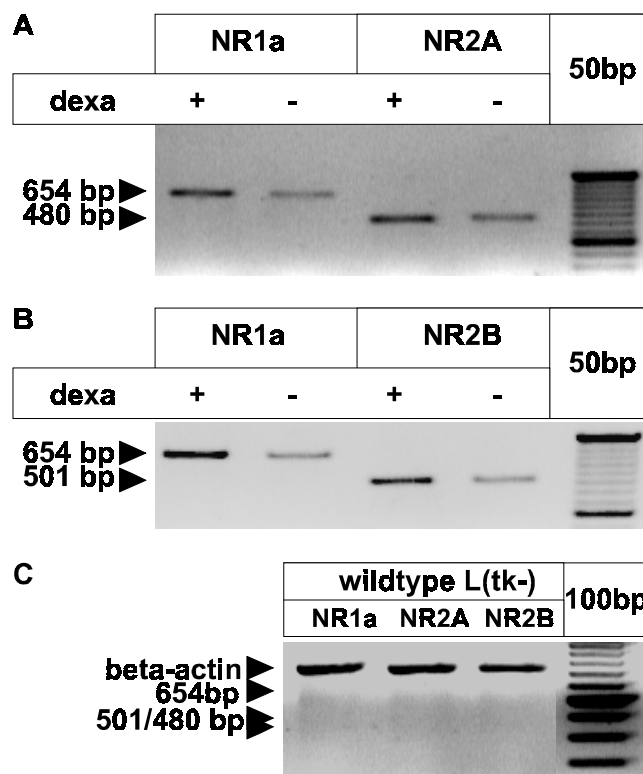
RT-PCR analysis of NMDA receptor mRNA, isolated from clones cultured for 12 hours in growth medium containing 2 μ M dexamethasone and 100 μ M ketamine, was performed for clone L12-G10 and L13-E6. Isolated RNA was reverse transcribed into cDNA using d(T)₁₂₋₁₈ priming. Reverse transcription of mature and immature transcripts was followed by PCR with primers corresponding to the distinct transfected cDNAs. As control for successful RNA isolation, amplicons from PCR with beta-actin priming were subjected to agarose gel electrophoresis. As shown in fig. 18, RT-PCR analysis revealed the transcription of transfected subunits in both clones. For clone L12-G10, amplicons in the predicted size of 654 bp (NR1-1a) and 480 bp (NR2A) were detected (fig. 18-A). Clone L13-E6 displayed the predicted 654 bp signal for NR1-1a and 501 bp for NR2B (fig. 18-B). Transcripts of the predicted size were also detected in uninduced cells but not in untransfected wildtype cells (fig. 18-C). To estimate the induction of transcription by dexamethasone, densitometric volume analysis was applied resulting in a 5-fold increase for hNR1-1a transcripts and a 2.3-fold increase for hNR2A in L12-G10. For clone L13-E6, ratios of 4.8 for hNR1-1a and 3.5 for hNR2B were calculated, respectively. This finding indicates an upregulation of mature transcripts for both transfected subunits. Hence, it is likely that exposure to glucocorticoids induces a co-synthesis of the NR1 and the NR2 subunits necessary for their functional assembly and cell surface targeting. The observed background transcription in uninduced clones does obviously not lead to detectable amounts of protein (see section 3.3.2). Additionally, uninduced cells cultured in growth medium lacking ketamine for more than 24

Results – characterization of clones

hours appeared healthy and no increased cell death rate could be detected, whereas dexamethasone treated cultures did undergo cell death.

Fig. 18 RT-PCR analysis

To verify the transcription of human NMDA receptor cDNA in transfected clones RT-PCR analysis was performed. Cells were cultured for 12 hours in growth medium \pm 2 μ M dexamethasone. Amplicons in the predicted size for hNR1-1a (654 bp), hNR2A (480 bp) and hNR2B (501 bp) were determined for the respective cell lines (A–B). Under treatment with dexamethasone clones showed an increase in transcription rate. Densitometric volume analysis leads to a 5-fold increase for hNR1-1a transcripts and a 2.3-fold increase for hNR2A in L12-G10 cells. For clone L13-E6 ratios of 4.8 for NR1-1a and 3.5 for NR2B were calculated. In wildtype L(tk-) cells no transcripts for hNR1-1a, hNR2A or hNR2B were detected (C).



3.3.2 Immunoblotting

Western blot analysis was performed using a monoclonal affinity purified mouse anti-NR1 antibody which was directed against the N-terminal region of rat NR1 (amino acids 1 – 564). L12-G10, L13-E6 and WT-cells were cultured in growth medium \pm 4 μ M dexamethasone and 100 μ M ketamine for 24 hours. Aliquots of solubilized membrane fractions (40 μ g) were subjected to gel electrophoresis. As positive control 5 μ g of rat brain membrane protein were probed.

In both clones a \sim 116 kDa polypeptide was recognised (fig. 19) which is in good agreement with the estimated molecular mass of rat NR1 transiently expressed in the human embryonal kidney cell line Hek 293 (Chazot et al., 1992), unglycosylated human NR1-1a (103.5 kDa) and the detected NR1 subunits in rat brain membranes. The slightly increased molecular weight compared to rat NR1 could be caused by different glycosylation. The observed lower molecular weight bands may be either proteolytic fragments or unglycosylated forms of the protein. In control lanes, no protein was detected neither in uninduced clone cultures nor in wildtype cells.

Results – characterization of clones

Fig. 19 Immunoblots of induced, uninduced clones and wildtype cells

Cells were cultured for 24 hours in growth medium containing 4 μ M dexamethasone and 100 μ M ketamine. Aliquots of solubilized membrane protein (40 μ g) were probed with N-terminal directed monoclonal mouse anti-NR1 antibody. As positive control 5 μ g rat brain membrane were loaded.

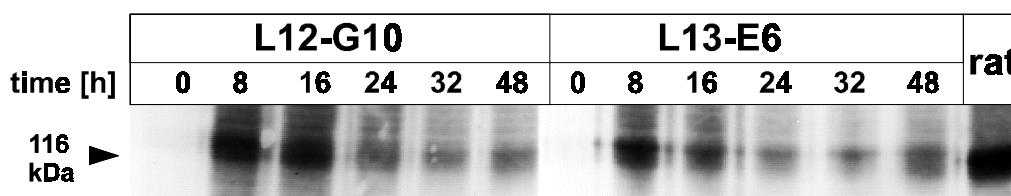
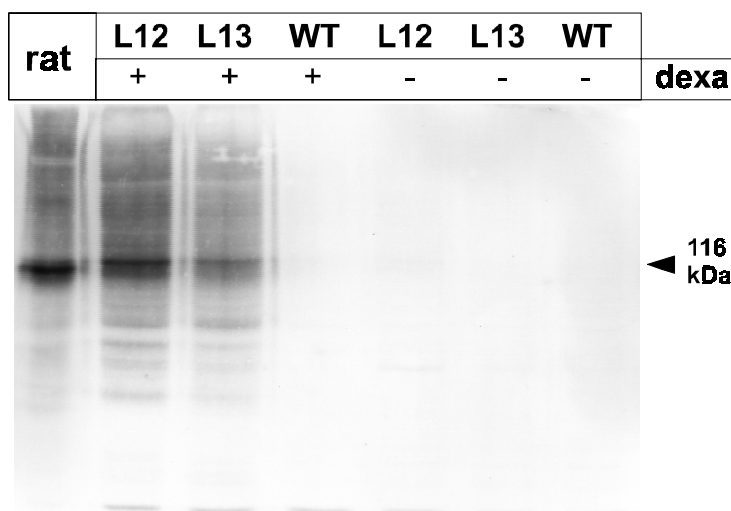


Fig. 20 Time course of hNR1-1a protein expression in L12-G10 and L13-E6 cells
Clones were cultured in growth medium containing 4 μ M dexamethasone and 100 μ M ketamine for the indicated time intervals. Aliquots of solubilized membrane protein (60 μ g) were loaded and NR1-1a subunit protein was detected with N-terminal directed monoclonal mouse anti-NR1 antibody (positive control 5 μ g rat brain membrane).

To examine the time course of hNR1a expression, cells were cultured in growth medium containing 4 μ M dexamethasone and 100 μ M ketamine and harvested after 0, 8, 16, 24, 32 and 48 hours. Aliquots of solubilized membrane protein (60 μ g) were probed (see fig. 20). As positive control, 5 μ g of rat brain membrane protein were subjected to gel electrophoresis. Surprisingly, both clones revealed a maximum protein amount after 8 hours of treatment with dexamethasone. Between 16 and 48 hours declining amounts of NR1 were detected.

In summary, results from immunoblotting revealed the expression of a 116 kDa protein detected with the monoclonal mouse anti-NR1 antibody. The size of the protein is consistent with the predicted molecular weight from the deduced amino acid sequence (103.5 kDa) and the size from the NR1 subunits detected in rat brain membranes. The maximum amount of protein is expressed between 8 and 16 hours after induction of receptor expression. This time course is consistent with the results from the RT-PCR analysis which revealed only 5 fold increase of hNR1-1a transcripts compared to background expression after 12 hours and may

also account for the lack of specific [³H]-MK801 binding at membranes from cells differentiated with dexamethasone / ketamine for 24 to 72 hours.

3.3.3 Immunocytochemistry

To investigate the cellular localization of the expressed recombinant NMDA receptor subunits, confocal laser microscopy was applied after immunofluorescence labelling with Cy-3 coupled rabbit anti-goat serum. As primary antibody we choose a polyclonal goat anti-NR1 serum which was directed against an intracellularly located C-terminal epitope of the NR1 subunit. The monoclonal mouse anti-NR1 antibody directed against the N-terminal region of NR1, which was used for immunoblotting, could not be used due to unspecific binding to L(tk-) cells.

Cell lines, grown on cover slides, were permeabilized and fixed with ice cold methanol / acetic acid (90:10). Receptors were labelled with goat anti-NR1 serum (1:500) and rabbit anti-goat serum (1:200) conjugated with Cy3 fluorescence dye. Fluorescence images were obtained by confocal laser microscopy.

As shown in fig. 21, strong fluorescence signals were observed within the plasma membrane indicating the cell surface targeting of the expressed NR1 subunits. Specificity of staining was verified by the lack of fluorescence signals from immunostained wildtype cells.

In contrast to other ion channels, e.g. AMPA or P2X receptors, which assemble to functional homo-oligomeric channels if expressed as single subunits, NMDA receptors seem to be different. As mentioned above, it has already been shown, both for transient and for stable heterologous transfection of recombinant NMDA receptor subunits, that cell surface expression of the NR1-1a subunit is found only in cells expressing both NR1 and NR2A subunits (McIlhinney et al., 1996). Same authors reported intracellular inclusions of NR1-1a subunits within the endoplasmatic reticulum of NR1-1a transfected COS cells which were lost when NR2A was co-transfected with NR1-1a (McIlhinney et al., 1998). This suggests that the two subunits are first associated in the ER. This hypothesis was supported by the co-precipitation of NR2A with NR1-1a in cells where normal transport out of the ER was blocked by Brefeldin-A (which disrupts transfer of proteins from the ER to the golgi apparatus within minutes after its addition to cells).

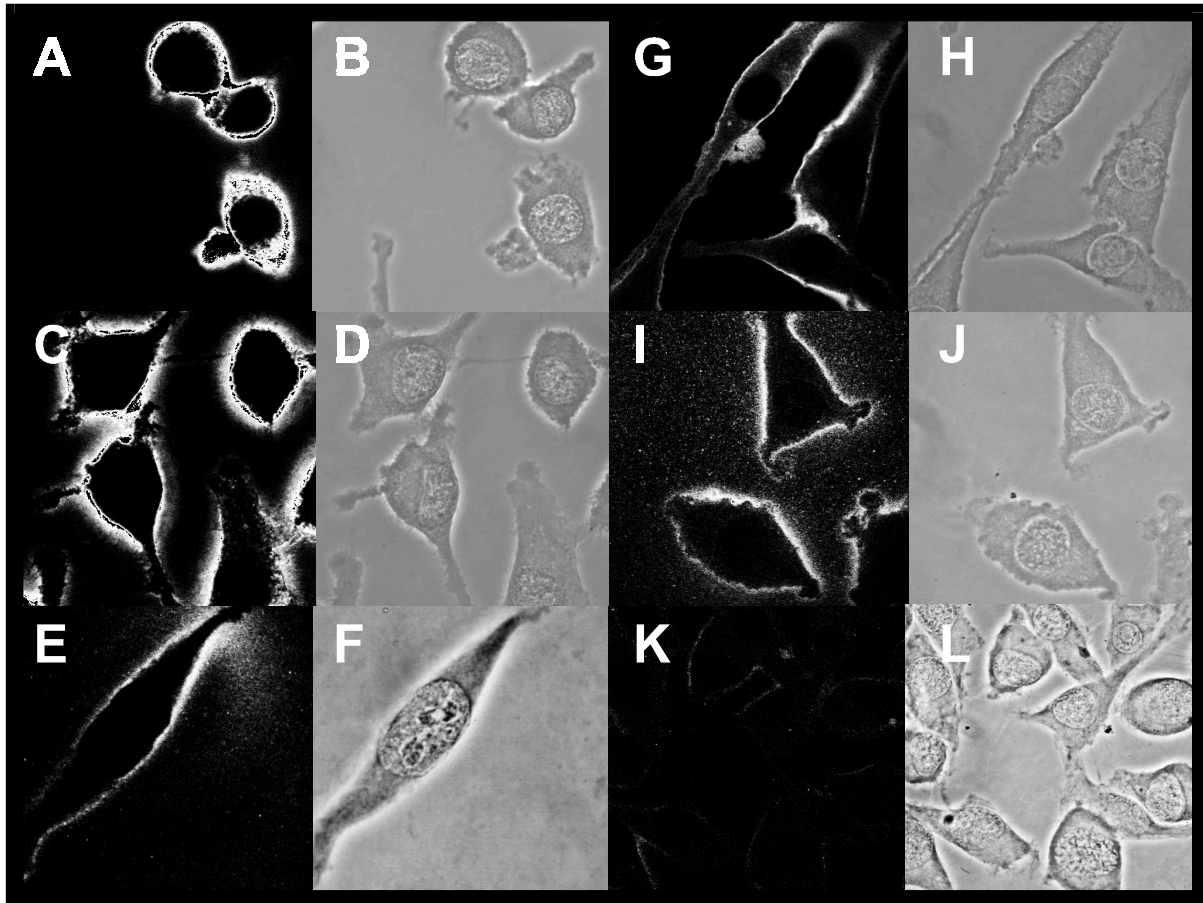


Fig. 21 *Immunofluorescent staining of subunit NR1-1a in permanently transfected cell clones.* Cells were differentiated with 2 μ M dexamethasone for 24 hours. After fixation and permeabilisation cultures were immunofluorescence labelled with primary goat anti-NR1 (1:500) and Cy3-conjugated rabbit anti-goat IgG (1:200) and imaged by confocal laser microscopy (ex 550nm; em 598nm). Fluorescence and phase contrast images of the following cultures are presented: L12-E3 (A, B), L12-G10 (C, D), L13-E6 (E, F), L42-C6 (G, H), L43-E8 (I, J), wildtype (K, L)

This requirement of NR1-1a association to NR2 for full surface expression in mammalian cells may not be valid for neurons, but there is some evidence that cell surface expression and functional channel formation of native NMDA receptors is regulated by the synthesis of the NR2 subunit family. Immunohistochemical studies found substantial NR1 immunoreactivity in neuronal cell bodies (Petralia et al., 1994b). Using NR2A/NR2B specific antibody same authors reported higher levels of dendritic staining than for cell body staining (Petralia et al., 1994a).

Supported by these findings it is most likely, that the fluorescence signals at the cell surface, detected by immunofluorescence labelling of NR1-1a subunits, result from functional hetero-oligomeric channels.

3.3.4 Calcium imaging

To confirm the functionality of expressed ion channels, calcium imaging was performed using the calcium sensitive fluorescence dye fluo-4 acetoxymethylester and confocal laser microscopy. Cells were plated in growth medium containing 4 μ M dexamethasone and 100 μ M ketamine for 16 to 20 hours. For dye loading cultures were treated with 1 μ M fluo-4 acetoxymethylester. Removal of ketamine enables calcium influx via NMDA receptor channels after stimulation with agonists. A set of functional experiments was performed with both clone L12–G10 and L13–E6.

Stimulation of clone L12–G10 with 100 μ M L–glutamate and glycine led to a rapid increase in intracellular calcium ($[Ca^{2+}]_i$) concentration as indicated by increasing fluorescence signal intensity (fig. 22-B to D). As control, an increase in $[Ca^{2+}]_i$ was elicited by 10 μ M ionomycin (fig. 22-A). Application of NMDA receptor specific open channel blockers abolished the increased $[Ca^{2+}]_i$. After exposure to 200 μ M ketamine (fig. 22-C) or 10 μ M MK801 (fig. 22-D) fluorescence signal intensity was reduced to starting levels. Receptors were also stimulated by the co–application of 200 μ M N-methyl-D-aspartate (NMDA) (fig. 22-E) or 1000 μ M L-aspartate with 100 μ M glycine (fig. 22-F). NMDA stimulation was inhibited by 10 μ M MK801 (fig 22-E). Addition of 100 μ M L-glutamate did not trigger response to 1000 μ M L-aspartate (fig. 22-F) indicating already saturated conditions after L–aspartate application. For clone L13–E6, a similar set of experiments was performed. Control experiments revealed the stability of fluorescence signals over the experimental interval in the absence of L–glutamate (fig. 23-A). Calcium influx was then elicited by the addition of 10 μ M ionomycin. In functional experiments with 100 μ M L–glutamate and glycine, a steep increase in $[Ca^{2+}]_i$ via stimulated NR1-1a / NR2B receptors was observed (fig. 23-B to D). Similar to L12–G10 cells increased $[Ca^{2+}]_i$ was abolished by the addition of 100 μ M ketamine (fig. 23-C) or 10 μ M MK801 (fig. 23-D). An increase of L–glutamate concentration to 200 μ M did not trigger peak level of fluorescence signal (fig. 23-E) which may be explained by either saturated agonist levels or by saturation of fluorescence dye by calcium. Subsequent application of competitive antagonist (R/S)–AP5 (400 μ M) reduced the increased $[Ca^{2+}]_i$ to approximately 50%. Figure 23-F demonstrates the calcium response of native glutamate receptors from mouse CGC cells to 100 μ M L–glutamate (data provided by E. Fava, Inst. for Molecular Toxicology, University of Konstanz). It should be noted that this increase in $[Ca^{2+}]_i$ is caused by the activation of distinct glutamate receptors and therefore represents the sum of calcium influx via NMDA receptors and release of calcium from intracellular stores via phospholipase C coupled mGluR1 / 5 stimulation.

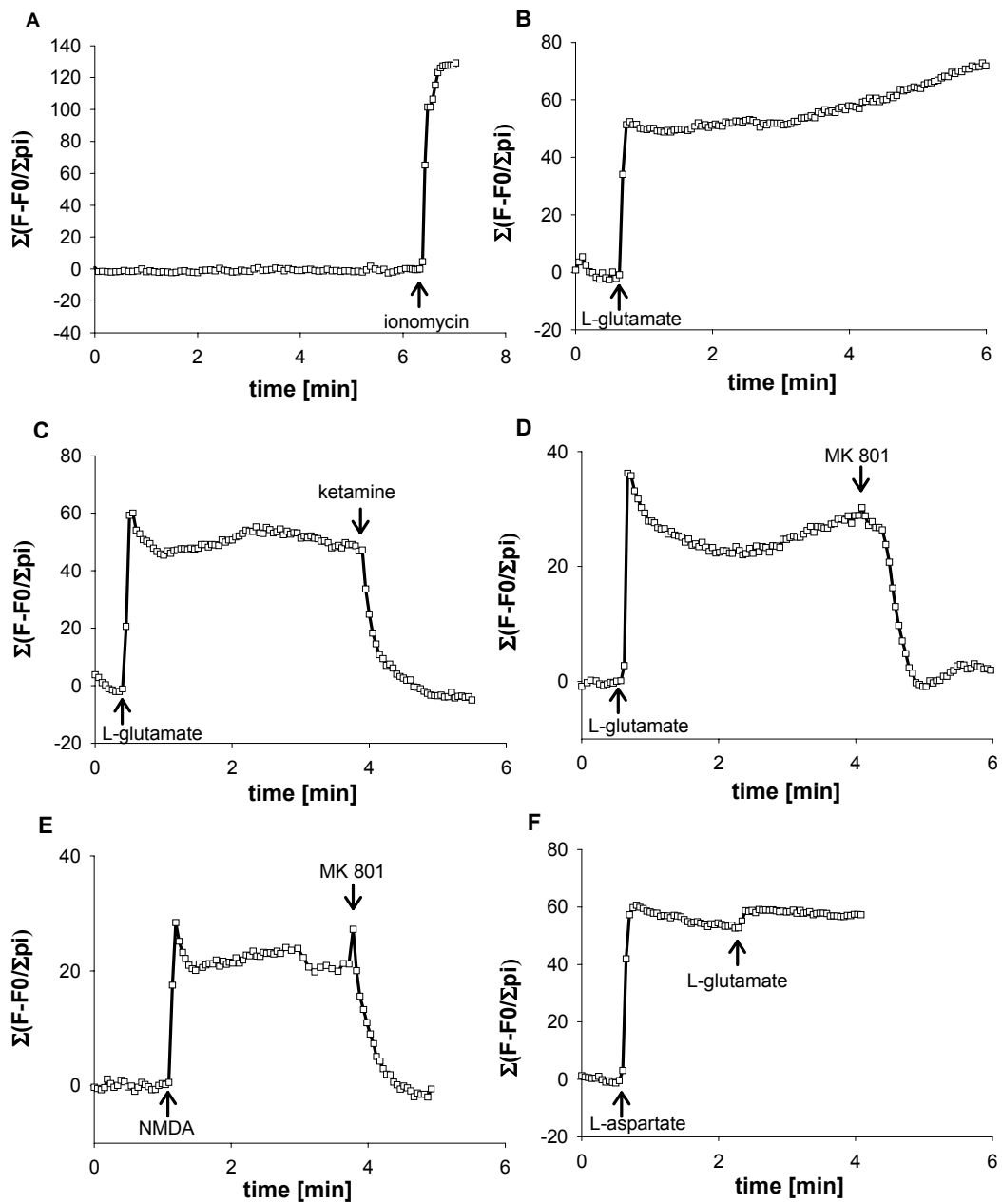


Fig. 22 Increase in intracellular calcium concentration via *hNR1-1a* / *hNR2A* expressed in L12-G10 cells

Cells were plated on coverslips in growth medium containing 4 μ M dexamethasone and 100 μ M ketamine for 16 to 20 hours. For dye loading, the cultures were treated with 1 μ M fluo-4 acetoxymethylester in original medium at 37°C. To remove ketamine, cells were washed 3 times. All experiments were performed in CSS pH 7.8 containing 50mM KCl, 1.8mM CaCl₂ and 100 μ M glycine. Presented data are mean values (n=6): (A) control (10 μ M ionomycin); application of 100 μ M L-glutamate (B-E), 200 μ M ketamine (C), 10 μ M MK801 (D and E), 200 μ M N-methyl-D-aspartate (E) and 1000 μ M L-aspartate (F).

Results – characterization of clones

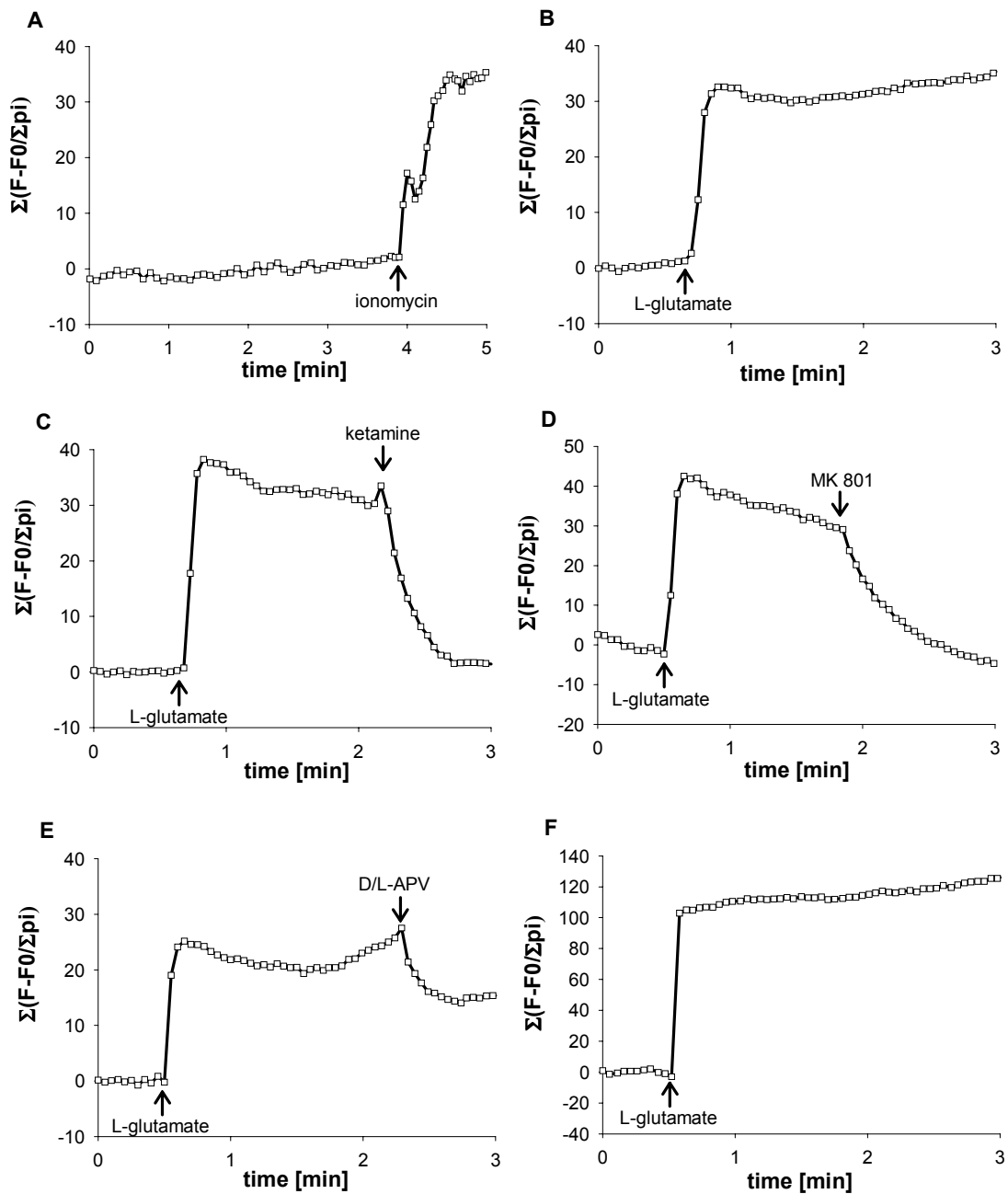


Fig. 23 Increase in intracellular calcium concentration via *hNR1-1a* / *hNR2B* expressed in L13-E6 cells and via native NMDA receptors in CGC cells. Clones were plated on coverslips in growth medium containing 4 μM dexamethasone and 100 μM ketamine for 16 to 20 hours. For dye loading, the cultures were treated with 1 μM fluo-4 acetoxymethylester in original medium at 37°C. To remove ketamine, cells were washed 3 times. All experiments were performed in CSS containing 50mM KCl, 1.8mM CaCl₂ and 100 μM glycine. Presented data are mean values (n=6): (A) control (10 μM ionomycin). Application of 100 μM L-glutamate (B-D), 200 μM ketamine (C), 10 μM MK801 (D), 200 μM L-glutamate and 400 μM (R/S)-AP5 (E). CGC cells were stimulated with 100 μM L-glutamate (F). CGC cell data were provided by E. Fava (Inst. for Molecular Toxicology, University of Konstanz).

3.4 Cell death based in vitro assays

3.4.1 LDH assay mixture

For economic reasons, a lactate dehydrogenase (LDH) assay mixture which is suitable for the performance of cell culture cytotoxicity assays was developed.

The developed assay is based on the same principle as the CytoTox 96[®] assay which was successfully used in clone screenings. LDH is a stable cytosolic enzyme that is released into the cell culture medium upon cell lysis. Released LDH activity in cell culture supernatants is quantitatively measured with a coupled enzymatic assay resulting in the conversion of a tetrazolium salt (INT) into a red formazan product. The formation of formazan is stopped through a pH shift by the addition of acetic acid. The amount of color formed, measured at 490nm, is proportional to the number of lysed cells. The general chemical reactions are as follows: Oxidation of L-lactate to pyruvate (catalysed by LDH) results in the generation of NADH which in turn reduces the tetrazolium salt to the red colored formazan (catalysed by diaphorase). The LDH-assay mixture was freshly prepared before each assay and contained approximately 1% sodium L-lactate, 0.1% NAD⁺, 75mM phosphate buffer (PB) pH 7.4, 0.08% BSA, Diaphorase (18 U / ml) and 0.4 % INT (for details see experimental procedures 5.4.1).

Initial studies with the developed LDH assay mixture displayed linear kinetics for the LDH dependent formation of formazan (fig. 24).

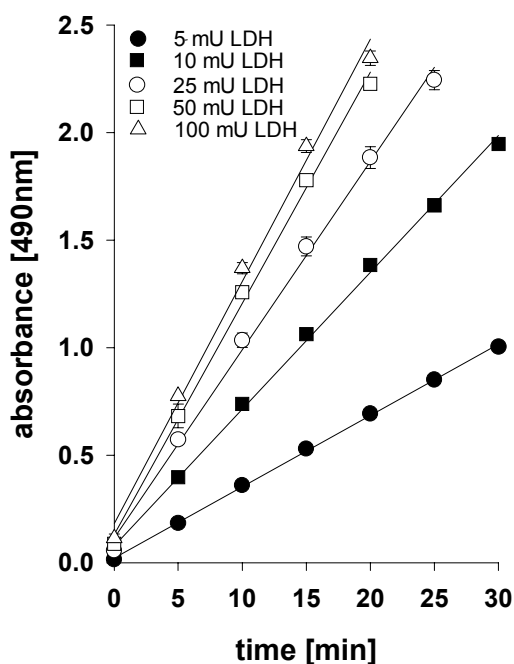


Fig. 24 Time course of formazan formation

50µl aliquots of samples which contained 5, 10, 25, 50 and 100 mU LDH (from rabbit muscle in 0.1M phosphate buffer pH 7.4) were incubated with 50µl assay mixture and absorbance was recorded at the indicated intervals.

Results – cell death based in vitro assays

A plot of the obtained slopes ($\Delta\text{absorbance} / \Delta\text{time}$) against spiked LDH activity (fig. 25-A) shows, that the rate of formazan formation varies with the LDH activity. The plot represents a function, that fits to the classical *Michaelis-Menten equation* ($r = 0.998$):

$$V = V_{\max} * [S]/([S] + K_M)$$

Hence, the provided amount of reduced NADH as a required substrate of diaphorase, is directly proportional to the added LDH activity. All other substrates are included in saturated concentrations under the described conditions. A *Lineweaver-Burk plot* of the obtained data allowed the estimation of a pseudo Michaelis constant of the used diaphorase for LDH (fig. 25-B), which was in the range of approximately 17 mU LDH / 50 μ l. From these data we conclude that, for the used activity of diaphorase (18 U / ml mixture), the time dependent formation of formazan is almost linearly proportional to LDH activity, if the sample contains less than 10mU LDH / 50 μ l.

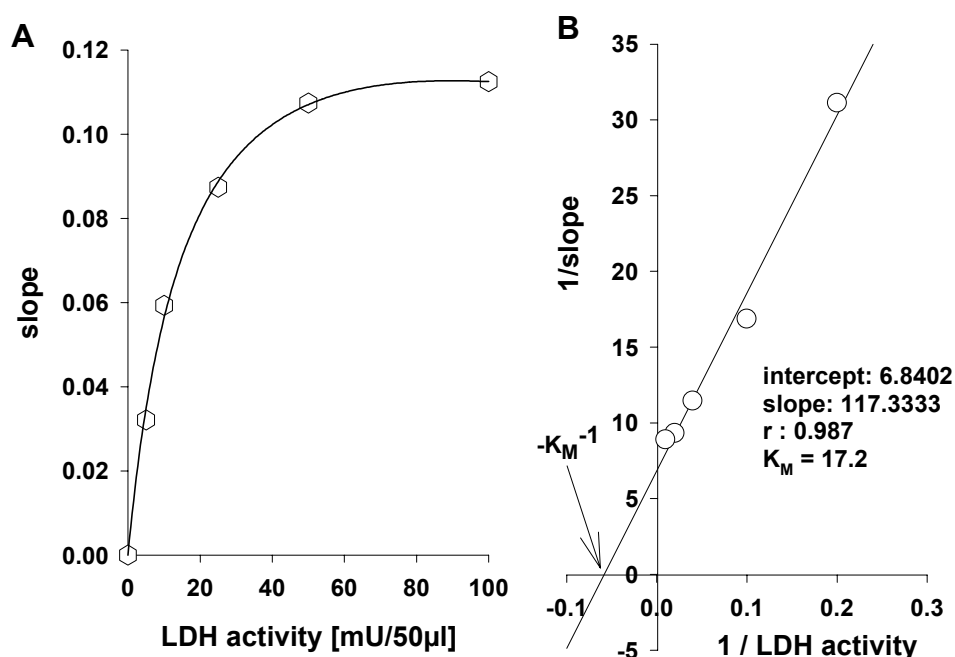


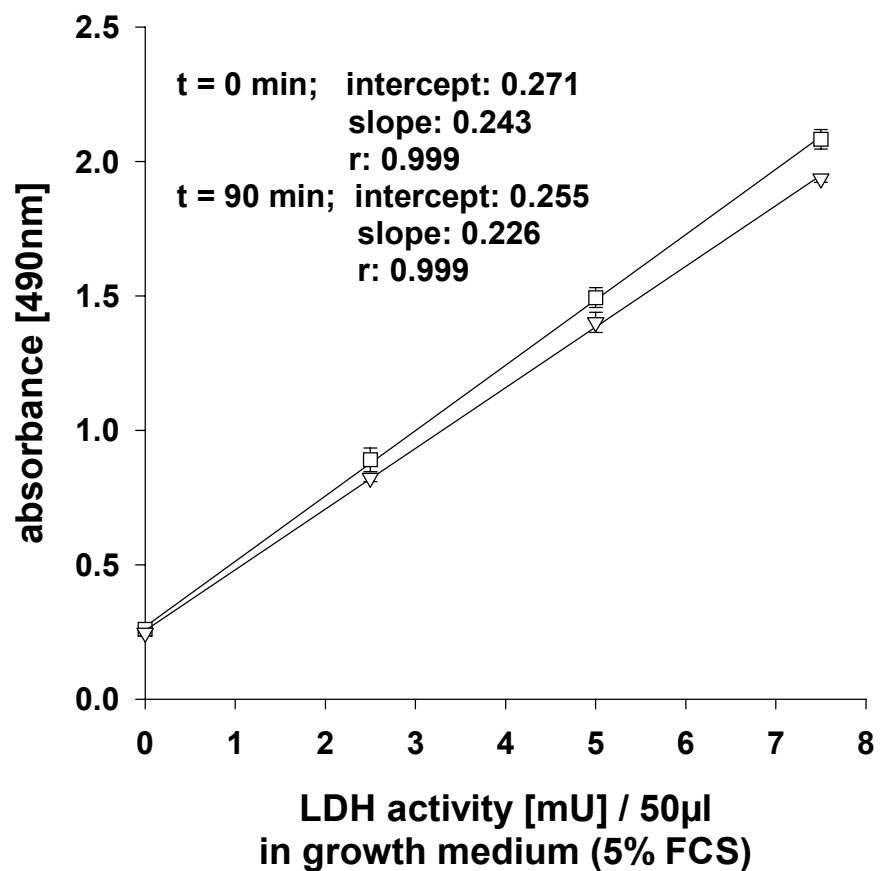
Fig. 25 Michaelis-Menten kinetics

(A) Slopes from graphs in fig. 1 dependent on the added LDH activity fitted to the Michaelis Menten equation. (B) Lineweaver-Burk plot of data in (A). The interception on the horizontal axis represents $-K_M^{-1}$.

Also in MEM containing 5% FCS, the amount of formed formazan is directly proportional to the spiked LDH activity (fig. 26). The high interception of ~ 0.2 derived from LDH within the supplemented FCS and is decreased to ~ 0.08 under the use CSS in the differentiation model. Formazan containing solutions exhibited a high stability over a period of 90 min if stored under light protection, since the parameters of the standard curve only slightly decreased under maintenance of linearity (fig. 26).

Fig. 26 **Linearity and stability of LDH dependent formazan formation**

Indicated LDH activity (0, 2.5, 5, 7.5mU) from rabbit muscle was spiked to growth medium containing 5% FCS. The resulting solutions were measured as triplicates. Absorbance was recorded immediately after the addition of stop solution ($t = 0$) or after a 90 min storage under light protection ($t = 90$).



To demonstrate the accuracy and precision of the developed assay, we quantified quality control samples (QCs; n = 9) which contained 7, 4.5 and 1.5mU LDH / ml growth medium (5% FCS). The amount of LDH activity within the samples was recalculated using a standard curve (0 – 7.5mU LDH). For both, precision and accuracy, we obtained satisfying results with coefficients of variation $< 4\%$ and relative errors $< 3\%$ (fig. 27).

Results – cell death based in vitro assays

	mean (n=9)	standard deviation	coefficient of variation	relative error	recovery
QC 7	6.90 mU LDH	0.13	1.9 %	1.4 %	98.6 %
QC 4.5	4.41 mU LDH	0.12	2.7 %	2 %	98.0 %
QC 1.5	1.54 mU LDH	0.06	3.9 %	2.7 %	102.7 %

calibration	0-7.5mU
intercept	0.211
slope	0.194
r	0.999

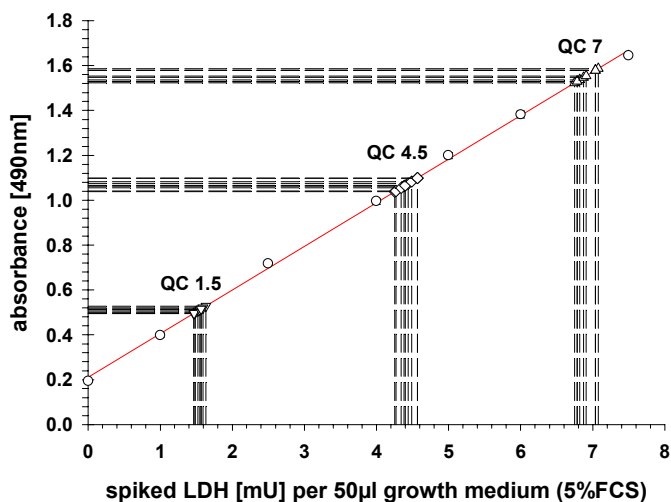


Fig. 27 Accuracy and precision of developed LDH assay QCs containing 1.5, 4.5 and 7mU LDH / ml growth medium (5% FCS) were assayed (n = 9) and the amount of added LDH was recalculated using a standard curve (0 - 7.5mU LDH).

To obtain a suitable total LDH activity < 10mU / 50µl cell culture supernatant, 15×10^3 L(tk-) cells were seeded overnight prior to receptor induction and the incubations were performed in a final volume of 200µl / well.

3.4.2 Cell culture models

Two models for the in vitro testing of compounds have been developed. Both models are based on the determination of cell death mediated by NMDA receptor activity using the quantification of released LDH from cell culture supernatants.

The first model, designated as **induction model**, is characterized by the simultaneous induction of NMDA receptor expression by addition of dexamethasone and application of increasing concentrations of NMDA receptor antagonists under sterile conditions at 37°C and 5% CO₂. As shown in fig. 28, induction of NMDA receptor expression leads to a steep increase in LDH release, as a parameter for the extent of NMDA receptor induced cytotoxicity. The increased LDH release started approximately 10 hours after receptor induction and reached a plateau after 20 hours. The addition of 50mM potassium triggered this L-glutamate mediated cytotoxicity whereas uninduced cultures remained unaffected. This

Results – cell death based in vitro assays

effect of potassium indicates a dependency of receptor activity upon membrane depolarisation.

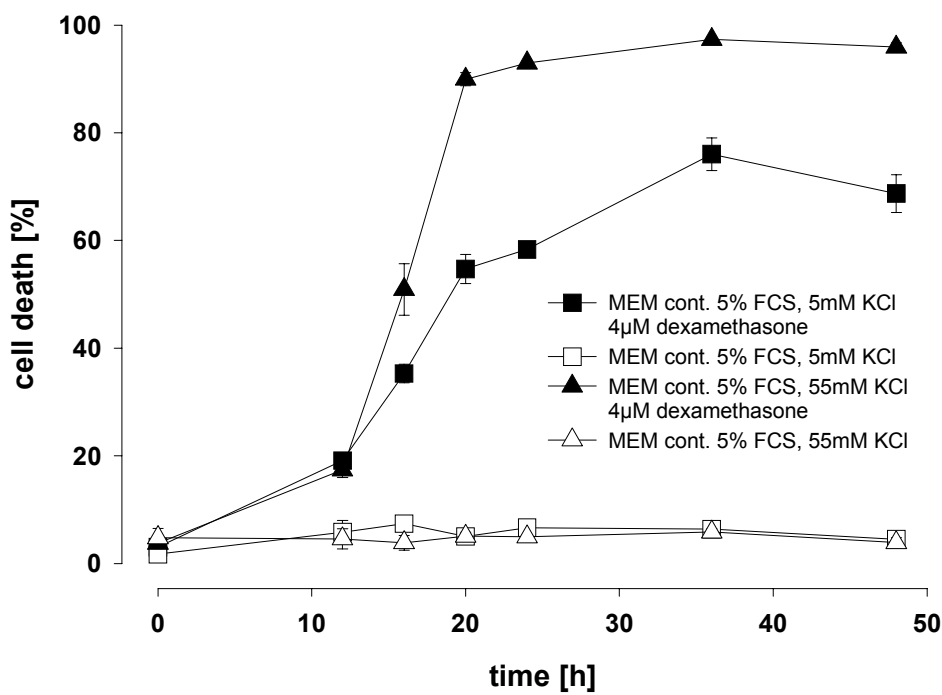


Fig. 28 LDH release after the induction of NMDA receptor expression

L12-G10 cells were exposed to MEM medium containing 5% FCS and 5 or 55mM potassium in the presence or absence of 4µM dexamethasone. LDH release was assayed after 0, 12, 16, 20, 24, 36 and 48 hours.

According to the time course of LDH release, cell death is quantified 20 to 24 hours after receptor induction. Due to the long incubation period and distinct growth of sister cultures, an individual cell amount should be taken into account. Therefore, to quantify the percentage of LDH release due to NMDA receptor activity, also the remaining cytosolic LDH activity in surviving cells was determined. This method exhibits some limitations due to the need of 5% FCS within the incubation medium. FCS is added to guarantee normal growth and low levels of unspecific cell death. Besides different growth factors, FCS contains high amounts of free amino acids. Therefore, addition of L-glutamate or glycine for stimulation of expressed NMDA receptors is not necessary. In turn, the application of this method is therefore restricted to NMDA receptor antagonists. This method was applied for the characterization of a series of thieno[2,3-b]pyridinones acting as glycine site antagonists.

Results – cell death based in vitro assays

The induction model was improved for the testing of compounds (agonists and antagonists) under more defined conditions. The developed model is designated as **differentiation model**.

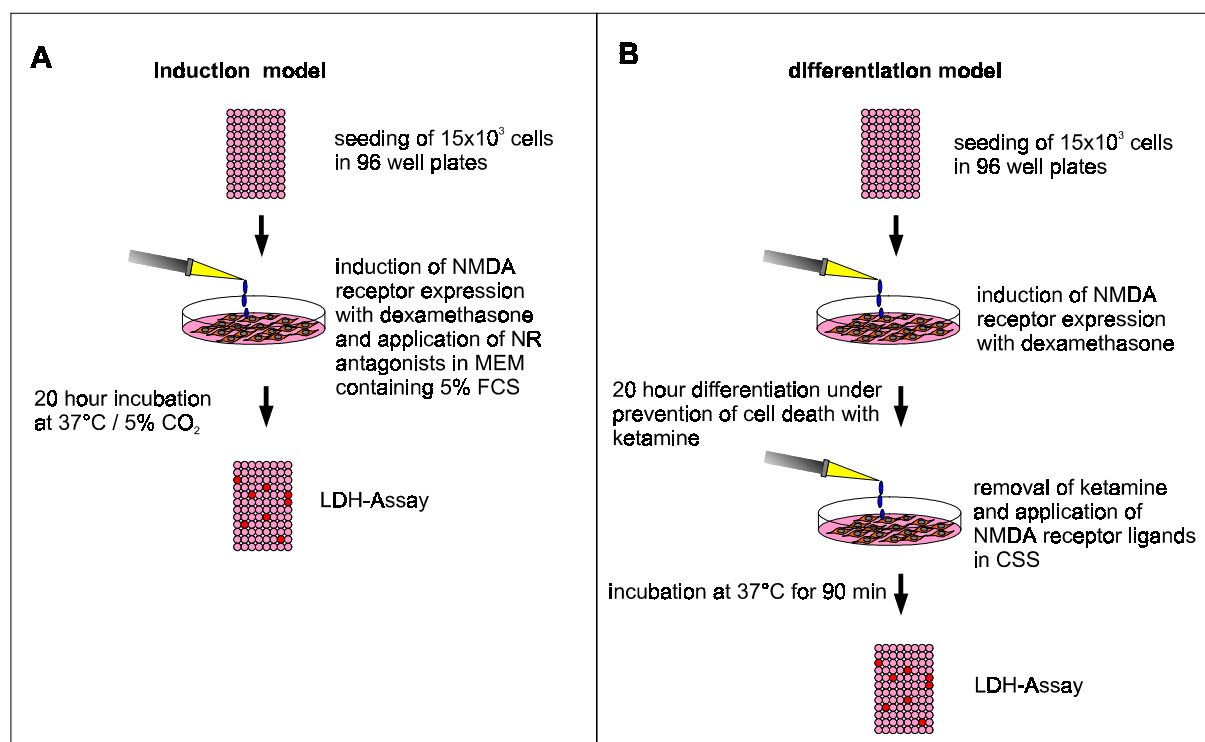


Fig. 29 Scheme of developed excitotoxicity models

In this design, NMDA receptors are pre-expressed by treatment with dexamethasone for 20 to 24 hours under sterile conditions. To avoid cell death, clones are exposed to $100\mu\text{M}$ ketamine during this period. For the testing of compounds, NMDA receptor activity is enabled by removal of ketamine and subsequent incubation in a controlled salt solution containing defined concentrations of agonists, antagonists or modulators such as protons or polyamines. Sterile conditions are not further required. The time course of LDH release is given in fig. 30. After stimulation with $30\mu\text{M}$ L-glu / gly, NR1-1a / 2A expressing L12-G10 cells showed a steep increase in LDH release, starting 5 min after the beginning of NMDA receptor stimulation and reaching their maximum cell death rate after 20 min, already. In contrast, NR1-1a / 2B expressing clone L13-E6 exhibited a more delayed cell death with a maximum cell death rate after 40 to 50 min.

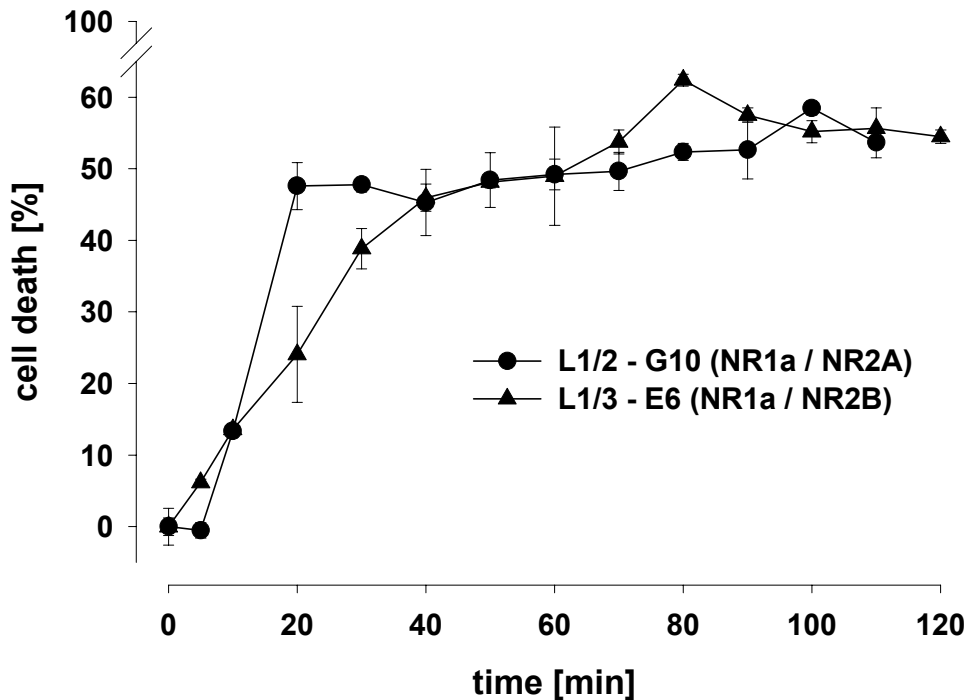


Fig. 30 Time course of LDH release in the differentiation model

L12-G10 (NR1-1a / NR2A) and L13-E6 (NR1-1a / NR2B) cells were differentiated for NMDA receptor expression in growth medium containing 4 μ M dexamethasone and 100 μ M ketamine for 24 hours. After removal of the induction medium cells were stimulated in CSS (pH 7.6 for L12-G10 or pH 8.0 for L13-E6) containing 1.8mM Ca²⁺, 50mM potassium and 30 μ M L-glu / gly). LDH-release was assayed after the indicated intervals.

This slower increase in cell death could be explained by a reduced calcium permeability of NR1-1a / NR2B receptors. In contrast to the onset of cell death, the final amount of cytotoxicity is comparable in both clones with cell death rates of 50 to 60% after 90 min of stimulation. According to these data, cells are incubated for 60 to 90 min at 37°C. Cell death is quantified by the determination of released LDH from test wells and total LDH from control wells released by addition of detergent. Due to the brief incubation period, differences in total cell amount do not occur and cytosolic LDH is not taken into account. Compared to the induction model, the amount of samples is therefore reduced to 50%.

The differentiation model was applied to the pharmacological characterization of the clones L12-G10 and L13-E6.

3.4.3 Structure - in vitro activity relationship of a series of thieno[2,3-b]pyridinones

A series of glycine site antagonists was used to demonstrate the usefulness of the created cell lines in drug screening and optimization of pharmacophores. The pharmacophore of the tested compounds is based on the structure of the 2-quinolone derivate L-701,324 (Kulagowski et al., 1994), one of the most potent antagonists at the glycine recognition site of the NMDA receptor yet described, with both high in vitro and in vivo activity. L-701,324 combines structural features present in 7-chlorokynurenic acid and quinoxaline-2,3-dione derivatives (see fig. 31) which were compounds early shown to have affinity for the glycine binding site (Kemp et al., 1988) (Kleckner and Dingledine, 1989). The special feature of 2-quinolone derivatives is the lack of the carboxylic acid function which is believed to improve the bioavailability within the CNS. Instead, the anionic function, which is necessary for high affinity, is restored as a vinylogous acid in tautomeric forms of the 4-hydroxyquinolin-2(1H)-one. The series of tested thieno[2,3-b]pyridin-6(7H)one compounds are derived from quinolones by bioisosteric replacement of the benzene nucleus with a thiophene (C. R. Noe et al, unpublished). Synthesis strategies of the thienopyridinones were driven by their ability to displace [³H]-glycine from rat hippocampal membranes (according to Berger, 1995). Hence, due to the availability of binding data, this series represented a suitable trial set.

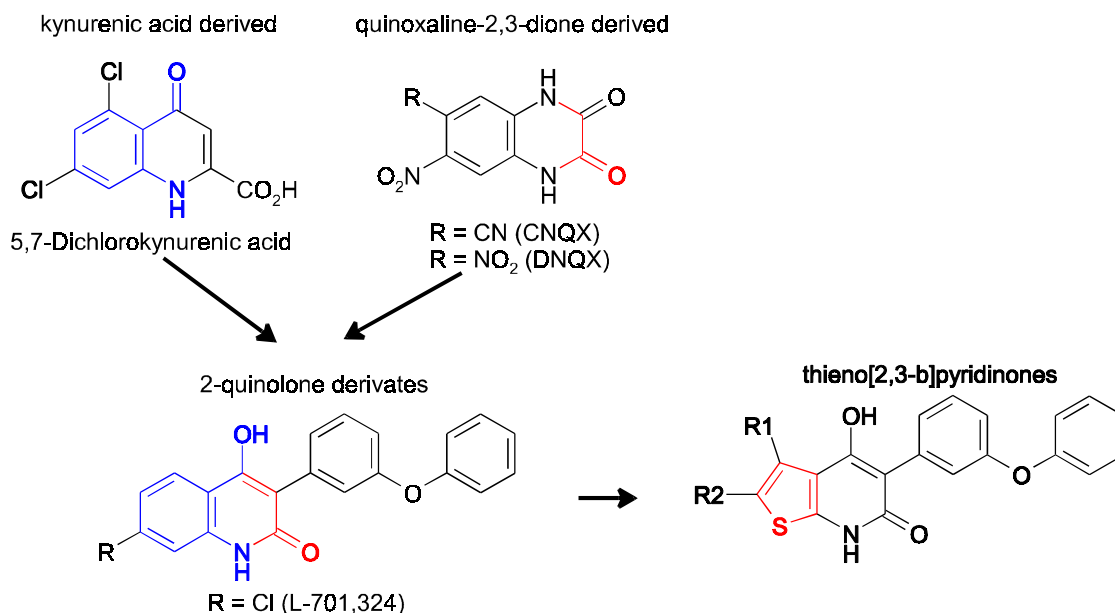


Fig. 31 Structure relationship between 2-quinolone and thieno[2,3-b]pyridinone derivatives

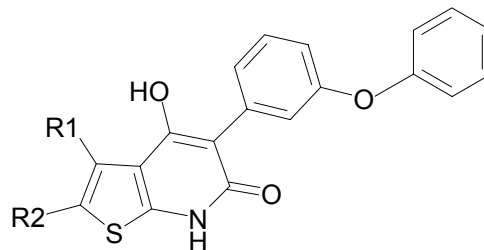
Results – cell death based in vitro assays

Compounds were characterized for their ability to prevent NMDA receptor mediated cell death in L12-G10 cells expressing hNR1-1a / hNR2A. Cell death rates were determined in the induction model. The obtained IC₅₀-values as well as K_i-values from [³H]-glycine binding are given in tab. 6. Not for all compounds IC₅₀-values were obtained. The determination of cytoprotective effects at higher concentration levels, for compounds such as 185, 323, 198 and 342 with lower affinity and increased lipophilicity, was not possible due to poor solubility of compounds in the incubation medium. Another limitation was the unspecific toxicity of some compounds (258, 234, 197) which occurred at concentrations > 50μM. Compound 186 exhibited no cytoprotective effects in concentrations up to 250μM. For high affinity compounds, IC₅₀-values obtained by cytotoxicity assays correlated well with the K_i values of the binding assays. For the 9 compounds active in both settings, a correlation coefficient of 0.90 (P = 0.001) was observed. The obtained IC₅₀-values in the cytotoxicity assay were between 4 and 90μM, whereas compounds were about thousand times more potent in the binding assay (K_i between 1 and 290nM). This discrepancy could be explained by high glycine concentrations within the micromolar range, since the used induction medium contained 5% FCS. According to its low activity in [³H]-glycine displacement (K_i=290nM), the 2-, 3-unsubstituted compound 256 exhibited a very low efficacy in cytoprotection of L12-G10 cells (IC₅₀=89.2μM). In radioligand studies, it was found that the introduction of a 2-chloro residue as well as a 3-alkyl residue leads to strongly increased affinity (see compounds 256 vs. 257 and 237 vs. 238). This increased affinity is also evident in our in vitro cytotoxicity model. Compared to compound 256 (R₁=H / R₂=H), introduction of a methoxymethyl residue at C-3 in compound 237 enhanced the cytoprotective efficacy (IC₅₀ = 55.8μM). Introduction of a 2-chloro residue in compound 257 enhanced the cytoprotective efficacy to a higher degree (IC₅₀=15.4μM). For compound 257 (R₁=H / R₂=Cl), results from cytotoxicity assays revealed a six-fold increase in cytoprotective potency compared to unsubstituted compound 256 (R₁=H / R₂=H) and a four-fold increase compared to the C-3 methoxymethyl substituted compound 237 (R₁=meOme / R₂=H). These results correspond to the data from radioligand binding studies which showed a 30-fold increased affinity for 2-chloro substitution compared to unsubstituted compound 256 and a four-fold increased affinity compared to compound 237 (R₁=meOme / R₂=H). For the combination of both substitution principles, the cytoprotective efficacy was further enhanced by the introduction of i-propyl (compound 191; IC₅₀=5.2μM) and i-butyl (compound 204; IC₅₀=7.9μM) residues but not by n-propyl (compound 233; IC₅₀ = 15.9μM) or tert-butyl (compound 199; IC₅₀=15.5).

Results – cell death based in vitro assays

These compounds exhibited the highest cytoprotective potency of all tested thienopyridinone derivatives.

Tab. 6. Results of the pharmacological characterization of 5-(3-phenoxyphenyl)-thieno[2,3-b]pyridin-6(7H)one derivatives by radioligand binding studies at rat brain membranes and cytotoxicity assays at clone L12-G10



Compound	R1	R2	K_i [^3H]-glycine [nM]	IC_{50} [μM] cytotoxicity assay
256	H	H	290 (410; 169)	89.2 (97.52; 80.90)
237	methoxymethyl	H	37 (24; 49)	55.8 (51.10; 60.54)
257	H	Cl	10.4 (13; 7.8)	15.4 (14.33; 16.55)
233	n-propyl	Cl	3.9 \pm 1.4 (3)	15.9 (20.54; 11.24)
199	tert.-butyl	Cl	3.3 \pm 0.4 (3)	15.5 (13.28; 15.74; 17.61)
204	i-butyl	Cl	2.0 \pm 0.2 (3)	7.9 (7.35; 8.46)
191	i-propyl	Cl	1.5 \pm 0.5 (5)	5.2 (6.27; 4.12)
238	methoxymethyl	Cl	0.99 \pm 0.65 (3)	15.7 (11.10; 20.32)
186	methyl	H	261 \pm 213 (9)	>250
323	ethyl	H	32	>50 ^b
258	i-butyl	H	66 (38; 156; 3.6)	>50 ^a
185	methyl	Cl	21 \pm 12 (7)	>200 ^b
234	n-hexyl	Cl	80 \pm 43 (5)	>50 ^a
197	cyclohexyl	Cl	>30000	>50 ^a
198	2,3-thiopyrane		35 \pm 10 (3)	>250 ^b
342	2,3-cyclohexane		500	>30 ^b
L-701,324 ¹⁾	H	Cl	1.35 \pm 0.2 (4)	3.8 (3.45, 4.13)

K_i values were determined by M. Berger (Berger, 1995) and are expressed as mean \pm SEM (n) or as arithmetic mean of two experiments (n_1, n_2). Inhibition constants (IC_{50}) in cytotoxicity assays are expressed as mean of two experiments (n_1, n_2).

¹⁾benzene analogous compound of thieno[3,2-b]pyridones with a chloride residue at C-7 of the chinoline ring

^a no effect; exceeding indicated concentrations led to unspecific cell death

^b no effect; insoluble at higher concentrations

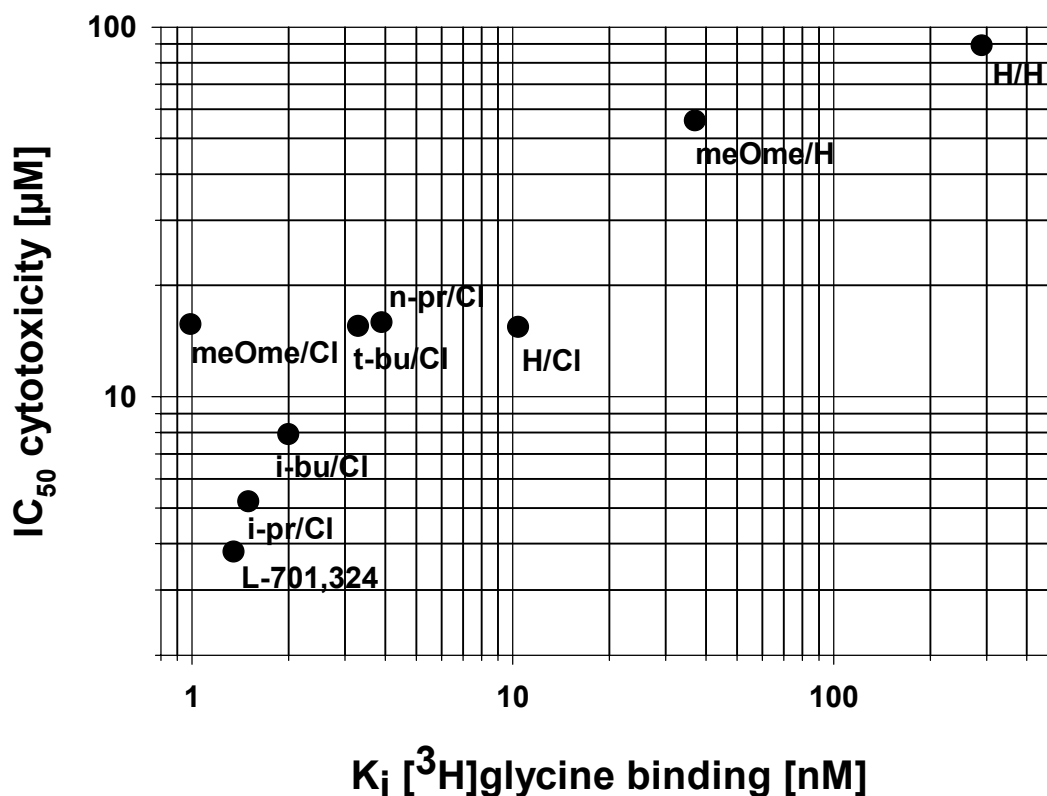


Fig. 32 Correlation between inhibition of NMDA receptor mediated cytotoxicity and inhibition of [^3H]-glycine binding to rat brain membranes by L-701,324 and eight thienopyridinones. Data points are marked with the corresponding residues R1/R2 from table 6.

Cytoprotective potencies of compounds 204 (R_1 =i-butyl / R_2 =Cl) and 191 (R_1 =i-propyl / R_2 =Cl) are comparable to the cytoprotective efficacy of the quinolone analogue L-701,324 which showed an IC_{50} -value of $3.8\mu\text{M}$. In the series of 2-chloro substituted compounds, introduction of a 3-methoxymethyl residue (compound 238) displayed the highest affinity in [^3H]-glycine binding with a K_i value of 0.99nM . The increased affinity of this compound, compared to n-propyl or tert-butyl substituted compounds 233 and 199, did not result in an improved cytoprotective efficacy. The IC_{50} -value of compound 238 was determined with $15.7\mu\text{M}$ corresponding to the IC_{50} -values determined for compounds 257, 233 and 199. A possible explanation for this discrepancy could be a different plasma protein binding of these compounds.

Results – cell death based in vitro assays

To investigate the presence of binding to plasma albumin, the high affinity compound L-701,324 and the low affinity compound 237 ($R_1 = \text{methoxymethyl} / R_2 = \text{H}$) (compound 238 was no more available!) were tested in the presence and absence of micromolar concentrations of warfarin. This 4-hydroxycoumarin is known for its high binding rate to plasma albumin (> 99%) and selectively competes for albumin binding site I. Although the structure of warfarin is closely related to those of 2-quinolone derived glycine site antagonists, it exhibited no cytoprotective effects in concentrations up to 300 μM . As shown in fig. 33-B 100 to 300 μM warfarin improved the efficacy of both compounds by approximately 2-fold. For L-701,324, the IC_{50} decreased from 4.2 μM to 2.6 μM in the presence of 100 μM warfarin. For compound 237, 300 μM warfarin shifted the IC_{50} -value from 58.3 μM to 28.0 μM . These data demonstrate, that binding to plasma albumin is present to a higher degree. Due to supplementation with 5% FCS, the assay medium contains at least 0.5 to 1% BSA. Since binding to plasma proteins limits the concentration of free antagonist in the pharmacodynamic phase, a higher affinity could be compensated by decreased effective concentrations of antagonist.

Summarizing, a 2-chloro residue, also present in the bioisosteric quinolone derivate L-701,324, seems to represent the major determinant for both, high affinity and high cytoprotective efficacy of this pharmacophore. This finding agrees with the proposed structure-activity model of Kemp and Leeson (Kemp and Leeson, 1993) who postulated a lipophilic pocket of the glycine binding site in this region. Compared to quinolones, in which the introduction of one Cl is sufficient for optimal affinity, thienopyridinones need an additional alkyl substituent (R_1) vicinal to the chloro residue (R_2) to reach high potency. The size of the 3-alkyl residue seems to influence the potency of the high affinity compounds, too. Radioligand binding data suggested a seven- to twenty-fold enhanced affinity for a C-3 methoxymethyl group (compounds 237 and 238) compared to methyl substituted compounds (compounds 186 and 185). This increased affinity is also evident in the cytoprotective efficacy of these compounds. The average IC_{50} -value of the C-2 unsubstituted methoxymethyl compound 237 was determined to 55.8 μM , whereas no cytoprotective effects were found for C-3 methyl substituted compound 186 up to 250 μM . The same results were obtained for the 2-chloro substituted analogues 238 ($R_1 = \text{methoxymethyl} / R_2 = \text{Cl}$; $\text{IC}_{50} = 15.7\mu\text{M}$) and 185 ($R_1 = \text{methyl} / R_2 = \text{Cl}$; $\text{IC}_{50} > 200$). On the other hand, bulky alkyl residues like n-hexyl (compound 234; $\text{IC}_{50} > 50$) or cyclohexyl (compound 197; $\text{IC}_{50} > 50$) led to decreased potencies. Therefore, the size of the introduced residue is critical with an

optimum for i-butyl and i-propyl.

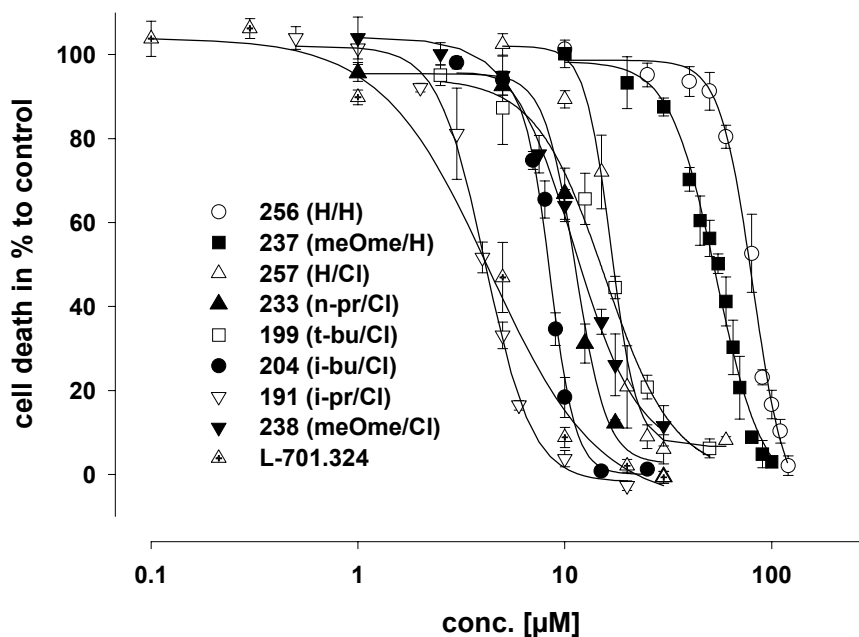


Fig. 33-A Inhibition of NMDA receptor mediated cell death by eight thieno[2,3-b]pyridinone derivatives and L-701,324. Compounds were incubated for 24h in MEM w/o Mg^{2+} containing 5% FCS, 55mM KCl and 4µM dexamethasone at 5% CO_2 . Cell death rate is expressed as percentage of positive control. Hill coefficients were > 1 for all tested compounds.

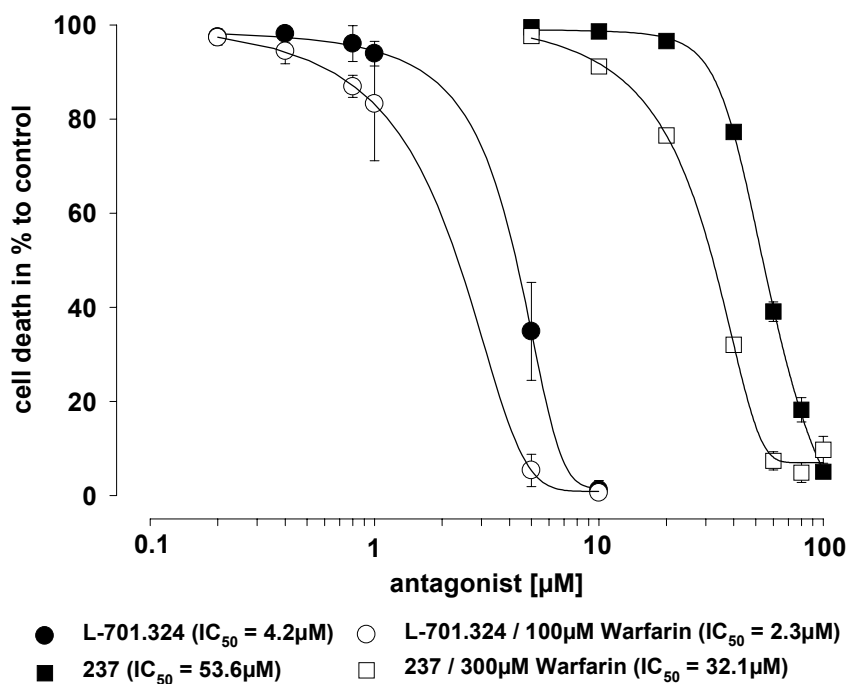


Fig. 33-B Warfarin increases the potency of L-701,324 and compound 237. Compounds were incubated for 24h in MEM w/o Mg^{2+} containing 5% FCS, 55mM KCl and 4µM dexamethasone at 5% CO_2 in the presence and absence of warfarin.

It should be noted, that the observed dose response curves displayed a very steep slope (see fig. 33-A) and Hill coefficients > 1 , which is a characteristic for the positive cooperativity of ligand binding. Since more than one glycine recognition site is present in the heteromultimer complex, this finding suggests, that the binding of one antagonist to a glycine recognition site lowers the affinity of glycine at the remaining binding sites.

3.4.4 Structure - in vitro activity relationship of quinoxaline-2,3-diones

Two 6,7-dihydro-1H,5H-pyrido[1,2,3-de]quinoxaline-2,3-diones (Nagata et al., 1994) were tested for their cytoprotective efficacy. The structure of these glycine site antagonists derived from the AMPA and NMDA receptor / glycine site antagonists CNQX and DNQX (see fig. 34). These compounds represent high affinity glycine antagonists (Nagata et al., 1994) with a 20-fold selectivity over AMPA receptors due to the substitution of one of the nitrogen atoms. For the determination of IC_{50} -values, hNR1-1a / hNR2A expressing L12-G10 cells were exposed to the compounds in the induction model. Nagata et al. evaluated the affinity for the glycine binding site of the NMDA receptor using a [3H]-5,7-dichlorokynurenic acid binding assay. The six-membered ring-fused tricyclic quinoxalinedione 18g displayed high affinity for the glycine site. The K_i -value was determined to 9.9 nM. The corresponding anilide derivative 20g was reported to be 4-fold more potent than 18g ($K_i = 2.6$ nM) and as potent as the tetrahydroquinolone derived compound L-689,560 (Leeson et al., 1992), one of the most potent glycine antagonists so far reported, whose structural features in position 4 are incorporated in these two compounds (fig. 34). The data obtained from the cytotoxicity assays confirmed the described structure affinity relationship between compounds 18g and 20g. For the anilide derivate 20g an IC_{50} -values of 4.7 μ M was determined. In contrast, the carboxylic acid derivative 18g was less effective with an IC_{50} -values of 17.2 μ M. From these data, an IC_{50} ratio of 3.7 is calculated which accurately fits to K_i -ratio of 3.8 obtained from the radioligand binding studies.

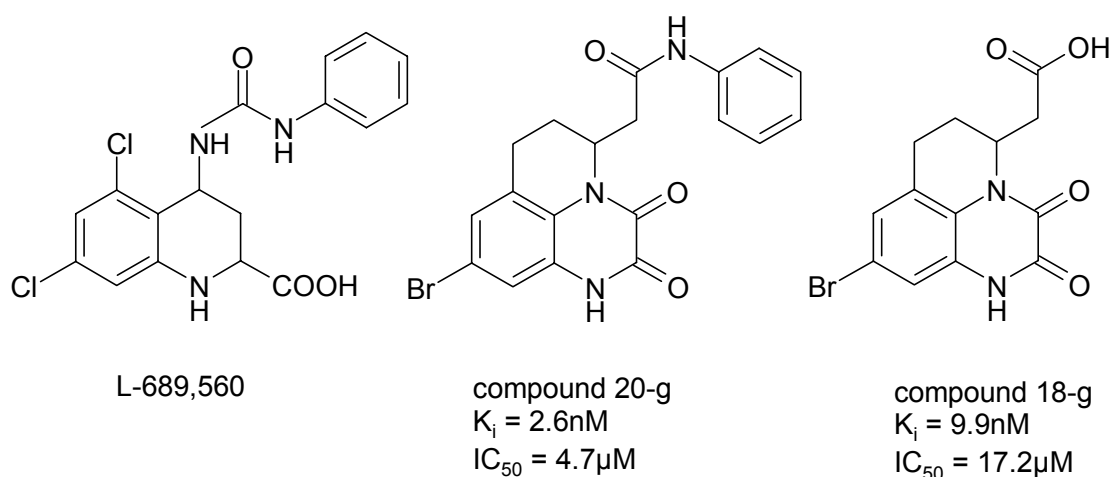


Fig. 34 Structure – activity relationship of 6,7-dihydro-1H,5H-pyrido[1,2,3-de] quinoxaline-2,3-dione derivatives 20-g and 18-g

K_i-values for displacement of [³H]-DCKA in rat brain membranes were taken from Nagata et al, 1994. IC₅₀-values represent the concentration for halfmaximum cytoprotection of L12-G10 cells in the induction model.

3.4.5 Pharmacology of clones

Since the induction model is limited by the presence of glutamate and glycine containing FCS, the further pharmacological characterization of clones was performed in the improved differentiation model. This design offers the possibility of cell death based in vitro assays under defined concentrations of agonists, antagonists and modulators.

Beside the determination of IC₅₀-values for competitive and non-competitive antagonists, the influence of modulators of the NMDA receptor complex, such as protons, polyamines, histamine and protein kinase C were examined. We have also addressed the question whether subunit specific antagonists like ifenprodil and haloperidol, exhibit a preference for distinct clones expressing different NMDA receptor subtypes.

3.4.5.1 Cell death caused by NMDA receptors is pH dependent

It has been reported from electrophysiological studies, that native NMDA receptors are sensitive to the extracellular proton concentration (Traynelis and Cull-Candy, 1990; Traynelis and Cull-Candy, 1991). In these receptor preparations, protons inhibit the NMDA receptor function by 50 percent at pH 7.3. Protons seem to mediate their NMDA receptor inhibition by interactions with the NR1 subunit, and both polyamines and presence of NR1 exon 5 potentiate receptor function through relief of the tonic proton inhibition present at physiological pH (Traynelis et al., 1995). Since the heteromultimeric channels expressed in

our cell lines contain the splicevariant NR1-1a lacking the 5'-insert (exon 5), these cell lines should be sensitive to proton inhibition. Therefore, the effects of various pH levels upon cell death rate were investigated.

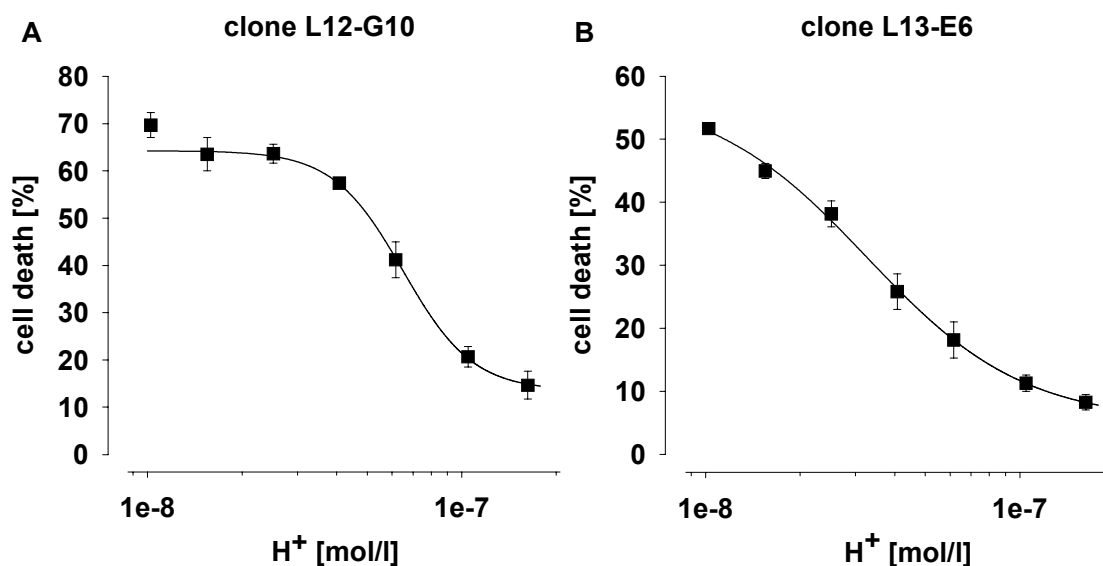


Fig. 35 Proton inhibition of NMDA receptor mediated cell death at clone L12-G10 (A) and L13-E6 (B)

Clones were cultured in growth medium containing 4 μ M dexamethasone and 100 μ M ketamine for 20 hours. After removal of ketamine, clones were stimulated in CSS containing 400 μ M L-glutamate and D-serine adjusted to pH levels between 6.8 and 8.0 for 90 min.

As shown in fig. 35, cell death rates of both clones depended on applied pH values. In clone L12-G10 expressing subunits NR1-1a / NR2A, an IC₅₀ of pH 7.2 was calculated. L13-E6 cells, expressing subunits NR1-1a / NR2B, showed a greater sensitivity to proton inhibition with a halfmaximum inhibition at pH 7.5. These results correspond to data from electrophysiological studies with NMDA receptor transformed *Xenopus oocytes* (Traynelis et al., 1995). Traynelis et al. reported IC₅₀-values for proton inhibition of pH 7.2 for NR1-1a / NR2A expression and pH 7.3 for NR1-1a / NR2B receptors. Further experiments were performed under the relief of proton inhibition (pH 7.6 for L12-G10 or 8.0 for L13-E6) unless indicated differently.

3.4.5.2 Spermine triggers cell death in a subunit specific manner

Polyamines like spermine are known to modulate the activity of the NMDA receptor complex by distinct mechanisms. One mechanism is the glycine independent stimulation. This stimulation depends on NR subunit composition, since only receptors containing NR1 splice

Results – cell death based in vitro assays

variants lacking the 5'-insert (such as NR1-1a) exhibit stimulation (Durand et al., 1993; Gallagher et al., 1996). In addition, glycine independent stimulation is only seen at receptors containing NR2B but not at NR2A-, NR2C-, NR-2D containing receptors (Kashiwagi et al., 1996a; Williams et al., 1994). Under saturated concentrations of glycine, it was proposed that polyamines act to shield the proton sensor, reducing the proton inhibition and therefore potentiating the activity of NMDA receptors (Traynelis et al., 1995). To confirm this hypothesis, the effect of 300 μ M spermine on proton inhibition was examined (fig. 36). After 20 hours of receptor induction and removal of ketamine, the cells were incubated in CSS containing 100 μ M L-glutamate and glycine in the presence or absence (control) of 300 μ M spermine at various pH values. Exposure of clone L13-E6 to spermine enhanced cell death rate from pH 6.8 to 8.0. The relative extent of increased cell death by spermine depended on the applied pH values. At pH 8.0, cell death at 300 μ M spermine was only slightly enhanced compared to control. In contrast, the relative extent of triggered cell death increased strongly if NMDA receptor activity in controls was reduced due to proton inhibition (pH 7.4 to 6.8).

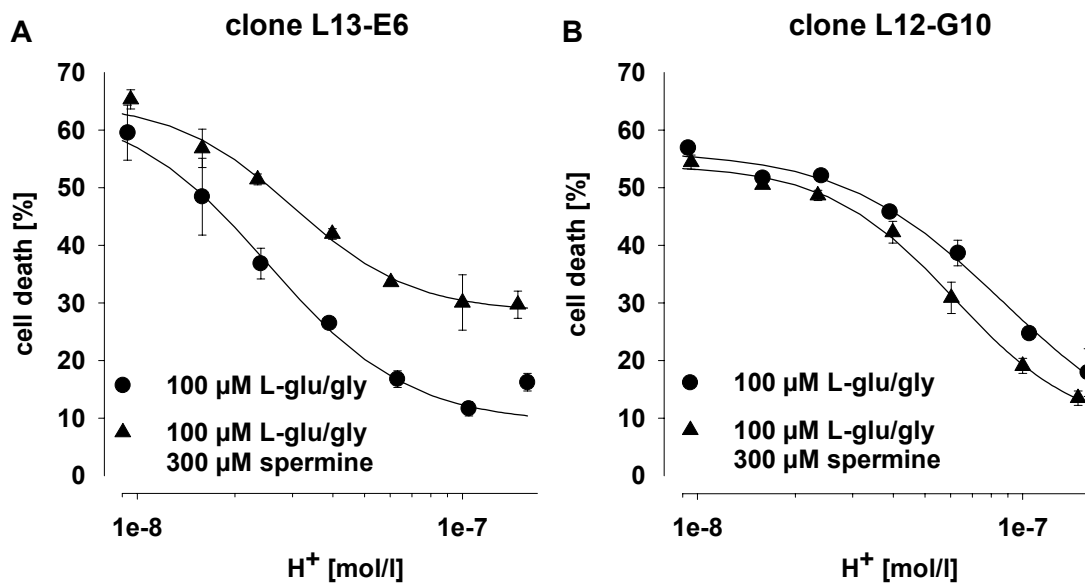


Fig. 36 *Proton and subunit dependent enhancement of cell death by spermine*
Clones were cultured in growth medium containing 4 μ M dexamethasone and 100 μ M ketamine for 20 hours. After removal of ketamine, clones were stimulated in CSS containing 100 μ M L-glutamate and glycine or CSS containing additional 300 μ M spermine. The pH of the incubation medium was varied from pH 6.8 to 8.0.

These findings suggest a partial relief of proton inhibition through the application of spermine at NR1-1a / NR2B expressing L13-E6 cells. With clone L12-G10, no receptor stimulation by spermine was observed. In contrast, a slight inhibition of cell death was detected.

3.4.5.3 Glycine site agonist D-serine enhances L-glutamate induced cell death

To demonstrate a coagonism at the L-glutamate and glycine binding sites of the expressed NMDA receptors, increasing concentrations of D-serine, L-glutamate and L-glutamate plus 100 μ M D-serine or D-serine plus 100 μ M L-glutamate were applied to both clones (fig. 37). During the application of D-serine at concentrations up to 100 μ M, both clones remained healthy and no LDH release could be determined. In contrast, L-glutamate induced cell death in both clones in a dose dependent manner. Maximum cell death rates of both clones were enhanced by addition of 100 μ M D-serine. Co-treatment with increasing concentrations of D-serine and 100 μ M L-glutamate exhibited a dose response to D-serine. But unexpectedly, enhanced cell death was even observed under low D-serine concentrations (0.1 μ M). This atypical dose dependency might be explained by glycine contamination due to the washing procedure with the BSA containing wash solutions.

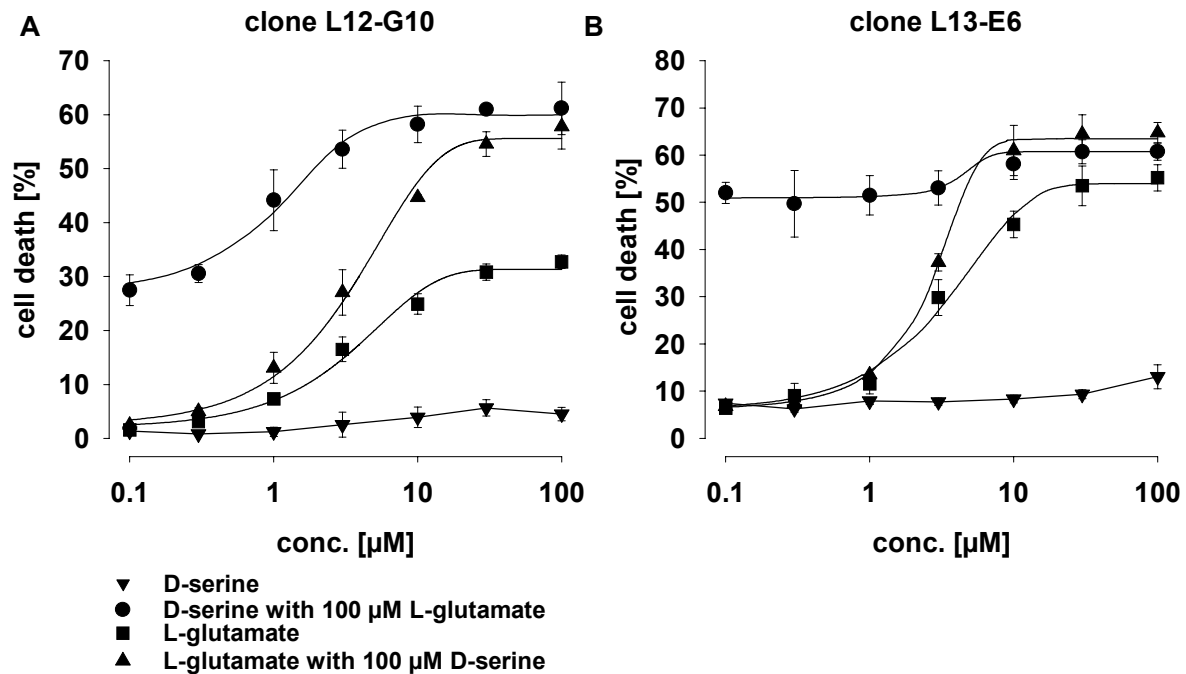


Fig. 37 Glycine site agonist D-serine enhanced L-glutamate mediated cell death
 Differentiated clones were stimulated in CSS containing increasing concentrations of D-serine, L-glutamate, L-glutamate with 100 μ M D-serine or D-serine with 100 μ M L-glutamate.

This contamination may also account for the lower enhancement of maximum cell death by co-application of 100 μ M D-serine and L-glutamate compared to single application of 100 μ M L-glutamate at clone L13-E6. As shown later, this clone has a stronger preference for agonists compared to clone L12-G10 reflecting the distinct pharmacological properties of the transfected NR2 subunits. Hence, the determination of concentrations required for halfmaximum cell death (EC_{50}) for glycine site agonists D-serine or glycine were not possible. The estimated EC_{50} for glutamate under saturated D-serine concentrations were 3.4 μ M (3.71 μ M, 3.12 μ M) for L12-G10 (fig. 37-A) and 2.7 μ M (2.80 μ M, 2.59 μ M) for L13-E6 (fig. 37-B).

3.4.5.4 Glutamate and glycine site antagonists inhibit NMDA receptor induced cell death

The ability of competitive antagonists at the glutamate and glycine binding site of NMDA receptors to prevent cells from undergoing cell death due to calcium overload was examined (tab. 7). For glutamate antagonism, (R/S)-AP5 and (R/S)-CPP were tested. Both antagonists prevented L12-G10 and L13-E6 cells from cell death. In both clones, (R/S)-CPP showed a 6- to 10-fold higher potency than (R/S)-AP5. Comparing the potency of antagonists in both clones there seems to be a dependency on receptor subunit composition which is in good agreement with data from radioligand binding studies at recombinant receptors (Laurie and Seeburg, 1994). The hNR1-1a / hNR2A expressing clone L12-G10 seems to be an antagonist preferring clone. The IC_{50} ratios (L12-G10:L13-E6) for (R/S)-AP5 (0.14) and for (R/S)-CPP (0.22) indicate a higher affinity of these antagonists to NR2A containing assemblies. The same preference was found for glycine site antagonist DCKA with a IC_{50} ratio of 0.15. Protection by 100 μ M DCKA was abolished in both clones by increasing concentrations of co-agonists glycine and D-serine, respectively. No significant difference in the potency of both co-agonists was observed. To abolish 50% of the cytoprotective effect of 100 μ M DCKA (EC_{50}) in L12-G10 cells, approximately 200 μ M of either glycine or D-serine were needed whereas L13-E6 showed a higher preference for co-agonists with EC_{50} of 70 μ M for glycine or 103 μ M for D-serine. Similar results were obtained using (R/S)-CPP and L-glutamate or L-aspartate. In L13-E6 cells the cytoprotective effect of 100 μ M CPP was abolished to 50% by 149 μ M L-glutamate or 1044 μ M L-aspartate whereas at clone L12-G10 EC_{50} -values of 182 μ M and 1769 μ M for displacement of 30 μ M (!) (R/S)-CPP were determined. Comparing efficacy of both agonists, L-glutamate is 7 to 10 fold more effective than L-aspartate.

Results – cell death based in vitro assays

Tab. 7. Pharmacological properties of clones L12-G10 and L13-E6 expressing hNR1-1a / NR2A and hNR1-1a / hNR2B, respectively (determined by cytotoxicity assays in the differentiation model). For tests with ketamine and competitive antagonists, cells were stimulated in CSS containing 30µM L-glutamate / glycine and increasing concentrations of compounds. Non-competitive compounds ifenprodil and haloperidol were applied in CSS containing 100µM L-glutamate and glycine. For agonist testing, the indicated concentration of antagonist was included and increasing concentrations of agonist were applied to abolish the cytoprotective effects of the antagonists. All concentrations were tested in triplicates. The ratios of respective IC₅₀-values indicate ligand preference for clone L12-G10 (<1) or for L13-G10 (>1).

Compound	L12-G10 cells	L13-E6 cells	ratio
	expressing NR1a/NR2A	expressing NR1a/NR2B	
	IC ₅₀ or EC ₅₀	IC ₅₀ or EC ₅₀	
	[µM]	[µM]	
Antagonists			
(RS)-APV	17.1 (14.4; 19.7)*	121.4 (115.2; 127.7)*	0.14
(RS)-CPP	2.6*	12.0*	0.22
DCKA	3.7*	24.6 (13.3; 36.0)*	0.15
Ifenprodil	>100	0.149 ± 0.019	>670
Haloperidol	>100	2.19 ± 1.55	>45
Ketamine	14.4*	14.9*	0.97
Agonists			
glycine	192.8**	70.3**	2.7
D-serine	206.9**	103.4**	2.0
L-glutamate	182.1***	148.6****	>1
L-aspartate	1769.5***	1043.9****	>1

* vs 30µM L-glutamate / glycine

** vs 100µM DCKA

*** vs 30µM (RS)-CPP

**** vs 100µM (RS)-CPP

3.4.5.5 Ifenprodil and haloperidol inhibit cell death selectively at NR2B expressing L13-E6 cells in the absence of spermine

Ifenprodil and haloperidol are known to be non-competitive antagonists selective for NMDA receptors containing the subunit NR2B. The mechanisms by which ifenprodil and haloperidol inhibit the ligand gated ion channel are still unknown. One proposed mechanism is the interaction with polyamine binding sites (Carter et al., 1990) in a competitive or more recently reported in an allosteric way (Kew and Kemp, 1998). Initially, both compounds were tested for their ability to protect clones from undergoing cell death in the absence of spermine. Both

Results – cell death based in vitro assays

compounds were cytoprotective to clone L13-E6 expressing subunits hNR1-1a / hNR2B (fig. 38-B). Ifenprodil strongly inhibits cell death with an IC_{50} of 149nM whereas haloperidol was 15-fold less effective (IC_{50} 2.19 μ M). In contrast, cell death of clone L12-G10 remained unaffected up to 100 μ M (fig. 38-A). Higher concentrations were not tested due to induction of unspecific cell death.

Since polyamines were not present under our standard settings, the mechanism of inhibition by these NR2B specific antagonists seems not to be restricted to a competition at polyamine binding sites. Hence, we wanted to elucidate whether spermine is able to abolish cytoprotective effects of both antagonists in a competitive way. As polyamines have several modes of action, e.g. potentiation by increasing the affinity for glycine or glycine independent stimulation by reducing proton inhibition, the proposed direct competition of spermine and NR2B specific antagonist should be best demonstrated under saturating glycine conditions (100 μ M glycine). To exclude an abolishment of proton inhibition by spermine, experiments were performed under relief of proton inhibition (pH 8.0).

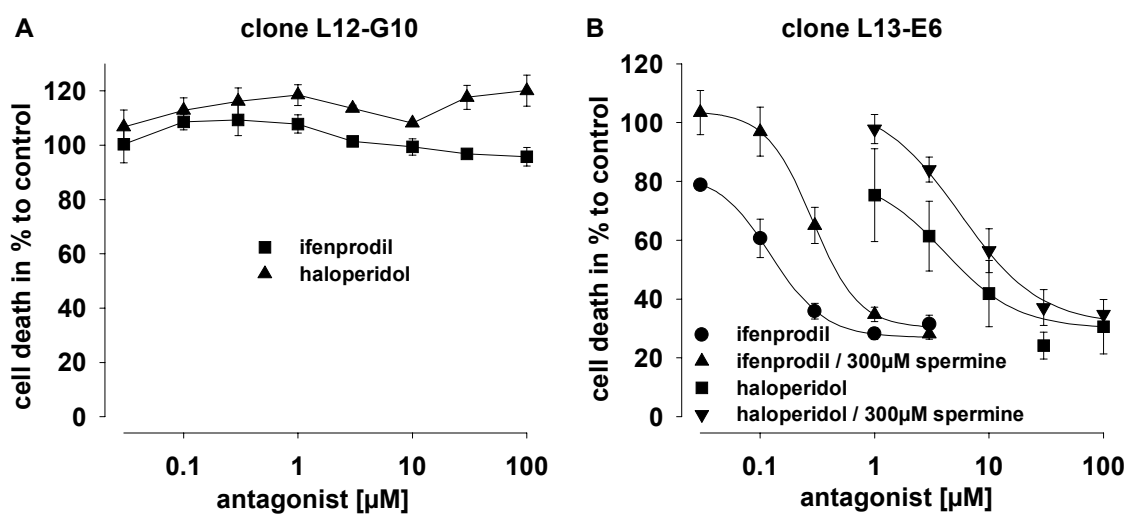


Fig. 38 Subunit dependency of cytoprotective effects of ifenprodil and haloperidol and interaction with spermine

Differentiated cells were stimulated in CSS containing 100 μ M L-glutamate and glycine under relief of proton inhibition. (A) Effects at NR1-1a / NR2A expressing L12-G10 cells; (B) Effects at NR1-1a / NR2B expressing L13-E6 cells in the presence and absence of 300 μ M spermine.

As shown in fig. 38-B, spermine failed to abolish cytoprotective effects of haloperidol and ifenprodil in a competitive way. The obtained dose response curves from controls and spermine treated cells exhibited significant different slopes. At non-protective concentrations of antagonist spermine increased the rate of cell death. In contrast, protective concentration levels remained nearly unaffected. Therefore, an allosteric interaction of spermine with both compounds is more likely.

3.4.5.6 Cell death is not triggered by histamine or activation of PKC

NT2 cells, representing a clonal line of human teratocarcinoma cells, exhibit NMDA receptor-mediated excitotoxicity after terminal differentiation into *NT2-N neurons* (Munir et al., 1996). Besides spermine and spermidine, histamine enhanced glutamate mediated excitotoxicity in a dose-dependent manner consistent with expression of an NR1 / NR2B combination of subunits. Examination of histamine effects on NMDA receptor-mediated ion current in cultured rat cortical neurones showed that in a subpopulation of the neurones tested, histamine (10-100 mM) enhanced the peak amplitude and slowed down the onset of desensitization of the NMDA-induced ion currents, both in a concentration-dependent manner (Zwart et al., 1996).

We have tested whether histamine triggers cell death in our recombinant cell lines (fig. 39), too. At clone L12-G10, neither 10 μ M nor 30 μ M histamine significantly influenced L-glutamate mediated cell death which was determined under relief of proton inhibition (pH 7.6). This is consistent with previous described findings which suggested that the NR1-1a / NR2A combination of subunits is not sensitive to histamine stimulation (Williams, 1994a). At NR1-1a / NR2B expressing L13-E6 cells, histamine also failed to enhance L-glutamate dependent cell death. At non saturated glutamate concentration levels (0.1 to 1 μ M), cell death rates were unchanged to control. In contrast, under saturated concentrations of L-glutamate (10 to 30 μ M), 30 μ M histamine significantly decreased cell death rates compared to control by approximately 10 to 20%. This unexpected inhibition by histamine is in contradiction with results obtained from *NT2-N cells* and heterologous expression in *Xenopus oocytes* as mentioned above. But it is consistent with the finding that histamine affects NMDA receptors in a pH-dependent manner. Whole cell records in the CA1 region of slices of rat hippocampus showed that histamine enhanced the N-methyl-D-aspartate (NMDA) component of the synaptic current at lowered pH (7.2) whereas at raised pH (7.6) it reduced them (Saybasili et al., 1995). At a pH of 7.4 no effects were observed. Since we performed the reported cell toxicity assays under relief of proton inhibition (pH 8.0 for clone L13-E6), our data support

Results – cell death based in vitro assays

the finding of a histamine mediated inhibition of NR2B containing NMDA receptors at raised pH levels. Contradictions to other observations may be caused by distinct pH conditions.

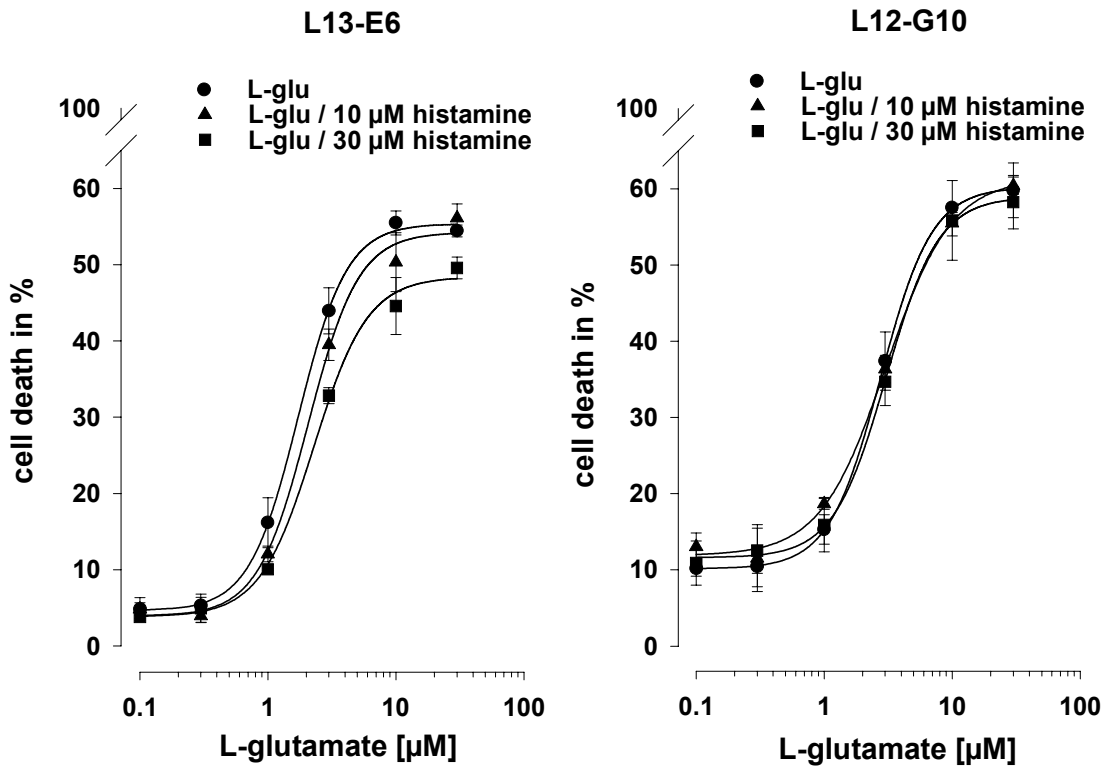


Fig. 39 **Effects of histamine**

Differentiated clones were stimulated with increasing concentrations of L-glu (0.1-30 μ M) in the absence or presence of 10 μ M or 30 μ M histamine. Experiments were performed under relief of proton inhibition (pH 7.6 for L12-G10 and pH 8.0 for L13-E6) and saturating glycine concentrations (100 μ M).

Since it has been reported that activation of PKC by 12-O-tetradecanoylphorbol 13-acetate (TPA) treatment in *Xenopus oocytes* potentiated the response of NR1 / NR ϵ 1 and NR1 / NR ϵ 2 assemblies (Kutsuwada et al., 1992; Mori et al., 1993) we tested the ability of TPA to trigger cell death in our cell culture models. L12-G10 and L13-E6 cells were stimulated with increasing concentrations of L-glutamate in the presence and absence of 100nM TPA for 90 min (fig. 40). With both cell lines, treatment with TPA failed to affect L-glutamate induced cell death. This finding suggests, that either the expressed receptors are highly phosphorylated due to basal activity of PKC or a putative phosphorylation did not affect receptors activity due to lack of calmodulin binding and inhibition.

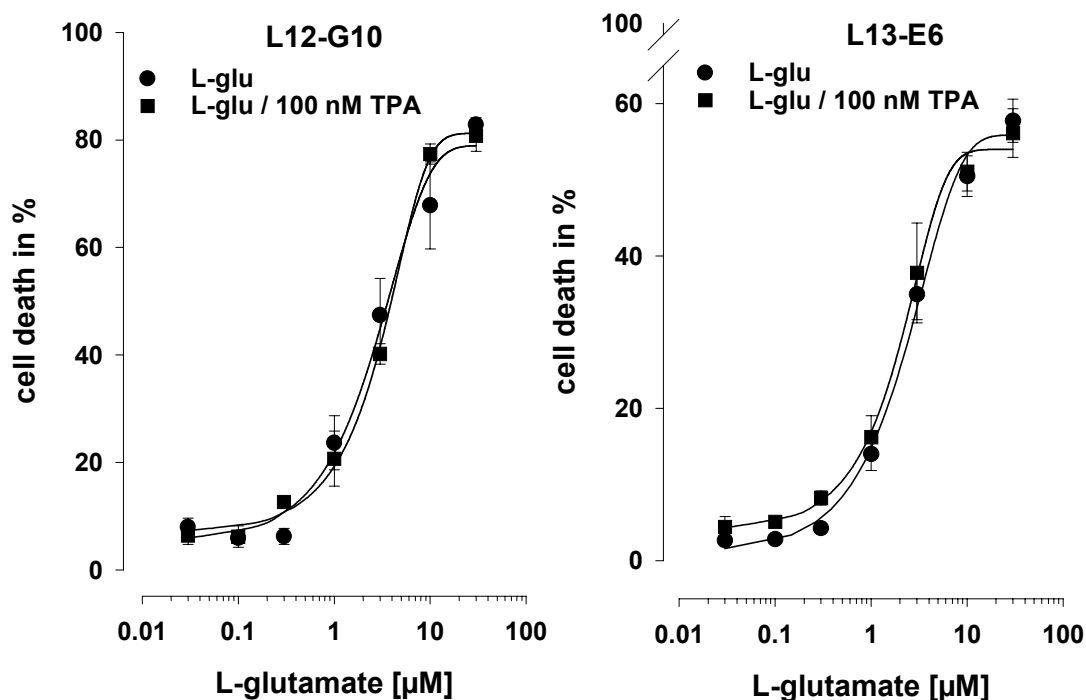


Fig. 40 Activation of PKC did not trigger cell death

Differentiated clones were stimulated with increasing concentrations of L-glutamate (0.03-30 μM) in the absence or presence of 100nM TPA. Experiments were performed under relief of proton inhibition (pH 7.6 for L12-G10 and pH 8.0 for L13-E6) and saturated glycine concentrations (100 μM).

3.5 Mechanism of cell death inhibition by cyclosporin A

The initial event in glutamate evoked excitotoxicity in neurons is an extensive entry of extracellular calcium through overstimulated NMDA receptors. Although it is well accepted that the subsequent intracellular accumulation of calcium plays a key role in the induction of excitotoxicity, the calcium dependent pathogenetic target is still unknown.

In cerebellar granule cells (CGC), continuous glutamate exposure is characterised by a transient elevation of cytoplasmic free calcium followed by a decay to a plateau after NMDA receptor desensitization. The plateau is maintained for a variable time (latent period) until a secondary, irreversible increase in intracellular calcium occurs (Nicholls and Budd, 1998). The raised calcium levels during the latent period as well as the delayed calcium deregulation do not depend on the presence of L-glutamate. Since the activity of calcium pumps within the plasma membrane could not only account for the decay of intracellular calcium to the plateau within the latent period, the involvement of calcium sequestering cellular organelles is likely. The dominant organelles capable of sequestering large quantities of calcium are the mitochondria. Meanwhile, it has been demonstrated that mitochondria

accumulate large quantities of calcium during a toxic glutamate stimulus (White and Reynolds, 1997) and that calcium efflux from mitochondria contributes to the delayed calcium deregulation after glutamate removal (White and Reynolds, 1996). Therefore, mitochondria are supposed to be the primary targets in glutamate induced excitotoxicity (Schinder et al., 1996).

It is known that mitochondria can actively accumulate calcium into their matrix using the electrical potential across the inner membrane as the driving force. This calcium transporting system operates as a uniporter whose activity depends on the intracellular calcium concentration with a set point of approximately 500nM as well as on the mitochondria membrane potential. In the presence of phosphate, substantial amounts of calcium can be taken up forming insoluble calcium phosphate complexes within the matrix. In the case of glutamate induced excitotoxicity, sequestering of calcium is accompanied by a depolarisation and finally by a disruption of the transmembrane potential $\Delta\psi$ which is detrimental for the oxidative phosphorylation. The loss of $\Delta\psi$ is explained by a permeability transition (PT) state, a phenomenon that is characterized by the opening of pores spanning the inner and outer membrane of mitochondria. Since these pores are permeable to compounds up to 1500 kDa, the opening of these PT pores allows the equilibration of protons and the release of respiratory substrates, sequestered calcium and other cell death inducing factors like cytochrome C (Kantrow and Piantadosi, 1997) and apoptosis-inducing factor (AIF) into the cytosol (Susin et al., 1996). The molecular composition of the PT pores is not entirely known but the adenine nucleotide translocator (ANT or ADC), the voltage dependent anion channel (VDAC), the peripheral benzodiazepine receptor (Szabo et al., 1993) and matrix cyclophilin (Connern and Halestrap, 1994; Crompton et al., 1992) are probable components of the PT pore. Similar to NMDA receptors this channel seems to be inhibited by protons (Halestrap, 1991) (Szabo et al., 1992) and sensitive to membrane potentials (Bernardi et al., 1993).

The immunosuppressant drug Cyclosporin A (CsA) has been reported to block pore conductance and to inhibit the onset of mitochondrial PT at isolated mitochondria from liver (Broekemeier et al., 1989; Davidson and Halestrap, 1990; Szabo and Zoratti, 1991) and heart cells (Crompton et al., 1988; Halestrap et al., 1997). Cytoprotective effects of CsA were shown in anoxic cultured hepatocytes (Broekemeier et al., 1992; Pastorino et al., 1993) and for neurons in an ischemic animal model (Friberg et al., 1998) and CGC cells (Ankarcrona et al., 1996). Also a delayed mitochondrial depolarization after treatment of cultured cortical neurons with CsA has been reported (Nieminen et al., 1996).

Results – inhibition of cell death by CsA

It should be noted that beside its inhibitory effect upon the cyclophilin proportion of the PT pore, CsA (in submicromolar concentrations) is also a known inhibitor of the Ca^{2+} /calmodulin dependent Ser/Thr phosphatase calcineurin. Inhibition of calcineurin is also mediated by the immuno-suppressive drug tacrolimus (FK506) in a submicromolar concentration range (10-100nM). Calcineurin has been shown to regulate the activity of native NMDA receptor channels at two different levels, gating and desensitization. FK506 has been shown to prolong the duration of single NMDA receptor channel openings (Lieberman and Mody, 1994). Inhibition of calcineurin by cyclosporin A (200-500nM) or FK506 (200-500nM) decreased the glycine insensitive desensitization after synaptic stimulation of NMDA receptors on rat hippocampal neurons (Tong et al., 1995). Thus, calcium entry through native NMDA receptors in neurons is limited by calcineurin activity and inhibition of calcineurin by cyclosporin A or FK506 results in a prolonged opening of channels. In contradiction, inhibition of calcineurin by 100nM CsA or FK506 has been reported to prevent the development of both early necrosis and delayed apoptosis in cerebellar granule cells (Ankarcrona et al., 1996). Although CsA and FK506 are structurally unrelated compounds, both bind to specific immunophilins (cyclophilin A and FKBP12). Inhibition of calcineurin activity is then mediated by the binding of cyclosporin A / cyclophilin or FK506 / FKBP12 complexes.

As already shown, even heterologous expression of recombinant NMDA receptors in non-neuronal cell lines leads to an increase in intracellular calcium concentration (Grant et al., 1997) and subsequent cell death (Anegawa et al., 1995) depending on subunit composition. To examine, whether even in heterologous expression systems the occurring excitotoxicity is related to an early damage of mitochondria, the influence of the extracellular calcium concentration upon intracellular ATP levels was investigated. Using the differentiation model, L12-G10 were stimulated in CSS pH 7.6 containing 100 μM L-glu / gly. The content of calcium chloride was varied from 1.8 μM to 0.1 μM , respectively. Differentiated L12-G10 cells, treated with CSS pH 7.6 with 1.8mM Ca^{2+} lacking L-glu / gly were used as control. ATP levels were determined using a luciferase based bioluminescence assay. ATP levels were assayed before and during stimulation with CSS (10, 20 and 30 min).

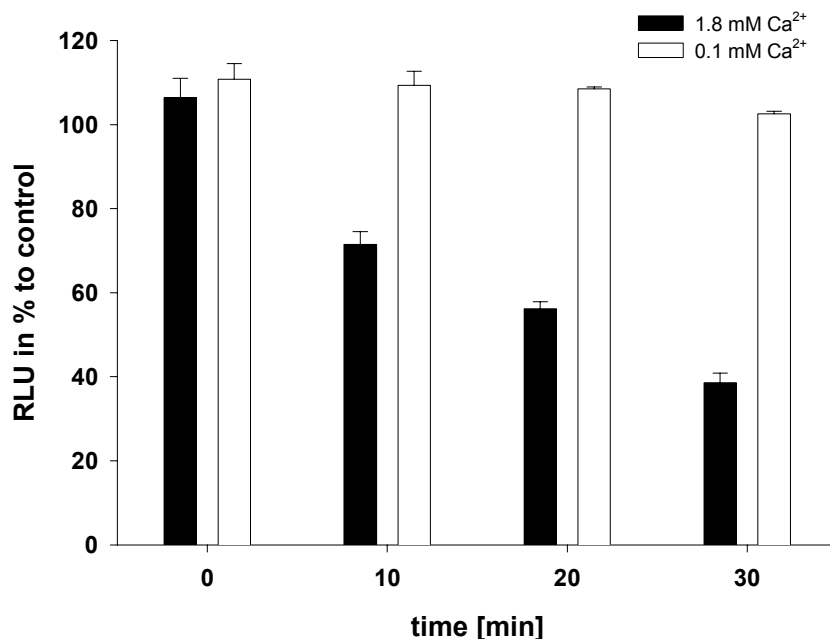


Fig. 41 Decrease of ATP levels after NMDA receptor stimulation is Ca²⁺ dependent

Differentiated L12-G10 cells were stimulated in CSS pH 7.6 containing 100µM L-glu / gly, 1% BSA and 1.8 or 0.1mM Ca²⁺, respectively (n = 3). Differentiated L12-G10 cells cultured in CSS pH 7.6 (1% BSA) w/o L-glu / gly were used as control. ATP samples were taken prior to stimulation and after the indicated time intervals. The ATP content of the samples was determined using a luciferase based bioluminescence assay. The obtained relative light units (RLU) are proportional to the amount of ATP within the samples. Results are expressed as RLU in % to control.

As shown in fig. 41, cultures stimulated in CSS containing 1.8mM Ca²⁺ exhibited decreased ATP levels whereas cultures stimulated in CSS with reduced Ca²⁺ content maintained ATP levels comparable to unstimulated control cultures. Although it cannot be excluded, that the decreased ATP levels are caused by the loss of plasma membrane integrity, these data clearly indicate the keyrole of Ca²⁺ and its involvement in the observed excitotoxicity.

For further investigations on the role of mitochondrial Ca²⁺ sequestration, CsA and FK506 were investigated for cytoprotective effects in a modified differentiation model. Clones, cultured in induction medium containing 4µM dexamethasone and 100µM ketamine for 16 h, were pre-treated with compounds for 4 hours followed by stimulation with L-glutamate and glycine in the presence of immunophilin ligands. Stimulation of L12-G10 cells with saturating agonist concentrations (400µM L-glu / gly) in the presence of CsA reduced cell

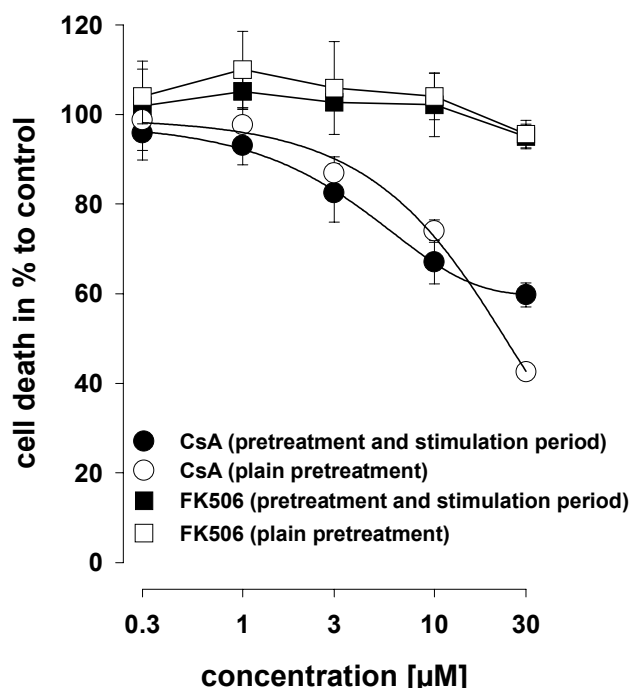
Results – inhibition of cell death by CsA

death by approximately 40% (fig. 42) with an IC_{50} -values of $7.1\mu\text{M}$. Similar results were obtained for L13-E6 cells (IC_{50} of $7.1\mu\text{M}$). Therefore, the cytoprotective effect of CsA seems not to be subunit specific. FK605, known to inhibit calcineurin but not the PTP (Friberg et al., 1998), did not exert significant cytoprotective effects in concentrations up to $30\mu\text{M}$. Higher concentrations induced unspecific toxicity.

To examine whether plain pre-treatment of cells is sufficient for a cytoprotective effect, L12-G10 cells, differentiated with $4\mu\text{M}$ dexamethasone and $100\mu\text{M}$ ketamine for 16 hours, were loaded with CsA ($0.3\text{--}30\mu\text{M}$) for 4 hours in induction medium prior to stimulation with CSS containing $100\mu\text{M}$ L-glutamate and glycine. As shown in fig. 42, cytoprotective effects obtained by plain pre-treatment of cells are similar to those obtained by pre-treatment and application during the stimulation interval. A prolonged pre-treatment of L12-G10 cells for 3h with increasing concentrations of FK506 did not lead to significant cytoprotection. Interestingly, these cytoprotective effects were only observed after a prolonged pre-treatment of cells with CsA.

Fig. 42 **Inhibition of cell death by CsA**

Cytoprotective efficacy of immunophilins CsA and FK506 was tested (A) by pre-treatment for 4 hours and presence during stimulation period or (B) by plain pre-treatment with CsA (4 hours) or FK506 (3 hours). L12-G10 cells were stimulated in CSS with saturating concentrations of L-glutamate and glycine under relief of proton inhibition (pH 7.6).



As shown in fig. 43 the cytoprotective effect decreases if the pre-treatment interval is reduced. Maximum cytoprotection is obtained after 4 hours and reduced the cell death rate by more than 60%. No significant prevention of cell death was observed with a brief pre-treatment interval of 10 minutes. Pre-treatment with $30\mu\text{M}$ FK506 was less effective with a maximum reduction of cell death by approximately 15% for pre-treatment intervals from one to three hours. After 4 hours of pre-treatment, cell death rate exceeded those of control cells due to unspecific

Results – inhibition of cell death by CsA

toxicity. Similar to CsA, a brief pre-treatment of 10 minutes failed to exert cytoprotection. The need of a prolonged pre-treatment by CsA for maximum cytoprotective effects is surprising and could not be explained by a delayed resorption of CsA to the cells since the cyclic undecapeptide has a highly lipophilic structure.

A possible explanation for this phenomenon could be effects on NMDA receptor expression. Studies concerning functional expression of potassium channels in *Xenopus oocytes* have shown that a prolonged treatment (16h) of RNA injected oocytes with CsA selectively reduces the functional expression of the transformed channels (Chen et al., 1998). Since the protein synthesis was not impaired by CsA, these authors conclude that the functional expression of these channels is facilitated by the peptidyl-prolyl isomerase cyclophilin. A similar hypothesis was proposed from another group (Helekar et al., 1994) who also demonstrated that functional surface expression of $\alpha 7$ neuronal nicotinic and a type 3 serotonin receptor is dependent on the activity of a cyclophilin.

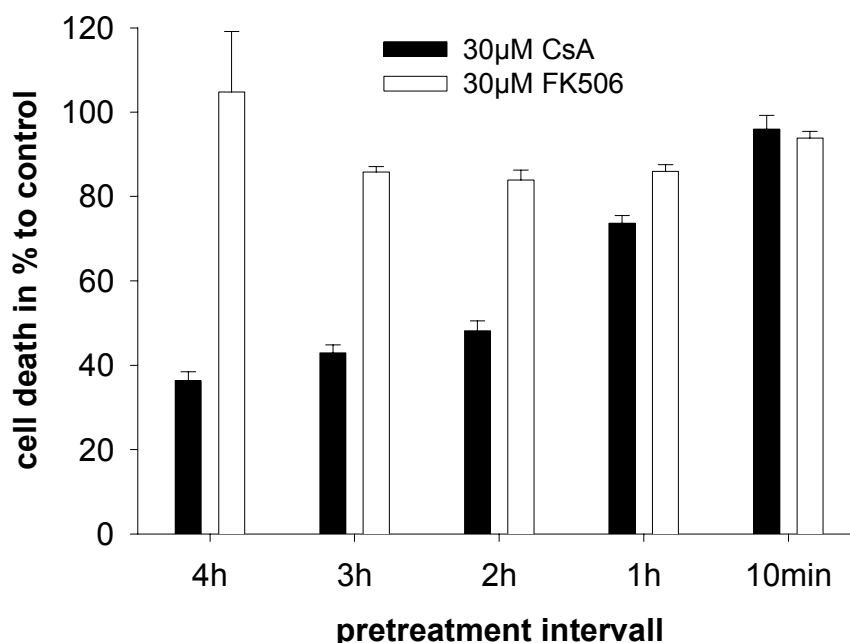


Fig. 43 *Cytoprotection by CsA depends on the duration of pre-treatment intervals*
L12-G10 cells expressing NMDA receptors were loaded with 30µM CsA for the indicated intervals. Ketamine and CsA were removed by washing. Cells were stimulated in CSS pH 7.6 containing 100µM L-glutamate and glycine.

Results – inhibition of cell death by CsA

Surface receptor expression was reduced in channel and cyclophilin co-injected *oocytes* by a treatment with 2 to 30 μ M CsA for 4 to 7 days. These authors concluded, that the oligomeric assembly of neurotransmitter-gated ion channels is a multi-step process involving the participation of cyclophilins. These immunophilins, which are present in the cytoplasm, the endoplasmic reticulum and the mitochondria, exhibit a peptidyl-prolyl isomerase activity and assist in the folding of polypeptides similar to classical heat shock proteins (chaperones).

To determine whether the cytoprotective effects after prolonged pre-treatment with CsA are caused by an inhibition of the PT pore or by a reduction of receptor surface expression, we investigated the surface expression of the NR1 keysubunit by densitometric volume analysis of immunoblots. L12-G10 cells were differentiated with 4 μ M dexamethasone and 100 μ M ketamine for 14 hours and an additional differentiation interval of 6 hours in the presence or absence of 30 μ M CsA. Plasma membranes were enriched by density centrifugation and subjected to gel electrophoresis. For relative quantification of subunit NR1-1a protein amounts of 8, 4, 2 and 1 μ g were probed with a mouse anti-NR1 (N-term) antibody. The resulting immunoblots were analysed by densitometric volume analysis. As shown in fig. 44, the amount of membrane bound NR1-1a receptor was drastically reduced to 28.5 % (29.76%; 27,32%) under treatment with 30 μ M CsA for 6 hours.

To investigate, whether the reduced protein amount of NR1a is accompanied by decreased mRNA levels, RT-PCR analysis was applied. L12-G10 cells were differentiated with 4 μ M dexamethasone and 100 μ M ketamine for 9 hours and an additional differentiation interval of 4 hours in the presence and absence of 30 μ M CsA. Uninduced L12-G10 cells were used as control. After 13 hours, total RNA was isolated and mRNA was transcribed into cDNA using d(T)₁₂₋₁₈ priming. Reverse transcription was followed by PCR with primers corresponding to the transfected NMDA receptor subunits NR1a and NR2A (same Primers were used for the detection of NMDA receptor mRNA; see chapter 3.3.1). Qualitative and quantitative template homogeneity was verified by PCR with β -actin primers. As shown in fig. 45, differentiation with 4 μ M dexamethasone for 13 hours increased the transcription rate of subunit NR1a and NR2A. These increased transcription levels were not affected by prolonged treatment with 30 μ M CsA. Hence, these results exclude an interference of CsA with the transcription of transfected cDNAs and favour the suggested CsA mediated inhibition of the peptidyl-prolyl isomerase cyclophilin as a mechanism for the reduced NMDA receptor expression.

Results – inhibition of cell death by CsA

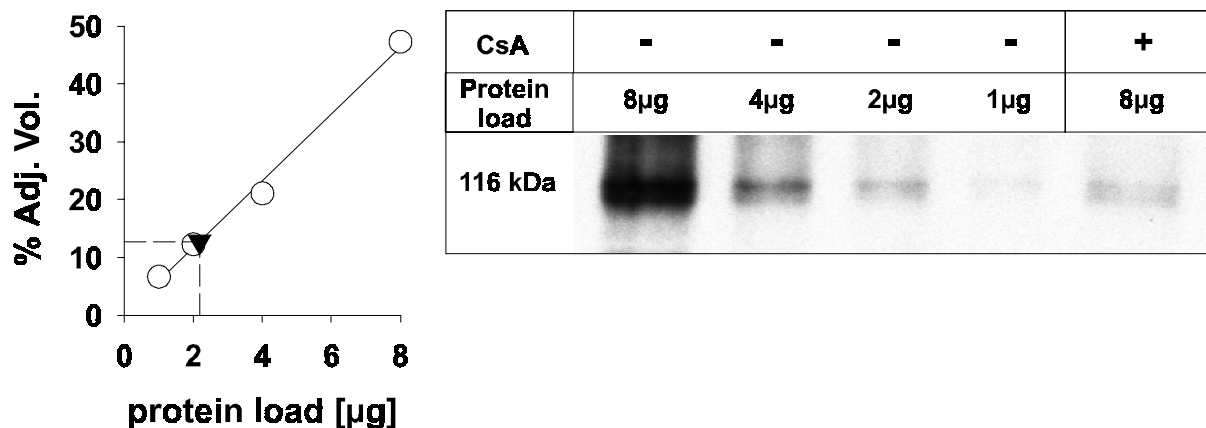


Fig. 44 Prolonged treatment with cyclosporine A decreases expression of NMDA receptor subunit NR1-1a

L12-G10 cells were differentiated with 4µM dexamethasone and 100µM ketamine for 14 hours and an additional differentiation interval of 6 hours in the presence and absence of 30µM CsA. Plasma membranes of cell lysates were enriched by density centrifugation and aliquots of solubilized membrane protein (8, 4, 2, 1µg) were probed with N-terminal directed monoclonal mouse anti-NR1 antibody. Decreased NR1a amount in CsA treated cells was estimated by linear regression of densitometric volume analysis data from controls.

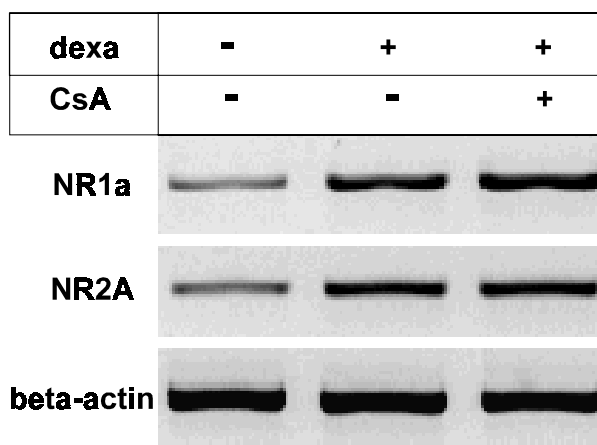


Fig. 45 Prolonged treatment with cyclosporin A does not affect transcription rates of transfected NMDA receptor subunits

L12-G10 cells were differentiated with 4µM dexamethasone and 100µM ketamine for 9 hours and an additional differentiation interval of 4 hours in the presence of 30µM CsA. As control, uninduced L12-G10 cells were used. Treatment with 4µM dexamethasone increased mRNA levels of NR1-1a and NR2A. Additional treatment with 30µM CsA did not alter the amount of NR1-1a or NR2A transcripts.

Results – inhibition of cell death by CsA

Since functional NMDA receptors represent heteromultimers consisting of NR1 and NR2 subunits (Chazot et al., 1994) and the NR1 subunit represents a key subunit necessary for successful surface expression (McIlhinney et al., 1996), the described reduction of NR1-1a expression by CsA may drastically alter the NMDA receptor mediated calcium influx. Hence, the functionality of expressed NMDA receptors after CsA treatment was characterized by fluo-4 calcium imaging. L12-G10 cells were differentiated with 4 μ M dexamethasone and 100 μ M ketamine for 15 hours and an additional differentiation interval of 5 hours in the presence and absence of 30 μ M CsA.

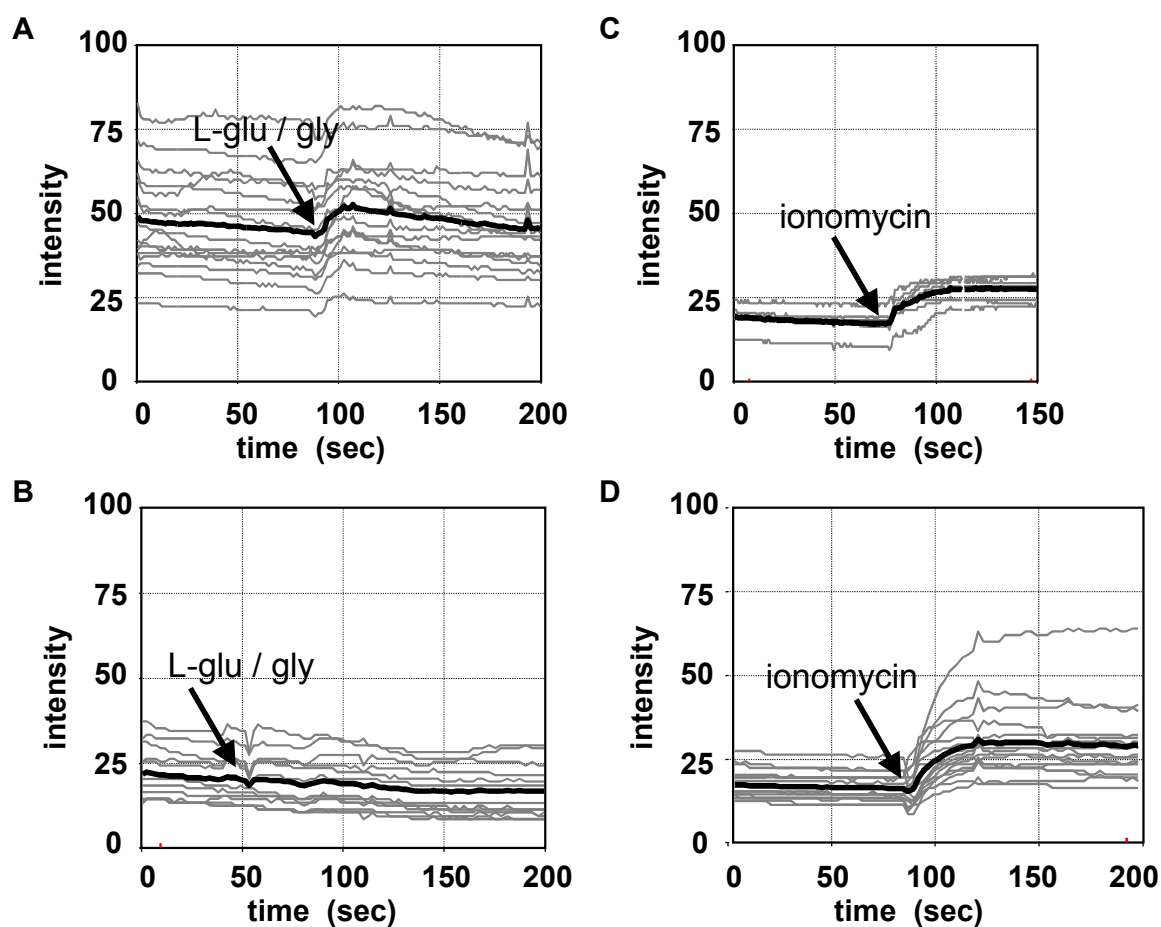


Fig. 46 Prolonged treatment with cyclosporine A leads to a loss of functional NMDA receptors

Cells were differentiated on coverslips in growth medium containing 4 μ M dexamethasone and 100 μ M ketamine for 15 hours and an additional differentiation interval of 5 hours in the presence or absence of 30 μ M CsA. For dye loading, the cultures were treated with 1 μ M fluo-4 acetoxymethylester in original medium at 37°C. To enable receptor activity, ketamine was removed by washing. All experiments were performed in CSS pH 7.6. Thick lines represent the obtained mean values: (A) Stimulation of control cells with 100 μ M L-glu / gly ($n=16$); (B) stimulation of CsA treated cells with 100 μ M L-glu / gly ($n=13$); (C) stimulation of control cells with 30 μ M ionomycin ($n=8$); (D) stimulation of CsA treated cells with 30 μ M ionomycin ($n=17$).

Results – inhibition of cell death by CsA

As shown in fig. 46-B, 100 μ M L-glu / gly failed to increase intracellular calcium levels in CsA treated cultures, whereas intracellular calcium significantly increased in control cells (fig. 46-A). Successful dye loading of CsA treated and untreated cells was demonstrated by the application of 30 μ M ionomycin (fig. 46-C and D).

From these data we conclude, that the observed cytoprotective effects exerted by prolonged pre-treatment with CsA are predominantly caused by an interaction with the NMDA receptor expression. Since we could exclude an influence on the transcription rate of transfected cDNAs, another possibility could be the suggested inhibition of the peptidyl-prolyl isomerase activity of immunophilin by CsA which will lead to the observed reduction of plasma membrane bound NR1-1a subunit and therefore prevent the formation of functional NMDA receptors. The influence of CsA upon the surface expression of NR2 subunits was not investigated. But since it has been shown, that heterologously expressed NMDA receptor subunits are assembled in the ER and that co-synthesis of the subunits is necessary for their successful cell surface targeting (McIlhinney et al., 1998), a reduction of cell surface expressed NR2 subunits seems to be likely. As shown in fig. 43, CsA failed to exert cytoprotective effects after a brief equilibration interval of 10 min.

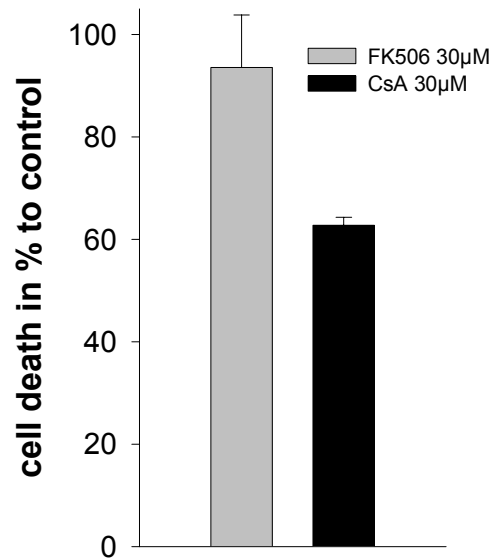
These investigations were performed under the relief of tonic proton inhibition (CSS pH 7.6) leading to highly permeable channels. It should be added that, in contrast to these results, cytoprotective effects were evident under partial proton inhibition of NMDA receptors (CSS pH 7.0). Under these modified conditions, a brief pre-treatment with 30 μ M CsA for 10 min reduced cell death by approximately 40% compared to control (fig. 47). FK506 (30 μ M) was only slightly effective and displayed a mean reduction of ~7% compared to control. From these results a calcineurin mediated cytoprotection of CsA could be excluded due to the lack of significant cytoprotection exerted by FK506.

But so far, we cannot clearly distinguish between the assumed inhibition of PT and a reduction of NR1 subunit expression by inhibition of cyclophilin A. Hence, the participation of mitochondrial damage after stimulation of heterologously expressed NMDA receptors remains elusive and instead of CsA, the use of more specific PT inhibitors like bongkrecic acid or inhibitors of mitochondrial calcium sequestration like ruthenium red or protonophores should be favoured in further investigations.

Results – inhibition of cell death by CsA

Fig. 47 *Inhibition of cell death by brief pre-treatment with 30 μ M CsA prior to NMDA receptor stimulation (under proton inhibition)*

NMDA receptors expressing L12-G10 cells were loaded with 30 μ M CsA for 10 min prior to stimulation in CSS pH 7.0 containing 100 μ M L-glutamate and glycine.



3.6 Characterization of cell death

3.6.1 Applied methods for studies on apoptosis and necrosis

Differences in morphology between necrotic and apoptotic cells include cellular appearance (cellular shrinking vs. swelling), nuclear changes (condensation and DNA fragmentation of apoptotic cells), cellular membrane changes (translocation of phosphatidylserines vs. lysis of membranes) and metabolic changes (e.g. activation of caspases during apoptosis). Apoptotic cells shrink and fragment, but remain metabolically intact (e.g. mitochondrial function, cell membrane integrity). In the following, the principles of the applied methods are briefly described.

Even though apoptotic cells are beginning to die, their plasma membrane remains intact. For studies on cell populations, the release of cytosolic lactate dehydrogenase into the cell culture supernatant indicates the break down of plasma membranes. The mode of cell death, apoptosis versus necrosis, was determined in part using the combination of two fluorescent dyes, Sytox and Hoechst 33342. Both dyes stain DNA; however Sytox is membrane non-permeable and yields green fluorescent chromatin, whereas Hoechst 33342 is membrane permeable and stains DNA blue. Viable cells display a normal nuclear size with a diffuse granular substructure and blue fluorescence. Necrotic cells manifest nuclei with strong green fluorescence and exhibit a typical chromatin pattern. Apoptotic cells exhibit a condensation of high molecular weight DNA. Hence, apoptotic nuclei show a dense blue staining caused by the formation of shrunken chromatin or lobular substructures, those being so called apoptotic bodies.

Additionally, apoptotic cells undergo endonuclease cleavage of their chromosomal DNA which leads to fragmentation into low molecular weight oligonucleosomes. This DNA cleavage leads to a nucleosomal banding pattern in nucleic acid gel electrophoresis analysis. The subsequent decreasing content of high molecular weight DNA in the apoptotic nuclei is detected by DNA staining with the fluorochrome propidium iodide and subsequent flow cytometry. Alive cells produced a pattern where their DNA content is normal diploid (G_0 and G_1 phase of the cell cycle) or greater when they begin to enter mitosis (S, G_2 and M phase of the cell cycle) (see fig. 48). The appearance of populations with a DNA content less than the G_1 amount indicates apoptosis. It should be noted that highly fragmented DNA is also found

in the late states of necrosis leading to signals in flow cytometry quite apart from the G₁ peak of the control.

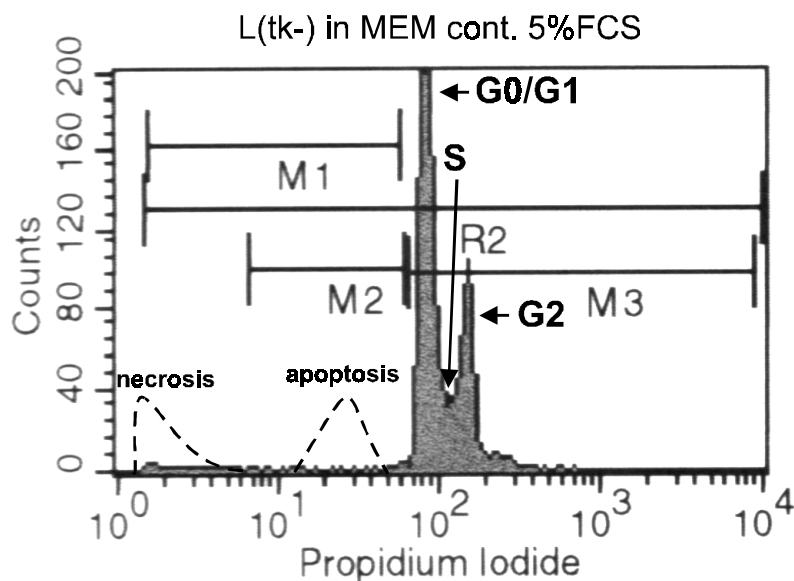


Fig. 48 Flow cytometric profiles of DNA content

L(tk-) wildtype cells were grown for 24 hours in MEM containing 5% FCS. Nuclei were stained with propidium iodide (50 µg/ml). Populations in different phases of the cell cycle are marked: gap₀/gap₁ phase (G0/G1); synthesis (S) and gap₂/mitose phase (G2). Apoptotic or necrotic nuclear populations cause the indicated changes in profile.

Besides nuclear changes, the externalisation of phosphatidylserine (PS) on the plasma membrane is another feature of apoptosis. During the early stages of apoptosis, PS is translocated from the inner part to the outer layer of the plasma membrane, thus exposing PS at the external surface of apoptotic cells, where it can be specifically recognised by macrophages. This translocation is indicated by the extracellular binding of annexin V, a Ca²⁺ dependent phospholipid-binding protein which possesses high affinity for phosphatidylserine. For the detection, the annexin-V is coupled to fluorochromes such as Alexa 568. Since annexin V can also detect necrotic cells as a result of the loss of membrane integrity, apoptotic cells have to be differentiated from these apoptotic cells by the use of propidium iodide or calcein-AM. This technique allows the concomitant detection of apoptosis and necrosis at a single-cell level.

3.6.2 Results of cell death studies

Initial studies on the time dependence of LDH release in the induction model indicated a steep increase in the loss of membrane integrity 12 hours after the induction of NMDA receptor

Results – characterization of cell death

expression (fig. 49). The detected membrane damage is caused either by secondary necrosis of apoptotic cells or simply accounts for a necrotic way of cell death.

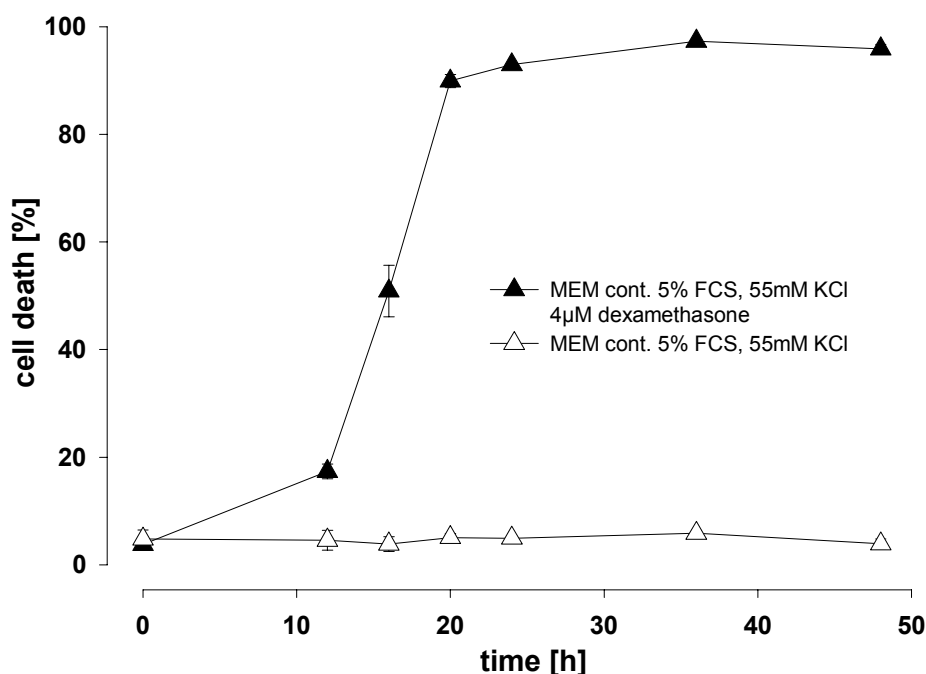


Fig. 49 *Loss of membrane integrity after the induction of NMDA receptor expression* L12-G10 cells were exposed to MEM medium containing 5% FCS and 55mM potassium in the presence and absence of 4µM dexamethasone. LDH release was assayed after 0, 12, 16, 20, 24, 36 and 48 hours.

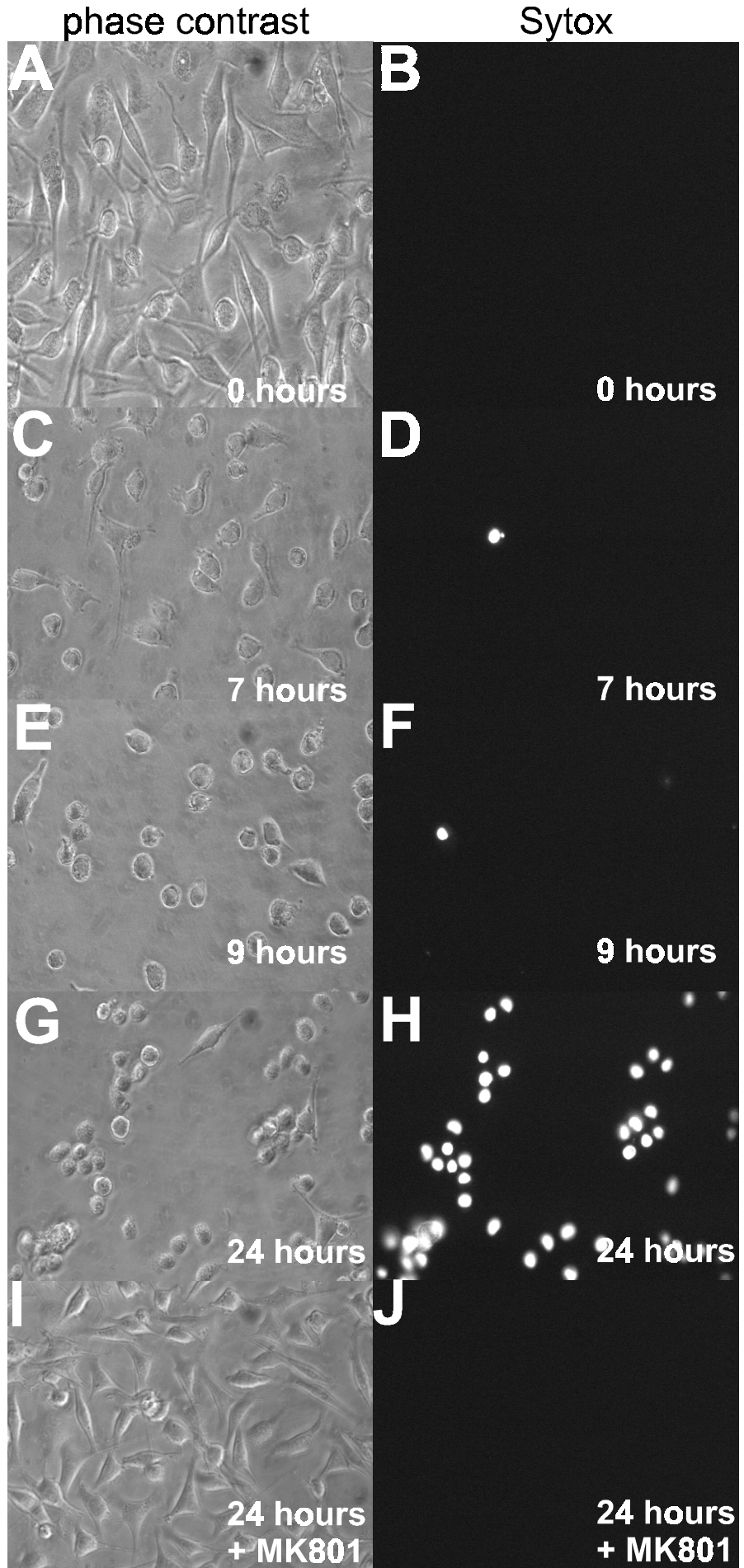
To look for phenotypic changes after the induction of NMDA receptor expression, L12-G10 cells were cultured in the presence or absence of NMDA receptor antagonist MK801 (10µM). Integrity of the plasma membrane was examined by the exclusion of the non-permeable, nuclein acid specific fluorochrome Sytox. Induced cultures developed drastic morphological changes (see fig. 50). The cells exhibited a certain shrinkage of the cytoplasm and changed their normal, oblong or angular appearance to almost round cell bodies (fig. 50-G vs. 50-A). Application of 10µM MK801 prevented cells from these phenotypic changes. 24 hours after NMDA receptor induction, MK801 treated cultures appeared healthy with similar morphology compared to uninduced control cells (fig. 50-I vs. 50-A).

In agreement with the LDH release studies, the expression of NMDA receptors led to an increased membrane leakage. 24 hours after the induction of NMDA receptors, more than 80% of cells were stained with Sytox (fig. 50-H).

Fig. 50

Morphological changes and plasma membrane leakage after induction of NMDA receptor expression

L12-G10 cells were grown in MEM w/o Mg^{2+} containing $4\mu M$ dexamethasone, 5% FCS and 55mM potassium (identical medium conditions to LDH release studies in the induction model) for the indicated intervals. Control cultures were treated with $10\mu M$ MK801 for 24 hours. Cultures were stained with Sytox (final $0.5\mu M$) after the indicated intervals and analysed by light and fluorescence microscopy.



Results – characterization of cell death

This cytotoxicity was mediated by NMDA receptors since it was prevented by the application of 10 μ M MK801 (fig. 50-J vs. 50 H) or 100 μ M ketamine (data not shown). Only a few cells exhibited a positive Sytox staining 7 and 9 hours after receptor induction (fig. 50-D / F). Hence, the increase in cytotoxicity occurred between 10 and 24 hours after NMDA receptor induction. This result confirms the described time course of LDH release (fig. 49). To examine whether the cellular shrinkage is linked to apoptosis, cells were investigated for changes in nuclear morphology by a nuclear co-staining with fluorescent dyes Hoechst 33342 (permeable) and Sytox (non-permeable). Apoptotic nuclear changes like chromatin condensation or nuclear DNA fragmentation are characterized by a dense staining of shrunken, intensely fluorescent nuclei or lobular structures (apoptotic bodies) in the absence of a nuclear staining with Sytox.

After 7 hours of induction, no significant changes in nuclear morphology were obvious compared to uninduced cells (fig. 51-E vs. 51-B). Nuclei showed a diffuse, granular substructure with fine fluorescence spots. Analogous results were obtained after 9 hours of NMDA receptor induction (fig. 51-H). After 24 hours of differentiation the majority of cells co-stained with Hoechst 33342 and Sytox (see fig. 51-K and 51-L). Sytox negative nuclei maintained their granular morphology whereas Sytox positive nuclei exhibited a dense, deep fluorescence; but regarding their size, these nuclei did not shrink, which is unusual for apoptosis. Therefore, the deeper staining of these nuclei is rather explained by an easier access of dye through the damaged plasma membranes than by nuclear apoptosis. Nuclei from MK801 treated cells maintained their granular structure up to 24 hours of differentiation (fig. 52).

For a further characterization, flow cytometric analysis of propidium iodide stained nuclei was applied. L12-G10 cells were exposed to induction medium containing 4 μ M dexamethasone with or without additional potassium (50mM). After 24 hours, cells were harvested, stained with propidium iodide (final 50 μ g/ml) and subjected to flow cytometry. As control, nuclei from wildtype cells, grown for 24 hours in induction medium, and from L12-G10 cells, cultured in induction medium lacking dexamethasone, were examined. Both controls showed normal profiles of DNA content with peaks for nuclei in the G₀ / G₁ and G₂ phase of the cell cycle (see fig. 53). The amount of smaller sized fragments and apoptotic nuclei was detected to 2.08% for L12-G10 cells and to 6.96% for WT cells (M1 marked range). For the treatment of L12-G10 cells in induction medium containing 5mM potassium, the amount of small sized nuclei and nuclear fragments within the M1 marked range slightly increased to 17.74%.

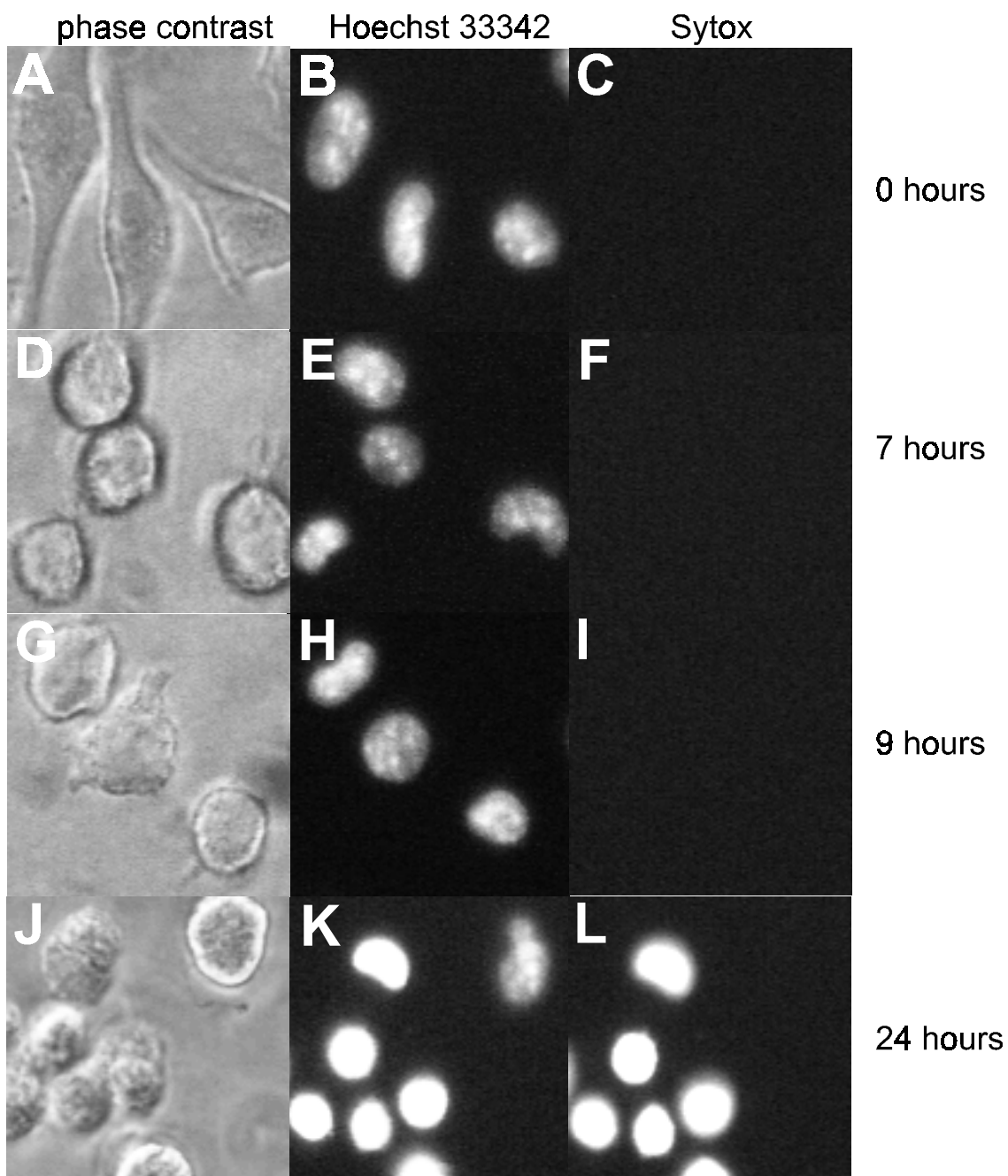


Fig. 51 Nuclear morphology of L12-G10 cells after induction of NMDA receptor expression

L12-G10 cells were grown in MEM w/o Mg^{2+} containing $4\mu M$ dexamethasone, 5% FCS and 55mM potassium (identical medium conditions to LDH release studies) for 0 (A-C), 7 (D-F), 9 (G-I) and 24 hours (J-L). Cultures were co-stained with Hoechst 33342 (final $0.5\mu g/ml$) (B, E, H, K) and Sytox (final $0.5\mu M$) (C, F, I, L) after the indicated intervals and analysed by fluorescence microscopy. A, D, G, J are the respective phase contrast images.

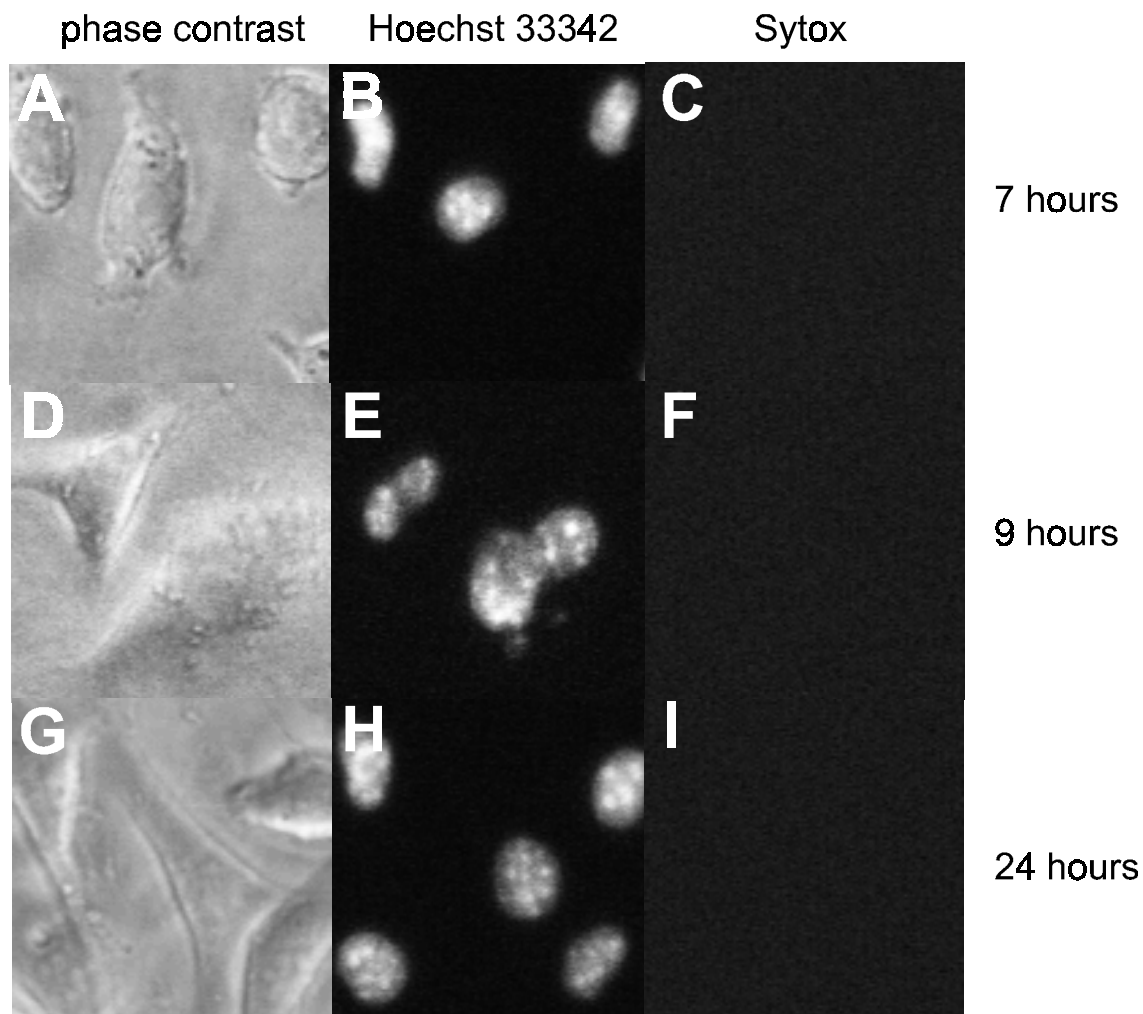


Fig. 52 Nuclear morphology of MK801 treated L12-G10 cells after induction of NMDA receptor expression

L12-G10 cells were grown in MEM w/o Mg^{2+} containing $4\mu M$ dexamethasone, 5% FCS, 1.8mM calcium, 55mM potassium and $10\mu M$ MK801 for 7 (A-C), 9 (D-F) and 24 hours (G-I). Cultures were co-stained with Hoechst 33342 (final $0.5\mu g/ml$) (B, E, H) and Sytox (final $0.5\mu M$) (C, F, I) after the indicated intervals and analysed by fluorescence microscopy. A, D, G are the respective phase contrast images.

Supplement with potassium to a final concentration of 55mM yielded highly fragmented, small sized DNA (M1 marked range 87.62%). The peak of this population is typical for necrotic DNA fragmentation.

Taking together, the data from LDH-release studies and nuclear staining experiments clearly indicate a NMDA receptor mediated loss of membrane integrity after 10 to 12 hours from

Results – characterization of cell death

induction of NMDA receptor expression which is not accompanied by nuclear, apoptotic features like chromatin condensation, DNA fragmentation and the development of apoptotic bodies.

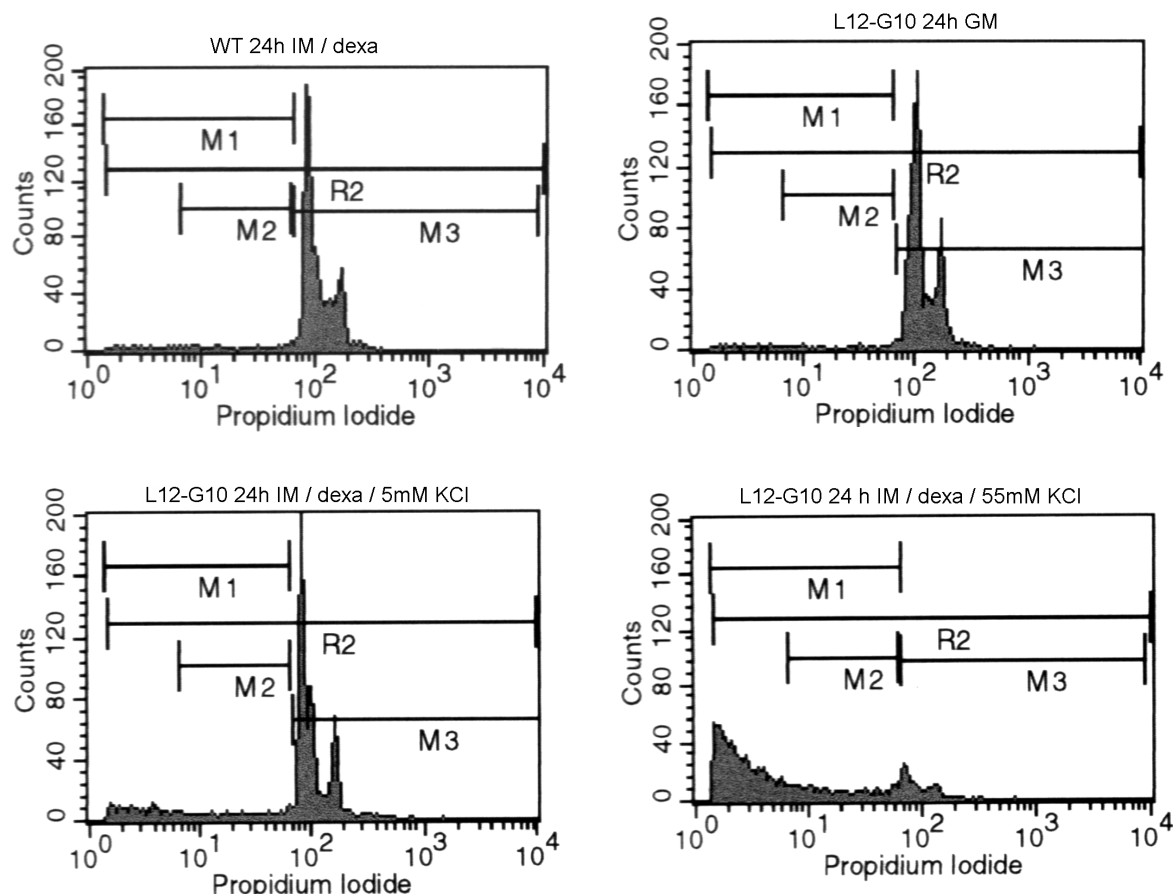


Fig. 53 Flow cytometry-histograms from propidium iodide stained nuclei

Cells were grown for 24 hours in the indicated medium (GM = growth medium (MEM containing 5% FCS); IM = induction medium (MEM containing 5% FCS, 4 μ M dexamethasone in the presence or absence of additional potassium (50mM))).

Since the development of nuclear changes displays a late event in the programmed cell death and may be blocked for unknown reasons, the translocation of phosphatidylserines (PS) was examined. The migration of PS is a very early event in the onset of apoptosis and distinct from nuclear changes. The binding of Alexa-568 labelled annexin V to L12-G10 cells was examined after 10 hours of differentiation (induction medium contained 55mM potassium). Representative images of the annexin V staining are given in fig. 54 and 55. Among the differentiated, NMDA receptor expressing L12-G10 cells, annexin V positive cells were only detected in cultures lacking ketamine (see fig. 54). Only a small amount of these cells (<10%) was annexin V positive. Necrotic cells exhibit a deep fluorescence in annexin V labelling and

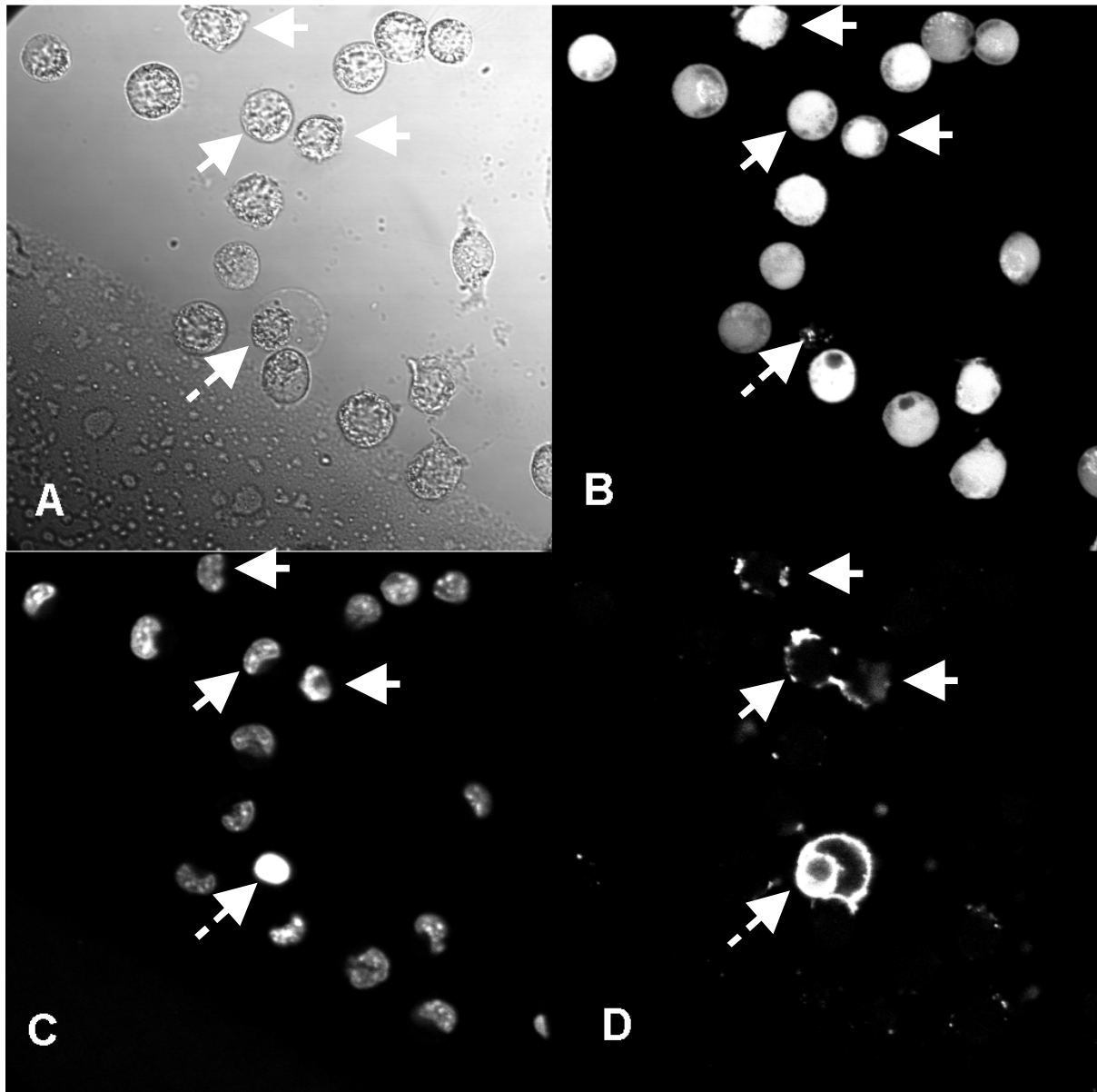


Fig. 54 Annexin-V staining of L12-G10 cells cultured for 10 hours in MEM containing 5% FCS, 4 μ M dexamethasone and 55mM potassium chloride
(A) phase contrast; (B) calcein staining; (C) Hoechst 33342 staining; (D) Annexin V staining. Annexin V positive cells are marked with solid arrows, necrotic cells with dashed arrows.

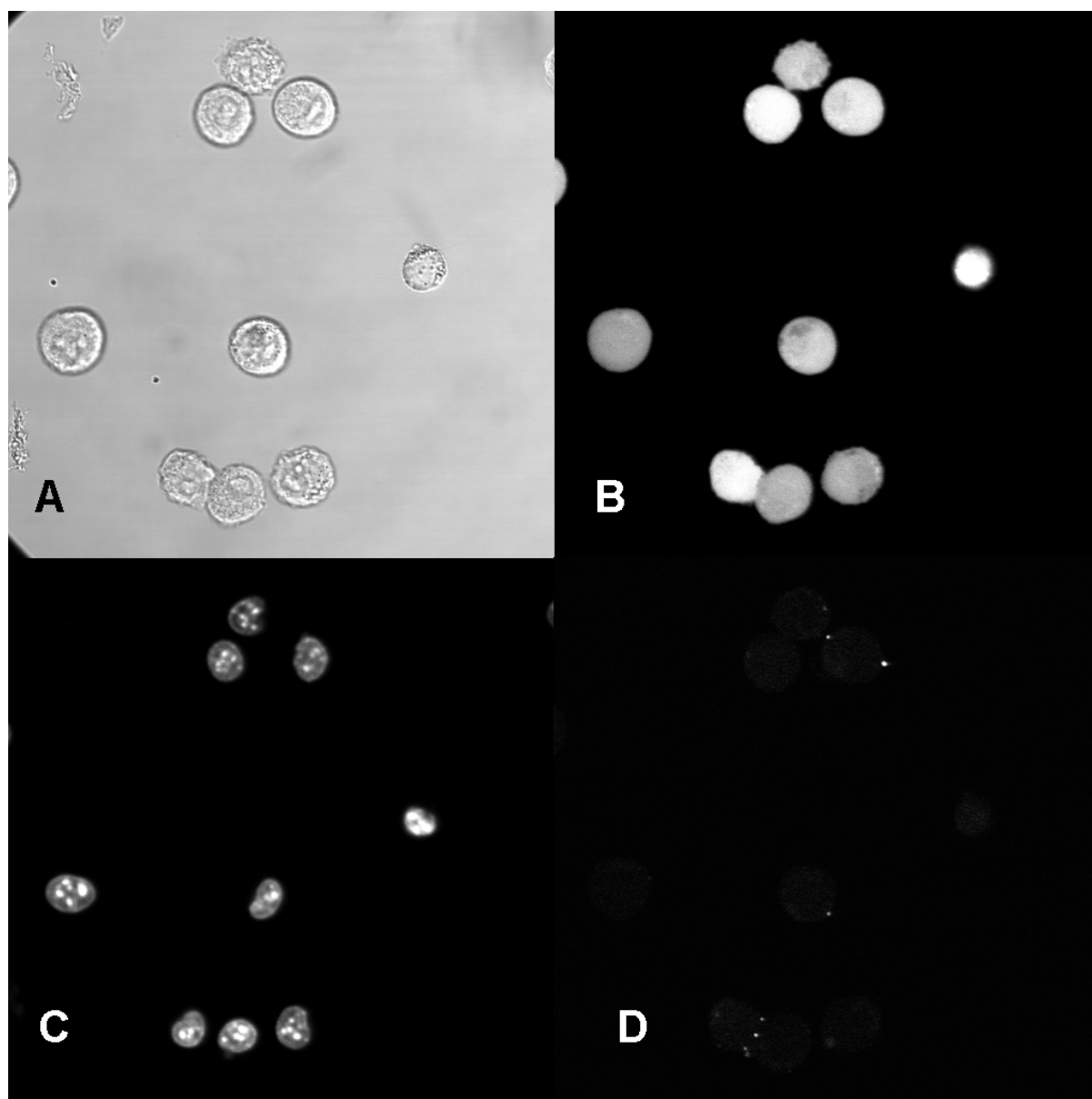


Fig. 55 *Annexin-V staining of L12-G10 cells cultured for 10 hours in MEM containing 5% FCS, 4 μ M dexamethasone, 55mM potassium and 100 μ M ketamine*
(A) phase contrast; (B) calcein-AM staining; (C) Hoechst 33342 staining; (D) Annexin V staining.

lack fluorescence signals resulting from calcein-AM treatment (fig. 54-D and B dashed arrow). Since these cells were calcein negative, the dense staining of their nuclei (fig. 54-C dashed arrow) is caused by a greater accumulation of dye through damaged plasma membranes and not by nuclear condensation. Additionally, the size of these nuclei is comparable to those of regular, healthy ones. Another population exhibited a positive annexin V staining accompanied by positive calcein staining (fig 54-D and B solid arrows). Therefore,

Results – characterization of cell death

these cells exhibit two major features of apoptotic cells – phosphatidyl turnover and membrane integrity. Consistent with the results of the nuclear staining, no changes in the chromatin pattern of these cells were obvious (fig. 54-C solid arrows). Exposure to the open channel blocker ketamine (100 μ M) prevented necrosis and annexin V staining (fig. 55). The nuclei of ketamine protected cells displayed a normal diffuse, granular staining. Although the extent of apoptotic PS turnover is very low, the onset of this apoptotic feature is clearly mediated by NMDA receptor stimulation proofed by the lack of annexin V positive cells in the ketamine control. Since “apoptotic“ annexin V stained cells lack any nuclear changes, this confirms the results from nuclear staining and led to the conclusion, that (i) necrosis is the predominant mode of cell death in the induction model and (ii) that there is some evidence for the inhibition of nuclear apoptosis by unknown mechanisms.

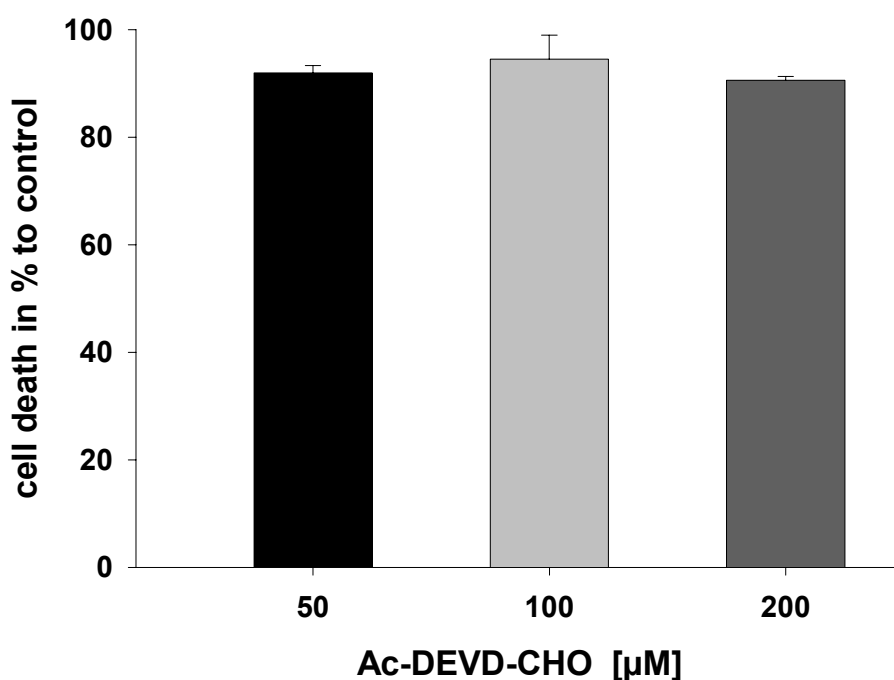


Fig. 56 **Effects of caspase-3 inhibitor Ac-DEVD-CHO on the NMDA receptor mediated cell death in L12-G10 cells**

L12-G10 cells were exposed to MEM medium containing 2 μ M dexamethasone, 5% FCS in the absence (control) or presence of 50, 100 and 200 μ M Ac-DEVD-CHO. LDH release was assayed after 24 hours.

This conclusion is supported by the finding, that the NMDA receptor mediated cell death of L12-G10 cells is only slightly decreased by application of cell permeable caspase-3 inhibitor

Results – characterization of cell death

Ac-DEVD-CHO (acetyl-Asp-Glu-Val-aspartic acid aldehyde) (fig. 56). Compared to control cells, 200 μ M Ac-DEVD-CHO decreased the cell death rate to approximately $91 \pm 0.7\%$. This result corresponds to the results of annexin V staining showing that apoptotic changes of the plasma membrane are apparent, but only in a small population of stimulated cells (<10%). Beside the induction model, the shape of cell death was also characterized in the differentiation model, since pre-expression of NMDA receptors resembles more excitotoxic processes in neurons. Initial studies characterized the time course of LDH release in the differentiation model (fig. 57). After stimulation with 30 μ M L-glu / gly, NR1-1a / 2A expressing L12-G10 cells showed a steep increase in LDH release, starting 5 min after the beginning of NMDA receptor stimulation and reaching their maximum cell death rate after 20 min, already. In contrast, NR1-1a / 2B expressing clone L13-E6 exhibited a more delayed cell death with a maximum cell death rate after 40 to 50 min. This attenuated increase in cell death

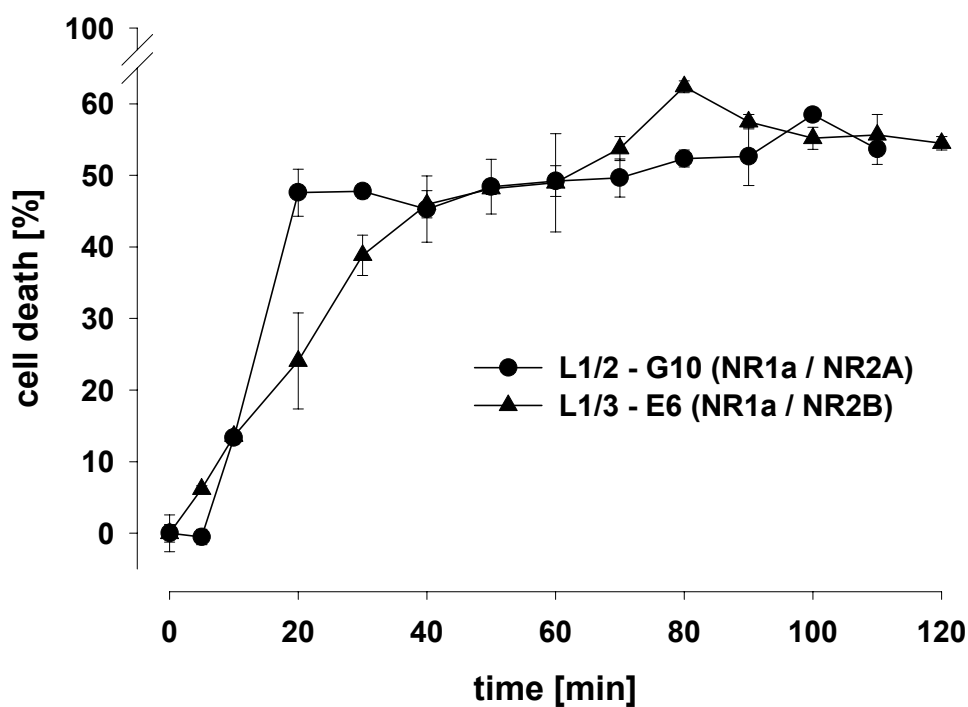


Fig. 57 *Loss of membrane integrity after stimulation of pre-expressed NMDA receptors in the differentiation model*

L12-G10 (NR1-1a / NR2A) and L13-E6 (NR1-1a / NR2B) cells were differentiated for NMDA receptor expression in growth medium containing 4 μ M dexamethasone and 100 μ M ketamine for 24 hours. After removal of the induction medium cells were stimulated in CSS (pH 7.6 for L12-G10 or pH 8.0 for L13-E6) cont. 1.8mM Ca²⁺, 50mM potassium and 30 μ M L-glu / gly). LDH-release was assayed after the indicated intervals.

Results – characterization of cell death

could be explained by a reduced calcium permeability of NR1-1a / 2B receptors. In contrast to the onset of cell death, the final amount of cytotoxicity is comparable in both clones with cell death rates of 50 to 60% after 90 min of stimulation. Stimulation periods exceeding 3 hours were not applied to avoid an unspecific cell death caused by growth factor withdrawal.

The early damage of the plasma membrane was confirmed by the nuclear staining with the non-permeable dye Sytox (fig. 58). 30 min after the beginning of stimulation with 30 μ M L-glu / gly, approximately 60% of L12-G10 cells displayed a Sytox positive staining (fig. 58-C), whereas inhibition of NMDA receptors by 100 μ M ketamine almost prevented cells from the loss of plasma membrane integrity (fig. 58-D). Ketamine treated cells maintained their normal oblong or angular phenotype (fig. 58-B). In contrast, unprotected cells flattened out, showed a rough surface and the nuclei of necrotic cells were clearly visible in the phase contrast (fig. 58-A and 59-A)). After 90 min of stimulation, NMDA receptor mediated cytotoxicity was increased to 75% (fig. 58-G) with similar morphological features (fig. 58-E vs. A). Ketamine treated cultures remained healthy, although the majority of cells changed their appearance to round cell bodies (fig. 58-H and F).

For the examination of changes in nuclear morphology, a co-staining with Hoechst 33342 and Sytox was applied (fig. 59). Similar to the results obtained from the induction model, necrotic L12-G10 cells displayed a dense nuclear staining with Hoechst 33342 dye, although nuclei did not shrink compared to those of alive, Sytox negative cells (fig. 59-B and C). Ketamine treated cells maintained the granular substructure of their nuclei up to 90 min of stimulation (fig. 59-E and K).

Taking together, even the results obtained from the differentiation model lead to the conclusion, that stimulation of heterologously expressed NMDA receptors in L(tk-) cells induces a predominant mode of necrotic cell death.

To investigate whether apoptosis is generally blocked in these cell lines, wildtype L(tk-) cells were treated with 1 μ M staurosporine for 8 hours. Staurosporine is an inhibitor of protein kinase C and a strong inducer of apoptosis in many cell lines. The results of the annexin V staining are given in fig. 60. The whole population showed a strong blebbing of the cytosol under maintenance of the membrane integrity (fig. 60-A and B). But only a minority of cells exhibited a positive annexin V staining (fig. 60-D solid arrows). In contrast to the investigations on NMDA receptor mediated cell death, the nuclei from annexin V positive cells exhibited intense fluorescent substructures which are typical for a chromatin condensation (fig. 60-C) or the formation of apoptotic bodies (fig. 60-G). Interestingly, only a

Fig. 58

Morphological changes and plasma membrane leakage after NMDA receptor stimulation in the differentiation model

L12-G10 cells were differentiated for NMDA receptor expression in growth medium cont. 4 μ M dexamethasone and 100 μ M ketamine for 24 hours. After removal of the induction medium cells were stimulated in CSS (pH 7.8 cont. 1.8mM Ca²⁺, 50mM potassium and 30 μ M L-glu / gly) in the absence (A / E) and presence (B / F) of 100 μ M ketamine for the following intervals: 30 min (A-B) and 90 min (E-F). For the detection of membrane leakage, cultures were stained with Sytox (final 0,5 μ M) (C, D, G, H) and analysed by light and fluorescence microscopy.

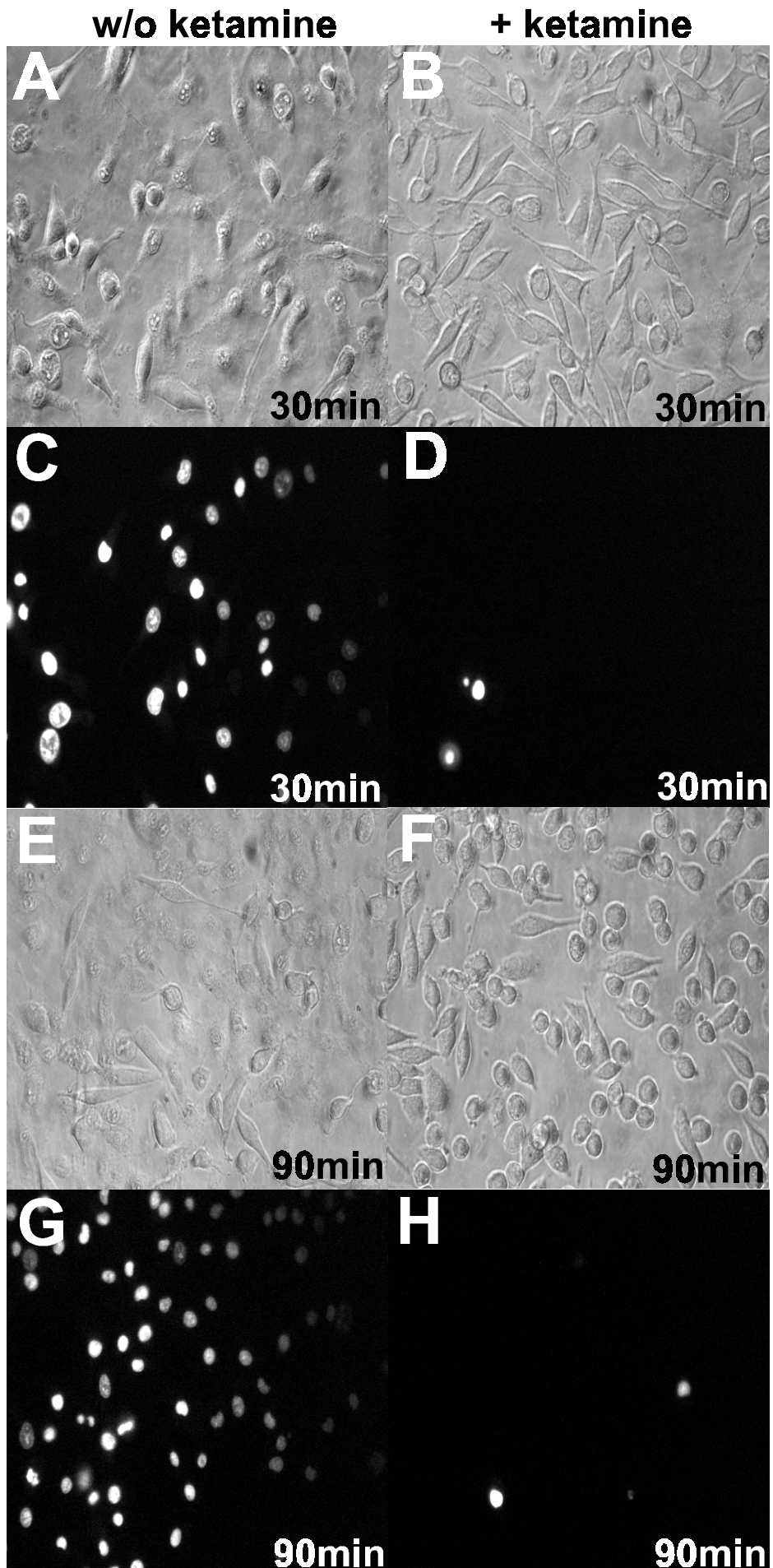
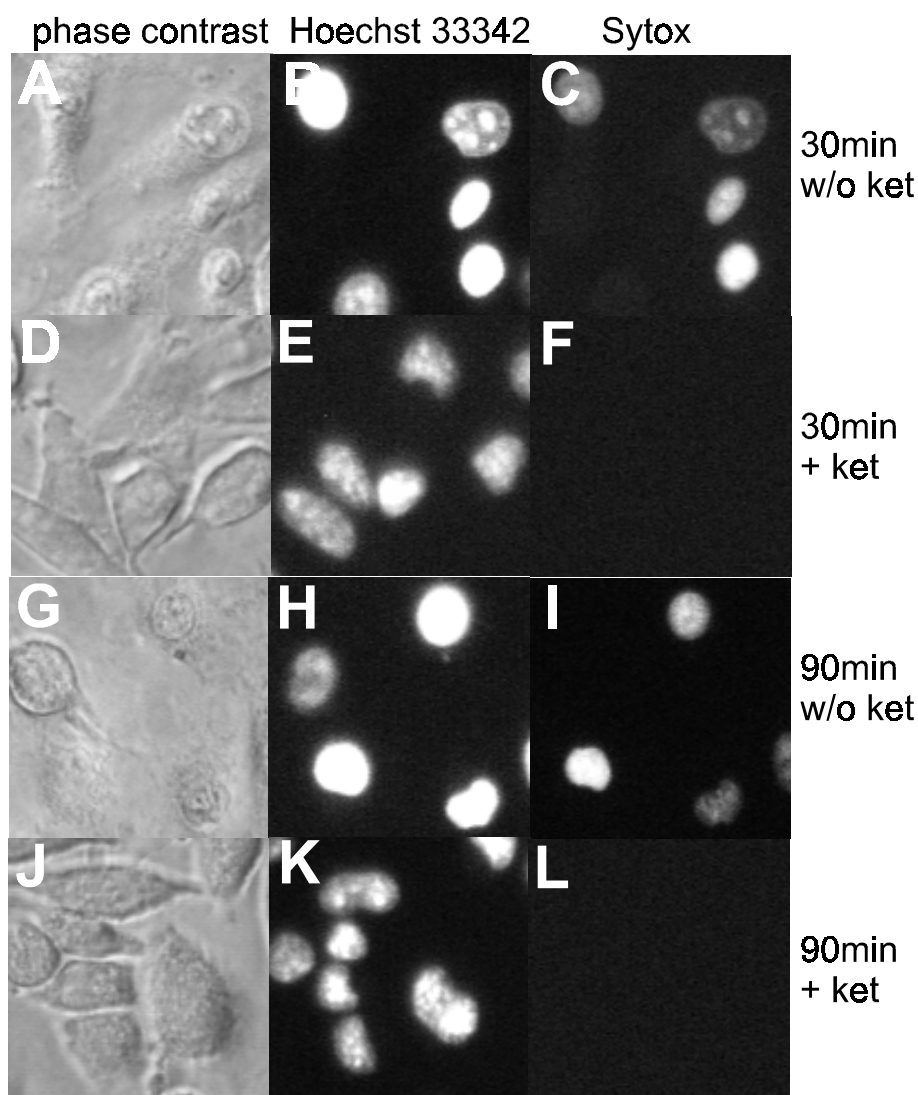


Fig. 59

Nuclear morphology of differentiated L12-G10 cells after stimulation of NMDA receptors

L12-G10 cells were differentiated for NMDA receptor expression in growth medium cont. 4µM dexamethasone and 100µM ketamine for 24 hours. After removal of the induction medium cells were stimulated in CSS (pH 7.8 cont. 1.8mM Ca²⁺, 50mM potassium and 30µM L-glu / gly) in the absence (A-C and G-I) and presence (D-F and J-L) of 100µM ketamine for the following intervals: 30 min (A-F) and 90 min (G-L). Cultures were co-stained with Hoechst 33342 (final 0.5µg/ml) (B, E, H, K) and Sytox[®] (final 0,5µM) (C, F, I, L) after the indicated intervals and analysed by fluorescence micros-copy. A, D, G and J are the respective phase contrast images.

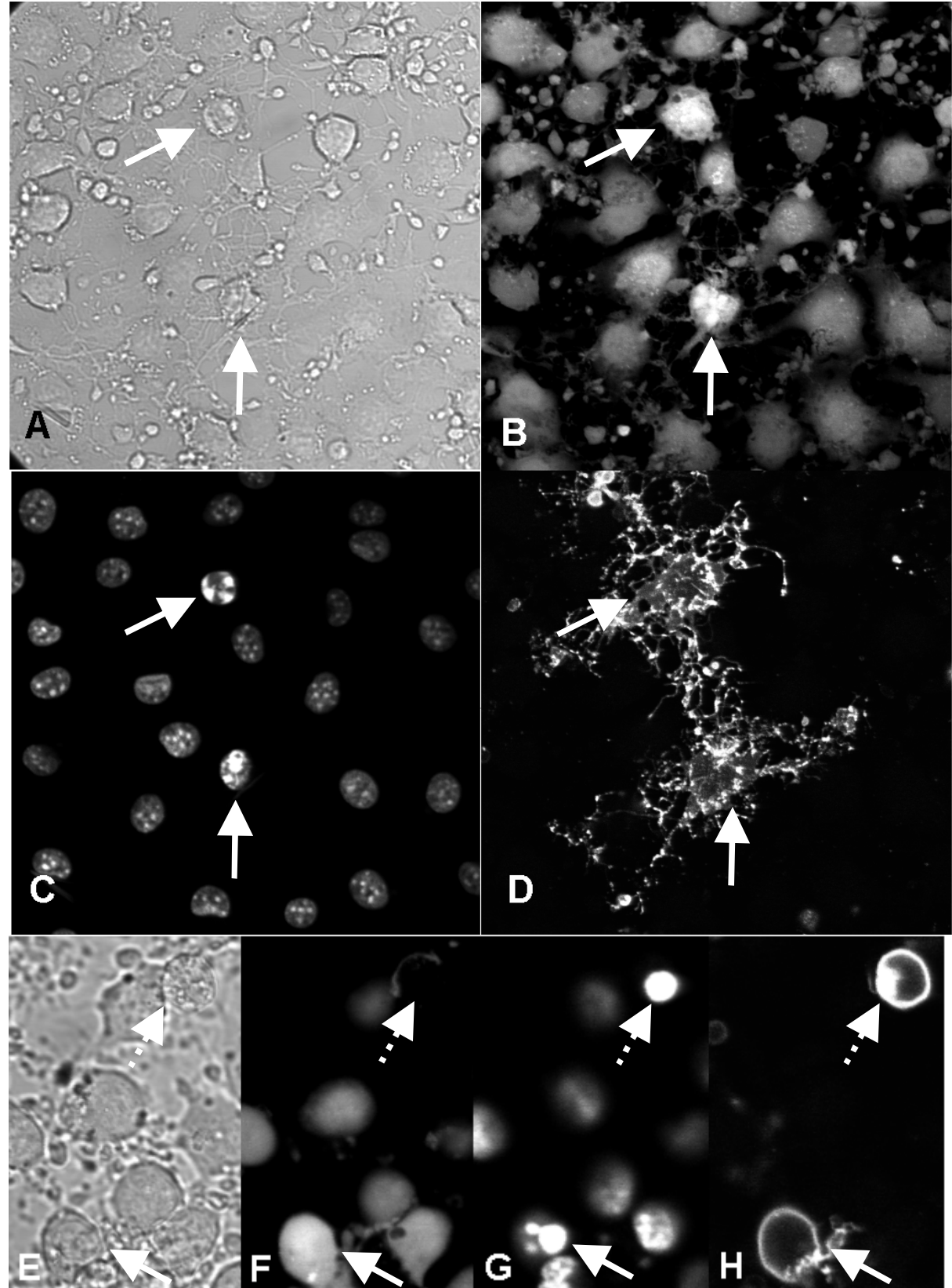


small proportion of the population (<10%) showed a positive annexin V staining accompanied by the maintenance of plasma membrane integrity. This indicates a general resistance of L(tk-) cells against apoptotic cell death since even a treatment with 0.5µM staurosporine for 20 hours led not to a significant nuclear condensation or the formation of apoptotic bodies (data not shown).

Results – characterization of cell death

Fig. 60 *Annexin-V staining of staurosporine treated L(tk-) cells*

L(tk-) wildtype cells were cultured for 8 hours in MEM containing 5% FCS, 55mM potassium and 1 μ M staurosporine. (A/E) phase contrast; (B/F) calcein-AM staining; (C/G) Hoechst 33342 staining; (D/H) Annexin V staining. Annexin V positive apoptotic cells are marked with solid arrows, necrotic cells with dashed arrows.



4. Conclusions

The current study was intended to develop an *in vitro* test system for NMDA receptor antagonists. Studies with primary cultures have some limitations in terms of characterizing antagonistic properties of compounds because there are several subtypes of NMDA receptors expressed in cultured neurons with different pharmacological properties. Besides, in toxicological studies investigating neurotoxic effects of compounds, it is useful to have molecularly defined receptors excluding an interaction with other glutamate receptors or NMDA receptor subtypes. Therefore, we favoured nonneuronal cell lines expressing recombinant NMDA receptors. After initial trials with transient expression of recombinant NMDA receptors in HEK 293 cells we decided to establish a stable expression system which should represent a more convenient and robust heterologous expression system.

We succeeded in the establishment of stably transformed mouse fibroblasts [L(tk-)] expressing recombinant human NMDA receptor subunits NR1-1a / NR2A (clone L12-G10) or NR1-1a / NR2B (clone L13-E6). The inherent excitotoxicity occurring while expressing recombinant NMDA receptors in mammalian cells (Anegawa et al., 1995; Cik et al., 1993) was used to create a cell death based *in vitro* test system for NMDA receptor ligands. During routine cell culture, the expression of NMDA receptors is avoided due to the use of a dexamethasone inducible expression system (Grimwood et al., 1996a). Selection due to background expression of receptors is prevented by the addition of the NMDA receptor antagonist ketamine. Our stable cell lines have proved their usefulness for more than 90 passages (~45 weeks); this is a great advantage compared to transiently transformed cells which could only be used for several days.

To characterize the expression and functionality of recombinant NMDA receptors in the obtained cell lines, RT-PCR analysis, Western blot and immunocytochemical analysis of subunit NR1-1a as well as calcium video imaging was applied. RT-PCR analysis of L12-G10 and L13-E6 cells differentiated for 12 hours with dexamethasone revealed an upregulation of NMDA receptor mRNA in both clones. By densitometric volume analysis we estimated a 5-fold increase for NR1-1a transcripts and a 2.3-fold increase for NR2A in L12-G10. For clone L13-E6, ratios of 4.8 for hNR1-1a and 3.5 for hNR2B were calculated.

These data are consistent with results from immunoblotting of subunit NR1-1a revealing a maximum of protein amount between 8 and 16 hours of treatment with dexamethasone, whereas no protein could be detected in uninduced clones and wildtype cells. The size of the detected 116 kDa protein is consistent with the predicted molecular weight from the deduced

Conclusions

amino acid sequence (103.5 kDa) and the size of NR1 subunits detected in rat brain membranes. Immunofluorescence labelling of subunit NR1-1a in induced clones suggested high amounts of receptor localized within the plasma membrane. Since it has been reported that co-expression with NR2 subunits is required for successful surface expression of subunit NR1 (McIlhinney et al., 1996; McIlhinney et al., 1998) we concluded a localization of hetero-oligomeric receptors within the plasma membrane. This conclusion was supported by results from calcium video imaging which indicated a strong increase in $[Ca^{2+}]_i$ after stimulation with L-glutamate and glycine. Subsequent treatment with open channel blockers ketamine and MK801 recovered $[Ca^{2+}]_i$ to basal levels. Since single expression of subunit NR1 failed to form functional receptors in mammalian cells, we have successfully demonstrated the surface co-expression of the transfected NMDA receptor subunits.

The developed cytotoxicity assay, using the measurement of LDH activity from lysed cells, represents a valid method with high precision, accuracy and easy performance for the evaluation of cell death. Other current methods have been described for the quantification of cell death, e.g. staining with vital dyes like trypan blue or fluorescent dyes like propidium iodide or Sytox. These approaches are based on the ability of alive cells, with intact cell membranes, to exclude these dyes and prevent nuclear staining. The disadvantage of these techniques is the need of multiple, time consuming cell counting. Therefore, results describing cell death rates under different conditions (e.g. dose response curves) at the same time point are hardly achieved. Other described cell death assays use the ability of mitochondria to convert tetrazolium salts like MTT or XTT into coloured formazan product that may be also measured spectrophotometrically. The disadvantage of these approaches is the need of an additional incubation period of 1 to 2 hours after treatment of cells, which prolongs assay time, and the immediate evaluation of cell death after short incubation periods is not possible. The method described here is suitable for the performance in 96 well or upper scale and offers an economic method for high throughput screening of compounds either in the induction or the differentiation model.

The developed cell culture designs were extensively characterized and successfully applied. For QSAR studies of thienopyridinones, we choose the induction model to evaluate its applicability. For high affinity compounds, IC_{50} -values obtained by cytotoxicity assays were well correlated to the K_i -values of binding assays. For the nine compounds active in both settings, a correlation coefficient of 0.90 ($P = 0.001$) was observed. The developed test system even considered compounds binding to plasma albumin which was demonstrated using the plasma albumin competitor warfarin. It should be noted, that binding to plasma albumin limits

Conclusions

compounds brain penetration *in vivo* (Rowley et al., 1997b). Therefore, the presence of plasma albumin binding in the developed test system seems to be an advantage compared to other routine methods like radioligand binding assays or electrophysiological methods, which do not consider this critical parameter.

Unfortunately, most low affinity compounds could not be characterized. The high agonist concentrations provided by the added FCS turned out to represent a disadvantage for competition assays of compounds with lower potency and poor solubility. Therefore, we developed an improved model, designated as differentiation model, which provides more defined experimental settings. This design, also based on the evaluation of cell death rates, allowed an extensive pharmacological characterization of clones L12-G10 and L13-E6. In part, we observed distinct pharmacological properties which are reflecting the different properties of NR1-1a / NR2A and NR1-1a / NR2B receptor assemblies. We demonstrated that the observed cell death in both cell lines is strictly dependent on the presence of L-glutamate and even depends on the applied pH. Proton sensitivity of NMDA receptors at the physiological pH has been established in patch clamp studies in cerebellar neurons (Traynelis and Cull-Candy, 1990). Now it is clear that proton inhibition is mediated by the absence of the 5'-insert in the NR1 subunit (Traynelis et al., 1995). Our results emphasize that experiments at functional NMDA receptors should only be performed under defined pH conditions (HEPES buffered salt solutions in the absence of CO₂ or carbonate buffered cell culture medium under strict CO₂ control). Since this proton inhibition appears in a narrow range close to physiological pH, the lack of receptor activity is often caused by unsuitable "acidic" pH conditions rather than by other reasons. Occurring cell death is triggered under the presence of glycine site agonists D-serine or glycine, but we failed to demonstrate a clear dose dependency for these compounds. This failure is probably caused by contamination of glycine which occurred during washing of the cells with MEM containing 1% BSA (required for the removal of ketamine to enable receptor activity). Since BSA enhanced adherence of cultures during the washing procedure, it was an ingredient of washing solutions which we could not substitute by other high molecular compounds (e.g. dextran). In competition assays, glycine and D-serine were able to completely abolish cytoprotective effects exerted by 100µM DCKA. The obtained EC₅₀-values indicated an agonist preference of L13-E6 cells (NR1-1a / NR2B) compared to NR1-1a / NR2A expressing L12-G10 cells. The estimated concentrations required to abolish 50% of cytoprotection were two to three fold higher with clone L12-G10. The same preference was evident in assays with the competitive antagonist (R/S)-CPP where L-glutamate and L-aspartate exhibited a higher potency at L13-E6 cells. In

Conclusions

turn, antagonists like (R/S)-CPP, (R/S)-AP5 or DCKA exhibited a 5 fold higher efficacy at L12-G10 cells. These findings are consistent with results from studies of NMDA receptor subunits expressed in *Xenopus oocytes* (Hess et al., 1996) and with the existence of agonist and antagonist preferring NMDA receptors in vivo. Compared to D-serine, the potency of glycine was slightly higher at both clones which is also consistent with earlier findings (Matsui et al., 1995). Efficacy of L-glutamate was 7 to 10 fold higher compared to L-aspartate. The open channel blocker ketamine did not discriminate between both clones which is also in accordance to literature. Ifenprodil and haloperidol exhibited cytoprotective effects only at clone L13-E6 (expressing NR1-1a / NR2B) but failed to reduce cell death at L12-G10 cells (NR1-1a / NR2A) in concentration up to 100 μ M. This preference (ifenprodil > 670 fold; haloperidol > 45 fold) is consistent with the finding that these compounds discriminate subtypes of recombinant heteromeric receptors with a preference for NR2B containing receptors. Patch clamp studies in *Xenopus oocytes* revealed a 400 fold NR2B preference for ifenprodil compared to NR2A (Williams, 1993a). For haloperidol a preference of > 100 has been described (Ilyin et al., 1996). The reported IC₅₀-values for ifenprodil (0.34 μ M) and haloperidol (\sim 3 μ M) correspond to the estimated IC₅₀-values for ifenprodil (0.15 \pm 0.02 μ M) and haloperidol (2.2 \pm 1.5 μ M) in our cytotoxicity model.

Interestingly, the requirement of NR2B subunits overlap with those for stimulation by polyamines. We have demonstrated, that spermine triggers the function of NR1-1a / NR2B (L13-E6) receptors resulting in an increased cell death rate. This glycine independent enhancement of cell death by spermine exhibited a clear dependency on applied proton concentrations. Increased cell death rates compared to control were obvious at pH levels which normally inhibit receptor function. At lower proton concentrations spermine failed to enhance cell death. At NR1-1a / NR2A expressing L12-G10 cells, spermine did not significantly affect cell death. These results suggest, that (i) spermine specifically affects NR2B containing receptors and (ii) mediates its positive modulating effect via relief of proton inhibition. These observations are consistent with the suggested mechanism of spermine modulation (Traynelis et al., 1995).

Under these predictions we have evaluated the ability of spermine to abolish the cytoprotective effects of ifenprodil and haloperidol at clone L13-E6. Spermine affected the cytoprotection by ifenprodil and haloperidol, but rather in an allosteric than direct competitive manner. At non-protective concentrations of antagonist, spermine increased the rate of cell death. In contrast, protective concentration levels remained nearly unaffected. These experiments were performed under relief of normal proton inhibition (pH 8.0). As previously

Conclusions

shown, spermine fails to trigger cell death under relief of proton inhibition but enhances cell death in the presence of non saturated concentrations of ifenprodil and haloperidol although these experiments were performed at pH 8.0. Hence, we conclude that these allosteric antagonists partially mediate their cytoprotective effects by facilitating proton inhibition. This hypothesis is supported by recent reports, which proposed that the allosteric block of NMDA receptors by ifenprodil is mediated by an increased potency of ambient protons to block the NMDA receptor (Mott et al., 1998). The authors concluded that ifenprodil causes a larger fraction of receptors to be protonated and thus inhibited by shifting the IC_{50} for proton block of NMDA receptors to more alkaline-values. Hence, spermine reduced cytoprotective effects of ifenprodil and haloperidol rather due to opposite effects on proton inhibition and not by direct competition at common binding sites.

Effects exerted by histamine were obvious at NR1-1a / NR2B expressing clone L13-E6 only, which is consistent with previous findings (Williams, 1994b). Unexpectedly we observed a dose dependent inhibition of cell death. Contradictions to earlier studies, which reported enhanced NMDA receptor function by the application of histamine (Bekkers, 1993) (Vorobjev et al., 1993) (Zwart et al., 1996), may be caused by distinct pH conditions, since it has been shown that histamine enhanced the NMDA component of the synaptic currents at lowered pH (7.2) while at raised pH (7.6) it reduced them (Saybasili et al., 1995). Since we performed the reported cell toxicity assays under relief of proton inhibition (pH 8.0 for clone L13-E6), our data support the finding of a histamine mediated inhibition of NR2B containing NMDA receptors at raised pH levels.

Although activation of PKC has been reported to enhance NMDA receptor activity (Chen and Huang, 1991) (Kelso et al., 1992) treatment with PKC activator TPA (100nM) failed to affect cell death in both clones. But our results may not be in direct contradiction to these observations, since different splice variants of subunit NR1 exhibit distinct sensitivity to PKC, and phosphorylation of splice variant NR1-1a exhibits an enhancement of only 3-fold (Tingley et al., 1993). In turn, a putative phosphorylation may not affect these heterologous NMDA receptors due to a high basal phosphorylation level which has been reported from transient expression experiments in Hek 293 cells (Tingley et al., 1993).

To investigate the participation of mitochondrial damage in NMDA receptor mediated excitotoxicity we used cyclosporin A (CsA) which is a known inhibitor of calcium induced permeability transition (PT) in mitochondria. Prolonged pre-treatment with CsA reduced cell death rates in a dose dependent manner. The selective calcineurin inhibitor FK506 failed to exert cytoprotection after NMDA receptor stimulation which excludes the involvement of

Conclusions

calcineurin inhibition by CsA. Unfortunately, we found that CsA did also affect the expression of the transfected NMDA receptor subunits. We could demonstrate that prolonged treatment with CsA reduced the expression of NMDA receptor subunit NR1-1a in our cell lines by 70%. This finding is in agreement with functional expression of other ion channels in *Xenopus oocytes* (Chen et al., 1998) (Helekar et al., 1994). These authors concluded that the functional expression of ion channels is facilitated by the peptidyl-prolyl isomerase cyclophilin and that the oligomeric assembly of neurotransmitter-gated ion channels represents a multi-step process involving the participation of cyclophilins. These immunophilins, which are present in the cytoplasm, the endoplasmic reticulum and the mitochondria, exhibit a peptidyl-prolyl isomerase activity and assist in the folding of polypeptides similar to classical heat shock proteins (chaperones). Since it has been suggested, that heterologously expressed NMDA receptor subunits are assembled in the ER and that co-synthesis of the subunits is necessary for their successful cell surface targeting (McIlhinney et al., 1998), it is likely that CsA also affects the surface expression of the transfected NR2 subunits. Brief pre-treatment with 30 μ M CsA (10min) failed to prevent cells from undergoing cell death when stimulated under the relief of tonic proton inhibition (CSS pH 7.6). But cytoprotective effects were evident under partial proton inhibition of NMDA receptors (CSS pH 7.0). Under these modified conditions, brief pre-treatment with CsA reduced cell death by approximately 40% compared to control. FK506, which did not affect the PT, displayed a mean reduction of \sim 7%. These results exclude a calcineurin mediated cytoprotection by CsA. But so far, we cannot clearly distinguish between the assumed inhibition of PT and a reduction of NR1 subunit expression by inhibition of cyclophilin A. Hence, the participation of mitochondrial damage after stimulation of heterologously expressed NMDA receptors remains elusive and instead of CsA, the use of more specific PT inhibitors like bongkrecic acid or inhibitors of mitochondrial calcium sequestration like ruthenium red or the uncoupler FCCP should be favoured in further investigations.

Studies on the shape of cell death suggested a predominant necrotic way of cell death due to early loss of plasma membrane integrity and the failure of nuclear apoptotic features related to the NMDA receptor stimulation. The lack of apoptosis in our excitotoxicity models is in contrast to the execution of neuronal glutamate induced cytotoxicity in vivo and in vitro. But the comparison of neuronal in vitro models (e.g. CGC cells) and heterologous expression models reveals some crucial differences in calcium metabolism. Due to their function, neurons have higher abilities to regulate oscillations of intracellular calcium levels and to

Conclusions

maintain calcium homeostasis. Ionized calcium as an intracellular second messenger, must be kept in a narrow concentration range in the resting cell (i. e. 100 – 300nM). Since the calcium concentration in the extracellular milieu is 1 - 2mM, this results in a very steep concentration gradient across the plasma membrane. Neurons possess a number of different transmembrane calcium transporting systems which participate in the control of the free calcium concentration within the cell. Most of these systems are located in the plasma membrane like voltage dependent or ligand directed calcium channels (e.g. L-type or NMDA receptor channels), the calcium pump for the ATP dependent export of calcium (Ca^{2+} -ATPase) and the Na^+ dependent Ca^{2+} exchanger, who transports three Na^+ ions for one Ca^{2+} (inward or outward depends on the transmembrane potential). Additionally, intracellular organelles are involved. The ER stores calcium, which can be released into the cytosol by the second messenger IP_3 (second messenger of metabotropic glutamate receptors mGluR1 and 5). Under pathological conditions, mitochondria possess by far the highest calcium storage capacity in cells. It has been shown, that the mitochondrial calcium uptake responds dynamically to changes in cytosolic calcium levels and plays a crucial role in the sequestration of large calcium loads induced by NMDA receptor activation (Stout et al., 1998b; White and Reynolds, 1997). Even a privileged access of calcium influx via NMDA receptors to mitochondria has been described (Peng and Greenamyre, 1998).

Only a few of the described mechanisms such as Ca^{2+} -ATPase and calcium sequestration by ER and mitochondria are ubiquitous and also present in the transfected fibroblasts. Since we have shown that the stimulation of the heterologously expressed NMDA receptors leads to a steep initial increase in intracellular calcium levels, the lack of an efficient calcium regulation system in L(tk-) cells (e.g. the Na^+ dependent Ca^{2+} exchanger) may lead to an increased sequestration of calcium by mitochondria, breakdown of mitochondrial membrane potential, loss of oxidative phosphorylation, lack of ATP synthesis and generation of reactive oxygen species. The decrease of ATP levels may also be triggered by an increased demand of ATP for membrane pumps (Ca^{2+} -ATPase). Results of ATP level determination after stimulation of the heterologous NMDA receptors confirm the calcium dependent decrease in cytosolic ATP levels. The ability of some neurons (e.g. CGC cells) to compensate the failure of oxidative phosphorylation by glycolysis has been shown (Budd and Nicholls, 1996). Interestingly, these cells predominantly undergo apoptotic excitotoxicity. In the presence of ATP synthase inhibitor oligomycin glycolysis supports the total cellular ATP demand of CGC cells. The combination of the complex I inhibitor rotenone with oligomycin allows the proton gradient at the inner-mitochondrial membrane to decay, preventing mitochondrial calcium loading and

Conclusions

reduced cell death. In our cell lines initial experiments with rotenone and oligomycin in the differentiation model did not lead to cytoprotective effects. After application of oligomycin, ATP levels in L12-G10 cells rapidly decreased, suggesting that glycolysis in L(tk-) cells is not sufficient to supply the total cellular ATP demand. Since ATP is required for the progression of programmed cell death, apoptosis seems to be hindered in our models for two reasons: (i) lack of efficient mechanisms to maintain calcium homeostasis after stimulation of heterologous NMDA receptors may lead to an early damage of Ca^{2+} - sequestering mitochondria and in consequence to (ii) ATP depletion since the ATP demand of these cells seems to be mainly supplied by mitochondria. Hence, predominant cell death might switch to necrosis. Since even staurosporine, which is a strong inducer of apoptosis in a number of cell lines, failed to induce higher rates of apoptosis, even a general resistance of L(tk-) cells against apoptosis is likely.

This hypothesis is also supported by the finding, that the murine fibrosarcoma cell line L929, representing the predecessor cell line of L(tk-) cells, rapidly dies in a necrotic way after exposure to TNF (Vercammen et al., 1998), which is a common inducer of apoptosis. In L929 cells, TNF seems to mediate its cytotoxicity through an early damage of mitochondria and the subsequent excessive formation of reactive oxygen intermediates (Schulze-Osthoff et al., 1992). Since we also assume a rapid damage of mitochondria in our excitotoxicity models, these findings support our results and lead to the conclusion, that the execution of apoptosis seems to be hindered due lack of maintenance of cellular ATP levels (Leist et al., 1997).

In summary, we could show that L(tk-) cells stably expressing recombinant human NMDA receptors inhere pharmacological properties, that correspond with the distinct NMDA receptor subunit assemblies. In our cell lines, stimulation of heterologous NMDA receptors elicits necrotic cell death, which was used to establish an efficient in vitro model for the characterization of NMDA receptor ligands. In this respect, expression of human NMDA receptor channels from cloned cDNAs in nonneuronal cell line L(tk-) will be useful because a molecularly defined selective subtype can be studied. The availability of recombinant L12-G10 and L13-E6 cell lines will facilitate the characterization of NR2B selective and non-selective antagonists. Furthermore, the cell death based functional assays applied here have proved to be convenient and pharmacologically valid experimental systems to study human NMDA receptors, to screen for new ligands or to improve structures of lead compounds in QSAR studies.

5. Experimental procedures

5.1 Transient expression of NMDA receptors in Hek 293 cells

For transfection, the constructs pCIS, pCISNR1-1a, pCISNR ϵ 1 and pCISNR ϵ 3 were amplified in DH5 α as host strain and large scale preparations were performed using the silica based anion exchanger Nucleobond[®]AX according to manufacturers instruction.

The transfection procedure was adapted from standard protocols (Chen and Okayama, 1987). Confluent cultures of Hek 293 cells were trypsinized in trypsin / EDTA 1x and diluted to obtain 3×10^6 cells per 10 cm cell culture dish. Cells were grown for 40 hours at 5% CO₂ in MEM supplemented with 10% FCS, 2mM L-glutamine, 100 U/ml penicillin, 100 μ g/ml streptomycin and 1% of a non-essential amino acids solution to obtain 50% confluent cultures. The respective constructs (10 μ g per plate) were diluted with water to final volume of 437 μ l. Then, 62.5 μ l 2M CaCl₂ and 500 μ l 2xBBS were added. 2xBBS contains 50mM BES, 280mM NaCl and 1.5mM Na₂HPO₄ accurately adjusted to pH 6.95. After 30 min and the formation of a very fine haze, the precipitate is added to the cell growth medium. The plates were incubated at 3% CO₂ for 24 hours. If indicated, AP5 was present during this period. Next day, cultures were harvested in trypsin / EDTA and centrifuged. The resulting cell pellet was resuspended in 5ml PBS. An aliquot was diluted 1:10 in 0.4% trypan blue (Sigma) in PBS and subjected to a haemocytometer. Using light microscopy, 150 to 200 cells were counted. Blue staining of chromatin indicated cell death.

5.2 Generation of cell lines stably expressing human NR1-1a / NR2A and NR1-1a / NR2B

5.2.1 Transfection

For plasmid preparation, the dexamethasone inducible mammalian transfection vectors pMSGNR1-1a, pMSGNR2A and pMSGNR2B were amplified in DH5 α as host strain and large scale preparations were performed using the silica based anion exchanger Nucleobond[®]AX according to manufacturers instruction.

L(tk-) cells were co-transfected with pMSGNR1-1a / pMSGNR2A and pMSGNR1-1a /

Experimental procedures

pMSG-NR2B in a 1:5 ratio (NR1 : NR2), respectively. Transfections were performed using the calcium phosphate co-precipitation method with 20µg of total DNA. 5×10^5 cells were plated overnight in a 250ml flask in MEM containing 10% heat inactivated FCS, 2 mM Glutamax I, 100 U/ml penicillin, 100 µg/ml streptomycin and 0.5 mM sodium pyruvate at 5% CO₂. 30 min prior to transfection, total DNA was precipitated in a final volume of 1ml as described above (section 5.1). The precipitate was added to the growth medium and the cells were maintained for 24h at 3% CO₂. Next day, cells were rinsed with serum free MEM and grown for another 24h at 5% CO₂ in growth medium containing 100µM ketamine. Two days after transfection, geneticine in a final concentration of 1mg per ml growth medium was added for 5 days. Between day 5 and 28 geneticine concentration was increased to 2mg/ml growth medium.

5.2.2 Cloning

After 4 weeks of selection, pool cultures were cloned using limiting dilution in 96 well plates (0.3 cells per well). Cloning was performed in growth medium containing 100µM ketamine and geneticine (2mg/ml). To improve the growth of single cells, 50% of “feeder medium“ were included. “Feeder medium“ was obtained from wildtype L(tk-) cells grown for two days in growth medium, centrifuged and deep frozen (-70°C) to delete contaminating cells. After 10 to 14 days various numbers of clones were obtained. Resulting clones were maintained in growth medium containing 100µM ketamine and geneticine (2mg/ml).

5.2.3 Screening

For the monitoring of NMDA receptor activity, clone cultures from 96 well plates were subdivided into 4 wells (96 well plates). Three wells were treated with either growth medium containing 5% FCS and 1µM dexamethasone or additionally 500µM ketamine or 100µM L-glutamate and glycine for 24 hours. The fourth well was maintained for further cultivation. Celltoxicity was determined after 24 hours using the CytoTox 96[®] cytotoxicity assay according to manufacturers instructions. Released LDH was directly measured from 50µl aliquots of cell culture supernatants. The induction medium was removed and the remaining cytosolic LDH was released into fresh growth medium (5% FCS) by a freeze-thaw-step at -70°C for the lysis of surviving cells. Aliquots of 50µl were used for the detection of LDH activity. The amount of formed red formazan was measured at 490nm in a Dynatech MR5000

Experimental procedures

ELISA-reader (96-well format). Cell death is expressed as ratio of absorption from released LDH and total LDH (released LDH plus unreleased cytosolic LDH). All absorptions were corrected for culture medium background caused by phenol red and LDH from FCS.

5.3 Characterization of clones L12-G10 and L13-E6

5.3.1 Reverse-transcription (RT)-PCR analysis

10 to 20x10⁶ cells were cultured in growth medium with or without 2 µM dexamethasone for 12 hours. After cell harvesting total cellular RNA was isolated after the guanidinium thiocyanate method (Chomczynski and Sacchi, 1987) and reverse transcribed into cDNA.

For reverse transcriptase (RT) reaction 5µg of total RNA were denatured in a final volume of 10 µl at 65°C for 10 min and chilled for 5 min on ice. After addition of 30 µl RT reaction mixture containing RT buffer (BRL Y00121), 14 mM DTT, 0.7 mM dNTPs, 37 units RNasin, 200ng Oligo d(T)₁₂₋₁₈ (Gibco) and 200 U reverse transcriptase Superscript plus, cDNA synthesis was carried out at 37°C for 60 min. After heating to 95°C for 5 min, the resulting cDNA template was stored at -20°C.

PCR was performed in a total volume of 50µl containing 2 µl template, 10x PCR buffer (500mM KCl, 100mM TrisCl pH 8.3, 20 mM MgCl₂ 0.1 % of gelatine), 0.2 mM dNTP and 1 µM of 3' and 5' primers. Amplification was carried out as follows: first cycle denaturation at 94°C for 5 min, addition of 2 U Taq polymerase, annealing at the indicated temperature (see primers sequence) for 2.5 min and extension at 72°C for 3.5 min; 26 cycles (for β-actin priming 22 cycles), denaturation at 94°C for 1 min, annealing at indicated temperature for 2.5 min and extension at 72°C for 3.5 min; last cycle, denaturation at 94°C for 1 min, annealing at indicated temperature for 2.5 min and extension at 72°C for 10 min. As subunit specific primers we have used the following oligomers with an annealing temperature of 62°C (5'-3'): GCAAGTGGGCATCTACAATGG (hNR1-1a-1); CAGCAGGTACAGCAT CACGG (hNR1-1a-2); TTGTTGAAAATGTGACCCTGCC (hNR2A-1); TGTTATCGT AGGAATGCTGACG (hNR2A-2); TTCTGACTGCAAATCCTACAACA (hNR2B-1); ACGGTAGGCCAGCTCGATCT (hNR2B-2). For β-actin determination, the following primers were used (5'-3') GAGGAGCACCCCGTGCTGCTG (β-actin A) and CTAGAAGCATTGCTGTGGACGAT (β-actin B) with 60°C as annealing temperature.

Experimental procedures

After amplification, 10 μ l of reaction mixture were separated by agarose gel electrophoresis (3%). Signal intensities were quantified by densitometry (BIO-RAD Gel Doc 1000 system).

5.3.2 Immunoblotting

Western blotting was performed according to standard protocols. 2×10^6 cells, containing approximately 80 μ g of total protein, were cultured in growth medium supplemented with 4 μ M dexamethasone and 100 μ M ketamine for the indicated intervals. Cells were harvested by scraping and centrifugation for 10 min at 3,000g. The resulting cell pellet was resuspended in 1ml PBS, recentrifuged at 3,000g and then frozen at -70°C . For Western blot analysis, the cell pellet was resuspended in 1ml 10mM Tris buffer pH 7.4 containing 1mM EDTA and 1mM PMSF. Membranes were obtained by centrifugation for 15 min at 4°C and 13,000g. From membrane pellets, receptors were solubilized into 10mM Tris buffer pH 7.4 containing 1mM EDTA, 1mM PMSF and 0.2% Triton X-100 to a final concentration of 4 μ g total protein per μ l solubilisation buffer. 40 to 60 μ g of protein (as indicated) were subjected to electrophoresis in a 7% SDS-polyacrylamid gel and transferred to a PVDF membrane (Biorad). Membranes were blocked overnight with blocking buffer (Tris-buffered saline / 0.05% Tween 20 (TBST) containing 5% dried skimmed milk). Anti-NR1 antibody (Chemicon) was diluted 1:400 into blocking buffer containing 0.05% sodium azide and incubated for 90 min. Membranes were washed 6 times with TBST and then incubated with horseradish peroxidase coupled donkey anti mouse antibody (Chemicon; 1:5000 in blocking buffer) for one hour. Membranes were washed 8 times and chemiluminescent/fluorescent detection was performed using the ECL *plus* kit (Amersham) according to the manufacturers instructions.

5.3.3 Immunocytochemistry

Cell cultures, grown on FCS coated cover slides in growth medium containing 2 μ M dexamethasone and 100 μ M ketamine for 24 hours, were washed with PBS for 5 min and permeabilized / fixed with ice cold methanol / acetic acid (90:10) for 5 min. The fluid was aspirated off and cover slides were allowed to air-dry for 10 min. After a overnight blocking step with phosphate buffered saline (PBS) containing 1% BSA at 4°C , blocking buffer was aspirated off and 10 μ l of primary antiserum (Santa Cruz; diluted 1:500 in blocking buffer) were placed on the permeabilized cells. After incubation in a moist environment for 1.5 hours, the primary antiserum was aspirated off and the cells were washed approximately 10 times

Experimental procedures

with blocking buffer. 10µl secondary antiserum (Cy3-conjugated affinity purified rabbit anti-goat IgG; Dianova; dilution 1:200 in blocking buffer) were placed on the cells and incubated for another 1.5 hours. Slides were washed 10 times with PBS and coverslipped on glass slides with mounting medium. Finally, objects were sealed with clear nail polish. For analysis of stained cells, confocal laser scanning microscopy (Leica TCS 4D) was applied using a 550 nm band pass excitation filter and 598 nm band pass emission filters.

5.3.4 Calcium imaging

The relative increase in $[Ca^{2+}]_i$ was monitored by imaging clones loaded with the calcium sensitive fluorescent dye fluo-4 acetoxymethyl ester. For NMDA receptor expression, the cells were plated on FCS coated coverslips for 16 to 20 hours in growth medium containing 4µM dexamethasone and 100µM ketamine to prevent cells from undergoing cell death caused by NMDA receptor activation. To monitor dynamic changes of $[Ca^{2+}]_i$, cells were loaded with 1µM fluo-4 acetoxymethyl ester at 37°C in original medium. After 20 min, cultures were washed 2 times with MEM w/o FCS, Mg^{2+} and phenolred containing 1% BSA and 25mM HEPES adjusted to pH 6.8 and once with MEM w/o FCS, Mg^{2+} and phenolred containing 1% BSA to remove surplus dye and ketamine. The wash medium was exchanged for a controlled salt solution (CSS) containing 120mM NaCl, 25mM HEPES, 50mM KCl, 1.8mM $CaCl_2$ and 15mM glucose adjusted to pH 7.8 (relief of proton inhibition). Cells were allowed to equilibrate at room temperature for 10 min before agonist exposure. Using the ion quantify domain of a Leica TCS 4D confocal system equipped with a Leica PL APO 63 x/1.2-0.6 lens, six cells and background area were marked and images were collected using a 488 nm band pass excitation filter and 520 nm band pass emission filters (wavelengths). Data were recorded at 3sec intervals. Relative mean fluorescence levels from defined areas corresponding to the position of cell bodies were recorded over the time course of the experiment. Values were corrected for background and arbitrarily set to zero at the beginning of each experiment.

Experimental procedures

5.4 Cell death based in vitro assays

5.4.1 LDH assay mixture

The following reagents are supplied:

reagents		storage
sodium lactate (60%)	Dissolve 6g sodium lactate in H ₂ O to a final volume of 10ml.	-20°C
buffered substrate	Dilute sodium lactate (60%) 1:20 in 0,1M Tris pH 9.0	fresh
NAD⁺	Dissolve NAD ⁺ in PB 0.5M pH 7.4 to a final conc. of 1%.	fresh
INT	Dissolve INT in MeOH / H ₂ O (1:1) at 70°C to a final concentration of 2%.	fresh
BSA	Dissolve BSA in H ₂ O to a final conc. of 0.8%.	fresh
enzyme buffer	Dilute PB 0.1M pH 7.4 1:10 in BSA solution (1%). Dilute the resulting solution 1:1 with glycerol (87%) and add sodium azide to a final concentration of 0.01%. The enzyme buffer is sterile filtered before use.	-20°C
Diaphorase-stock	Dissolve lyophilised diaphorase from Clostridium Kluveri in enzyme buffer to a final concentration of 1600 U / ml.	-20°C
LDH-stock	Dissolve lyophilised LDH from rabbit muscle in enzyme buffer to a final concentration of 200 U / ml.	-20°C
PB 0.5M pH 7.4	Adjust a 0.5M Na ₂ HPO ₄ to pH 7.4 with 0.5M KH ₂ PO ₄ .	RT
PB 0.1M pH 7.4	Adjust a 0.1M Na ₂ HPO ₄ to pH 7.4 with 0.1M KH ₂ PO ₄ .	RT
Stop solution	Dilute 2.222ml acetic acid with H ₂ O to a final volume of 40ml.	RT
Blocking solution	Dissolve BSA in H ₂ O to a final conc. of 1%.	fresh

The following volumes are combined to obtain 1000µl LDH-assay mixture:

<u>reagent</u>	<u>volume [µl]</u>
Buffered substrate	333
NAD ⁺	111
BSA	111
PB 0.1M pH 7.4	212
INT	222
Diaphorase	11

Experimental procedures

50µl aliquots of cell culture supernatants are transferred to a 96 well flat bottom (enzymatic assay) plate which was previously blocked overnight with blocking solution (100µl / well). 50µl of LDH-assay mixture are added and the plate is incubated at 25°C for 30 min under light protection. After 30 min, 50µl of stop solution are added to each well. Large bubbles are removed with a syringe needle and the absorbance at 490nm is recorded in a common ELISA-reader (Dynatech MR5000). To obtain a suitable total LDH activity < 10mU / 50µl cell culture supernatant, 15×10^3 L(tk-) cells were seeded and the incubations were performed in a final volume of 200µl / well.

5.4.2 Induction model

15×10^3 cells per well were seeded in a 96 well plate which was previously coated with heat inactivated FCS for 30 min. Cells were grown overnight in growth medium at 5% CO₂. Stocks of DMSO, methanol or ethanol dissolved compounds were regarded as sterile. Hydrophilic compounds were dissolved in PBS and sterile filtered. Stock solutions were diluted 1:100 in induction medium (MEM w/o Mg²⁺ and phenolred containing 5% FCS, 50mM KCl, 2 mM Glutamax I, 100 U/ml ampicillin, 100 µg/ml streptomycin, 0.5 mM sodium pyruvate and 4µM dexamethasone). As FCS contains saturating concentrations of glutamate and glycine, addition of agonists was not necessary. To avoid variations in agonist concentration, always the same FCS batch was used. Receptor expression was induced by replacing growth medium with antagonist containing induction medium (200µl per well). 96 well plates were incubated at 37°C and 5% CO₂. Every concentration of antagonists was incubated as triplicate. As positive control, cultures were treated with induction medium containing 1% solvent (n = 6). For background subtraction, 200µl of induction medium were incubated in blank wells (n = 6). After 20 to 24 hours, plates were carefully agitated and 50µl aliquots of each well were transferred to assay plates (released LDH). Residual medium was removed from wells and cytosolic LDH of surviving cells was released into blank induction medium containing 0.1 % Triton X 100. 50µl samples of each well were transferred to assay plates and determined as described above. Data were corrected for cell culture medium background. Cell death rate (CD) was calculated as follows:

$$CD (\%) = A_{LDH \text{ rel}} / (A_{LDH \text{ rel}} + A_{LDH \text{ cyt}}) * 100$$

Experimental procedures

Cell death rates in % to control were fitted to a four parameter logistic function using Sigma Plot. From the resulting dose response curve, the concentration displaying 50% of the observed cytoprotective effect was calculated (IC_{50}). To prevent measurement of non-specific toxicity, the applicable concentration range of each compound was determined prior to LDH assays by trypan blue exclusion of non-dexamethasone treated cells. After 24 hours of incubation, 50 μ l of 0.04% trypan-blue in PBS were added and dye exclusion was checked using light microscopy. Only non-toxic inhibitor concentrations were used.

5.4.3 Differentiation model

15x10³ cells per well were seeded in a 96 well plate which were previously coated with heat inactivated FCS. Cultures were grown overnight in growth medium at 37°C / 5% CO₂. To induce receptor expression, the growth medium was exchanged for growth medium containing 4 μ M dexamethasone and 100 μ M ketamine (alternative seeding of 20x10³ cells / well in growth medium containing 4 μ M dexamethasone and 100 μ M ketamine is possible). After 20 to 24 hours, ketamine was removed from cultures. Wells were washed twice with 100 μ l MEM w/o FCS containing 1% BSA and 25mM HEPES (adjusted to pH 6.8) and once with MEM w/o FCS containing 1% BSA. Incubations were carried out in a controlled salt solution (CSS). 100ml CSS were prepared as described:

<i>ingredient</i>	<i>added volume [ml]</i>	<i>final concentration [mM]</i>
sterile glucose solution (40%)	0.676	15
sterile normal saline solution	77.922	120
1M HEPES solution	2.5	25
1M KCl solution	5	50
1M CaCl ₂ solution	0.18	1.8
H ₂ O	13.722	–
10 mM dexamethasone in DMSO	0.04	0.004

Ligands applied in constant concentrations (e.g. agonists like L-glu and glycine or D-serine), were added from concentrated stock solutions and pH was adjusted to 7.6 for clone L12-G10 or 8.0 for clone L13-E6, respectively, to abolish proton inhibition. The wash medium was removed and 200 μ l CSS containing the indicated concentrations of test compounds (diluted 1:100 from concentrated stocks) were added. Test compounds were incubated as triplicates

Experimental procedures

for 90 min at 37°C. Total LDH activity was determined in sister well cultures treated with lysis medium (CSS containing 0.1 % Triton-X-100; n = 6). Plates were carefully agitated and 50 µl supernatant of each well were transferred to assay plates and measured as mentioned above. Data were corrected for background controls (CSS and lysis medium; n = 3) and cell death was calculated as absorbance ratio of records from released LDH and total LDH:

$$\text{CD (\%)} = A_{\text{LDH rel}} / A_{\text{LDH total}} * 100$$

For curve fitting, estimation of IC₅₀-values and exclusion of unspecific cell death see section 5.4.2.

5.5 Inhibition of cell death by cyclosporin A

Cytotoxicity assays were performed using the differentiation model (see previous section). Pre-treatment with compounds was performed as follows: Cell cultures were differentiated in growth medium, containing 4µM dexamethasone and 100µM ketamine (induction medium) for 20 hours minus the indicated pre-treatment interval. The induction medium was removed and immunophilin ligand containing induction medium was incubated for the indicated time. Stock solutions of compounds were prepared by dissolving CsA in ethanol and FK506 in DMSO. Stocks were diluted 1:100 in fresh induction medium and if present during stimulation 1:100 in CSS. Control cultures were exposed to the respective solvent diluted 1:100 in induction medium or CSS.

For **immunoblotting**, 25x10⁶ L12-G10 cells were seeded overnight in growth medium. Next day, growth medium was exchanged for induction medium followed by 6 hours of CsA pre-treatment. Control cultures were exposed to induction medium containing corresponding amounts of ethanol. Pre-treated cultures were washed three times with 20ml PBS and scraped off into 10ml PBS. Cell suspensions were centrifuged at 500g for 10 min. The supernatant was discarded and the pellets were shock frozen in nitrogen and stored at -70°C. For sonification lysis, cell pellets were resuspend in 2ml of ice cold PBS containing 1mM PMSF and 1mM EDTA. Cells were homogenized in a BANDELEIN SONOPULS HD200 sonifier (30% efficacy; 3 x 3 sec on; 10 sec off) and chilled on ice. Homogenates were centrifuged for 20 min at 500g at 4°C. Supernatants were subjected to density centrifugation. The density fraction consisted of 3ml sucrose (25% in PBS) containing 1mM PMSF and 1mM EDTA and was carefully overlaid with supernatants. The density centrifugation was carried out in a

Experimental procedures

Beckman Ultracentrifuge using a Beckman SW 55 Ti rotor at 150,000g for 30 min at 4°C with low deceleration. The supernatants were discarded and the pelleted plasma membranes were resuspended in 50µl of hypotonic buffer (10mM Tris; 1mM EDTA; 1mM PMSF). 10µl aliquots were used for detection of protein amount (BIO-RAD protein assay according to manufacturer's instruction). For solubilization, 0.8µl Triton-X-100 (10%) were added to the residual volume and chilled on ice for at least 15 min. Non dissolved ingredients were separated by centrifugation (4°C; 14000g; 15 min). Supernatant (37.5µl) was diluted 1:2 with standard loading buffer, boiled for 10 min and stored at -20°C. Under consideration of protein amounts, sample volumes containing 8, 4, 2, 1 µg protein were subjected to gel electrophoresis in a 7% SDS-polyacrylamide gel and transferred to a PVDF membrane (Amersham). Membranes were blocked overnight with blocking buffer (Tris-buffered saline (TBS) containing 5% dried skimmed milk). Anti-NR1 antibody (Chemicon) was diluted 1:400 into blocking buffer containing 0.05% sodium azide and incubated for 90 min. Membranes were washed 6 times with TBST and then incubated with horseradish peroxidase coupled donkey anti mouse antibody (Chemicon; 1:5000 in blocking buffer) for one hour. Membranes were washed 8 times and chemiluminescent/fluorescent detection was performed using the ECL *plus* kit (Amersham) according to the manufacturer's instructions.

For **calcium imaging** 6×10^5 cells were seeded on poly-L-lysine (1mg / ml) coated cover slides (32mm diameter) in induction medium for 15 hours, followed by pre-treatment with 30µM CsA for 5 hours. Calcium imaging was performed as described in section 1.1.4 using an Zeiss Axiovert S 100 video imaging system equipped with 488nm (excitation) and 520nm (emission) band pass filters. Data were obtained and transformed using ATTOFLUOR ratio vision software.

For the **determination of intracellular ATP levels**, differentiated L12-G10 cells were stimulated in CSS pH 7.6 containing 100µM L-glu / gly, 1% BSA and 1.8 or 0.1mM Ca²⁺, respectively (n = 3). Differentiated L12-G10 cells cultured in CSS pH 7.6 (1% BSA) w/o L-glu / gly were used as control. ATP samples (trial and control; n = 3) were taken prior to stimulation and after 10, 20 and 30 min. The medium was removed from cell cultures and ATP was released into 200µl of ice cold ATP releasing buffer (Sigma). 80µl of each sample were immediately frozen in nitrogen and stored at -20°C to avoid ATP decay caused by ATPases. ATP content of the samples was determined using a luciferase based bioluminescence assay (CLS II ATP bioluminescence kit Boehringer Mannheim). Samples were thawed on ice water for 10 min, agitated and centrifuged for 2 min at 4°C and 14000g. 50µl of each sample were added to 50µl of ice cold ATP assay mixture. The 96 well

Experimental procedures

luminescence plate was gently agitated and the developed bioluminescence was assayed in a Microplate Luminometer LB 96V (EG&G BERTHOLD). The obtained relative light units (RLU; integration interval = 6sec) are direct proportional to the amount of ATP within the samples. Although the consumption of ATP by luciferase is regarded as low, a timed dependent decay of approximately 2% RLU / min was observed (linear plot!). Therefore, to shorten run time, the number of samples within one run was limited to the samples of one stimulation interval (run time < 1 min). Results were expressed as RLU in % to control samples.

5.6 Characterization of cell death

5.6.1 Plasma membrane damage and morphological characterization

Necrosis (plasma membrane damage) was calculated using the described LDH assay (see section 5.4.1). To distinguish morphologically apoptotic, necrotic and living cells, cultures were stained with a mixture of the membrane permeable chromatin dye Hoechst 33342 (stock 50mg / ml DMSO; working solution 50 μ g / ml DMSO; 0.5 μ g/ml final; staining all nuclei) and the membrane nonpermeable dye Sytox (stock 250 μ M in DMSO; working solution 50 μ M in DMSO; 0.5 μ M final). Cells stained with different fluorescent probes were imaged in a Leica DM-IRB microscope equipped with a video camera. Blue Hoechst 33342 fluorescence was excited with UV and green Sytox fluorescence with blue band pass filters.

5.6.2 Flow cytometry

L12-G10 cells were cultured in MEM containing 5% FCS, 4 μ M dexamethasone, 5mM or 55mM potassium. After 24 hours, cells were harvested into the original medium using a cell rubber. After centrifugation, the resulting pellet were lysed in 0.1% Triton-X-100 / 0.1% sodium citrate and stained with propidium iodide (final 50 μ g/ml) for 6 hours. Nuclei were then subjected to flow cytometry (FACS Calibur; Becton Dickinson). Using CELL Quest software, 5000 events were gated. As control, nuclei from WT cells, grown for 24 hours in growth medium containing 5% FCS and 4 μ M dexamethasone, and from L12-G10 cells, cultured in MEM lacking dexamethasone, were examined.

5.6.3 Phosphatidyl serine translocation

Surface phosphatidylserine (PS) expression was analysed by annexin V-staining and confocal microscopy (TCS-4D UV/VIS confocal scanning system; Leica AG). For NMDA receptor expression, the L12-G10 cells were plated on poly-L-lysine coated coverslips in induction medium containing 5% FCS and 4 μ M dexamethasone in the presence and absence of 100 μ M ketamine. After 10 hours of differentiation, cells were analysed for PS translocation. L(tk-) wildtype cells, exposed to 1 μ M staurosporine in growth medium, were assayed after 8 hours. Incubation medium was removed and cells were rinsed with annexin-V binding buffer (containing 1% BSA, 140mM NaCl, 2.5mM CaCl₂ and 10mM HEPES adjusted to 7.4). Buffer was removed and a 1:100 dilution of labelled annexin-V was added. After 5 min, cells were gently rinsed with annexin binding buffer. To ensure that the red fluorescence signals from Alexa 568 labelled annexin-V results from the binding to translocated PS, a co-staining with calcein-AM was performed. The accumulation of this fluorochrome in the cytoplasm depends on the activity of esterases. Calcein is not enriched in the cytoplasm if the plasma membrane is damaged. To examine whether the phosphatidyl turnover is accompanied by nuclear changes, an additional staining with Hoechst 33342 was applied. Cultures were loaded with Hoechst 33342 (0.5 μ g / ml) and calcein-AM (1 μ M final) for 2 min before observation. Cells were imaged under phase contrast optics and with three fluorescent filter sets (red fluorescence, Alexa-568 labelled annexin V; green fluorescence, calcein-AM; blue fluorescence, Hoechst 33342).

6. Materials

The following materials were used (alphabetical order):

materials	purchased from
(R/S)-AP5; ketamine hydrochloride; DCKA; (R/S)-CPP; ifenprodil; haloperidol; (+)-MK801 hydrogen maleate; D-serine; L-glutamate hydrochloride	RBI distributed by BIOTREND Chemikalien GmbH Köln
Ac-DEVD-CHO	BACHEM Biochemica GmbH, Heidelberg
Acrylamid solution	BIO-RAD
Albumine from bovine serum (BSA) fraction V	FLUKA Chemie AG, Switzerland
Annexin-V (Alexa 568 labelled)	Boehringer Mannheim, Germany
ATP Bioluminescence Assay Kit CLS II	Boehringer Mannheim, Germany
ATP Releasing Reagent for Somatic Cells (FL-SAR)	SIGMA-Aldrich, Deisenhofen, Germany
BES (N,N-bis[2-Hydroxyethyl]-2-aminoethanesulfonic acid)	SIGMA-Aldrich, Deisenhofen, Germany
Calcein-AM	Molecular Probes, Leiden, Netherlands
Cell culture materials	Greiner GmbH, Frickenhausen, Germany
Cy3 conjugated rabbit anti goat polyclonal IgG	Dianova, Hamburg, Germany
Cyclosporin A	ALEXIS
Cyto Tox 96™	Promega, Heidelberg, Germany
Dexamethasone	FLUKA Chemie AG, Switzerland
Diaphorase, Clostridium kluveri	Calbiochem, Bad Soden, Germany
dNTPs; DTT	GIBCO BRL Life Technologies
Donkey anti mouse IgG (horseradish peroxidase conjugated)	CHEMICON International Inc., Canada
ECL-Plus Kit	Amersham Buchler GmbH, Germany
Fluo-4-AM	Molecular Probes, Leiden, Netherlands
Fetal calf serum (FCS)	Boehringer Mannheim, Germany
Geneticin (G418)	GIBCO BRL Life Technologies
Glutamax I (100x); sterile filtered	GIBCO BRL Life Technologies
Glycine	SIGMA-Aldrich, Deisenhofen, Germany
Goat anti-NR1 polyclonal IgG (C-terminal)	SANTA CRUZ Biotechnology Inc.,
HEPES (4-(2-Hydroxyethyl)piperazine-1-ethanesulfonic acid)	FLUKA Chemie AG, Switzerland
Hoechst 33342	Molecular Probes, Leiden, Netherlands
Human embryonal kidney cells (Hek 293) (American Type Culture Collection CRL 1573)	Generous gift from Prof. Dr. H. Betz (Max Planck Inst. for Brain Research, Frankfurt, Germany)
INT (Iodonitrotetrazolium chloride)	FLUKA Chemie AG, Switzerland

Materials

L(tk-) cells (American Type Culture Collection CCL1.3)	Generous gift from Prof. Dr. Engels (Dept. of Organic Chemistry, University of Frankfurt, Germany)
Lactate dehydrogenase from rabbit muscle	Calbiochem, Bad Soden, Germany
L-Glutamine (200mM)	SIGMA-Aldrich, Deisenhofen, Germany
L-Lactic acid sodium salt	FLUKA Chemie AG, Switzerland
MEM non essential amino acid solution (100x); sterile filtered	SIGMA-Aldrich, Deisenhofen, Germany
MEM with Earle's salts w/o L-glutamine	GIBCO BRL Life Technologies
MEM with Earle's salts w/o L-glutamine, Mg ²⁺ and phenolred	GIBCO BRL Life Technologies
Mouse anti-NR1 monoclonal IgG (N-terminal)	CHEMICON International Inc., Canada
NAD ⁺ (β-Nicotinamide adenine dinucleotide from yeast)	SIGMA-Aldrich, Deisenhofen, Germany
Nucleobond AX	Macherey und Nagel, Düren, Germany
Oligo d(T) ₁₂₋₁₈	GIBCO BRL Life Technologies
PBS (Buffer substance Dulbecco's powder)	SERVA, Heidelberg, Germany
pCIS vectors and respective rodent cDNAs	Generous gift from Prof. Dr. F. A. Stevenson (Dept. of Pharmaceutical Chemistry, School of Pharmacy, London, UK)
Penicillin-Streptomycin (10,000 IU/ml-10,000µg/ml)	GIBCO BRL Life Technologies
PMSF	FLUKA Chemie AG, Switzerland
pMSG vectors and respective human cDNAs	Generous gift from Dr. P.J. Whiting (Merck, Sharp and Dohme Research Laboratories, UK)
Poly-L-lysine	SIGMA-Aldrich, Deisenhofen, Germany
Primer specific for transfected hNRs	GIBCO BRL Life Technologies
Protein assay	BIO-RAD
PVDF-Membrane	BIO-RAD
RNasin	GIBCO BRL Life Technologies
SDS	MERCK, Darmstadt, Germany
Sodium pyruvate 100mM solution; sterile filtered	SIGMA-Aldrich, Deisenhofen, Germany
Superscript Plus	GIBCO BRL Life Technologies
Sytox	Molecular Probes, Leiden, Netherlands
Tacrolimus (FK 506)	ALEXIS
Tris	SIGMA-Aldrich, Deisenhofen, Germany
Triton X-100	FLUKA Chemie AG, Switzerland
Trypsin-EDTA-solution (10x); sterile filtered	SIGMA-Aldrich, Deisenhofen, Germany

All other not further specified chemicals were obtained from Merck Darmstadt, Germany.

7. Zusammenfassung (German summary)

Das Ziel der vorliegenden Arbeit war die Etablierung eines funktionellen in vitro Testsystems für NMDA-Rezeptor Antagonisten. Primäre neuronale Zellkulturen weisen ein sehr komplexes Expressionsmuster einer Vielzahl von Ionenkanälen und unterschiedlichen Glutamatrezeptoren auf. So werden neben metabotropen (G-Protein gekoppelten) Glutamatrezeptoren und ionotropen AMPA- und Kainatrezeptoren auch verschiedene NMDA-Rezeptorsubtypen mit unterschiedlichen pharmakologischen Eigenschaften exprimiert. Im Vergleich dazu ermöglicht ein heterologes Expressionssystem die pharmakologische Charakterisierung von NMDA-Rezeptorantagonisten an molekular definierten Rezeptoren. Hinsichtlich der Entwicklung eines „Screening“ fähigen Testsystems stellt die fehlende Proliferation der isolierten Neurone eine weitere Limitierung dar. Aufgrund dieser Tatsachen wurde die heterologe Expression von rekombinanten NMDA-Rezeptoruntereinheiten in eukaryotischen Zelllinien favorisiert.

Zu Beginn der Entwicklung wurden transiente Co-Expressionen der Untereinheiten NR1-1a (Ratte), NR ϵ 1 (NR2A; Maus) und NR ϵ 3 (NR2C; Maus) in Hek 293 Zellen durchgeführt (Abschnitt 3.1). In den hierfür verwendeten pCIS-Konstrukten steht die Expression der transfizierten cDNAs unter der Kontrolle des konstitutiv aktiven hCMV Promotors. Da funktionelle NMDA-Rezeptoren Heteromultimere aus Subtypen der NR1- und NR2-Familie darstellen, wurde die NR1-1a Untereinheit mit den Untereinheiten NR ϵ 1 bzw. NR ϵ 3 im Verhältnis 1:3 co-transfiziert. Die Kombination aus NR1-1a / NR ϵ 1 führte nach 24 Stunden zu einer signifikant erhöhten Zelltodrate ($28,2 \pm 3,7$ %). Die Zelltodrate der Transfektion der Untereinheiten NR1-1a / NR ϵ 3 ($8,7 \pm 2,1$ %) unterschied sich dagegen nicht signifikant von der Zelltodrate der mit dem pCIS Kontrollvektor transfizierten Kulturen ($7,3 \pm 2,5$ %). Der kompetitive NMDA-Rezeptorantagonist (R/S)-AP5 ($150\mu\text{M}$) reduzierte die Zelltodrate der NR1-1a / NR ϵ 1 Transfektion auf $16,5 \pm 1,5$ %. Diese Ergebnisse sind in guter Übereinstimmung mit Resultaten aus anderen Untersuchungen. Cik et al. (1993) berichteten eine 24 Stunden Mortalität von 21,7 % für die Co-Expression von pCISNR1-1a / pCISNR ϵ 1 in Hek 293 Zellen. (R/S)-AP5 ($200\mu\text{M}$) reduzierte die Zelltodrate auf 8,3 %. Anegawa et al. (1995) fanden nach 48 Stunden eine Mortalität von 57,9 % für die Co-Expression der Untereinheiten NR1-1a (Ratte) und NR2A (Ratte) sowie eine im Vergleich zur Kontrolle unveränderte Mortalität für die Co-Expression der Untereinheiten NR1-1a (Ratte) / NR2C (Ratte).

Der unter der Co-Expression von NR1-1a / NR2A beobachtete Mortalitätsanstieg scheint

durch die Aktivierung von funktionellen NMDA-Rezeptoren durch im Zellkulturmedium enthaltenes Glutamat und Glycin hervorgerufen zu sein, da der kompetitive Glutamatantagonist AP5 die Zelltodrate signifikant reduzierte. Das Fehlen einer gesteigerten Mortalitätsrate unter der Co-Expression der Untereinheiten NR1-1a / NR2C kann in der geringeren Calcium-Permeabilität dieses NMDA-Rezeptorsubtyps begründet liegen (Monyer et al., 1992).

Nach diesen ersten transienten Expressionsstudien wurde die Etablierung eines stabilen heterologen Expressionssystems angestrebt. Für die stabile Expression der humanen cDNAs der NMDA-Rezeptoruntereinheiten NR1-1a, NR2A und NR2B wurde die Maus-Fibroblasten Zelllinie L(tk-) verwendet. Da sowohl für die Co-Expression von NR1-1a / NR2A als auch für NR1-1a / NR2B eine erhöhte Zelmortalität beschrieben ist (Anegawa et al., 1995), mußte ein induzierbares Expressionssystem gewählt werden. In den für die Transfektion verwendeten Vektoren steht die Expression der transfizierten cDNAs unter der Kontrolle eines Dexamethasone induzierbaren MMTV-Promotors (Grimwood et al., 1996a). Durch Zusatz von Dexamethasone wird die Expression der NMDA-Rezeptoruntereinheiten und ein damit verbundener Zelltod induziert, während unter normalen Zellkulturbedingungen in der Abwesenheit von Dexamethasone ein normales Wachstum der Zellkulturen gewährleistet ist (Selektion durch Hintergrundexpression wurde durch Zusatz des nicht kompetitiven NMDA-Rezeptorantagonisten Ketamin (100µM) verhindert). Die Erhöhung der Zelmortalität unter der Expression von funktionellen NMDA-Rezeptoren stellt das Prinzip des entwickelten Testsystems dar, da in der Gegenwart von NMDA-Rezeptorantagonisten eine Erhöhung der Zelltodrate unterdrückt werden kann. Die Co-Transfektionen wurden in einem Vektor-Verhältnis von 1:5 (NR1 : NR2) durchgeführt. Nach vierwöchiger Selektionierung mit Geneticin (2mg/ml) und anschließender Klonierung durch limitierende Verdünnung wurden verschiedene Zelllinien erhalten, die für funktionelle Experimente in einem Zeitraum von mehr als 90 Passagen (~ 45 Wochen) verwendet werden können. Nach Screening-Versuchen mit verschiedenen NMDA-Rezeptorantagonisten (Abschnitt 3.2.3) wurden die Klone L12-G10 (NR1-1a / NR2A) und L13-E6 (NR1-1a / NR2B) zur molekularbiologischen Charakterisierung herangezogen. Die RT-PCR Analyse (Abschnitt 3.3.1) des Klones L12-G10 ergab für ein Differenzierungsintervall von 12 Stunden mit 2µM Dexamethasone einen 5-fachen Anstieg der mRNA für die Untereinheit NR1-1a und einen 2,3-fachen Anstieg für NR2A. Analoge Ergebnisse wurden für den Klon L13-E6 erhalten, der einen 4,8-fachen Anstieg der NR1-1a mRNA und einen 3,5-fachen Anstieg der NR2B mRNA zeigte. Diese Ergebnisse zur Transkription der transfizierten Untereinheiten sind in Übereinstimmung mit

Untersuchungen zum immunologischen Nachweis der exprimierten NR1-1a Untereinheit. Die Westernblot-Analyse von Zelllysaten ergab ein Maximum an NR1-1a Protein zwischen 8 und 16 Stunden nach Induktion mit Dexamethasone. NR1-1a Protein konnte dagegen weder in L(tk-) Wildtyp Zellen noch in nicht induzierten Klonen nachgewiesen werden (Abschnitt 3.3.2). Die Größe des 116 kDa Proteins ist in Übereinstimmung mit dem detektierten Protein aus Rattenhirn Membranhomogenaten und dem aus der Aminosäuresequenz unter Vernachlässigung der Glykosylierung abgeleiteten Molekulargewicht von 103,5 kDa. Die immunozytochemische Untersuchung der Lokalisation der NR1-1a Untereinheit mittels confocaler Lasermikroskopie ergab den Nachweis größerer Mengen an NR1-1a Rezeptorprotein innerhalb der Zytoplasma Membran (Abschnitt 3.3.3). Da gezeigt werden konnte, dass die Co-Expression der NR2 Untereinheit für eine erfolgreiche Oberflächenexpression der NR1-Untereinheit notwendig ist (McIlhinney et al., 1996), kann aus diesen Ergebnissen auf eine Co-Lokalisation der transfizierten NMDA-Rezeptoruntereinheiten innerhalb der Zytoplasma Membran geschlossen werden. Diese Schlußfolgerung wurde durch Ergebnisse aus Calcium Video-Imaging Untersuchungen bestätigt (Abschnitt 3.3.4). Hierfür wurden beide Klone für 16 bis 20 Stunden mit Dexamethasone und Ketamin behandelt. Nach Beladung der Zellen mit dem Calcium sensitiven Fluorochrome Fluo-4, der Entfernung von Ketamin und anschließender Stimulation mit L-Glutamat und Glycin konnte in beiden Klonen ein starker Anstieg der intrazellulären Ca^{2+} -Konzentration ($[\text{Ca}^{2+}]_i$) festgestellt werden. Die anschließende Zugabe der nicht kompetitiven Antagonisten Ketamin oder MK801 führte zum Absinken der $[\text{Ca}^{2+}]_i$ auf ein basales Niveau. Da die alleinige Expression der NR1 Untereinheit in eukaryotischen Zellen nicht zur Ausbildung funktioneller Ionenkanäle führt, kann anhand dieser Ergebnisse ebenfalls auf eine funktionelle Co-Lokalisation der transfizierten cDNAs an der Zelloberfläche geschlossen werden.

Zur Bestimmung der auftretenden Exzitotoxizität nach Induktion der NMDA-Rezeptorexpression wurde eine Methode etabliert, die die Freisetzung von Lactat-Dehydrogenase (LDH) aus lysierten, nekrotischen Zellen nutzt (Abschnitt 3.4.1). Die Aktivität der von lysierten Zellen abgegebenen LDH kann direkt aus dem Zellkulturmedium bestimmt werden. Der hierfür selbst entwickelte „Assay-Mix“ enthält ca. 1 % Natrium-L-Lactat, 0,1 % NAD^+ , 0,08 % Albumin, 18 U / ml Diaphorase und 0,4 % Iodnitrotetrazoliumchlorid (INT). Das Prinzip der Methode stellt eine gekoppelte Enzymreaktion dar: Die die Reaktionsgeschwindigkeit limitierende LDH-Aktivität katalysiert die Reduktion von NAD^+ zu $\text{NADH} + \text{H}^+$, welches als Substrat für die Reduktion des

farblosen INT zum Rot gefärbten Formazan dient. Die Menge an gebildeten Formazan ist direkt proportional zur eingesetzten LDH-Aktivität und kann im 96-well-Format bei 490nm photometrisch bestimmt werden. Die Reaktion folgt bei 25°C einer klassischen Michaelis-Menten Kinetik mit einer pseudo Michaelis-Konstanten von ca. 17mU LDH / 50µl. Die zu bestimmenden Proben sollten deshalb weniger als 10mU LDH / 50µl Zellkulturmedium enthalten. Die hohe Präzision und Richtigkeit der Methode wurde in einem Meßbereich von 0 bis 7,5 mU LDH / ml Zellkulturmedium mit Variationskoeffizienten von < 4 % sowie relative Fehlern < 3 % belegt.

Zur Testung von NMDA-Rezeptorliganden wurden zwei verschiedene Versuchsdesigns entwickelt und charakterisiert (Abschnitt 3.4.2). Bei dem als Induktionsmodell bezeichneten Verfahren werden über Nacht 15×10^3 Zellen pro well angesetzt. Am nächsten Tag erfolgt die Induktion der NMDA-Rezeptorexpression unter Zugabe von Dexamethasone und gleichzeitigem Zusatz der zu testenden Rezeptorantagonisten. Die Stimulation der rekombinanten Rezeptoren erfolgt durch die im zugesetzten foetalen Kälberserum (5% FKS) enthaltenen Co-Agonisten Glutamat und Glycin. Die Zelltodrate wird nach 20 bis 24 Stunden unter Verwendung des entwickelten „LDH Assays“ bestimmt.

Um die Anwendbarkeit dieser Methode zu zeigen, wurde für eine Serie von Thieno[2,3-b]pyridinonen (C. Noe, Institut für Pharmazeutische Chemie, Universität Wien) auf ihre Zytoprotektivität getestet (Abschnitt 3.4.3). Diese Verbindungen stellen Bioisostere zu L-701,324 dar, einem hochaffinen Glycin-Antagonisten mit in vivo Aktivität. Die Affinität der einzelnen Verbindungen zur Glycin-Bindungsstelle von NMDA-Rezeptoren aus Hippocampus-Membranen der Ratte wurde durch [³H]-Glycin Bindungsstudien charakterisiert (M. Berger, Institut für Hirnforschung, Universität Wien). Aufgrund der Verfügbarkeit von K_i -Werten stellt diese Verbindungsklasse somit ein geeignetes Test-Set zur Überprüfung der Anwendbarkeit der entwickelten Methode in QSAR-Studien dar. Für die neun hochaffinen Substanzen, die mit beiden Methoden charakterisiert werden konnten, ergab sich eine gute Korrelation zwischen den ermittelten IC_{50} -Werten im Exzitotoxizitätsmodell (4 bis 90 µM) und den K_i -Werten der Bindungsexperimente (1 bis 290 nM) (Korrelationskoeffizient = 0,90; P = 0,001). Unter Verwendung des Albumin-Kompetitors Warfarin konnte gezeigt werden, dass die entwickelte Zellkulturmethode im Gegensatz zu den Bindungsexperimenten auch die für Glycin-Antagonisten typische und als problematisch zu bewertende Bindung zu Plasmaalbumin berücksichtigt. Da eine hohe Bindungsrate an Plasmaalbumin in vivo die Penetration der Verbindungen ins ZNS behindert und somit die zentrale Bioverfügbarkeit herabsetzt (Rowly et al., 1997b), stellt die Berücksichtigung dieses

Parameters sicherlich einen Vorteil gegenüber anderen Routinemethoden wie Radioligand-Bindungsstudien oder elektrophysiologische Untersuchungen dar.

Aufgrund des durch FKS verursachten hohen Glycingehaltes und der geringen Löslichkeit der Verbindungen im Inkubationsmedium, konnten Substanzen mit „niederer“ Affinität nicht charakterisiert werden. Deshalb wurde ein Test-Design entwickelt, das die Charakterisierung von Agonisten und Antagonisten unter definierteren Bedingungen erlaubt. Bei diesem als Differenzierungsmodell bezeichneten Design (Abschnitt 3.4.2) werden die Zellkulturen für 20 bis 24 Stunden mit Dexamethasone in der Gegenwart von Ketamin differenziert. Nach anschließender Entfernung des Ketamin werden die zu untersuchenden Substanzen in einer kontrollierten Salzlösung unter definierten Bedingungen (variierbarer pH-Wert und Agonist-Konzentrationen) für 60 bis 90 Minuten bei 37°C inkubiert und anschließend die Zelltoderate bestimmt. Aufgrund des wesentlich verkürzten Test-Intervalls kann sowohl auf sterile Bedingungen als auch auf den Zusatz von FKS verzichtet werden. Dieses Design erlaubte eine umfassende pharmakologische Charakterisierung der Klone L12-G10 und L13-E6. Die hier ermittelten pharmakologischen Profile der beiden Klone reflektieren die unterschiedlichen Eigenschaften der exprimierten Rezeptoren (NR1-1a / NR2A gegenüber NR1-1a / NR2B).

Es konnte eine Abhängigkeit der Rezeptoraktivität vom pH-Wert des verwendeten Inkubationsmediums gezeigt werden (Abschnitt 3.4.5.1). Protonen inhibieren die maximale Zelltoderate mit IC_{50} -Werten nahe des physiologischen pH-Wertes von 7,4. Für Klon L12-G10 wurde ein IC_{50} von pH 7,2 ermittelt, während Klon L13-E6 eine noch größere Sensitivität für Protonen mit einem IC_{50} von pH 7,5 aufzeigt. Diese Ergebnisse sind in guter Übereinstimmung mit elektrophysiologischen Untersuchungen zur Inhibition von NMDA-Rezeptoren durch Protonen (Traynelis et al., 1995). Für die in *Xenopus* Oozyten exprimierten NR1-1a / NR2A-Rezeptoren wurde ein IC_{50} von pH 7,2 berichtet, während NR1-1a / NR2B Rezeptoren mit einem IC_{50} von pH 7,3 bestimmt wurden. Aufgrund der gezeigten Sensitivität gegenüber Protonen sollten funktionelle Experimente an NMDA-Rezeptoren nur unter strikter Kontrolle des pH-Wertes durchgeführt werden.

Es konnte weiterhin gezeigt werden, dass der in beiden Zelllinien auftretende Zelltod von der applizierten Dosis an Glutamat abhängig ist (Abschnitt 3.4.5.3). Für die Zelllinie L12-G10 wurde unter sättigenden Glycinkonzentrationen ein EC_{50} von 3,4 μ M (3,7 μ M; 3,1 μ M) ermittelt. Für Klon L13-E6 ergab sich ein EC_{50} von 2,7 μ M (2,8 μ M; 2,6 μ M). Der auftretende Zelltod wurde durch den Zusatz von Glycin oder D-Serin verstärkt, jedoch konnte keine klassische Dosis-Wirkungsbeziehung für diese Substanzen gezeigt werden. Dies liegt

wahrscheinlich in Glycin Kontaminationen begründet, die durch das Waschen der Zellkulturen mit 1% BSA enthaltendem MEM-Medium hervorgerufen werden (Auswaschen von Ketamin zur Aktivierung der exprimierten NMDA-Rezeptoren). BSA wurde zur Verstärkung der Zelladherenz zugesetzt und konnte nicht durch andere Polymere wie z.B. Dextran ersetzt werden. Dagegen konnten in Kompletionsversuchen mit dem Glycin-Antagonisten DCKA (100 μ M) klassische Dosis-Wirkungskurven beobachtet werden. Der Vergleich der hierfür erhaltenen EC₅₀-Werte für Glycin und D-Serin weist auf eine Präferenz des Klons L13-E6 (NR1-1a / NR2B) für Agonisten an der Glycin-Bindungsstelle hin, da die EC₅₀-Werte für Klon L12-G10 (NR1-1a / NR2A) um Faktor 2 bis 3 höher liegen. Ebenso war in Kompletionsversuchen mit dem Glutamat-Antagonisten (R/S)-CPP eine Präferenz für Agonisten an der Glutamat-Bindungsstelle evident. L-Glutamat und L-Aspartat zeigten hierbei eine wesentlich höhere Wirksamkeit an Klon L13-E6 als an Klon L12-G10 (s. Abschnitt 3.4.5 Tab.7). Dagegen zeigen die ermittelten IC₅₀-Werte für den Glutamat-Antagonisten (R/S)-AP5 und den Glycin-Antagonisten DCKA eine ca. 7-fach höhere Effizienz an L12-G10 Zellen an. Der offene Kanalblocker Ketamin diskriminiert dagegen nicht zwischen beiden Klonen. Diese Ergebnisse sind in Übereinstimmung mit Patch-Clamp Studien an NMDA-Rezeptor exprimierenden *Xenopus* Oozyten (Hess et al., 1996) und der Existenz von Agonist oder Antagonist bevorzugenden NMDA-Rezeptoren *in vivo*.

Im Vergleich zu D-Serin war die Wirksamkeit von Glycin an beiden Klonen leicht erhöht, was ebenfalls mit früheren Beobachtungen übereinstimmt (Matsui et al., 1995). Die Effizienz von L-Glutamat ist im Vergleich zu L-Aspartat 7- bis 10-fach höher.

Die NR2B selektiven allosterischen Antagonisten Ifenprodil und Haloperidol zeigten zytoprotektive Effekte an Klon L13-E6 (NR1-1a / NR2B) (IC₅₀ Ifenprodil = 0,15 \pm 0,02 μ M; IC₅₀ Haloperidol = 2,2 \pm 1,5 μ M), blieben aber in der Testung an Klon L12-G10 (NR1-1a / NR2A) in Konzentrationen bis zu 100 μ M ohne Effekt (Abschnitt 3.4.5.5). Diese Ergebnisse bestätigen frühere Studien, die eine NR2B-Selektivität für Ifenprodil (Williams et al., 1993a) und Haloperidol (Ilyin et al., 1996) beobachteten. Die berichteten IC₅₀-Werte für Ifenprodil (0,34 μ M) und Haloperidol (3 μ M) stimmen mit den ermittelten IC₅₀-Werten überein.

Für das positiv modulatorische Polyamin Spermin (300 μ M) konnte ebenfalls eine Selektivität zugunsten des Klons L13-E6 gezeigt werden (Abschnitt 3.4.5.2). Das Ausmaß dieser glycinunabhängigen Verstärkung der Zelltodrate durch Spermin war abhängig vom pH-Wert des Inkubationsmediums und stieg mit steigender Inhibition durch Protonen an. An L12-G10 Zellen blieb Spermin dagegen ohne signifikanten Effekt. Diese Ergebnissen bestätigen, dass Polyamin-Effekte nur an solchen Rezeptoren auftreten, an denen neben bestimmten NR1-

Speißvarianten wie NR1-1a (Abwesenheit von Exon 5!) die Untereinheit NR2B beteiligt ist. Die pH-Wert Abhängigkeit des beobachteten Effektes weist darauf hin, dass der glycinunabhängige positiv modulatorische Effekt der Polyamine über eine Aufhebung der Inhibition durch Protonen vermittelt wird. Somit sind diese Beobachtungen in Übereinstimmung mit dem von Traynelis (1995) vorgeschlagenen Mechanismus zur glycinunabhängigen Stimulation von NMDA-Rezeptoren durch Polyamine.

Obwohl für die NR2B selektiven Verbindungen Ifenprodil und Haloperidol bereits früher eine Interaktion mit der Polyamin-Bindungsstelle des NMDA-Rezeptors diskutiert wurde, zeigen diese Verbindungen auch in der Abwesenheit von Spermin starke zytoprotektive Wirkung (s.o.). Eine zusätzliche Competition um die Polyamin-Bindungsstelle scheint allerdings nicht vorzuliegen, da unter Zusatz von 300µM Spermin die Dosis-Wirkungskurve nicht parallel verschoben wird. Die Zelltodrate wird lediglich bei nicht voll inhibierenden Konzentrationen an Ifenprodil oder Haloperidol erhöht. Somit scheint eine allosterische Interaktion dieser Verbindungen wahrscheinlicher zu sein. Die diskutierten Experimente wurden bei einem pH-Wert von 8,0 durchgeführt wurden, bei dem normalerweise keine Inhibition durch Protonen mehr vorliegt. Da Spermin seinen positiv modulatorischen Effekt normalerweise über eine Aufhebung der Inhibition durch Protonen vermittelt, könnte die teilweise Aufhebung der zytoprotektiven Effekte von Ifenprodil und Haloperidol durch Spermin darauf hinweisen, dass die Zytoprotektivität dieser Verbindungen in einer Erleichterung der Inhibition durch Protonen begründet liegt. Diese Interpretation der Ergebnisse ist in Übereinstimmung mit dem von Mott et al. (1998) vorgeschlagenem Mechanismus zur allosterischen Blockade von NMDA-Rezeptoren durch Phenylethanolamine.

In Übereinstimmung mit früheren Beobachtungen (Williams et al., 1993b) traten Histamin-Effekte nur an dem NR1-1a / NR2B exprimierenden Klon L13-E6 auf (Abschnitt 3.4.5.6). Anstatt einer Erhöhung der NMDA-Rezeptoraktivität (Bekkers, 1993; Vorobjev et al., 1993; Zwart et al., 1996) wurde jedoch eine dosisabhängige Inhibition des Zelltodes beobachtet. Diese Unterschiede könnten auf unterschiedliche pH-Bedingungen zurückzuführen sein. Saybasili et al. (1995) beobachteten für Histamin bei pH-Werten um pH 7,2 eine Verstärkung von NMDA induzierten Strömen, während bei einem erhöhten pH-Werten von 7,6 eine Reduktion der Ströme auftrat. Die Behandlung der Klone L12-G10 bzw. L13-E6 mit dem Protein Kinase C (PKC) Aktivator TPA (100nM) bei gleichzeitiger Stimulation der NMDA-Rezeptoren führte nicht zu einer erhöhten Mortalität (Abschnitt 3.4.5.6), obwohl elektrophysiologische Untersuchungen eine Verstärkung der NMDA-Rezeptoraktivität durch Phosphorylierung der beteiligten NR1 Untereinheit zeigten (Chen et al., 1991; Kelso et al.,

1992). Es muß dabei aber berücksichtigt werden, dass verschiedene Spleißvarianten eine unterschiedliche Sensitivität gegenüber der PKC aufweisen (Tingley et al., 1993) und die Untereinheit NR1-1a nur eine dreifache Erhöhung der Spitzenströme aufzeigte. Andererseits kann bereits ein hohes basales Phosphorylierungsniveau vorliegen, vergleichbar dem der in Hek 293 Zellen exprimierten Rezeptoren (Tingley et al., 1993).

Für Untersuchungen zur Ca^{2+} induzierten mitochondrialen Schädigung als Ursache für den NMDA-Rezeptor vermittelten Zelltod wurde Cyclosporin A (CsA) verwendet. CsA ist ein Inhibitor der sogenannten „permeability transition pore“ (PTP), einer Ca^{2+} induzierbaren Pore innerhalb der inneren mitochondrialen Membran. Die Induktion dieser PTP führt zu einer Depolarisation der inneren mitochondrialen Membran und mit dem Verlust des Membranpotentials $\Delta\psi$ zu einer Entkopplung der mitochondrialen Atmungskette und zum Abfallen der intrazellulären ATP-Spiegel. Eine mehrstündige Vorbehandlung mit CsA führte nach anschließender Stimulation zu einer signifikanten Reduktion der Zellmortalität um maximal 40 bis 60% ($\text{IC}_{50} \sim 7\mu\text{M}$) (Abschnitt 3.5). Da CsA ebenfalls die NMDA-Rezeptor regulierende Ca^{2+} /Calmodulin abhängige Ser/Thr-Phosphatase Calcineurin inhibiert, wurde der selektive Calcineurin Inhibitor FK506 (Tacrolimus) auf seine zytoprotektiven Eigenschaften getestet. Für eine mehrstündige Vorbehandlung mit FK506 konnten keine signifikanten zytoprotektiven Effekt gezeigt werden. Deshalb kann der zytoprotektive Effekt von CsA nicht durch Inhibition von Calcineurin vermittelt sein. Überraschenderweise wurde aber festgestellt, dass CsA mit der Expression der transfizierten NMDA-Rezeptoruntereinheiten interagiert. Eine sechsstündige Vorbehandlung der NMDA-Rezeptor induzierten Zellen mit $30\mu\text{M}$ CsA reduzierte die Menge an NR1-1a Protein um $\sim 70\%$. Dieser Effekt könnte mit einer CsA vermittelten Inhibition der Peptidyl-Prolyl-Isomerase-Aktivität von Cyclophilinen zusammenhängen (Chen et al., 1998; Helekar et al., 1994). Diese im Zytoplasma, im ER und in Mitochondrien vorkommenden Immunophilinen sind an der Faltung von Polypeptiden ähnlich den klassischen „heat shock“ Proteinen (Chaperone) beteiligt. Da gezeigt werden konnte, dass heterolog exprimierte NMDA-Rezeptoren innerhalb des ER assembliert werden und zur Oberflächenexpression eine Co-Synthese von NR1 und NR2 Untereinheiten notwendig ist (McIlhinney et al., 1998), kann somit auch von einer Beeinflussung der Oberflächenexpression der transfizierten NR2 Untereinheiten ausgegangen werden. Calcium Video Imaging Studien belegten den Verlust funktioneller NMDA-Rezeptoren nach mehrstündiger Vorbehandlung mit $30\mu\text{M}$ CsA. Im Gegensatz zur mehrstündigen Präinkubation von $30\mu\text{M}$ CsA führte ein kurzes Vorbehandlungsintervall von 10 min bei pH 7,6 zu keinem zytoprotektiven Effekt. Dagegen konnte bei eingeschränkter

Rezeptoraktivität (pH 7,0) die Zelltodrate um 40% gesenkt werden (FK506 ohne signifikanten Effekt!). Insofern kann eine zusätzliche Beeinflussung der PTP durch CsA nicht ausgeschlossen werden. Um die Beteiligung einer mitochondrialen Schädigung nach Stimulation heterolog exprimierter NMDA-Rezeptoren eingehender zu charakterisieren, sollten in zukünftigen Studien selektivere PTP-Inhibitoren wie Bongkrekische Säure oder Inhibitoren der mitochondrialen Ca^{2+} -Speicherung wie „ruthenium red“ oder FCCP Verwendung finden. Nach Untersuchungen zur Charakterisierung des vorherrschenden Zelltodtyps kann auf einen vorwiegend nekrotischen Zelltod geschlossen werden. Der auftretende Zelltod ist in beiden Modellen durch einen raschen Verlust der Integrität der Zytoplasma Membran gekennzeichnet (Abschnitt 3.6.2). Die für apoptotische Prozesse charakteristischen nukleären Veränderungen des Chromatins wie Kondensation und DNA-Fragmentierung konnten weder mit FACS-Analysen noch mit fluoreszenzmikroskopischen Methoden beobachtet werden.

Das fehlende Auftreten von Apoptose in den entwickelten Exzitotoxizitätsmodellen steht in Kontrast zur neuronalen Glutamat induzierbaren Zytotoxizität in vivo und in vitro. Als Ursache hierfür sind Unterschiede im Ca^{2+} -Metabolismus (z.B. das Fehlen wichtiger Ca^{2+} -Transporter wie dem Na^+ abhängigen Ca^{2+} -Austauscher) zu sehen. Der Mangel an einer effizienten Ca^{2+} -Regulation kann zu einer verstärkten Ca^{2+} -Speicherung innerhalb der Mitochondrien, dem Zusammenbruch von $\Delta\psi$, dem Verlust der oxidativen Phosphorylierung mit anschließendem Abfall der ATP-Spiegel und Generierung reaktiver Sauerstoffspezies (Peroxiden und Superoxidradikalen) führen. Dieser Abfall der ATP-Spiegel kann durch einen erhöhten ATP-Bedarf für Membranpumpen (z.B. Ca^{2+} -ATPase) noch verstärkt werden. Der gemessene Ca^{2+} abhängige Abfall der ATP-Spiegel während der Stimulation der heterolog exprimierten NMDA-Rezeptoren (Abschnitt 3.5) weist auf eine solche mitochondriale Schädigung hin. Da eine Aufrechterhaltung der intrazellulären ATP-Spiegel als Voraussetzung für Entwicklung apoptotischer Prozesse angesehen wird (Nicotera et al., 1998; Leist et al., 1999), erklärt dies die nach Stimulation der heterologen NMDA-Rezeptoren rasch eintretende Nekrose.

Zusammenfassend kann gesagt werden, dass das Ziel der Etablierung eines funktionellen in vitro Testsystems zur Charakterisierung von NMDA-Rezeptorliganden erreicht wurde. Die mit humanen NMDA-Rezeptoruntereinheiten stabil transfizierten Zelllinien wurden molekularbiologisch eingehend charakterisiert und die Funktionalität der exprimierten Rezeptoren mit verschiedenen Methoden belegt. Auf der Basis der nach Stimulation der ligandgesteuerten Ionenkanäle rasch auftretenden Nekrose wurden zwei eingehend

untersuchte *in vitro* Modelle entwickelt, die der pharmakologischen Charakterisierung der vorgestellten Zelllinien dienen. Es konnte gezeigt werden, dass die unterschiedlichen pharmakologischen Profile der Zelllinien in der jeweiligen molekularen Zusammensetzung der exprimierten heteromultimeren Rezeptoren begründet liegen.

Abschließend bleibt festzuhalten, dass die hier vorgestellten, auf exzitotoxischen Prozessen basierenden Modelle im Vergleich zu elektrophysiologischen Methoden und Radioligand-Bindungsstudien experimentell sehr einfache, aber zugleich pharmakologisch valide Testsysteme darstellen, die der weiteren Untersuchung humaner NMDA-Rezeptoren, dem Screening neuer NMDA-Rezeptorliganden sowie der Verbesserung von Leitstrukturen in QSAR-Studien dienen können.

8. References

1. Adams, S. L., Foldes, R. L., and Kamboj, R. K.: Human N-methyl-D-aspartate receptor modulatory subunit hNR3: cloning and sequencing of the cDNA and primary structure of the protein. *Biochimica et Biophysica Acta* 1260 (1): 105-8, 1995.
2. Aizenmann, E., Lipton, S. A., and Loring, R. H.: Selective modulation of NMDA responses by reduction and oxidation. *Neuron* 2: 1257-63, 1989.
3. Akazawa, C., Shigemoto, R., Bessho, Y., Nakanishi, S., and Mizuno, N.: Differential expression of five N-methyl-D-aspartate receptor subunit mRNAs in the cerebellum of developing and adult rats. *Journal of Comparative Neurology* 347 (1): 150-60, 1994.
4. Allaoua, H., Chaudieu, I., Boksa, P., Perry, T. L., Krieger, C., and Quirion, R.: Excitatory amino acid receptors in human spinal cord. Evaluation in amyotrophic lateral sclerosis patients. *Annals of the New York Academy of Sciences* 648: 260-2, 1992.
5. Andine, P., Sandberg, M., Bangenholm, R., Lehmann, A., and Hagberg, H.: Intra- and extracellular changes of amino acids in the cerebral cortex of the neonatal rat during hypoxic-ischemia. *Develop Brain Res* 64: 115-20, 1991.
6. Andreyev, A. Y., Fahy, B., and Fiskum, G.: Cytochrome c release from brain mitochondria is independent of the mitochondrial permeability transition. *FEBS Lett* 439 (3): 373-6, 1998.
7. Anegawa, N. J., Lynch, D. R., Verdoorn, T. A., and Pritchett, D. B.: Transfection of N-methyl-D-aspartate receptors in a nonneuronal cell line leads to cell death. *Journal of Neurochemistry* 64 (5): 2004-12, 1995.
8. Ankarcrona, M., Dypbukt, J. M., Bonfoco, E., Zhivotovsky, B., Orrenius, S., Lipton, S. A., and Nicotera, P.: Glutamate-induced neuronal death: a succession of necrosis or apoptosis depending on mitochondrial function. *Neuron* 15 (4): 961-73, 1995.
9. Ankarcrona, M., Dypbukt, J. M., Orrenius, S., and Nicotera, P.: Calcineurin and mitochondrial function in glutamate-induced neuronal cell death. *FEBS Lett* 394 (3): 321-4, 1996.
10. Anthony, E. W., and Nevins, M. E.: Anxiolytic-like effects of N-methyl-D-aspartate-associated glycine receptor ligands in the rat potentiated startle test. *European Journal of Pharmacology* 250 (2): 317-24, 1993.

References

11. Auer, R. N.: Assessing structural changes in the brain to evaluate neurotoxicological effects of NMDA receptor antagonists. *Psychopharmacology Bulletin* 30 (4): 585-91, 1994.
12. Avenet, P., Leonardon, J., Besnard, F., Graham, D., Frost, J., Depoortere, H., Langer, S. Z., and Scatton, B.: Antagonist properties of the stereoisomers of ifenprodil at NR1A/NR2A and NR1A/NR2B subtypes of the NMDA receptor expressed in *Xenopus* oocytes. *European Journal of Pharmacology* 296 (2): 209-13, 1996.
13. Baron, B. M., Harrison, B. L., Kehne, J. H., Schmidt, C. J., van Giersbergen, P. L., White, H. S., Siegel, B. W., Senyah, Y., McCloskey, T. C., Fadayel, G. M., Taylor, V. L., Murawsky, M. K., Nyce, P., and Salituro, F. G.: Pharmacological characterization of MDL 105,519, an NMDA receptor glycine site antagonist. *European Journal of Pharmacology* 323 (2-3): 181-92, 1997.
14. Baron, B. M., Harrison, B. L., McDonald, I. A., Meldrum, B. S., Palfreyman, M. G., Salituro, F. G., Siegel, B. W., Slone, A. L., Turner, J. P., and White, H. S.: Potent indole- and quinoline-containing N-methyl-D-aspartate antagonists acting at the strychnine-insensitive glycine binding site. *Journal of Pharmacology & Experimental Therapeutics* 262 (3): 947-56, 1992.
15. Baron, B. M., Harrison, B. L., Miller, F. P., McDonald, I. A., Salituro, F. G., Schmidt, C. J., Sorensen, S. M., White, H. S., and Palfreyman, M. G.: Activity of 5,7-dichlorokynurenic acid, a potent antagonist at the N-methyl-D-aspartate receptor-associated glycine binding site. *Molecular Pharmacology* 38 (4): 554-61, 1990.
16. Baron, B. M., Siegel, B. W., Harrison, B. L., Gross, R. S., Hawes, C., and Towers, P.: [3H]MDL 105,519, a high-affinity radioligand for the N-methyl-D-aspartate receptor-associated glycine recognition site. *Journal of Pharmacology & Experimental Therapeutics* 279 (1): 62-8, 1996.
17. Baudy, R. B., Greenblatt, L. P., Jirkovsky, I. L., Conklin, M., Russo, R. J., Bramlett, D. R., Emrey, T. A., Simmonds, J. T., Kowal, D. M., Stein, R. P., and et al.: Potent quinoxaline-spaced phosphono alpha-amino acids of the AP-6 type as competitive NMDA antagonists: synthesis and biological evaluation. *Journal of Medicinal Chemistry* 36 (3): 331-42, 1993.
18. Beaton, J. A., Stemsrud, K., and Monaghan, D. T.: Identification of a novel N-methyl-D-aspartate receptor population in the rat medial thalamus. *Journal of Neurochemistry* 59 (2): 754-7, 1992.

References

19. Bekkers, J. M.: Enhancement by histamine of NMDA-mediated synaptic transmission in the hippocampus. *Science* 261 (5117): 104-6, 1993.
20. Bennett, J. A., and Dingledine, R.: Topology profile for a glutamate receptor: three transmembrane domains and a channel-lining reentrant membrane loop. *Neuron* 14 (2): 373-84, 1995.
21. Berger, M. L.: On the true affinity of glycine for its binding site at the NMDA receptor complex. *Journal of Pharmacological & Toxicological Methods* 34 (2): 79-88, 1995.
22. Bernardi, P., Colonna, R., Costantini, P., Eriksson, O., Fontaine, E., Ichas, F., Massari, S., Nicolli, A., Petronilli, V., and Scorrano, L.: The mitochondrial permeability transition. *Biofactors* 8 (3-4): 273-81, 1998.
23. Bernardi, P., Veronese, P., and Petronilli, V.: Modulation of the mitochondrial cyclosporin A-sensitive permeability transition pore. I. Evidence for two separate Me²⁺ binding sites with opposing effects on the pore open probability. *J Biol Chem* 268 (2): 1005-10, 1993.
24. Birch, P. J., Grossman, C. J., and Hayes, A. G.: Kynurenic acid antagonises responses to NMDA via an action at the strychnine-insensitive glycine receptor. *Eur J Pharmacol* 154 (1): 85-7, 1988.
25. Biton, B., Granger, P., Carreau, A., Depoortere, H., Scatton, B., and Avenet, P.: The NMDA receptor antagonist eliprodil (SL 82.0715) blocks voltage-operated Ca²⁺ channels in rat cultured cortical neurons. *European Journal of Pharmacology* 257 (3): 297-301, 1994.
26. Bordi, F., Pietra, C., Ziviani, L., and Reggiani, A.: The glycine antagonist GV150526 protects somatosensory evoked potentials and reduces the infarct area in the MCAo model of focal ischemia in the rat. *Experimental Neurology* 145 (2 Pt 1): 425-33, 1997.
27. Bristow, L. J., Landon, L., Saywell, K. L., and Tricklebank, M. D.: The glycine/NMDA receptor antagonist, L-701,324 reverses isolation-induced deficits in prepulse inhibition in the rat. *Psychopharmacology* 118 (2): 230-2, 1995.
28. Broekemeier, K. M., Carpenter-Deyo, L., Reed, D. J., and Pfeiffer, D. R.: Cyclosporin A protects hepatocytes subjected to high Ca²⁺ and oxidative stress. *FEBS Lett* 304 (2-3): 192-4, 1992.
29. Broekemeier, K. M., Dempsey, M. E., and Pfeiffer, D. R.: Cyclosporin A is a potent inhibitor of the inner membrane permeability transition in liver mitochondria. *J Biol Chem* 264 (14): 7826-30, 1989.

References

30. Budd, S. L., and Nicholls, D. G.: Mitochondria, calcium regulation, and acute glutamate excitotoxicity in cultured cerebellar granule cells. *J Neurochem* 67 (6): 2282-91, 1996.
31. Buller, A. L., Larson, H. C., Schneider, B. E., Beaton, J. A., Morrisett, R. A., and Monaghan, D. T.: The molecular basis of NMDA receptor subtypes: native receptor diversity is predicted by subunit composition. *Journal of Neuroscience* 14 (9): 5471-84, 1994.
32. Bullock, R., McCulloch, J., Graham, D. I., Lowe, D., Chen, M. H., and Teasdale, G. M.: Focal ischemic damage is reduced by CPP-ene studies in two animal models. *Stroke* 21 (11 Suppl): III32-6, 1990.
33. Burnashev, N., Monyer, H., Seeburg, P. H., and Sakmann, B.: Divalent ion permeability of AMPA receptor channels is dominated by the edited form of a single subunit. *Neuron* 8 (1): 189-98, 1992a.
34. Burnashev, N., Schoepfer, R., Monyer, H., Ruppersberg, J. P., Gunther, W., Seeburg, P. H., and Sakmann, B.: Control by asparagine residues of calcium permeability and magnesium blockade in the NMDA receptor. *Science* 257 (5075): 1415-9, 1992b.
35. Camins, A., Sureda, F. X., Gabriel, C., Pallas, M., Escubedo, E., and Camarasa, J.: Effect of 1-methyl-4-phenylpyridinium (MPP⁺) on mitochondrial membrane potential in cerebellar neurons: interaction with the NMDA receptor. *Journal of Neural Transmission* 104 (6-7): 569-77, 1997.
36. Carling, R. W., Leeson, P. D., Moore, K. W., Moyes, C. R., Duncton, M., Hudson, M. L., Baker, R., Foster, A. C., Grimwood, S., Kemp, J. A., Marshall, G. R., Tricklebank, M. D., and Saywell, K. L.: 4-substituted-3-phenylquinolin-2(1H)-ones: acidic and nonacidic glycine site N-methyl-D-aspartate antagonists with in vivo activity. *Journal of Medicinal Chemistry* 40 (5): 754-65, 1997.
37. Carlton, S. M., and Hargett, G. L.: Treatment with the NMDA antagonist memantine attenuates nociceptive responses to mechanical stimulation in neuropathic rats. *Neuroscience Letters* 198 (2): 115-8, 1995.
38. Carlton, S. M., Hargett, G. L., and Coggeshall, R. E.: Localization and activation of glutamate receptors in unmyelinated axons of rat glabrous skin. *Neuroscience Letters* 197 (1): 25-8, 1995.
39. Carter, C., Rivy, J. P., and Scatton, B.: Ifenprodil and SL 82.0715 are antagonists at the polyamine site of the N-methyl-D-aspartate (NMDA) receptor. *European Journal of Pharmacology* 164 (3): 611-2, 1989.

References

40. Carter, C. J., Lloyd, K. G., Zivkovic, B., and Scatton, B.: Ifenprodil and SL 82.0715 as cerebral antiischemic agents. III. Evidence for antagonistic effects at the polyamine modulatory site within the N-methyl-D-aspartate receptor complex. *Journal of Pharmacology & Experimental Therapeutics* 253 (2): 475-82, 1990.
41. Chandler, L. J., Norwood, D., and Sutton, G.: Chronic ethanol upregulates NMDA and AMPA, but not kainate receptor subunit proteins in rat primary cortical cultures. *Alcohol Clin Exp Res* 23 (2): 363-70, 1999.
42. Charriaut-Marlangue, C., Margaille, I., Borrega, F., Plotkine, M., and Ben-Ari, Y.: NG-nitro-L-arginine methyl ester reduces necrotic but not apoptotic cell death induced by reversible focal ischemia in rat. *Eur J Pharmacol* 310 (2-3): 137-40, 1996.
43. Chazot, P. L., Cik, M., and Stephenson, F. A.: Immunological detection of the NMDAR1 glutamate receptor subunit expressed in embryonic kidney 293 cells and in rat brain. *Journal of Neurochemistry* 59 (3): 1176-8, 1992.
44. Chazot, P. L., Coleman, S. K., Cik, M., and Stephenson, F. A.: Molecular characterization of N-methyl-D-aspartate receptors expressed in mammalian cells yields evidence for the coexistence of three subunit types within a discrete receptor molecule. *Journal of Biological Chemistry* 269 (39): 24403-9, 1994.
45. Chen, C., and Okayama, H.: High-efficiency transformation of mammalian cells by plasmid DNA. *Mol Cell Biol* 7 (8): 2745-52, 1987.
46. Chen, H., Kubo, Y., Hoshi, T., and Heinemann, S. H.: Cyclosporin A selectively reduces the functional expression of Kir2.1 potassium channels in *Xenopus* oocytes. *FEBS Lett* 422 (3): 307-10, 1998.
47. Chen, L., and Huang, L. Y.: Sustained potentiation of NMDA receptor-mediated glutamate responses through activation of protein kinase C by a mu opioid. *Neuron* 7 (2): 319-26, 1991.
48. Chenard, B. L., and Menniti, F. S.: Antagonists selective for NMDA receptors containing the NR2B subunit. *Current Pharmaceutical Design* 5: 381-404, 1999.
49. Chenard, B. L., Shalaby, I. A., Koe, B. K., Ronau, R. T., Butler, T. W., Prochniak, M. A., Schmidt, A. W., and Fox, C. B.: Separation of alpha 1 adrenergic and N-methyl-D-aspartate antagonist activity in a series of ifenprodil compounds. *Journal of Medicinal Chemistry* 34 (10): 3085-90, 1991.
50. Chenu, C., Serre, C. M., Raynal, C., Burt-Pichat, B., and Delmas, P. D.: Glutamate receptors are expressed by bone cells and are involved in bone resorption. *Bone* 22 (4): 295-9, 1998.

References

51. Chomczynski, P., and Sacchi, N.: Single-step method of RNA isolation by acid guanidinium thiocyanate-phenol-chloroform extraction. *Analytical Biochemistry* 162 (1): 156-9, 1987.
52. Christine, C. W., and Choi, D. W.: Effect of zinc on NMDA receptor-mediated channel currents in cortical neurons. *J Neurosci* 10 (1): 108-16, 1990.
53. Cik, M., Chazot, P. L., and Stephenson, F. A.: Optimal expression of cloned NMDAR1/NMDAR2A heteromeric glutamate receptors: a biochemical characterization. *Biochemical Journal* 296 (Pt 3): 877-83, 1993.
54. Collingridge, G. L., Kehl, S. J., and McLennan, H.: Excitatory amino acids in synaptic transmission in the Schaffer collateral-commissural pathway of the rat hippocampus. *J. Physiology* 334: 33-46, 1983.
55. Collingridge, G. L., and Watkins, J. C.: *The NMDA Receptor*. Oxford University Press Second Edition: 31-104, 1994.
56. Connern, C. P., and Halestrap, A. P.: Recruitment of mitochondrial cyclophilin to the mitochondrial inner membrane under conditions of oxidative stress that enhance the opening of a calcium-sensitive non-specific channel. *Biochem J* 302 (Pt 2): 321-4, 1994.
57. Coughenour, L. L., and Cordon, J. J.: Characterization of haloperidol and trifluoperidol as subtype-selective N-methyl-D-aspartate (NMDA) receptor antagonists using [³H]TCP and [³H]ifenprodil binding in rat brain membranes. *Journal of Pharmacology & Experimental Therapeutics* 280 (2): 584-92, 1997.
58. Cowburn, R. F., Wiehager, B., Trief, E., Li-Li, M., and Sundstrom, E.: Effects of beta-amyloid-(25-35) peptides on radioligand binding to excitatory amino acid receptors and voltage-dependent calcium channels: evidence for a selective affinity for the glutamate and glycine recognition sites of the NMDA receptor. *Neurochemical Research* 22 (12): 1437-42, 1997.
59. Crompton, M., Ellinger, H., and Costi, A.: Inhibition by cyclosporin A of a Ca²⁺-dependent pore in heart mitochondria activated by inorganic phosphate and oxidative stress. *Biochem J* 255 (1): 357-60, 1988.
60. Crompton, M., McGuinness, O., and Nazareth, W.: The involvement of cyclosporin A binding proteins in regulating and uncoupling mitochondrial energy transduction. *Biochim Biophys Acta* 1101 (2): 214-7, 1992.
61. Danysz, W., Dyr, W., Jankowska, E., Glazewski, S., and Kostowski, W.: The involvement of NMDA receptors in acute and chronic effects of ethanol. *Alcoholism, Clinical & Experimental Research* 16 (3): 499-504, 1992.

References

62. Danysz, W., and Parsons, C. G.: Glycine and N-Methyl-D-Aspartate Receptors: Physiological Significance and Possible Therapeutic Applications. *Pharmacological Reviews* 50 (4): 598-664, 1998.
63. Das, S., Sasaki, Y. F., Rothe, T., Premkumar, L. S., Takasu, M., Crandall, J. E., Dikkes, P., Conner, D. A., Rayudu, P. V., Cheung, W., Chen, H. S., Lipton, S. A., and Nakanishi, N.: Increased NMDA current and spine density in mice lacking the NMDA receptor subunit NR3A. *Nature* 393 (6683): 377-81, 1998.
64. Davidson, A. M., and Halestrap, A. P.: Partial inhibition by cyclosporin A of the swelling of liver mitochondria in vivo and in vitro induced by sub-micromolar $[Ca^{2+}]$, but not by butyrate. Evidence for two distinct swelling mechanisms. *Biochem J* 268 (1): 147-52, 1990.
65. Di Fabio, R., Capelli, A. M., Conti, N., Cugola, A., Donati, D., Feriani, A., Gastaldi, P., Gaviraghi, G., Hewkin, C. T., Micheli, F., Missio, A., Mugnaini, M., Pecunioso, A., Quaglia, A. M., Ratti, E., Rossi, L., Tedesco, G., Trist, D. G., and Reggiani, A.: Substituted indole-2-carboxylates as in vivo potent antagonists acting as the strychnine-insensitive glycine binding site. *J Med Chem* 40 (6): 841-50, 1997.
66. DiFiglia, M.: Excitotoxic injury of the neostriatum: a model for Huntington's disease. *Trends in Neurosciences* 13 (7): 286-9, 1990.
67. Durand, G. M., Bennett, M. V., and Zukin, R. S.: Splice variants of the N-methyl-D-aspartate receptor NR1 identify domains involved in regulation by polyamines and protein kinase C. *Proceedings of the National Academy of Sciences of the United States of America* 90 (14): 6731-5, 1993.
68. Durand, G. M., Gregor, P., Zheng, X., Bennett, M. V., Uhl, G. R., and Zukin, R. S.: Cloning of an apparent splice variant of the rat N-methyl-D-aspartate receptor NMDAR1 with altered sensitivity to polyamines and activators of protein kinase C. *Proceedings of the National Academy of Sciences of the United States of America* 89 (19): 9359-63, 1992.
69. During, M. J., Symes, C. W., Lawlor, P. A., Lin, J., Dunning, J., Fitzsimons, H. L., Poulsen, D., Leone, P., Xu, R., Dicker, B. L., Lipski, J., and Young, D.: An oral vaccine against NMDAR1 with efficacy in experimental stroke and epilepsy [see comments]. *Science* 287 (5457): 1453-60, 2000.
70. Dyker, A. G., Edwards, K. R., Fayad, P. B., Hormes, J. T., and Lees, K. R.: Safety and tolerability study of aptiganel hydrochloride in patients with an acute ischemic stroke. *Stroke* 30 (10): 2038-42, 1999.

References

71. Enari, M., Sakahira, H., Yokoyama, H., Okawa, K., Iwamatsu, A., and Nagata, S.: A caspase-activated DNase that degrades DNA during apoptosis, and its inhibitor ICAD [see comments] [published erratum appears in Nature 1998 May 28;393(6683):396]. *Nature* 391 (6662): 43-50, 1998.
72. Fedele, E., Smith, D., and Foster, A. C.: Autoradiographical evaluation of [3H]glycine uptake in rat forebrain: cellular localization in the hippocampus. *Neurosci Lett* 161 (1): 4-8, 1993.
73. Foster, A. C., and Kemp, J. A.: HA-966 antagonizes N-methyl-D-aspartate receptors through a selective interaction with the glycine modulatory site. *J Neurosci* 9 (6): 2191-6, 1989.
74. Foster, A. C., Kemp, J. A., Leeson, P. D., Grimwood, S., Donald, A. E., Marshall, G. R., Priestley, T., Smith, J. D., and Carling, R. W.: Kynurenic acid analogues with improved affinity and selectivity for the glycine site on the N-methyl-D-aspartate receptor from rat brain. *Molecular Pharmacology* 41 (5): 914-22, 1992.
75. Friberg, H., Ferrand-Drake, M., Bengtsson, F., Halestrap, A. P., and Wieloch, T.: Cyclosporin A, but not FK 506, protects mitochondria and neurons against hypoglycemic damage and implicates the mitochondrial permeability transition in cell death. *J Neurosci* 18 (14): 5151-9, 1998.
76. Gallagher, M. J., Huang, H., Grant, E. R., and Lynch, D. R.: The NR2B-specific interactions of polyamines and protons with the N-methyl-D-aspartate receptor. *Journal of Biological Chemistry* 272 (40): 24971-9, 1997.
77. Gallagher, M. J., Huang, H., Pritchett, D. B., and Lynch, D. R.: Interactions between ifenprodil and the NR2B subunit of the N-methyl-D-aspartate receptor. *Journal of Biological Chemistry* 271 (16): 9603-11, 1996.
78. Globus, M. Y. T., Busto, R., Dietrich, W. D., Martinez, E., Valdes, I., and Ginsberg, M. D.: Effect of ischemia on the in vivo release of striatal dopamine, glutamate, and GABA studied in intracerebral microdialysis. *Journal of Neurochemistry* 51: 1455-64, 1988.
79. Gorman, C. M., Gies, D., McCray, G., and Huang, M.: The human cytomegalovirus major immediate early promoter
80. Graham, F. L., Smiley, J., Russell, W. C., and Nairn, R.: Characteristics of a human cell line transformed by DNA from human adenovirus type 5. *J. gen. Virol.* 36: 59-74, 1977.
81. Graham, F. L., and Van der Eb, A. J.: A new technique for the assay of the infectivity of human adenovirus 5 DNA. *Virology* 52: 456-67, 1973.

References

- 82.** Grant, E. R., Bacskai, B. J., Pleasure, D. E., Pritchett, D. B., Gallagher, M. J., Kendrick, S. J., Kricka, L. J., and Lynch, D. R.: N-methyl-D-aspartate receptors expressed in a nonneuronal cell line mediate subunit-specific increases in free intracellular calcium. *Journal of Biological Chemistry* 272 (1): 647-56, 1997.
- 83.** Gredal, O., Werdelin, L., Bak, S., Christensen, P. B., Boysen, G., Kristensen, M. O., Jespersen, J. H., Regeur, L., Hinge, H. H., and Jensen, T. S.: A clinical trial of dextromethorphan in amyotrophic lateral sclerosis. *Acta Neurol Scand* 96 (1): 8-13, 1997.
- 84.** Greenamyre, J. T.: The role of glutamate in neurotransmission and in neurologic disease. *Archives of Neurology* 43: 1058-63, 1986.
- 85.** Grimwood, S., Le Bourdelles, B., Atack, J. R., Barton, C., Cockett, W., Cook, S. M., Gilbert, E., Hutson, P. H., McKernan, R. M., Myers, J., Ragan, C. I., Wingrove, P. B., and Whiting, P. J.: Generation and characterisation of stable cell lines expressing recombinant human N-methyl-D-aspartate receptor subtypes. *Journal of Neurochemistry* 66 (6): 2239-47, 1996a.
- 86.** Grimwood, S., Le Bourdelles, B., and Whiting, P. J.: Recombinant human NMDA homomeric NR1 receptors expressed in mammalian cells form a high-affinity glycine antagonist binding site. *Journal of Neurochemistry* 64 (2): 525-30, 1995.
- 87.** Gusev, E. I., Skvortsova, V. I., Izykenova, G. A., Alekseev, A. A., and Dambinova, S. A.: [The level of autoantibodies to glutamate receptors in the blood serum of patients in the acute period of ischemic stroke]. *Zhurnal Nevropatologii i Psikhiiatrii Imeni S - S - Korsakova* 96 (5): 68-72, 1996.
- 88.** Halestrap, A. P.: Calcium-dependent opening of a non-specific pore in the mitochondrial inner membrane is inhibited at pH values below 7. Implications for the protective effect of low pH against chemical and hypoxic cell damage. *Biochem J* 278 (Pt 3): 715-9, 1991.
- 89.** Halestrap, A. P., Connern, C. P., Griffiths, E. J., and Kerr, P. M.: Cyclosporin A binding to mitochondrial cyclophilin inhibits the permeability transition pore and protects hearts from ischaemia/reperfusion injury. *Mol Cell Biochem* 174 (1-2): 167-72, 1997.
- 90.** Hargreaves, R. J., Rigby, M., Smith, D., Hill, R. G., and Iversen, L. L.: Competitive as well as uncompetitive N-methyl-D-aspartate receptor antagonists affect cortical neuronal morphology and cerebral glucose metabolism. *Neurochemical Research* 18 (12): 1263-9, 1993.
- 91.** Hawkinson, J. E., Huber, K. R., Sahota, P. S., Han Hsu, H., Weber, E., and Whitehouse, M. J.: The N-methyl-D-aspartate (NMDA) receptor glycine site antagonist ACEA 1021 does not produce pathological changes in rat brain. *Brain Research* 744 (2): 227-34, 1997.

References

92. Hayashi, T. A.: Effects of sodium glutamate on the nervous system. *J. Medicine* 3: 183-92, 1954.
93. Helekar, S. A., Char, D., Neff, S., and Patrick, J.: Prolyl isomerase requirement for the expression of functional homo- oligomeric ligand-gated ion channels. *Neuron* 12 (1): 179-89, 1994.
94. Hess, S. D., Daggett, L. P., Crona, J., Deal, C., Lu, C. C., Urrutia, A., Chavez-Noriega, L., Ellis, S. B., Johnson, E. C., and Velicelebi, G.: Cloning and functional characterization of human heteromeric N-methyl-D-aspartate receptors. *Journal of Pharmacology & Experimental Therapeutics* 278 (2): 808-16, 1996.
95. Hess, S. D., Daggett, L. P., Deal, C., Lu, C. C., Johnson, E. C., and Velicelebi, G.: Functional characterization of human N-methyl-D-aspartate subtype 1A/2D receptors. *Journal of Neurochemistry* 70 (3): 1269-79, 1998.
96. Hetman, M., Danysz, W., and Kaczmarek, L.: Increased expression of cathepsin D in retrosplenial cortex of MK-801-treated rats. *Experimental Neurology* 147 (2): 229-37, 1997.
97. Hirai, H., Kirsch, J., Laube, B., Betz, H., and Kuhse, J.: The Glycine Binding Site Of the N-Methyl-D-Aspartate Receptor Subunit Nr1 - Identification Of Novel Determinants Of Co-Agonist Potentiation In the Extracellular M3-M4 Loop Region. *Proceedings of the National Academy of Sciences of the United States of America* 93 (12): 6031-6036, 1996a.
98. Hirai, H., Kirsch, J., Laube, B., Betz, H., and Kuhse, J.: The glycine binding site of the N-methyl-D-aspartate receptor subunit NR1: identification of novel determinants of co-agonist potentiation in the extracellular M3-M4 loop region. *Proceedings of the National Academy of Sciences of the United States of America* 93 (12): 6031-6, 1996b.
99. Hisatsune, C., Umemori, H., Inoue, T., Michikawa, T., Kohda, K., Mikoshiba, K., and Yamamoto, T.: Phosphorylation-dependent regulation of N-methyl-D-aspartate receptors by calmodulin. *Journal of Biological Chemistry* 272 (33): 20805-10, 1997.
100. Hoffman, P. L., Iorio, K. R., Snell, L. D., and Tabakoff, B.: Attenuation of glutamate-induced neurotoxicity in chronically ethanol-exposed cerebellar granule cells by NMDA receptor antagonists and ganglioside GM1. *Alcoholism, Clinical & Experimental Research* 19 (3): 721-6, 1995.
101. Hollmann, M., and Heinemann, S.: Cloned glutamate receptors. *Annu. Rev. Neurosci.* 17: 31-108, 1994.

References

102. Hollmann, M., Maron, C., and Heinemann, S.: N-glycosylation site tagging suggests a three transmembrane domain topology for the glutamate receptor GluR1. *Neuron* 13 (6): 1331-43, 1994.
103. Honer, M., Benke, D., Laube, B., Kuhse, J., Heckendorn, R., Allgeier, H., Angst, C., Monyer, H., Seeburg, P. H., Betz, H., and Mohler, H.: Differentiation of glycine antagonist sites of N-methyl-D-aspartate receptor subtypes. Preferential interaction of CGP 61594 with NR1/2B receptors. *Journal of Biological Chemistry* 273 (18): 11158-63, 1998.
104. Horvath, Z. C., Czopf, J., and Buzsaki, G.: MK-801-induced neuronal damage in rats. *Brain Res* 753 (2): 181-95, 1997.
105. Hu, X. J., Follsea, P., and Ticku, M. K.: Chronic ethanol treatment produces a selective upregulation of the NMDA receptor subunit gene expression in mammalian cultured cortical neurons. *Brain Research. Molecular Brain Research* 36 (2): 211-8, 1996.
106. Hume, R. I., Dingledine, R., and Heinemann, S. F.: Identification of a site in glutamate receptor subunits that controls calcium permeability. *Science* 253 (5023): 1028-31, 1991.
107. Ikeda, K., Nagasawa, M., Mori, H., Araki, K., Sakimura, K., Watanabe, M., Inoue, Y., and Mishina, M.: Cloning and expression of the epsilon 4 subunit of the NMDA receptor channel. *FEBS Letters* 313 (1): 34-8, 1992.
108. Ilyin, V. I., Whittemore, E. R., Guastella, J., Weber, E., and Woodward, R. M.: Subtype-selective inhibition of N-methyl-D-aspartate receptors by haloperidol. *Molecular Pharmacology* 50 (6): 1541-50, 1996.
109. Inagaki, N., Kuromi, H., Gonoi, T., Okamoto, Y., Ishida, H., Seino, Y., Kaneko, T., Iwanaga, T., and Seino, S.: Expression and role of ionotropic glutamate receptors in pancreatic islet cells. *FASEB Journal* 9 (8): 686-91, 1995.
110. Ishii, T., Moriyoshi, K., Sugihara, H., Sakurada, K., Kadotani, H., Yokoi, M., Akazawa, C., Shigemoto, R., Mizuno, N., Masu, M., and et al.: Molecular characterization of the family of the N-methyl-D-aspartate receptor subunits. *Journal of Biological Chemistry* 268 (4): 2836-43, 1993.
111. Janicke, R. U., Sprengart, M. L., Wati, M. R., and Porter, A. G.: Caspase-3 is required for DNA fragmentation and morphological changes associated with apoptosis. *J Biol Chem* 273 (16): 9357-60, 1998.
112. Javitt, D. C., and Zukin, S. R.: Recent advances in the phencyclidine model of schizophrenia [see comments]. *American Journal of Psychiatry* 148 (10): 1301-8, 1991.

References

- 113.** Johnson, J. W., and Ascher, P.: Glycine potentiates the NMDA response in cultured mouse brain neurons. *Nature* 325 (6104): 529-31, 1987.
- 114.** Kantrow, S. P., and Piantadosi, C. A.: Release of cytochrome c from liver mitochondria during permeability transition. *Biochem Biophys Res Commun* 232 (3): 669-71, 1997.
- 115.** Karcz-Kubicha, M., Jessa, M., Nazar, M., Plaznik, A., Hartmann, S., Parsons, C. G., and Danysz, W.: Anxiolytic activity of glycine-B antagonists and partial agonists--no relation to intrinsic activity in the patch clamp. *Neuropharmacology* 36 (10): 1355-67, 1997.
- 116.** Karp, S. J., Masu, M., Eki, T., Ozawa, K., and Nakanishi, S.: Molecular cloning and chromosomal localization of the key subunit of the human N-methyl-D-aspartate receptor. *Journal of Biological Chemistry* 268 (5): 3728-33, 1993.
- 117.** Kashiwagi, K., Fukuchi, J., Chao, J., Igarashi, K., and Williams, K.: An Aspartate Residue In the Extracellular Loop Of the N-Methyl-D-Aspartate Receptor Controls Sensitivity to Spermine and Protons. *Molecular Pharmacology* 49 (6): 1131-1141, 1996a.
- 118.** Kehne, J. H., Baron, B. M., Harrison, B. L., McCloskey, T. C., Palfreyman, M. G., Poirot, M., Salituro, F. G., Siegel, B. W., Slone, A. L., Van Giersbergen, P. L., and et al.: MDL 100,458 and MDL 102,288: two potent and selective glycine receptor antagonists with different functional profiles. *European Journal of Pharmacology* 284 (1-2): 109-18, 1995.
- 119.** Kehne, J. H., McCloskey, T. C., Baron, B. M., Chi, E. M., Harrison, B. L., Whitten, J. P., and Palfreyman, M. G.: NMDA receptor complex antagonists have potential anxiolytic effects as measured with separation-induced ultrasonic vocalizations. *European Journal of Pharmacology* 193 (3): 283-92, 1991.
- 120.** Kelso, S. R., Nelson, T. E., and Leonard, J. P.: Protein kinase C-mediated enhancement of NMDA currents by metabotropic glutamate receptors in *Xenopus* oocytes. *Journal of Physiology* 449: 705-18, 1992.
- 121.** Kemp, J. A., Foster, A. C., Leeson, P. D., Priestley, T., Tridgett, R., Iversen, L. L., and Woodruff, G. N.: 7-Chlorokynurenic acid is a selective antagonist at the glycine modulatory site of the N-methyl-D-aspartate receptor complex. *Proc Natl Acad Sci U S A* 85 (17): 6547-50, 1988.
- 122.** Kemp, J. A., and Leeson, P. D.: The glycine site of the NMDA receptor--five years on. *Trends in Pharmacological Sciences* 14 (1): 20-5, 1993.

References

123. Kerr, J. F., Wyllie, A. H., and Currie, A. R.: Apoptosis: a basic biological phenomenon with wide-ranging implications in tissue kinetics. *Br J Cancer* 26 (4): 239-57, 1972.
124. Kessler, M., Terramani, T., Lynch, G., and Baudry, M.: A glycine site associated with N-methyl-D-aspartic acid receptors: characterization and identification of a new class of antagonists. *J Neurochem* 52 (4): 1319-28, 1989.
125. Kew, J. N., and Kemp, J. A.: An allosteric interaction between the NMDA receptor polyamine and ifenprodil sites in rat cultured cortical neurones. *J Physiol (Lond)* 512 (Pt 1): 17-28, 1998.
126. Kieburz, K., Feigin, A., McDermott, M., Como, P., Abwender, D., Zimmerman, C., Hickey, C., Orme, C., Claude, K., Sotack, J., Greenamyre, J. T., Dunn, C., and Shoulson, I.: A controlled trial of remacemide hydrochloride in Huntington's disease. *Movement Disorders* 11 (3): 273-7, 1996.
127. Kleckner, N. W., and Dingledine, R.: Requirement for glycine in activation of NMDA-receptors expressed in *Xenopus* oocytes. *Science* 241 (4867): 835-7, 1988.
128. Kleckner, N. W., and Dingledine, R.: Selectivity of quinoxalines and kynurenes as antagonists of the glycine site on N-methyl-D-aspartate receptors. *Mol Pharmacol* 36 (3): 430-6, 1989.
129. Klepstad, P., Maurset, A., Moberg, E. R., and Oye, I.: Evidence of a role for NMDA receptors in pain perception. *European Journal of Pharmacology* 187 (3): 513-8, 1990.
130. Koh, J. Y., and Choi, D. W.: Zinc toxicity on cultured cortical neurons: involvement of N-methyl-D-aspartate receptors. *Neuroscience* 60 (4): 1049-57, 1994.
131. Kohr, G., Eckardt, S., Luddens, H., Monyer, H., and Seeburg, P. H.: NMDA receptor channels: subunit-specific potentiation by reducing agents. *Neuron* 12 (5): 1031-40, 1994.
132. Kohr, G., and Seeburg, P. H.: Subtype-specific regulation of recombinant NMDA receptor-channels by protein tyrosine kinases of the src family. *Journal of Physiology* 492 (Pt 2): 445-52, 1996.
133. Kornhuber, J., Weller, M., Schoppmeyer, K., and Riederer, P.: Amantadine and memantine are NMDA receptor antagonists with neuroprotective properties. *Journal of Neural Transmission. Supplementum* 43: 91-104, 1994.
134. Kretschmer, B. D., Kratzer, U., Breithecker, K., and Koch, M.: ACEA 1021, a glycine site antagonist with minor psychotomimetic and amnestic effects in rats. *European Journal of Pharmacology* 331 (2-3): 109-16, 1997.

References

- 135.** Kristensen, J. D., Karlsten, R., Gordh, T., and Berge, O. G.: The NMDA antagonist 3-(2-carboxypiperazin-4-yl)propyl-1-phosphonic acid (CPP) has antinociceptive effect after intrathecal injection in the rat. *Pain* 56 (1): 59-67, 1994.
- 136.** Krystal, J. H., Karper, L. P., Seibyl, J. P., Freeman, G. K., Delaney, R., Bremner, J. D., Heninger, G. R., Bowers, M. B., Jr., and Charney, D. S.: Subanesthetic effects of the noncompetitive NMDA antagonist, ketamine, in humans. Psychotomimetic, perceptual, cognitive, and neuroendocrine responses. *Archives of General Psychiatry* 51 (3): 199-214, 1994.
- 137.** Kulagowski, J. J., Baker, R., Curtis, N. R., Leeson, P. D., Mawer, I. M., Moseley, A. M., Ridgill, M. P., Rowley, M., Stansfield, I., Foster, A. C., and et al.: 3'-(Arylmethyl)- and 3'-(aryloxy)-3-phenyl-4-hydroxyquinolin-2(1H)-ones: orally active antagonists of the glycine site on the NMDA receptor. *Journal of Medicinal Chemistry* 37 (10): 1402-5, 1994.
- 138.** Kuryatov, A., Laube, B., Betz, H., and Kuhse, J.: Mutational analysis of the glycine-binding site of the NMDA receptor: structural similarity with bacterial amino acid-binding proteins. *Neuron* 12 (6): 1291-300, 1994.
- 139.** Kutsuwada, T., Kashiwabuchi, N., Mori, H., Sakimura, K., Kushiya, E., Araki, K., Meguro, H., Masaki, H., Kumanishi, T., Arakawa, M., and et al.: Molecular diversity of the NMDA receptor channel [see comments]. *Nature* 358 (6381): 36-41, 1992.
- 140.** Laird, J. M., Mason, G. S., Webb, J., Hill, R. G., and Hargreaves, R. J.: Effects of a partial agonist and a full antagonist acting at the glycine site of the NMDA receptor on inflammation-induced mechanical hyperalgesia in rats. *British Journal of Pharmacology* 117 (7): 1487-92, 1996.
- 141.** Laube, B., Hirai, H., Sturgess, M., Betz, H., and Kuhse, J.: Molecular determinants of agonist discrimination by NMDA receptor subunits: analysis of the glutamate binding site on the NR2B subunit. *Neuron* 18 (3): 493-503, 1997.
- 142.** Laube, B., Kuhse, J., and Betz, H.: Evidence for a tetrameric structure of recombinant NMDA receptors. *Journal of Neuroscience* 18 (8): 2954-61, 1998.
- 143.** Laurie, D. J., and Seeburg, P. H.: Ligand affinities at recombinant N-methyl-D-aspartate receptors depend on subunit composition. *European Journal of Pharmacology* 268 (3): 335-45, 1994.
- 144.** Le Bourdelles, B., Wafford, K. A., Kemp, J. A., Marshall, G., Bain, C., Wilcox, A. S., Sikela, J. M., and Whiting, P. J.: Cloning, functional coexpression, and pharmacological

References

- characterisation of human cDNAs encoding NMDA receptor NR1 and NR2A subunits. *Journal of Neurochemistry* 62 (6): 2091-8, 1994.
- 145.** Lee, F., Mulligan, R., Berg, P., and Ringold, G.: Glucocorticoids regulate expression of dihydrofolate reductase cDNA in mouse mammary tumor virus chimaeric plasmids. *Nature* 294: 228-32, 1981.
- 146.** Lees, G. J.: Contributory mechanisms in the causation of neurodegenerative disorders. *Neuroscience* 54: 287-322, 1993.
- 147.** Leeson, P. D., Carling, R. W., Moore, K. W., Moseley, A. M., Smith, J. D., Stevenson, G., Chan, T., Baker, R., Foster, A. C., Grimwood, S., and et al.: 4-Amido-2-carboxytetrahydroquinolines. Structure-activity relationships for antagonism at the glycine site of the NMDA receptor. *Journal of Medicinal Chemistry* 35 (11): 1954-68, 1992.
- 148.** Leeson, P. D., and Iversen, L. L.: The glycine site on the NMDA receptor: structure-activity relationships and therapeutic potential. *Journal of Medicinal Chemistry* 37 (24): 4053-67, 1994.
- 149.** Legendre, P., and Westbrook, G. L.: The inhibition of single N-methyl-D-aspartate-activated channels by zinc ions on cultured rat neurones. *J Physiol (Lond)* 429: 429-49, 1990.
- 150.** Leist, M., and Nicotera, P.: The shape of cell death. *Biochem Biophys Res Commun* 236 (1): 1-9, 1997.
- 151.** Leist, M., Single, B., Castoldi, A. F., Kuhnle, S., and Nicotera, P.: Intracellular adenosine triphosphate (ATP) concentration: a switch in the decision between apoptosis and necrosis. *J Exp Med* 185 (8): 1481-6, 1997.
- 152.** Leist, M., Single, B., Naumann, H., Fava, E., Simon, B., Kuhnle, S., and Nicotera, P.: Inhibition of mitochondrial ATP generation by nitric oxide switches apoptosis to necrosis. *Exp Cell Res* 249 (2): 396-403, 1999.
- 153.** Li, P., Nijhawan, D., Budihardjo, I., Srinivasula, S. M., Ahmad, M., Alnemri, E. S., and Wang, X.: Cytochrome c and dATP-dependent formation of Apaf-1/caspase-9 complex initiates an apoptotic protease cascade. *Cell* 91 (4): 479-89, 1997.
- 154.** Lieberman, D. N., and Mody, I.: Regulation of NMDA channel function by endogenous Ca(2+)-dependent phosphatase. *Nature* 369 (6477): 235-9, 1994.
- 155.** Liebmann, J. M., and Bennett, D. A.: Anxiolytic actions of N-methyl-D-aspartate receptor antagonists: a comparison with benzodiazepine modulators and dissociative anesthetics. *Frontiers in excitatory amino acid research* : 301-8, 1988.

References

- 156.** Lin, Y. J., Bovetto, S., Carver, J. M., and Giordano, T.: Cloning of the cDNA for the human NMDA receptor NR2C subunit and its expression in the central nervous system and periphery. *Brain Research. Molecular Brain Research* 43 (1-2): 57-64, 1996.
- 157.** Löscher, W.: Basic aspects of epilepsy. *Current Opinion in Neurology & Neurosurgery* 6: 223-32, 1993.
- 158.** Loscher, W., and Honack, D.: Anticonvulsant and behavioral effects of two novel competitive N-methyl-D-aspartic acid receptor antagonists, CGP 37849 and CGP 39551, in the kindling model of epilepsy. Comparison with MK-801 and carbamazepine. *Journal of Pharmacology & Experimental Therapeutics* 256 (2): 432-40, 1991.
- 159.** Lunn, W. H., Schoepp, D. D., Calligaro, D. O., Vasileff, R. T., Heinz, L. J., Salhoff, C. R., and PJ, O. M.: DL-tetrazol-5-ylglycine, a highly potent NMDA agonist: its synthesis and NMDA receptor efficacy. *Journal of Medicinal Chemistry* 35 (24): 4608-12, 1992.
- 160.** Luo, J., Wang, Y., Yasuda, R. P., Dunah, A. W., and Wolfe, B. B.: The majority of N-methyl-D-aspartate receptor complexes in adult rat cerebral cortex contain at least three different subunits (NR1/NR2A/NR2B). *Molecular Pharmacology* 51 (1): 79-86, 1997.
- 161.** Lutfy, K., and Weber, E.: Attenuation of nociceptive responses by ACEA-1021, a competitive NMDA receptor/glycine site antagonist, in the mice. *Brain Research* 743 (1-2): 17-23, 1996.
- 162.** Lynch, D. R., Anegawa, N. J., Verdoorn, T., and Pritchett, D. B.: N-methyl-D-aspartate receptors: different subunit requirements for binding of glutamate antagonists, glycine antagonists, and channel-blocking agents. *Molecular Pharmacology* 45 (3): 540-5, 1994.
- 163.** Matsui, T., Sekiguchi, M., Hashimoto, A., Tomita, U., Nishikawa, T., and Wada, K.: Functional comparison of D-serine and glycine in rodents: the effect on cloned NMDA receptors and the extracellular concentration. *Journal of Neurochemistry* 65 (1): 454-8, 1995.
- 164.** Mayhan, W. G., and Didion, S. P.: Glutamate-induced disruption of the blood-brain barrier in rats. Role of nitric oxide. *Stroke* 27 (5): 965-9; discussion 970, 1996.
- 165.** McBain, C. J., Kleckner, N. W., Wyrick, S., and Dingledine, R.: Structural requirements for activation of the glycine coagonist site of N-methyl-D-aspartate receptors expressed in *Xenopus* oocytes. *Mol Pharmacol* 36 (4): 556-65, 1989.
- 166.** McIlhinney, R. A., Molnar, E., Atack, J. R., and Whiting, P. J.: Cell surface expression of the human N-methyl-D-aspartate receptor subunit 1a requires the co-expression of the NR2A subunit in transfected cells. *Neuroscience* 70 (4): 989-97, 1996.

References

167. McIlhinney, R. A. J., Le Bourdellès, B., Molnár, E., Tricaud, N., Streit, P., and Whiting, P. J.: Assembly intracellular targeting and cell surface expression of the human N-methyl-D-aspartate receptor subunits NR1a and NR2A in transfected cells. *Neuropharmacology* 37: 1355-67, 1998.
168. Meguro, H., Mori, H., Araki, K., Kushiya, E., Kutsuwada, T., Yamazaki, M., Kumanishi, T., Arakawa, M., Sakimura, K., and Mishina, M.: Functional characterization of a heteromeric NMDA receptor channel expressed from cloned cDNAs. *Nature* 357 (6373): 70-4, 1992.
169. Meldrum, B., and Garthwaite, J.: Excitatory amino acid neurotoxicity and neurodegenerative disease. *Trends in Pharmacological Sciences* 11 (9): 379-87, 1990.
170. Mishina, M., Mori, H., Araki, K., Kushiya, E., Meguro, H., Kutsuwada, T., Kashiwabuchi, N., Ikeda, K., Nagasawa, M., Yamazaki, M., and et al.: Molecular and functional diversity of the NMDA receptor channel. *Annals of the New York Academy of Sciences* 707: 136-52, 1993.
171. Molnar, P., and Erdo, S. L.: Differential effects of five glycine site antagonists on NMDA receptor desensitisation. *European Journal of Pharmacology* 311 (2-3): 311-4, 1996.
172. Monyer, H., Burnashev, N., Laurie, D. J., Sakmann, B., and Seeburg, P. H.: Developmental and regional expression in the rat brain and functional properties of four NMDA receptors. *Neuron* 12 (3): 529-40, 1994.
173. Monyer, H., Sprengel, R., Schoepfer, R., Herb, A., Higuchi, M., Lomeli, H., Burnashev, N., Sakmann, B., and Seeburg, P. H.: Heteromeric NMDA receptors: molecular and functional distinction of subtypes. *Science* 256 (5060): 1217-21, 1992.
174. Mori, H., Masaki, H., Yamakura, T., and Mishina, M.: Identification by mutagenesis of a Mg(2+)-block site of the NMDA receptor channel. *Nature* 358 (6388): 673-5, 1992.
175. Mori, H., Yamakura, T., Masaki, H., and Mishina, M.: Involvement of the carboxyl-terminal region in modulation by TPA of the NMDA receptor channel. *Neuroreport* 4 (5): 519-22, 1993.
176. Moriyoshi, K., Masu, M., Ishii, T., Shigemoto, R., Mizuno, N., and Nakanishi, S.: Molecular cloning and characterization of the rat NMDA receptor [see comments]. *Nature* 354 (6348): 31-7, 1991.
177. Moroni, F., Russi, P., Lombardi, G., Beni, M., and Carla, V.: Presence of kynurenic acid in the mammalian brain. *J Neurochem* 51 (1): 177-80, 1988.

References

- 178.** Mott, D. D., Doherty, J. J., Zhang, S., Washburn, M. S., Fendley, M. J., Lyuboslavsky, P., Traynelis, S. F., and Dingledine, R.: Phenylethanolamines inhibit NMDA receptors by enhancing proton inhibition. *Nat Neurosci* 1 (8): 659-67, 1998.
- 179.** Muir, K. W., Grosset, D. G., Gamzu, E., and Lees, K. R.: Pharmacological effects of the non-competitive NMDA antagonist CNS 1102 in normal volunteers. *British Journal of Clinical Pharmacology* 38 (1): 33-8, 1994.
- 180.** Muir, K. W., Grosset, D. G., and Lees, K. R.: Effects of prolonged infusions of the NMDA antagonist aptiganel hydrochloride (CNS 1102) in normal volunteers. *Clinical Neuropharmacology* 20 (4): 311-21, 1997.
- 181.** Munir, M., Lu, L., Wang, Y. H., Luo, J., Wolfe, B. B., and McGonigle, P.: Pharmacological and immunological characterization of N-methyl-D-aspartate receptors in human NT2-N neurons. *Journal of Pharmacology & Experimental Therapeutics* 276 (2): 819-28, 1996.
- 182.** Murata, S., and Kawasaki, K.: Common and uncommon behavioural effects of antagonists for different modulatory sites in the NMDA receptor/channel complex. *European Journal of Pharmacology* 239 (1-3): 9-15, 1993.
- 183.** Nagata, R., Tanno, N., Kodo, T., Ae, N., Yamaguchi, H., Nishimura, T., Antoku, F., Tatsuno, T., Kato, T., Tanaka, Y., and et al.: Tricyclic quinoxalinediones: 5,6-dihydro-1H-pyrrolo[1,2,3-de] quinoxaline-2,3-diones and 6,7-dihydro-1H,5H-pyrido[1,2,3-de] quinoxaline-2,3-diones as potent antagonists for the glycine binding site of the NMDA receptor. *Journal of Medicinal Chemistry* 37 (23): 3956-68, 1994.
- 184.** Nagata, S.: Apoptosis by death factor. *Cell* 88 (3): 355-65, 1997.
- 185.** Nakanishi, N., Axel, R., and Shneider, N. A.: Alternative splicing generates functionally distinct N-methyl-D-aspartate receptors. *Proceedings of the National Academy of Sciences of the United States of America* 89 (18): 8552-6, 1992.
- 186.** Nicholls, D. G., and Budd, S. L.: Mitochondria and neuronal glutamate excitotoxicity. *Biochim Biophys Acta* 1366 (1-2): 97-112, 1998.
- 187.** Nicholson, D. W., Ali, A., Thornberry, N. A., Vaillancourt, J. P., Ding, C. K., Gallant, M., Gareau, Y., Griffin, P. R., Labelle, M., Lazebnik, Y. A., and et al.: Identification and inhibition of the ICE/CED-3 protease necessary for mammalian apoptosis [see comments]. *Nature* 376 (6535): 37-43, 1995.
- 188.** Nicotera, P., Leist, M., and Ferrando-May, E.: Intracellular ATP, a switch in the decision between apoptosis and necrosis. *Toxicol Lett* 102-103: 139-42, 1998.

References

- 189.** Nieminen, A. L., Petrie, T. G., Lemasters, J. J., and Selman, W. R.: Cyclosporin A delays mitochondrial depolarization induced by N-methyl-D-aspartate in cortical neurons: evidence of the mitochondrial permeability transition. *Neuroscience* 75 (4): 993-7, 1996.
- 190.** Okakura, K., Yamatodani, A., Mochizuki, T., Horii, A., and Wada, H.: Glutamatergic regulation of histamine release from rat hypothalamus. *European Journal of Pharmacology* 213 (2): 189-92, 1992.
- 191.** Olney, J. W., Labruyere, J., and Price, M. T.: Pathological changes induced in cerebrocortical neurons by phencyclidine and related drugs. *Science* 244: 1360-62, 1989.
- 192.** Omerovic, A., Chen, S. J., Leonard, J. P., and Kelso, S. R.: Subunit-specific redox modulation of NMDA receptors expressed in *Xenopus* oocytes. *Journal of Receptor & Signal Transduction Research* 15 (6): 811-27, 1995.
- 193.** Paoletti, P., Ascher, P., and Neyton, J.: High-affinity zinc inhibition of NMDA NR1-NR2A receptors [published erratum appears in *J Neurosci* 1997 Oct 15;17(20):following table of contents]. *Journal of Neuroscience* 17 (15): 5711-25, 1997.
- 194.** Paoletti, P., Neyton, J., and Ascher, P.: Glycine-independent and subunit-specific potentiation of NMDA responses by extracellular Mg²⁺. *Neuron* 15 (5): 1109-20, 1995.
- 195.** Park, C. K., Nehls, D. G., Graham, D. I., Teasdale, G. M., and McCulloch, J.: The glutamate antagonist MK-801 reduces focal ischemic brain damage in the rat. *Ann Neurol* 24 (4): 543-51, 1988.
- 196.** Parsons, C. G., Danysz, W., Quack, G., Hartmann, S., Lorenz, B., Wollenburg, C., Baran, L., Przegalinski, E., Kostowski, W., Krzascik, P., Chizh, B., and Headley, P. M.: Novel Systemically Active Antagonists Of the Glycine Site Of the N-Methyl-D-Aspartate Receptor - Electrophysiological, Biochemical and Behavioral Characterization. *Journal of Pharmacology & Experimental Therapeutics* 283 (3): 1264-1275, 1997a.
- 197.** Parsons, C. G., Danysz, W., Quack, G., Hartmann, S., Lorenz, B., Wollenburg, C., Baran, L., Przegalinski, E., Kostowski, W., Krzascik, P., Chizh, B., and Headley, P. M.: Novel systemically active antagonists of the glycine site of the N-methyl-D-aspartate receptor: electrophysiological, biochemical and behavioral characterization. *Journal of Pharmacology & Experimental Therapeutics* 283 (3): 1264-75, 1997b.
- 198.** Parsons, C. G., Gruner, R., Rozental, J., Millar, J., and Lodge, D.: Patch clamp studies on the kinetics and selectivity of N-methyl-D-aspartate receptor antagonism by memantine (1-amino-3,5-dimethyladamantan). *Neuropharmacology* 32 (12): 1337-50, 1993a.

References

- 199.** Parsons, C. G., Zong, X., and Lux, H. D.: Whole cell and single channel analysis of the kinetics of glycine-sensitive N-methyl-D-aspartate receptor desensitization. *British Journal of Pharmacology* 109 (1): 213-21, 1993b.
- 200.** Pastorino, J. G., Snyder, J. W., Serroni, A., Hoek, J. B., and Farber, J. L.: Cyclosporin and carnitine prevent the anoxic death of cultured hepatocytes by inhibiting the mitochondrial permeability transition. *J Biol Chem* 268 (19): 13791-8, 1993.
- 201.** Patton, A. J., Genever, P. G., Birch, M. A., Suva, L. J., and Skerry, T. M.: Expression of an N-methyl-D-aspartate-type receptor by human and rat osteoblasts suggests a novel glutamate signaling pathway in bone. *Bone* 22 (6): 645-49, 1998.
- 202.** Peng, T. I., and Greenamyre, J. T.: Privileged access to mitochondria of calcium influx through N-methyl-D-aspartate receptors. *Mol Pharmacol* 53 (6): 974-80, 1998.
- 203.** Petralia, R. S., Wang, Y. X., and Wenthold, R. J.: The NMDA receptor subunits NR2A and NR2B show histological and ultrastructural localization patterns similar to those of NR1. *Journal of Neuroscience* 14 (10): 6102-20, 1994a.
- 204.** Petralia, R. S., Yokotani, N., and Wenthold, R. J.: Light and electron microscope distribution of the NMDA receptor subunit NMDAR1 in the rat nervous system using a selective anti-peptide antibody. *Journal of Neuroscience* 14 (2): 667-96, 1994b.
- 205.** Planells-Cases, R., Sun, W., Ferrer-Montiel, A. V., and Montal, M.: Molecular cloning, functional expression, and pharmacological characterization of an N-methyl-D-aspartate receptor subunit from human brain. *Proceedings of the National Academy of Sciences of the United States of America* 90 (11): 5057-61, 1993.
- 206.** Popik, P., and Skolnick, P.: The NMDA antagonist memantine blocks the expression and maintenance of morphine dependence. *Pharmacology, Biochemistry & Behavior* 53 (4): 791-7, 1996.
- 207.** Pud, D., Eisenberg, E., Spitzer, A., Adler, R., Fried, G., and Yarnitsky, D.: The NMDA receptor antagonist amantadine reduces surgical neuropathic pain in cancer patients: a double blind, randomized, placebo controlled trial. *Pain* 75 (2-3): 349-54, 1998.
- 208.** Raboisson, P., Flood, K., Lehmann, A., and Berge, O. G.: MK-801 neurotoxicity in the guinea pig cerebral cortex: susceptibility and regional differences compared with the rat. *Journal of Neuroscience Research* 49 (3): 364-71, 1997.
- 209.** Randle, J. C., Guet, T., Bobichon, C., Moreau, C., Curutchet, P., Lambolez, B., de Carvalho, L. P., Cordi, A., and Lepagnol, J. M.: Quinoxaline derivatives: structure-activity relationships and physiological implications of inhibition of N-methyl-D-aspartate

References

- and non-N-methyl-D-aspartate receptor-mediated currents and synaptic potentials. *Molecular Pharmacology* 41 (2): 337-45, 1992.
- 210.** Randolph, C., Roberts, J. W., Tierney, M. C., Bravi, D., Mouradian, M. M., and Chase, T. N.: D-cycloserine treatment of Alzheimer disease. *Alzheimer Dis Assoc Disord* 8: 198-205, 1994.
- 211.** Reddy, N. L., Hu, L. Y., Cotter, R. E., Fischer, J. B., Wong, W. J., McBurney, R. N., Weber, E., Holmes, D. L., Wong, S. T., Prasad, R., and et al.: Synthesis and structure-activity studies of N,N'-diarylguanidine derivatives. N-(1-naphthyl)-N'-(3-ethylphenyl)-N'-methylguanidine: a new, selective noncompetitive NMDA receptor antagonist. *Journal of Medicinal Chemistry* 37 (2): 260-7, 1994.
- 212.** Reilmann, R., Rolf, L. H., and Lange, H. W.: Huntington's disease: N-methyl-D-aspartate receptor coagonist glycine is increased in platelets. *Experimental Neurology* 144 (2): 416-9, 1997.
- 213.** Reynolds, I. J., and Palmer, A. M.: Regional variations in [3H]MK801 binding to rat brain N-methyl-D-aspartate receptors. *Journal of Neurochemistry* 56 (5): 1731-40, 1991.
- 214.** Rock, D. M., and MacDonald, R. L.: Spermine and related polyamines produce a voltage-dependent reduction of N-methyl-D-aspartate receptor single-channel conductance. *Molecular Pharmacology* 42 (1): 157-64, 1992.
- 215.** Rothstein, J. D., Martin, L. J., and Kuncl, R. W.: Decreased glutamate transport by the brain and spinal cord in amyotrophic lateral sclerosis. *New England Journal of Medicine* 326: 1464-8, 1992.
- 216.** Rowley, M., Kulagowski, J. J., Watt, A. P., Rathbone, D., Stevenson, G. I., Carling, R. W., Baker, R., Marshall, G. R., Kemp, J. A., Foster, A. C., Grimwood, S., Hargreaves, R., Hurley, C., Saywell, K. L., Tricklebank, M. D., and Leeson, P. D.: Effect of plasma protein binding on in vivo activity and brain penetration of glycine/NMDA receptor antagonists. *J Med Chem* 40 (25): 4053-68, 1997.
- 217.** Russi, P., Alesiani, M., Lombardi, G., Davolio, P., Pellicciari, R., and Moroni, F.: Nicotinylalanine increases the formation of kynurenic acid in the brain and antagonizes convulsions. *Journal of Neurochemistry* 59 (6): 2076-80, 1992.
- 218.** Sakurada, K., Masu, M., and Nakanishi, S.: Alteration of Ca²⁺ permeability and sensitivity to Mg²⁺ and channel blockers by a single amino acid substitution in the N-methyl-D-aspartate receptor. *Journal of Biological Chemistry* 268 (1): 410-5, 1993.
- 219.** Salituro, F. G., Harrison, B. L., Baron, B. M., Nyce, P. L., Stewart, K. T., Kehne, J. H., White, H. S., and McDonald, I. A.: 3-(2-Carboxyindol-3-yl)propionic acid-based

References

- antagonists of the N-methyl-D-aspartic acid receptor associated glycine binding site. *Journal of Medicinal Chemistry* 35 (10): 1791-9, 1992.
- 220.** Santamaria, A., Rios, C., Solis-Hernandez, F., Ordaz-Moreno, J., Gonzalez-Reynoso, L., Altagracia, M., and Kravzov, J.: Systemic DL-kynurenine and probenecid pretreatment attenuates quinolinic acid-induced neurotoxicity in rats. *Neuropharmacology* 35 (1): 23-8, 1996.
- 221.** Saybasili, H., Stevens, D. R., and Haas, H. L.: pH-dependent modulation of N-methyl-D-aspartate receptor-mediated synaptic currents by histamine in rat hippocampus in vitro. *Neuroscience Letters* 199 (3): 225-7, 1995.
- 222.** Schell, M. J., Brady, R. O., Jr., Molliver, M. E., and Snyder, S. H.: D-serine as a neuromodulator: regional and developmental localizations in rat brain glia resemble NMDA receptors. *Journal of Neuroscience* 17 (5): 1604-15, 1997.
- 223.** Schell, M. J., Molliver, M. E., and Snyder, S. H.: D-serine, an endogenous synaptic modulator: localization to astrocytes and glutamate-stimulated release. *Proc Natl Acad Sci U S A* 92 (9): 3948-52, 1995.
- 224.** Schinder, A. F., Olson, E. C., Spitzer, N. C., and Montal, M.: Mitochondrial dysfunction is a primary event in glutamate neurotoxicity. *Journal of Neuroscience* 16 (19): 6125-33, 1996.
- 225.** Schulze-Osthoff, K., Bakker, A. C., Vanhaesebroeck, B., Beyaert, R., Jacob, W. A., and Fiers, W.: Cytotoxic activity of tumor necrosis factor is mediated by early damage of mitochondrial functions. Evidence for the involvement of mitochondrial radical generation. *J Biol Chem* 267 (8): 5317-23, 1992.
- 226.** Schwarcz, R.: Metabolism and function of brain kynurenines. *Biochemical Society Transactions* 21 (1): 77-82, 1993.
- 227.** Sherman, A. D., Hegwood, T. S., Baruah, S., and Waziri, R.: Deficient NMDA induced glutamate release from synaptosomes of schizophrenics. *Biological Psychiatry* 30: 1191-8, 1991.
- 228.** Smith, K. E., Borden, L. A., Hartig, P. R., Branchek, T., and Weinshank, R. L.: Cloning and expression of a glycine transporter reveal colocalization with NMDA receptors. *Neuron* 8 (5): 927-35, 1992.
- 229.** Sommer, B., Kohler, M., Sprengel, R., and Seeburg, P. H.: RNA editing in brain controls a determinant of ion flow in glutamate-gated channels. *Cell* 67 (1): 11-9, 1991.

References

- 230.** Speciale, C., Wu, H. Q., Cini, M., Marconi, M., Varasi, M., and Schwarcz, R.: (R,S)-3,4-dichlorobenzoylalanine (FCE 28833A) causes a large and persistent increase in brain kynurenic acid levels in rats. *Eur J Pharmacol* 315 (3): 263-7, 1996.
- 231.** Stern, P., Behe, P., Schoepfer, R., and Colquhoun, D.: Single-channel conductances of NMDA receptors expressed from cloned cDNAs: comparison with native receptors. *Proceedings of the Royal Society of London - Series B: Biological Sciences* 250 (1329): 271-7, 1992.
- 232.** Stone, T. W.: Neuropharmacology of quinolinic and kynurenic acids. *Pharmacological Reviews* 45 (3): 309-79, 1993.
- 233.** Stout, A. K., Raphael, H. M., Kanterewicz, B. I., Klann, E., and Reynolds, I. J.: Glutamate induced neuron death requires mitochondrial calcium uptake. *Nature* 5 (1): 366-73, 1998.
- 234.** Sucher, N. J., Akbarian, S., Chi, C. L., Leclerc, C. L., Awobuluyi, M., Deitcher, D. L., Wu, M. K., Yuan, J. P., Jones, E. G., and Lipton, S. A.: Developmental and regional expression pattern of a novel NMDA receptor-like subunit (NMDAR-L) in the rodent brain. *Journal of Neuroscience* 15 (10): 6509-20, 1995.
- 235.** Sullivan, J. M., Traynelis, S. F., Chen, H. S., Escobar, W., Heinemann, S. F., and Lipton, S. A.: Identification of two cysteine residues that are required for redox modulation of the NMDA subtype of glutamate receptor. *Neuron* 13 (4): 929-36, 1994.
- 236.** Supplisson, S., and Bergman, C.: Control of NMDA receptor activation by a glycine transporter co-expressed in *Xenopus* oocytes. *Journal of Neuroscience* 17 (12): 4580-90, 1997.
- 237.** Susin, S. A., Zamzami, N., Castedo, M., Hirsch, T., Marchetti, P., Macho, A., Daugas, E., Geuskens, M., and Kroemer, G.: Bcl-2 inhibits the mitochondrial release of an apoptogenic protease. *J Exp Med* 184 (4): 1331-41, 1996.
- 238.** Sveinbjornsdottir, S., Sander, J. W. A. S., Upton, D., Thompson, P. J., Patsalos, P. N., Hirt, D., Emre, M., Lowe, D., and Duncan, J. S.: The excitatory amino acid antagonist D-CPP-ene (SDZ EAA-494) in patients with epilepsy. *Epilepsy Research* 16: 165-74, 1993.
- 239.** Szabo, I., Bernardi, P., and Zoratti, M.: Modulation of the mitochondrial megachannel by divalent cations and protons. *J Biol Chem* 267 (5): 2940-6, 1992.
- 240.** Szabo, I., De Pinto, V., and Zoratti, M.: The mitochondrial permeability transition pore may comprise VDAC molecules. II. The electrophysiological properties of VDAC are compatible with those of the mitochondrial megachannel. *FEBS Lett* 330 (2): 206-10, 1993.

References

- 241.** Szabo, I., and Zoratti, M.: The giant channel of the inner mitochondrial membrane is inhibited by cyclosporin A. *J Biol Chem* 266 (6): 3376-9, 1991.
- 242.** Takaoka, S., Bart, R. D., Pearlstein, R., Brinkhous, A., and Warner, D. S.: Neuroprotective effect of NMDA receptor glycine recognition site antagonism persists when brain temperature is controlled. *Journal of Cerebral Blood Flow & Metabolism* 17 (2): 161-7, 1997.
- 243.** Tang, L. H., and Aizenman, E.: The modulation of N-methyl-D-aspartate receptors by redox and alkylating reagents in rat cortical neurones in vitro. *Journal of Physiology* 465: 303-23, 1993.
- 244.** Tingley, W. G., Roche, K. W., Thompson, A. K., and Huganir, R. L.: Regulation of NMDA receptor phosphorylation by alternative splicing of the C-terminal domain. *Nature* 364 (6432): 70-3, 1993.
- 245.** Tiseo, P. J., and Inturrisi, C. E.: Attenuation and reversal of morphine tolerance by the competitive N-methyl-D-aspartate receptor antagonist, LY274614. *Journal of Pharmacology & Experimental Therapeutics* 264 (3): 1090-6, 1993.
- 246.** Toggas, S. M., Masliah, E., and Mucke, L.: Prevention of HIV-1 gp120-induced neuronal damage in the central nervous system of transgenic mice by the NMDA receptor antagonist memantine. *Brain Research* 706 (2): 303-7, 1996.
- 247.** Tong, G., Shepherd, D., and Jahr, C. E.: Synaptic desensitization of NMDA receptors by calcineurin. *Science* 267 (5203): 1510-2, 1995.
- 248.** Toth, E., and Lajtha, A.: Antagonism of phencyclidin induced hyperactivity by glycine in mice. *Neurochemistry International* 11: 393-400, 1986.
- 249.** Traynelis, S. F., and Cull-Candy, S. G.: Proton inhibition of N-methyl-D-aspartate receptors in cerebellar neurons. *Nature* 345 (6273): 347-50, 1990.
- 250.** Traynelis, S. F., and Cull-Candy, S. G.: Pharmacological properties and H⁺ sensitivity of excitatory amino acid receptor channels in rat cerebellar granule neurones. *Journal of Physiology* 433: 727-63, 1991.
- 251.** Traynelis, S. F., Hartley, M., and Heinemann, S. F.: Control of proton sensitivity of the NMDA receptor by RNA splicing and polyamines. *Science* 268 (5212): 873-6, 1995.
- 252.** Trujillo, K. A.: Effects of noncompetitive N-methyl-D-aspartate receptor antagonists on opiate tolerance and physical dependence. *Neuropsychopharmacology* 13 (4): 301-7, 1995.
- 253.** Trujillo, K. A., and Akil, H.: Inhibition of morphine tolerance and dependence by the NMDA receptor antagonist MK-801. *Science* 251 (4989): 85-7, 1991.

References

- 254.** Turski, L., Bressler, K., Rettig, K. J., Loschmann, P. A., and Wachtel, H.: Protection of substantia nigra from MPP⁺ neurotoxicity by N-methyl-D-aspartate antagonists [see comments]. *Nature* 349 (6308): 414-8, 1991.
- 255.** Uchino, S., Kudo, Y., Wanatabe, W., Nakajima-Iijima, S., and Mishina, M.: Inducible expression of N-methyl-D-aspartate (NMDA) receptor channels from cloned cDNAs in CHO cells. *Molecular Brain Research* 44: 1-11, 1997.
- 256.** Vaccarino, A. L., Marek, P., Kest, B., Weber, E., Keana, J. F., and Liebeskind, J. C.: NMDA receptor antagonists, MK-801 and ACEA-1011, prevent the development of tonic pain following subcutaneous formalin. *Brain Research* 615 (2): 331-4, 1993.
- 257.** Varney, M. A., Jachec, C., Deal, C., Hess, S. D., Daggett, L. P., Skvoretz, R., Urcan, M., Morrison, J. H., Moran, T., Johnson, E. C., and Velicelebi, G.: Stable expression and characterization of recombinant human heteromeric N-methyl-D-aspartate receptor subtypes NMDAR1A/2A and NMDAR1A/2B in mammalian cells. *Journal of Pharmacology & Experimental Therapeutics* 279 (1): 367-78, 1996.
- 258.** Vercammen, D., Beyaert, R., Denecker, G., Goossens, V., Van Loo, G., Declercq, W., Grooten, J., Fiers, W., and Vandenabeele, P.: Inhibition of caspases increases the sensitivity of L929 cells to necrosis mediated by tumor necrosis factor. *J Exp Med* 187 (9): 1477-85, 1998.
- 259.** Vorobjev, V. S., Sharonova, I. N., Walsh, I. B., and Haas, H. L.: Histamine potentiates N-methyl-D-aspartate responses in acutely isolated hippocampal neurons. *Neuron* 11 (5): 837-44, 1993.
- 260.** Wafford, K. A., Bain, C. J., Le Bourdelles, B., Whiting, P. J., and Kemp, J. A.: Preferential co-assembly of recombinant NMDA receptors composed of three different subunits. *Neuroreport* 4 (12): 1347-9, 1993.
- 261.** Wafford, K. A., Kathoria, M., Bain, C. J., Marshall, G., Le Bourdelles, B., Kemp, J. A., and Whiting, P. J.: Identification of amino acids in the N-methyl-D-aspartate receptor NR1 subunit that contribute to the glycine binding site. *Molecular Pharmacology* 47 (2): 374-80, 1995.
- 262.** Wako, K., Ma, N., Shiroyama, T., and Semba, R.: Glial uptake of intracerebroventricularly injected D-serine in the rat brain: an immunocytochemical study. *Neurosci Lett* 185 (3): 171-4, 1995.
- 263.** Wang, Y. T., and Salter, M. W.: Regulation of NMDA receptors by tyrosine kinases and phosphatases. *Nature* 369 (6477): 233-5, 1994.

References

- 264.** Warncke, T., Jorum, E., and Stubhaug, A.: Local treatment with the N-methyl-D-aspartate receptor antagonist ketamine, inhibit development of secondary hyperalgesia in man by a peripheral action. *Neuroscience Letters* 227 (1): 1-4, 1997.
- 265.** Warner, D. S., Martin, H., Ludwig, P., McAllister, A., Keana, J. F., and Weber, E.: In vivo models of cerebral ischemia: effects of parenterally administered NMDA receptor glycine site antagonists. *Journal of Cerebral Blood Flow & Metabolism* 15 (2): 188-96, 1995.
- 266.** Watanabe, M., Inoue, Y., Sakimura, K., and Mishina, M.: Developmental changes in distribution of NMDA receptor channel subunit mRNAs. *Neuroreport* 3 (12): 1138-40, 1992.
- 267.** Watanabe, M., Inoue, Y., Sakimura, K., and Mishina, M.: Distinct distributions of five N-methyl-D-aspartate receptor channel subunit mRNAs in the forebrain. *Journal of Comparative Neurology* 338 (3): 377-90, 1993.
- 268.** Watanabe, M., Mishina, M., and Inoue, Y.: Differential distributions of the NMDA receptor channel subunit mRNAs in the mouse retina. *Brain Research* 634 (2): 328-32, 1994a.
- 269.** Watanabe, M., Mishina, M., and Inoue, Y.: Distinct distributions of five NMDA receptor channel subunit mRNAs in the brainstem. *Journal of Comparative Neurology* 343 (4): 520-31, 1994b.
- 270.** Watanabe, M., Mishina, M., and Inoue, Y.: Distinct gene expression of the N-methyl-D-aspartate receptor channel subunit in peripheral neurons of the mouse sensory ganglia and adrenal gland. *Neuroscience Letters* 165 (1-2): 183-6, 1994c.
- 271.** Watanabe, M., Mishina, M., and Inoue, Y.: Distinct spatiotemporal distributions of the N-methyl-D-aspartate receptor channel subunit mRNAs in the mouse cervical cord. *Journal of Comparative Neurology* 345 (2): 314-9, 1994d.
- 272.** Watanabe, M., Mishina, M., and Inoue, Y.: Distinct spatiotemporal expressions of five NMDA receptor channel subunit mRNAs in the cerebellum. *Journal of Comparative Neurology* 343 (4): 513-9, 1994e.
- 273.** Watson, G. B., and Lanthorn, T. H.: Pharmacological characteristics of cyclic homologues of glycine at the N-methyl-D-aspartate receptor-associated glycine site. *Neuropharmacology* 29 (8): 727-30, 1990.
- 274.** Waziri, R.: Glycine therapy of schizophrenia. *Biological Psychiatry* 23: 209-14, 1988.

References

275. White, R. J., and Reynolds, I. J.: Mitochondrial depolarization in glutamate-stimulated neurons: an early signal specific to excitotoxin exposure. *J Neurosci* 16 (18): 5688-97, 1996.
276. White, R. J., and Reynolds, I. J.: Mitochondria accumulate Ca²⁺ following intense glutamate stimulation of cultured rat forbrain neurones. *J. Physiology* 498: 31-47, 1997.
277. Willetts, J., Balster, R. L., and Leander, J. D.: The behavioral pharmacology of NMDA receptor antagonists [see comments]. *Trends in Pharmacological Sciences* 11 (10): 423-8, 1990.
278. Williams, K.: Ifenprodil discriminates subtypes of the N-methyl-D-aspartate receptor: selectivity and mechanisms at recombinant heteromeric receptors. *Mol Pharmacol* 44 (4): 851-9, 1993.
279. Williams, K.: Subunit-specific potentiation of recombinant N-methyl-D-aspartate receptors by histamine. *Mol Pharmacol* 46 (3): 531-41, 1994.
280. Williams, K., Kashiwagi, K., Fukuchi, J., and Igarashi, K.: An acidic amino acid in the N-methyl-D-aspartate receptor that is important for spermine stimulation. *Molecular Pharmacology* 48 (6): 1087-98, 1995.
281. Williams, K., Zappia, A. M., Pritchett, D. B., Shen, Y. M., and Molinoff, P. B.: Sensitivity of the N-methyl-D-aspartate receptor to polyamines is controlled by NR2 subunits. *Molecular Pharmacology* 45 (5): 803-9, 1994.
282. Wood, M. W., VanDongen, H. M., and VanDongen, A. M.: An alanine residue in the M3-M4 linker lines the glycine binding pocket of the N-methyl-D-aspartate receptor. *Journal of Biological Chemistry* 272 (6): 3532-7, 1997.
283. Woodward, R. M., Huettner, J. E., Guastella, J., Keana, J. F., and Weber, E.: In vitro pharmacology of ACEA-1021 and ACEA-1031: systemically active quinoxalinediones with high affinity and selectivity for N-methyl-D-aspartate receptor glycine sites. *Molecular Pharmacology* 47 (3): 568-81, 1995.
284. Wu, H. Q., Salituro, F. G., and Schwarcz, R.: Enzyme-catalyzed production of the neuroprotective NMDA receptor antagonist 7-chlorokynurenic acid in the rat brain in vivo. *European Journal of Pharmacology* 319 (1): 13-20, 1997.
285. Wu, P., Price, P., Du, B., Hatch, W. C., and Terwilliger, E. F.: Direct cytotoxicity of HIV-1 envelope protein gp120 on human NT neurons. *Neuroreport* 7 (5): 1045-9, 1996.
286. Xie, X. M., and Smart, T. G.: A physiological role for endogenous zinc in rat hippocampal synaptic neurotransmission. *Nature* 349 (6309): 521-4, 1991.

References

- 287.** Yamakura, T., Mori, H., Masaki, H., Shimoji, K., and Mishina, M.: Different sensitivities of NMDA receptor channel subtypes to non-competitive antagonists. *Neuroreport* 4 (6): 687-90, 1993a.
- 288.** Yamakura, T., Mori, H., Shimoji, K., and Mishina, M.: Phosphorylation of the carboxyl-terminal domain of the zeta 1 subunit is not responsible for potentiation by TPA of the NMDA receptor channel. *Biochemical & Biophysical Research Communications* 196 (3): 1537-44, 1993b.
- 289.** Yamazaki, M., Mori, H., Araki, K., Mori, K. J., and Mishina, M.: Cloning, expression and modulation of a mouse NMDA receptor subunit. *FEBS Letters* 300 (1): 39-45, 1992.
- 290.** Yang, J. C., and Cortopassi, G. A.: Induction of the mitochondrial permeability transition causes release of the apoptogenic factor cytochrome c. *Free Radic Biol Med* 24 (4): 624-31, 1998.
- 291.** Yoneda, Y., and Ogita, K.: Heterogeneity of the N-methyl-D-aspartate receptor ionophore complex in rat brain, as revealed by ligand binding techniques. *Journal of Pharmacology & Experimental Therapeutics* 259 (1): 86-96, 1991.
- 292.** Zheng, F., Gingrich, M. B., Traynelis, S. F., and Conn, P. J.: Tyrosine kinase potentiates NMDA receptor currents by reducing tonic zinc inhibition [see comments]. *Nat Neurosci* 1 (3): 185-91, 1998.
- 293.** Zhou, S., Bonasera, L., and Carlton, S. M.: Peripheral administration of NMDA, AMPA or KA results in pain behaviors in rats. *Neuroreport* 7 (4): 895-900, 1996.
- 294.** Zou, H., Henzel, W. J., Liu, X., Lutschg, A., and Wang, X.: Apaf-1, a human protein homologous to *C. elegans* CED-4, participates in cytochrome c-dependent activation of caspase-3 [see comments]. *Cell* 90 (3): 405-13, 1997.
- 295.** Zwart, R., Blank, T., and Spiess, J.: Histamine slows the onset of desensitization of rat cortical NMDA receptors. *Neuroreport* 7 (13): 2206-10, 1996.

9. Curriculum Vitae

Ralf Dirk Steinmetz

Geburtsdatum 01.11.1968
Geburtsort Frankfurt am Main
Staatsangehörigkeit deutsch

E-mail R.Steinmetz@pharmchem.uni-frankfurt.de



Curriculum Vitae

schulische Ausbildung	1975 - 1979	Friedrich Ebert-Schule	Schöneck
	1979 - 1988	Otto Hahn-Schule	Hanau
	■ Allgemeine Hochschulreife		
Ersatzdienst	1988 - 1990	Martin Luther-Stiftung	Hanau
Studium	WS 90/91 - WS 94/95	Johann Wolfgang Goethe-Universität	Frankfurt
	■ Studium der Pharmazie		
	■ 1. Staatsexamen März 1993		
	■ 2. Staatsexamen April 1995		
Tätigkeiten neben dem Studium	1990 - 1994	Zentrallaboratorium Dt. Apotheker	Eschborn
	■ Tätigkeiten in den Abteilungen Bioanalytik und Biopharmazie		
Pharmaziepraktikum	Mai 1995 - Okt 1995	Zentrallaboratorium Dt. Apotheker	Eschborn
	Nov 1995 - Apr 1996	Apotheke am Weissen Stein	Frankfurt
Approbation zum Apotheker	Mai 1996		
Promotion	1996 - 2000	Institut für Pharmazeutische Chemie der Johann Wolfgang Goethe-Universität	Frankfurt
	■ Mitglied im Graduierten Kolleg „Arzneimittel: Entwicklung und Analytik“		
	■ Anfertigung einer Dissertationsarbeit zur funktionellen Expression von rekombinanten NMDA-Rezeptoren in eukaryotischen Zelllinien im Arbeitskreis von Prof. Dr. Dieter Steinhilber		
	seit Juni 1999		
	■ wissenschaftlicher Mitarbeiter im Arbeitskreis von Prof. Dr. Dieter Steinhilber		
	■ Leitung des 2. Fachsemesters „Quantitative anorganische Analyse“		